Evolutionary Origins, Palaeoecology and Systematics of Placodont Marine Reptiles from the Triassic of Europe and China

---

Dissertation

zur

Erlangung der naturwissenschaftlichen Doktorwürde
(Dr. sc. nat.)

vorgelegt der

Mathematisch-naturwissenschaftlichen Fakultät

der

Universität Zürich

von

James Michael Neenan

aus dem

Vereinigten Königreich Grossbritannien

Promotionskomitee

Dr. Torsten Scheyer
(Leitung der Dissertation)
Prof. Dr. Marcelo Sánchez (Vorsitz)
Prof. Dr. Hugo Bucher
Dr. Nick Fraser

Zürich, 2014

Evolutionary Origins, Palaeoecology and Systematics of Placodont Marine Reptiles from the Triassic of Europe and China

James M. Neenan

University of Zurich, 2014

Title page image:

“Out of Time”, painting by Jane Neenan, 2014

CONTENTS

ACKNOWLEDGEMENTS

I am extremely grateful to my supervisor, Dr. Torsten Scheyer, whose constant support and patience over the years have helped me beyond words. I have learnt a great deal from him: scientific methods, diplomacy, self-confidence and the ability to appreciate fine music and beers. I am incredibly grateful to him for choosing me for this project and consider him a friend as well as a mentor. I am also extremely grateful to Prof. Dr. Marcelo Sánchez for his constant good advice, useful discussions and constructive criticism. I feel truly privileged to have been a member of his working group, and have become a better scientist because of it. Prof. Dr. Hugo Bucher is also thanked for being a supportive, helpful director with a good sense of humour.

I would also like to thank all the colleagues from outside the PIMUZ with whom I have had the honour of collaborating: Olivier Rieppel (Field Museum, Chicago), Li Chun (IVPP, Beijing), Da-Yong Jiang (GMPKU, Beijing), Nicole Klein (SIPG, Bonn), Hans Hagdorn (MHI, Ingelfingen), Andrea Tintori (Milan, Italy), Silvio Renesto (Varese, Italy), Franco Saller (Bozen, Italy), Federico Bernardini, Claudio Tuniz (both ICTP; Trieste), and Giuseppe Muscio (MFSN, Udine). Access to specimens was vital for the success of this project, so my deepest thanks go to Heinz Furrer (PIMUZ, Zurich), Joachim Rabold and Stefan Eggmaier (UMO, Bayreuth), Markus Moser and Oli Rauhut (BSPG, Munich), Rainer Schoch (SMNS, Stuttgart), Li Chun (IVPP, Beijing), and Da-Yong Jiang (GMPKU, Beijing), for allowing me to examine specimens and take many of them to be CT scanned. I am also very grateful to Walter Leis (Hochschule Aalen), Hou Yemao (IVPP, Beijing), Nicole Klein (SIPG, Bonn) and Federico Bernardini (ICTP, Trieste), who all assisted in the CT scanning of

specimens. Indeed, processing and segmenting the vast amounts of CT data would have been impossible without the help of Lisa Rager (SMNS, Stuttgart) and Constanze Bickelmann (MHUB, Berlin). My deepest thanks also go to those who were always willing to discuss my project and help me with various issues: Robin O'Keefe (Marshall), Nick Fraser, Steve Brusatte (both in Edinburgh), Mike Benton, Tom Stubbs, Aude Caromel (all Bristol), Darren Naish (Southampton), Neil Kelley and Ryosuke Motani (both UC Davis).

My sincerest thanks also go to my officemates and very good friends, Christian Kolb and Juan Carillo who have both supported me through the tougher periods of my PhD and have always been available for discussion and advice. I would also like to thank all my other friends at the PIMUZ, who have all made my time here both enjoyable and rewarding: Åsa Frisk, Fiona Straehl, Pat Putzi-Meier, Carlo Romano, David Ware, Morgane Brosse, Marc Leu, Lorena Tessitore, Borhan Bagherpour, Conni Bickelmann, Jorge Carillo, Linda Frey, Maddy Geiger, Markus Hebeisen, Dick Hofmann, Jasi Hugi, Romain Jattiot, Christian Klug, Dai Koyabu, Erin Maxwell, Carole 'Bronzie' Naglik, Lisa Rager, Anna Sanson, Beat Scheffold, Madlen Stange, Mirjam Fehlmann, Viv Jaquier, Alex Wegmann, Ingmar Werneburg and Laura Wilson. This thesis would not have been possible without the heroic efforts of Heike Götzmann, who has the ability to solve any problem without breaking a sweat, and Heini Walter, who can fix any IT-related issue. Nor could have I survived my time here without the love and support of Artemis Treindl and Christa Finkenwirth, who have both been incredible friends to me.

Finally and most importantly, I would like to thank my family, Jane, Mike and Jordan for being incredibly supportive, patient and loving over my many years of education.

SUMMARY

Placodonts are a basal clade of sauropterygian marine reptiles that inhabited the eastern and western margins of the Tethys Ocean from the earliest Middle Triassic until the latest Triassic (~247–201 mya). They are characterised by a highly specialised dentition that was adapted for, in most cases, a durophagous diet. Many taxa also feature heavy armour, with superficially turtle-like carapaces. While the first placodonts were described during the 1830's, the group is still fairly under-studied, with relatively little known about their evolutionary origins, palaeoecology, or even phylogenetic relationships. The aims of this study were to clarify these omissions, mostly by using micro-computed tomographic (μCT) scanning on placodont crania from both Europe and South China (which correspond to the western and eastern margins of the Tethys Ocean respectively). A more in-depth introduction to placodonts and the project is outlined in Chapter 1.

In Chapter 2, recent publications questioning the traditionally-held view that placodonts were durophagous inspired a thorough literature review on placodont palaeoecology, combined with a comment in response to these claims. The original author concluded that fossil evidence, combined with tooth wear, indicates an herbivorous diet for placodonts, describing them as Triassic 'sea cows' that fed on macroalgae. However, osteological, biomechanical and taphonomic evidence were used to effectively counter this, concluding that, apart from the enigmatic *Henodus chelyops*, it is very unlikely that placodonts were herbivorous.

Chapter 3 is a study of two exceptionally well preserved skulls of the basal placodont *Placodus gigas* using μCT scanning to shed light on braincase morphology and palaeoecology. This resulted in a revised reconstruction of braincase osteology,

the first reconstruction of a sauropterygian inner ear (vestibular apparatus) and a new reconstruction of the cranial endocast of *Placodus*. The vestibular apparatus is characterised by dorsoventrally compressed vertical semi-circular canals, a common feature of extant marine reptiles. The position of the horizontal canal also indicates an 'alert' head position of about 20º, indicating a highly aquatic lifestyle even in basal placodonts.

Chapter 4 is a description of a new taxon from the early Middle Triassic of Winterswijk in the Netherlands, which sheds light on the palaeogeographic origins of the placodonts, as well as the evolutionary origins of their highly-derived dentition. µCT data were used to identify, amongst other diagnostic features, a single row of teeth on the palatine, similar to that seen in placodonts. However these teeth were small and pointed rather than large and flattened for durophagy. Phylogenetic analyses indicated that the specimen is sister taxon to Placodontia, thus indicating that the clade first evolved in the western Tethys, and that their palatine dentition was not initially used for durophagous feeding.

Investigations into placodont dentition are continued in Chapter 5, where patterns of tooth replacement were studied, as well as a description of the dentition of Chinese placodonts. Placodonts exhibit a unique method of tooth replacement, with basal, non-armoured taxa exhibiting seemingly random replacement patterns, while the more derived, armoured taxa show highly-organised unilateral replacement, often in functional units. This allowed these taxa to continue feeding efficiently, despite some functional teeth being missing while being replaced.

Placodont phylogenetic relationships are investigated in Chapter 6. Despite the cranial osteology of European placodonts being relatively well understood, Chinese placodonts have been neglected, resulting in a lack of comprehensive phylogenetic studies on this group. Thorough cranial osteological descriptions were

conducted for the four Chinese placodont holotype crania using a combination of µCT data and specimen study. These taxa were then included in the first placodont phylogeny to include all genera from both the eastern and western Tethys. Results support a monophyletic Placodontia, with eastern taxa interspaced among western taxa, indicating no significant geographic separation between the two regions. Unarmoured as well as armoured placodonts appear to have evolved in the western Tethys, although the highly nested Placochelyidae probably first appeared in the Middle Triassic of the eastern Tethys.

KEYWORDS: Placodontia, Sauropterygia, Triassic, Tethys, µCT scanning, durophagy, phylogeny, palaeoecology

ZUSAMMENFASSUNG

Placodontier sind eine basale Gruppe mariner Reptilien innerhalb der Sauropterygier, welche die östlichen und westlichen Bereiche des Tethys-Ozeans von der frühesten Mitteltrias bis in die späte Obertrias (vor ca. 247-201 Millionen Jahren) besiedelten. Sie sind charakterisiert durch ihre hoch spezialisierte Knackbezahnung, welche das Knacken hartschaliger Nahrung ermöglicht. Viele Taxa besitzen auch eine stark entwickelte Panzerung die oberflächlich an Schildkröten erinnert. Obwohl die ersten Placodontierfunde bereits in den 1830er Jahren beschrieben wurden, ist die Gruppe dennoch wenig untersucht worden in Bezug auf deren Ursprung, Paläoökologie oder die intraspezifischen Verwandtschaftsbeziehungen. Die Ziele dieser Arbeit sind unter anderem diese Punkte genauer zu beleuchten, hauptsächlich durch den Einsatz von Microcomputertomographie-Untersuchungen (µCT) von sowohl europäischen als auch chinesischen Placodontierschädeln (Zentraleuropa und China entsprechen heute etwa den damaligen westlichen und östlichen Randgebieten des Tethysozeans). Eine tiefer gehende Einführung in die Gruppe der Placodontier sowie die Ziele der vorliegenden Arbeit befindet sich in Kapitel 1.

In Kapitel 2 haben kürzlich veröffentlichte Studien, welche die traditionelle Sichtweise der durophagen Lebensweise der Placodontier in Frage stellten, den Ausschlag zu einer eingehenden Literaturarbeit zur Überprüfung der Paläoökologie dieser Tiere gegeben. Der Autor der kontrovers diskutierten Studie postulierte, dass das stratigraphische Auftreten der Fossilien zusammen mit Spuren von Zahnabnutzungen allein auf Herbivorie (pflanzliche Ernährungsweise) hindeutet, sodass die Tiere analog zu Seekühen anzusehen wären, welche sich in der Triaszeit

von Makroalgen (Seetangen) ernährten. Die osteologischen, biomechanischen und taphonomischen Beweise sprechen allerdings dagegen, sodass nicht davon auszugehen ist, dass die Placodontier (vielleicht mit Ausnahme des enigmatischen *Henodus chelyops*) herbivor waren.

In Kapitel 3 ist in zwei außergewöhnlich gut erhaltenen Schädeln des basalen Placodontiers *Placodus gigas* mittels µCT-Aufnahmen die innere Hirnschädelmorphologie untersucht worden, um mehr über die Paläoökologie der Tiere zu erfahren. Die Ergebnisse führten zu einer überarbeiteten Osteologie des Hirnschädels, der ersten Rekonstruktion eines Sauropterygier-Innenohrs (Gleichgewichtsorgan), sowie eine neue, virtuelle Rekonstruktion der Hirnschädelausgusses. Das Gleichgewichtsorgan ist charakterisiert durch dorsoventral komprimierte vertikale Bogengänge, ein Merkmal welches bei vielen verschiedenen Meeresreptilien auftritt. Die Position des horizontalen Bogengangs zeigt zudem eine um etwa 20° geneigte 'alert' Kopfp osition an, was schon auf eine hoch entwickelte Anpassungsstufe der Placodontier an ein Leben im Wasser hindeutet.

Kapitel 4 beschäftigt sich mit der Neubeschreibung eines Taxons aus der frühen Mitteltrias von Winterswijk, Niederlande, welches für die paläogeographischen Ursprünge und die Entstehung der stark abgeleiteten Bezahnung der Placodontier aufschlussreich ist. µCT-Daten wurden benutzt um diagnostische Merkmale, wie etwa ein Palatinum, welches wie bei den Placodontier nur eine einzelne Zahnreihe trägt, zu identifizieren. Die Zähne dieser Zahnreihe waren allerdings nicht grosse und flache Mahlzähne sondern klein und spitz zulaufend. Phylogenetische Analysen zeigten zudem dass es sich bei dem Tier um das Schwestertaxon zu Placodontia handelt, was zum einen die Vermutung stützt, dass die ganze Gruppe zuerst in der

westlichen Tethys entstand und zum anderen, dass die Palatinalbezahnung nicht ursprünglich zum Knacken hartschaliger Nahrung auftrat.

Weitere Untersuchungen zur Bezahnung der Placodontier finden sich im Kapitel 5, wobei sowohl die Zahnwechsel innerhalb der Gruppe als auch die Bezahnung der chinesischen Arten im Speziellen untersucht wurden. Die Placodontier zeigen eine einzigartige Methode des Zahnwechsels, welche sich in den basalen, nicht gepanzerten Vertretern durch scheinbar zufällige Ersatzmuster äussert, wogegen die stärker abgeleiteten, gepanzerten Taxa höher organisierte Muster erkennen lassen, in denen die Zähne häufig in funktionellen Einheiten gewechselt werden. Diese erlauben den letzteren Arten eine effiziente Nahrungsaufnahme, obwohl einige funktionelle Zähne während des Zahnwechselvorgangs fehlen.

Die Verwandtschaftsbeziehungen der Placodontier werden eingehender in Kapitel 6 untersucht. Die Schädelosteologie der europäischen Placodontier ist relativ gut verstanden, wogegen die der chinesischen Vertreter eher untergeordnet behandelt wurde, was wiederum dazu führt, dass vergleichende phylogenetische Arbeiten bisher nicht durchgeführt wurden. Gründliche osteologische Beschreibungen der Holotypenschädel aller vier bisher beschriebenen chinesischen Arten basieren hierin nun auf einer Kombination von äußeren anatomischen Merkmalen und µCT Daten. Diese Taxa wurden zudem in die erste phylogenetische Analyse eingearbeitet, welche nun sowohl Vertreter der westlichen als auch alle der östlichen Tethysbereiche beinhaltet. Die Resultate der Untersuchung unterstützen die Monophylie der Placodontia, wobei die fernöstlichen und die westlichen Taxa vermischt sind und somit keine eindeutige geographische Trennung zwischen den beiden Regionen erkennbar ist. Sowohl die ungepanzerten als auch die gepanzerten Formen scheinen sich in der westlichen Tethys entwickelt zu haben, wobei die

Placochelyidae dagegen vielleicht als erstes während der Mitteltrias in der östlichen Tethys auftritt.

SCHLÜSSELWÖRTER: Placodontia, Sauropterygia, Trias, Tethys, µCT scanning, Durophagie, Phylogenie, Paläoökologie

CHAPTER 1

INTRODUCTION

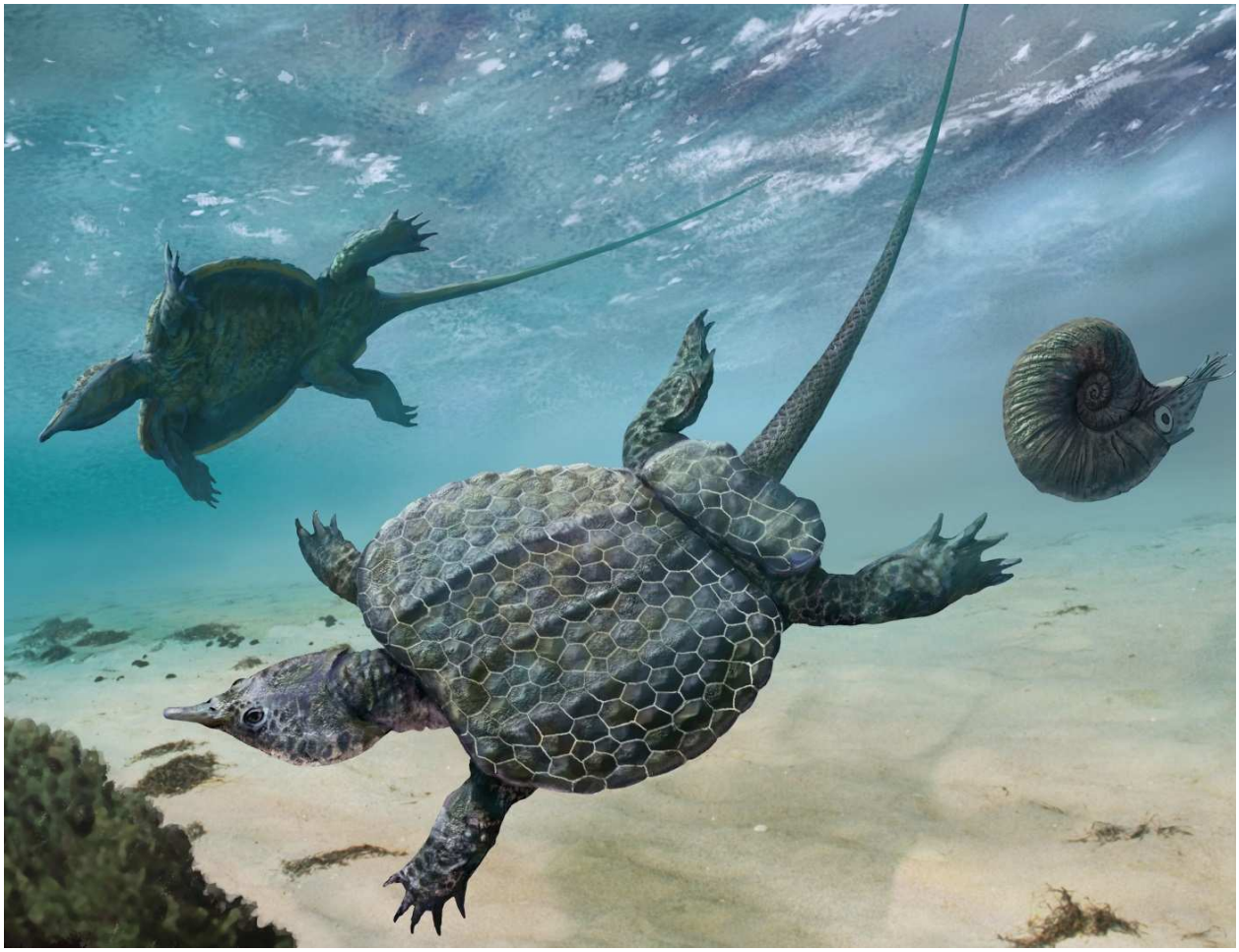

Psephoderma alpinum by Jaime Chirinos

1.1 PLACODONTIA

Placodonts are members of Sauropterygia, the most successful radiation of marine reptiles known (Cheng et al., 2004; Motani, 2009), with a wide range of morphologies and ecologies (Rieppel, 2000a; O'Keefe and Chiappe, 2011) that spanned almost the entire Mesozoic Era (~245–65.5 mya; Benson et al., 2010; Motani, 2010). As the most 'basal' group of sauropterygians (i.e., retaining the most plesiomorphic characters; e.g., Rieppel, 2000a), placodonts are extremely important for understanding the evolutionary origins of the Sauropterygia. Like all other sauropterygians, placodonts lack not only any modern descendants (e.g., Meyer, 1863; Peyer & Kuhn-Schnyder, 1955) but also show ecomorphologies that lack modern counterparts among living reptile species. The earliest placodonts are known from about 245 million years ago in the lower Anisian of the Triassic, and the group diversified in the Anisian and Ladinian (Pinna, 1990; Pinna and Mazin, 1993). While the clade flourished during the Triassic, placodonts died out at the Triassic/Jurassic boundary around 201 million years ago.

A prominent feature of all placodonts and the characteristic for which the clade is named is the highly specialised crushing dentition, not only located on the usual marginal tooth-bearing elements, but also on the enlarged palatine bones (Mazin and Pinna, 1993; Rieppel, 2001b, a). Placodont skull morphologies range from robust skulls that carry anterior grasping teeth, to broad blunt-snouted forms, to skulls with elongate slender rostra, exemplifying the ecological variation within the group (Fig. 1.1: Mazin and Pinna, 1993; Rieppel and Zanon, 1997). However it is clear that the majority of taxa would have had a durophagous diet, with the exception of the highly derived *Henodus*, which may have been a filter feeder, sieving food with baleen-like structures (Rieppel, 2002b).

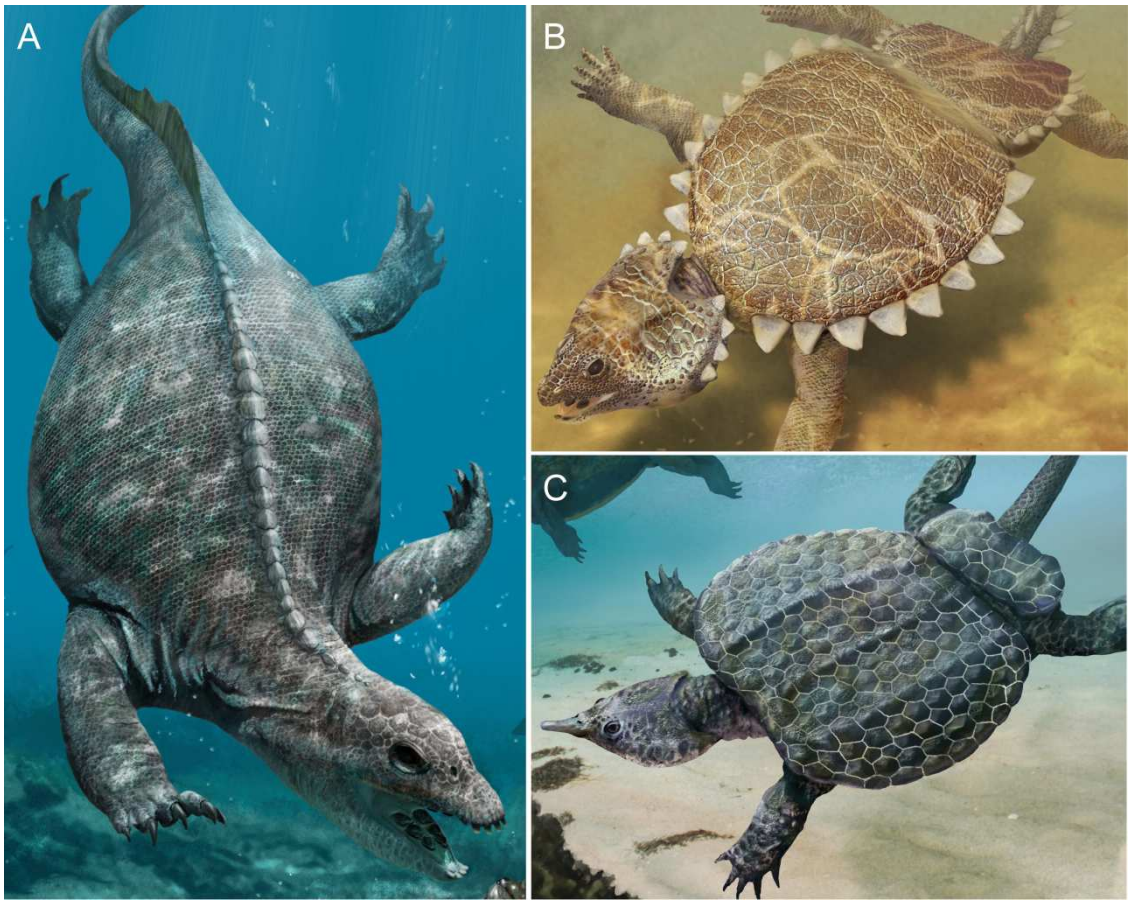

Figure 1.1. Examples of placodont morphotypes. **A**, The unarmoured basal 'placodontoid' *Placodus gigas*. **B**, The heavily armoured cyamodontoid *Cyamodus hildegardis*. **C**, The armoured cyamodontoid *Psephoderma alpinum*, with elongate edentulous rostrum. Reconstructions by Jaime Chirinos.

Placodontia is comprised of less armoured forms ('placodontoids'; Fig. 1.1A; 1.2) and the monophyletic, well armoured Cyamodontoidea (Fig. 1.1B, C; 1.2). Following the newest phylogenetic analyses (Rieppel, 2001a; Jiang et al., 2008; Klein and Scheyer, in press; Fig. 1.2), the 'placodontoids' are paraphyletic. The 'placodontoid' *Paraplacodus broilii*a lacks dermal armour, while *Pararcus diepenbroeki* and *Placodus gigas* do have it, the latter having a single row of dermal plates running over its vertebral column (e.g. Rieppel, 2000b; Drevermann, 1933; Klein and Scheyer, in press). The well armoured cyamodontoids, on the other hand, carry a turtle-like armour shell encasing their trunk (e.g. Rieppel, 2002b; Scheyer,

2010; Fig. 1.1B, C), although the histology of this armour differs from turtles in that it exhibits the unique morphology of postcranial fibrocartilaginous bone (Scheyer, 2007). The general body shape of the unarmoured taxa such as *Placodus* was squared or box-like (Fig. 1A), with the rather flat belly being strengthened by a well-developed gastral apparatus. The superficial similarity of the well armoured cyamodontoid placodonts and turtles, on the other hand, was first noted over a century ago (e.g., Jaekel, 1902) and taxon names, e.g., *Placochelys placodonta* and *Henodus chelyops*, were chosen in reference to this similarity. By looking more closely, though, placodont armour was found to be fundamentally different from that of turtles in that it lacks connection to the underlying endoskeleton (e.g., Gregory, 1946).

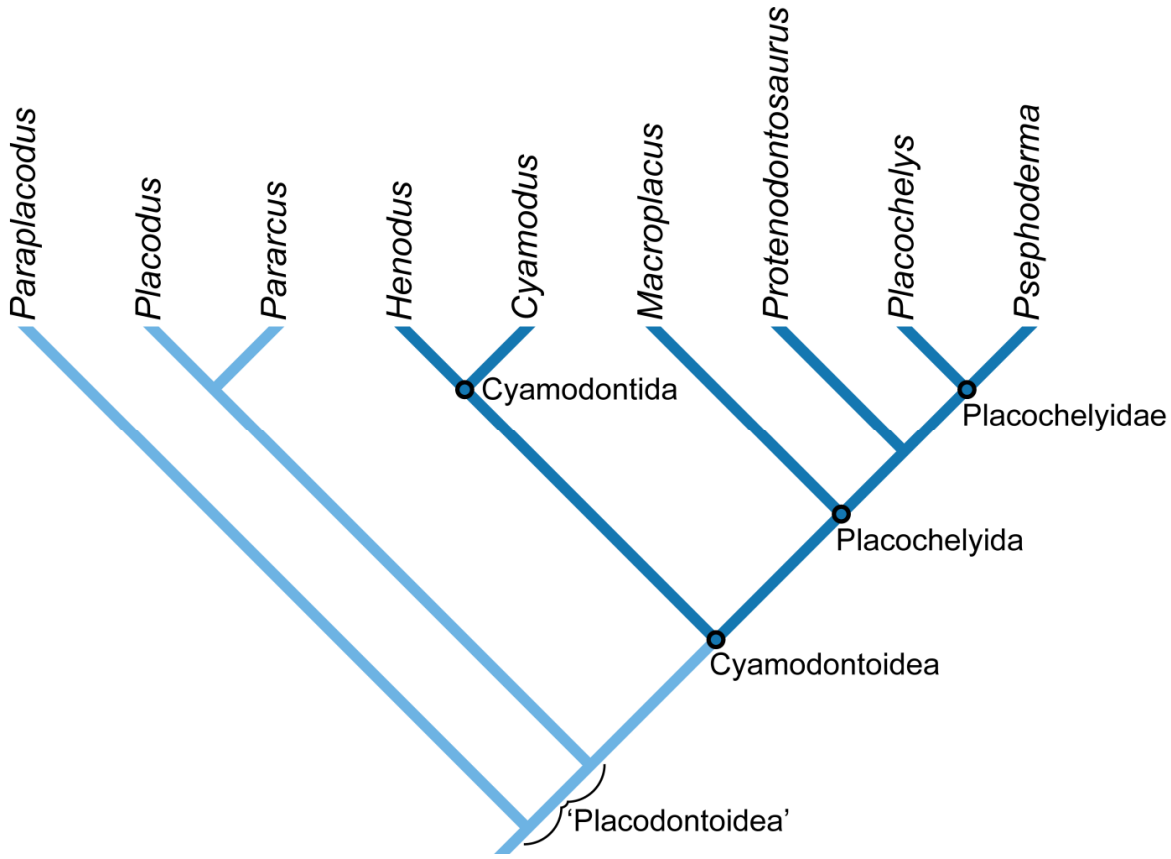

Figure 1.2. Ingroup relationships of placodont genera, modified from Rieppel (2001a), Jiang et al. (2008), and Klein and Scheyer (in press). Note that, with the exception of *Placodus*, only European taxa are included as no phylogenetic studies have yet been conducted on Chinese taxa.

Until recently, placodonts were thought to be restricted to the western margin of the ancient Tethys Ocean, which corresponds to modern-day Europe and Middle East (Brotzen, 1956; Haas, 1969; Pinna, 1990; Rieppel and Hagdorn, 1997; Rieppel, 2002a). However, in the last fourteen years, four valid placodont species have been described from the eastern Tethys, i.e., southern China: *Sinocyamodus xinpuensis* (Li, 2000); *Psephochelys polyosteoderma* (Li and Rieppel, 2002); *Placodus inexpectatus* (Jiang et al., 2008); and *Glyphoderma kangi* (Zhao et al., 2008). A palaeobiogeographic model of the evolution and dispersal of Sauropterygia, including few placodont genera (i.e., *Cyamodus*, *Placodus*) was presented by Rieppel and Hagdorn (1997; see also Rieppel, 2001a) for the Germanic and Alpine Triassic. However, this scenario has to be modified to include these new findings from China.

1.2 STUDY AIMS

Since the first placodonts were described in the 1830's (*Placodus gigas* Agassiz, 1833; *Cyamodus rostratus* Munster, 1839), relatively few analyses have been conducted on the clade that did not focus on simple description of primary anatomy. Vogt (1983) and Rieppel (2001a; 2002a) are exceptions, as they examined tooth implantation and replacement in placodonts and other sauropterygians, as well as the feeding biomechanics of some members of the group. However it is still not clear how placodonts replaced their teeth while maintaining feeding ability, or how their extremely specialised and characteristic dentition evolved. While placodont palaeoecology has been studied (e.g., Mazin and Pinna, 1993), many questions remain regarding their diets and lifestyles, especially with regard to recent claims that they may have been herbivorous rather than durphagous. In addition, while phylogenetic analyses have been carried out on placodonts (e.g., Rieppel, 2000b,

2001a: Jiang et al. 2008), no comprehensive analysis has yet been conducted that incorporates all placodont taxa from both the western and eastern Tethyan realms.

The aims of this study were to clarify the evolutionary and palaeogeographic origins of Placodontia, as well as shedding light on aspects of their palaeoecology and elucidating their phylogenetic relationships. This was mostly done with data obtained from micro-computed tomographic (µCT) scanning on placodont crania from throughout Europe and southern China. µCT scanning has the unique ability to reveal and identify internal as well as external structures that would otherwise have remained obscured to the naked eye (see Abel et al. 2012, for a description of µCT scanning and reconstructing fossil material). This is of great value when attempting to identify morphological characters for phylogenetic analyses, or to reveal structures that would otherwise require the destruction of the specimen to expose, such as the inner ears or replacement teeth.

In Chapter 2, a detailed literature review on placodont palaeoecology is presented as a response to recent publications that argue that placodonts, namely *Placodus* and *Cyamodus*, were herbivorous macroalgae feeders rather than durophagous (e.g., Diedrich 2010, 2011a, b). In response to this claim, an international collaboration of colleagues, including myself, use detailed osteological, biomechanical and taphonomic evidence to show that most placodonts were much more likely to be durophagous than herbivorous. Placodont skulls were over-engineered for herbivory, and would have had an incredibly powerful crushing bite. They were also unable to grind food, an important feature of most herbivores. Moreover, there is no evidence of macroalgae in the same fossil-bearing localities as where placodonts are found.

Chapter 3 is a redescription of the braincase of the ‘basal’, unarmoured placodont, *Placodus gigas*, using µCT data of two exceptionally preserved skulls

from the German Muschelkalk (~243–235 mya, Menning et al. 2011). In addition to a clarification of the braincase anatomy, the morphology of the sphenoid region is described, as well as a reinterpretation of the enigmatic ‘alisphenoid bridge’ as a dorsally expanded dorsum sellae. The first virtual cranial endocast of *Placodus* is presented, as is the first reconstruction of a sauropterygian inner ear. The vertical semicircular canals are dorsoventrally compressed, similar to those of modern marine reptiles. The position of the horizontal canal also indicates that the head of the animal was most ‘alert’ at an incline of about 20º, an ideal position for feeding on the sea floor, thus indicating that even ‘basal’ placodonts were well adapted to life in aquatic environments.

Chapter 4 is concerned with both the palaeogeographic origins of the Placodontia and the evolutionary origins of their highly specialised crushing dentition. A new taxon from the early Anisian (early Middle Triassic) of Winterswijk in the Netherlands is described with the aid of µCT data. The skull of the juvenile sauropterygian exhibits an array of external osteological similarities with the basal-most placodont *Paraplacodus*. However, with the addition of µCT data, a palatine with a single row of teeth can be identified, much like the condition found in placodonts. However these teeth are small and pointed rather than the enlarged crushing teeth of a durophagous animal. Phylogenetic analyses reveal that the new taxon, *Palatodonta bleekeri*, is sister taxon to the placodonts and indicates that the presence of palatine teeth did not initially evolve for a durophagous diet. It also indicates that the placodonts initially appeared in the western Tethys before dispersing to the eastern Tethyan realm.

Chapter 5 continues the theme of placodont teeth, but with a focus on replacement patterns and the dental morphology/formulae of Chinese taxa. The exceptionally enlarged teeth in placodonts cooperated to form functional crushing

areas that could efficiently process hard-shelled prey (Mazin and Pinna, 1993). However this presents a problem for tooth replacement, as if any teeth from a functional unit are lost, then this may prevent the animal from feeding. µCT data for 11 placodont specimens that span all placodont morphotypes were used to investigate replacement patterns. Results show that the plesiomorphic *Placodus* species exhibited seemingly random patterns of tooth replacement, with replacement teeth at several stages of growth throughout the skull. However the more derived, armoured placodonts show highly modular, unilateral replacement that often occurs in functional units. Thus, at least one functional unit is always preserved to allow feeding. Importantly, there was always one replacement tooth growing at the posterior-most palatine teeth, indicating increased wear here and the most efficient site of crushing.

Chapter 6 combines µCT datasets and detailed specimen study to present the first cranial reconstructions for all Chinese placodont holotype skulls, as well as incorporating them into the first comprehensive phylogenetic analyses with European taxa. Two phylogenetic matrices are used: a general diapsid dataset based on the matrix from Chapter 4, and a placodont-only cranial dataset mostly based on Rieppel (2001b), but with additional characters from Rieppel (2000b) and Jiang et al. (2008). While results vary between analyses, both support a monophyletic Placodontia and have Chinese taxa interspersed with European ones. This indicates that there was no major barrier between placodont populations in the eastern and western Tethys. A European origin for both ‘placodonoid’ and cyamodontoid placodonts is suggested, with the highly-nested Placochelyidae originating in the Middle Triassic of the eastern Tethys. We propose that all placodont clades originated in a period of intense speciation during the Middle Triassic.

1.3 THESIS OUTLINE

This is a cumulative thesis and all chapters subsequent to this one are presented either as fully-formatted articles as published in their respective journals (Chapters 2–5), or in manuscript form (Chapter 6). Co-author affiliations can be found at the beginning of each chapter, and any supplementary material can be found at the end of each chapter. All art in this thesis has been used with the artists' permission. Authors, publication details and author contributions are outlined for each chapter below.

Chapter 2

Authors: Scheyer T.M., Neenan J.M., Renesto S., Saller F., Hagdorn H., Furrer H., Rieppel O., Tintori A

Publication: 2012, *Historical Biology*, 24(3): 257-267.

Author Contributions: TMS and JMN wrote the majority of the manuscript. SR, FS, HH, HF, OR and AT all contributed data and discussion points.

Chapter 3

Authors: Neenan J.M., Scheyer T.M.

Publication: 2012, *Journal of Vertebrate Paleontology* 32(6): 1350-1357.

Author Contributions: TMS and JMN designed the project. JMN carried out model segmentation, analysed the data and wrote the manuscript. TMS supervised the project.

Chapter 4

Authors: Neenan J.M., Klein N., Scheyer T.M.

Publication: 2013, *Nature Communications* 4:1621.

Author Contributions: “J.M.N. and T.M.S. wrote the manuscript and prepared the figures. N.K. and J.M.N. conducted the morphological description of outwardly visible structures. N.K. carried out the CT scanning. T.M.S. and J.M.N. performed the phylogenetic analysis. J.M.N. created the three-dimensional reconstruction and conducted the morphological description of the concealed elements.”

Chapter 5

Authors: Neenan J.M., Li C., Rieppel O., Bernardini F., Tuniz C., Muscio G., Scheyer T.M.

Publication: 2014, *Journal of Anatomy* 224(5): 603-613.

Author Contributions: “TMS and JMN designed the research. JMN carried out the segmentation, analysis and wrote the manuscript. OR and CL provided expert knowledge and insight. CL enabled and supported scanning of the Chinese material at the IVPP. GM made the specimen of Protenodontosaurs available for scanning and transported it to Trieste, where FB and CT carried out the scan.”

Chapter 6

Authors: Neenan J.M., Li C., Jiang D-Y., Rieppel O., Scheyer T.M.

Publication: To be submitted to the Zoological Journal of the Linnean Society.

Author Contributions: “TMS and JMN designed the research and examined specimens in China together. JMN carried out model segmentation, osteological descriptions, skull reconstructions, phylogenetic analyses and wrote the manuscript. TMS, CL, D-YJ and OR provided expert knowledge and advice. CL and DY-J provided permission and access for the examination of specimens, and CL facilitated the CT scanning process at the IVPP. TMS supervised the project.”

1.4 REFERENCES

Abel, R. L., C. R. Laurini, and M. Richter. 2012. A palaeobiologist's guide to 'virtual' micro-CT preparation. *Palaeontologia Electronica* 15:6T.

Agassiz, L. 1833-43. *Recherches sur les Poissons Fossiles, Vol. I-V*. Imprimaire de Petitpierre, Neuchâtel, 336 pp.

Benson, R. B. J., R. J. Butler, J. Lindgren, and A. S. Smith. 2010. Mesozoic marine tetrapod diversity: mass extinctions and temporal heterogeneity in geological megabiases affecting vertebrates. *Proceedings of the Royal Society of London, B* 277:829-834.

Brotzen, F. 1956. Stratigraphical studies on the Triassic vertebrate fossils from Wadi Raman, Israel. *Arkiv for Mineralogi och Geologi* 2:191-217.

Cheng, Y.-n., X.-c. Wu, and Q. Ji. 2004. Triassic marine reptiles gave birth to live young. *Nature* 432:383-386.

Diedrich, C. G. 2010. Palaeoecology of *Placodus gigas* (Reptilia) and other placodontids — Middle Triassic macroalgae feeders in the Germanic Basin of central Europe — and evidence for convergent evolution with Sirenia. *Palaeogeography, Palaeoclimatology, Palaeoecology* 285:287-306.

Diedrich, C. G. 2011a. The shallow marine placodont *Cyamodus* of the central European Germanic Basin: its evolution, paleobiogeography and paleoecology. *Historical Biology* 23:391-409.

Diedrich, C. G. 2011b. Fossil middle triassic "sea cows" – placodont reptiles as macroalgae feeders along the north-western tethys coastline with pangaea and in the germanic basin. *Natural Science* 3:9-27.

Drevermann, F. 1933. Die Placodontier. 3. Das Skelett von *Placodus gigas* Agassiz im Senckenberg-Museum. Abhandlungen der Senckenbergischen *Naturforschenden Gesellschaft* 38:319-364.

Gregory, W. K. 1946. Pareiasaurs versus placodonts as near ancestors to the turtles. *Bulletin of the American Museum of Natural History* 86:275-326.

Haas, G. 1969. The armour of placodonts from the Muschelkalk of Wadi Ramon (Israel). *Israel Journal of Zoology* 18:135-147.

Jaekel, O. 1902. Wirbelthierreste aus der Trias des Bakonyerwaldes. *Resultate der Wissenschaftlichen Erforschung des Balatonsees, 1. Band. 1. Teil. Paläontologischer Anhang III. Band* 1-22.

Jiang, D.-Y., R. Motani, W.-C. Hao, O. Rieppel, Y.-L. Sun, L. Schmitz, and Z.-Y. Sun. 2008. First record of Placodontoidea (Reptilia, Sauropterygia, Placodontia) from the Eastern Tethys. *Journal of Vertebrate Paleontology* 28:904-908.

Klein, N., and T. M. Scheyer. In press. A new placodont sauropterygian from the Middle Triassic of the Netherlands. *Acta Palaeontologica Polonica*. (doi:10.4202/app.2012.0147).

Li, C. 2000. Placodont (Reptilia: Placodontia) from Upper Triassic of Guizhou, Southwest China. *Vertebrata PalAsiatica* 38:314-317.

Li, C., and O. Rieppel. 2002. A new cyamodontoid placodont from Triassic of Guizhou, China. *Chinese Science Bulletin* 47:156-159.

Mazin, J.-M., and G. Pinna. 1993. Palaeoecology of the armoured placodonts. *Paleontologia Lombarda N. S.* 2:83-91.

Menning, M., B. Schröder, E. Plein, T. Simon, J. Lepper, H.-G. Röhling, C. Heunisch, K. Stapf, H. Lützner, K.-C. Käding, J. Paul, M. Horn, H. Hagdorn, G. Beutler, and E. Nitsch. 2011. Beschlüsse der Deutschen Stratigraphischen Kommission 1991–2010 zu Perm und Trias von Mitteleuropa. *Zeitschrift der Deutschen Gesellschaft für Geowissenschaften* 162:1-18.

Meyer, H. v. 1863. Die Placodonten, eine Familie von Sauriern der Trias. *Palaeontographica* 11:175-221.

Motani, R. 2009. The evolution of marine reptiles. *Evolution: Education and Outreach* 2:224-235.

Motani, R. 2010. Warm-blooded "sea dragons"? *Science* 328:1361-1362.

Münster, G. 1839. *Beiträge zur Petrefaktenkunde, mit XVIII nach der Natur gezeichneten Tafeln der Herren Hermann v. Meyer und Professor Rudolph Wagner*. Buchner'sche Buchhandlung, Bayreuth.

O'Keefe, F. R., and L. M. Chiappe. 2011. Viviparity and k-selected life history in a Mesozoic marine plesiosaur (Reptilia, Sauropterygia). *Science* 333:870-873.

Peyer, B., and E. Kuhn-Schnyder. 1955. Placodontia; pp. 459-486 in J. Piveateau (ed.), *Traité de Paléontologie*. Masson et Cie, Paris.

Pinna, G. 1990. Notes on stratigraphy and geographical distribution of placodonts. *Atti della Società Italiana di Scienze Naturali e del Museo Civico di Storia Naturale di Milano* 131:145-156.

Pinna, G., and J.-M. Mazin. 1993. Stratigraphy and paleobiogeography of the Placodontia. *Paleontologia Lombarda N. S.* 2:125-130.

Rieppel, O. 2000a. Sauropterygia I - Placodontia, Pachypleurosauria, Nothosauroidea, Pistosauroidea; pp. 134 in P. Wellnhofer (ed.), *Encyclopedia of Paleoherpetology*. Verlag Dr. Friedrich Pfeil, Munich.

Rieppel, O. 2000b. *Paraplacodus* and the phylogeny of the Placodontia (Reptilia: Sauropterygia). *Zoological Journal of the Linnean Society* 130:635-659.

Rieppel, O. 2001a. Tooth implantation and replacement in Sauropterygia. *Paläontologische Zeitschrift* 75:207-217.

Rieppel, O. 2001b. The cranial anatomy of *Placochelys placodonta* Jaekel, 1902, and a review of the Cyamodontoidea (Reptilia, Placodonta). *Fieldiana: Geology, New Series* 45:1-104.

Rieppel, O. 2002a. The dermal armor of the cyamodontoid placodonts (Reptilia, Sauropterygia): morphology and systematic value. *Fieldiana: Geology, New Series* 46:1-41.

Rieppel, O. 2002b. Feeding mechanics in Triassic stem-group sauropterygians: the anatomy of a successful invasion of Mesozoic seas. *Zoological Journal of the Linnean Society* 135:33-63.

Rieppel, O., and R. T. Zanon. 1997. The interrelationships of Placodontia. *Historical Biology* 12:211-227.

Rieppel, O., and H. Hagdorn. 1997. Paleobiogeography of Middle Triassic Sauropterygia in central and western Europe; pp. 121-144 in J. M. Callaway and E. L. Nicholls (eds.), *Ancient Marine Reptiles*. Academic Press, San Diego, California.

Scheyer, T. M. 2007. Skeletal histology of the dermal armor of Placodontia: the occurrence of 'postcranial fibro-cartilaginous bone' and its developmental implications. *Journal of Anatomy* 211:737-753.

Scheyer, T. M. 2010. New interpretation of the postcranial skeleton and overall body shape of the placodont *Cyamodus hildegardis* Peyer, 1931 (Reptilia, Sauropterygia). *Palaeontologia Electronica* 13:1-15.

Vogt, C. 1983. Evolutive Palökologie der Placodontier (*Placodus*, *Henodus*; Euryapsida, Trias). Geowissenschaftliche Fakultät, Eberhard-Karls-Universität, Tübingen, 99 pp.

Zhao, L.-J., C. Li, J. Liu, and T. He. 2008. A new armored placodont from the Middle Triassic of Yunnan Province, southwestern China. *Vertebrata PalAsiatica* 46:171-177.

CHAPTER 2

REVISED PALEOECOLOGY OF PLACODONTS – WITH A COMMENT ON 'THE SHALLOW MARINE PLACODONT *CYAMODUS* OF THE CENTRAL EUROPEAN GERMANIC BASIN: ITS EVOLUTION, PALEOBIOGEOGRAPHY AND PALEOECOLOGY' BY C.G. DIEDRICH

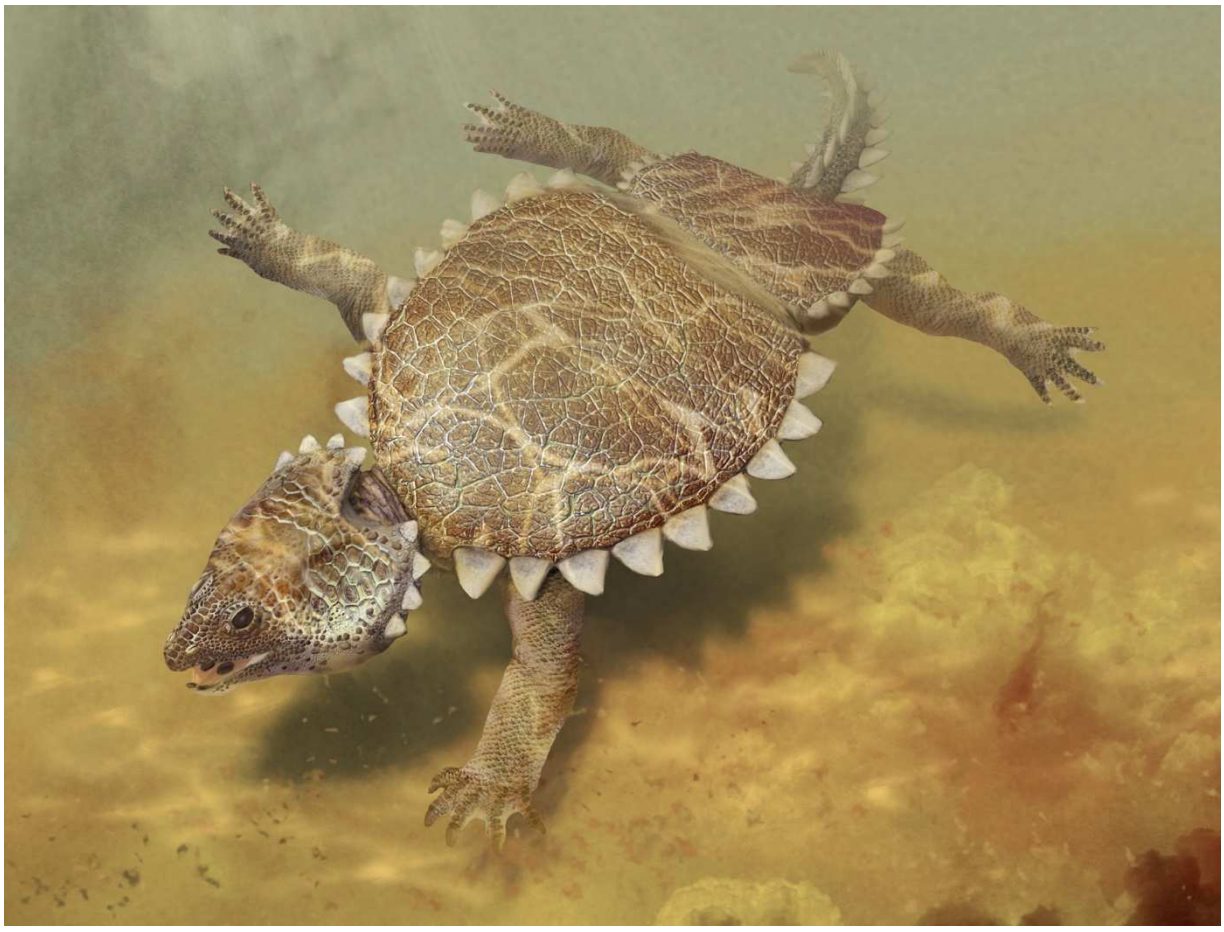

Cyamodus hildegardis by Jaime Chirinos

Historical Biology
Vol. 24, No. 3, June 2012, 257–267

Revised paleoecology of placodonts – with a comment on 'The shallow marine placodont *Cyamodus* of the central European Germanic Basin: its evolution, paleobiogeography and paleoecology' by C.G. Diedrich (Historical Biology, iFirst article, 2011, 1–19, doi: 10.1080/08912963.2011.575938)

Torsten M. Scheyer[a]*, James M. Neenan[a], Silvio Renesto[b], Franco Saller[c], Hans Hagdorn[d], Heinz Furrer[a], Olivier Rieppel[e] and Andrea Tintori[f]

[a]*Paläontologisches Institut und Museum der Universität Zürich, Karl Schmid-Strasse 4, 8006 Zürich, Switzerland;* [b]*Dipartimento di Biologia Strutturale e Funzionale, Università degli Studi dell'Insubria, via Dunant 3, I-21100 Varese, Italy;* [c]*Weingarterstrasse 3, Gargazzone, Bozen, Italy;* [d]*Muschelkalkmuseum Hagdorn Ingelfingen, Schlossstraße 11, 74653 Ingelfingen, Germany;* [e]*The Field Museum, Department of Geology, 1400 S. Lake Shore Drive, Chicago, IL 60605-2496, USA;* [f]*Dipartimento di Scienze della Terra 'A. Desio', Università degli Studi di Milano, Mangiagalli 34 – 20133 Milano, Italy*

(*Received 6 July 2011; final version received 3 September 2011*)

A recent article published by Diedrich (2011a, Hist Biol. iFirst online, 1–19, doi: 10.1080/08912963.2011.575938) aspired to provide a complete revision of the known material of the placodont genus *Cyamodus* Meyer, 1863 from the Germanic Basin of central Europe. It is the latest in a series of similar articles by the same author (see Diedrich 2010, Palaeogeogr Palaeoclimatol Palaeoecol. 285(3–4):287–306; 2011b, Nat Sci. 3(1):9–27 for overview) focussing on the European members of the Placodontia (Reptilia: Sauropterygia), a diverse group of enigmatic marine reptiles known from Triassic shallow marine deposits. In a similar fashion to some previous works by Diedrich (see Tintori 2011, Palaeogeogr Palaeoclimatol Palaeoecol. 300(1–4):205–207 for similar points of criticism), this newest article demonstrates a narrow scope of presenting and discussing data, including omitted articles relevant to the topic, and over-interpretation of results, all with the aim of embedding the idea of placodonts being herbivorous Triassic 'sea cows' feeding on macroalgae (Diedrich 2010, 2011b). The present contribution is intended to clarify mistakes and misinterpretations made by Diedrich (2011a), to incorporate vital citations previously omitted which allow alternative interpretations, and to put the paper into perspective by including a more general evolutionary and paleoecological overview of the remaining placodonts.

Keywords: Triassic; Placodontia; Cyamodontoidea; sea cows; durophagous; *Cyamodus hildegardis*

Introduction

Placodontia (Reptilia: Sauropterygia), currently recognised as sister group to the remaining eosauropterygians including groups such as pachypleurosaurs, nothosaurs, pistosaurs and plesiosaurs, are known to occur in both the western and eastern Tethys [e.g. Hagdorn and Rieppel 1999; Li 2000; Rieppel 2000; Li and Rieppel 2002; Jiang et al. 2008 (not Yiang et al. 2008 in Diedrich 2011a, p. 4); Zhao et al. 2008]. *Cyamodus* is the name-giving genus of the monophyletic group of heavily armoured placodonts, the Cyamodontoidea (Rieppel 2001a).

In the introduction, Diedrich (2011a) provides a historical overview of the collection and description of fossil placodont material from the Germanic Basin with a special emphasis on the material attributable to the genus *Cyamodus*. Although there is no doubt that the author identified or discovered many specimens (especially isolated tooth material) either in the field or in historical fossil collections mainly in Germany, it is the interpretations (often based on scanty material) presented as fact and not tested against all available data which are the most problematic. The new data from facies analyses and stratigraphic sections from Bindlach, Laineck and Hegnabrunn on the one hand and Bissendorf and Lamerden on the other are regarded as the only evidence for the presence of the three species *Cyamodus rostratus, Cyamodus muensteri* and *Cyamodus kuhnschnyderi* occurring in the Germanic Basin, forming a monophyletic grade that reflects a trend of tooth reduction as an adaptation to macroalgae feeding (Diedrich 2011a, p. 1, 4). Unfortunately, the main reference provided by the author to support this is another publication by Diedrich (2011a, p. 1, 4, 5, 12, 17; Diedrich 2011) cited as being 'in review' – a condition which should generally be avoided, because the data and interpretations therein are not available for study and comparison. In addition, previous cladistic approaches (e.g. Rieppel 2000, 2001a; Jiang et al. 2008), as well as functional interpretations relying on the osteological and myological study of skulls and the function of the dentition [e.g. Vogt 1983; Massare 1987, 1997; Westphal 1988; Mazin 1989; Mazin and Pinna 1993; Renesto and Tintori 1995;

*Corresponding author. Email: tscheyer@pim.uzh.ch

ISSN 0891-2963 print/ISSN 1029-2381 online

http://dx.doi.org/10.1080/08912963.2011.621083
http://www.tandfonline.com

Rieppel 2002a (note that with the exception of Westphal 1988, none of these works was mentioned or discussed in Diedrich 2010, 2011a, b)] are dismissed *a priori* as leading to biased results. Diedrich's rejection of these methods is based on the supposed exclusion of stratigraphic and ontogenetic age data of the fossils (Diedrich 2011a, p. 12). This rejection was substantiated by a dubious point of criticism of Rieppel's (2001a) analysis on the same page, in which Rieppel supposedly mentioned erroneously that *C. rostratus* was younger than *C. muensteri*. A review of the systematic paleontology section in Rieppel (2001a, p. 76–77), however, revealed that *C. rostratus* and *C. muensteri* were regarded as contemporaneous species, with the holotypes both occurring in the Trochitenkalk Formation and the lower part of the Meissner Formation (*atavus* through *postspinosus* biozone), Upper Muschelkalk (mo1), latest Illyrian, late Anisian, Middle Triassic. Although the stratocladistic approach (e.g. Fisher 2008) was mentioned as an improvement to traditional cladistic studies, such an analysis was, unfortunately, not performed either.

Rieppel and Reisz (1999) and Scheyer (2008) are cited to indicate the value of "Middle Triassic sauropterygian placodonts [...] for developing new ideas to the evolutionary history of their relatives, the turtles [...]" (Diedrich 2011a, p. 4). While the former study is based on an 'osteology-based cladistic analysis' (other cladistic analyses like this were rejected elsewhere in the article by Diedrich), the latter based its discussion and conclusions on the differences in histology and microanatomy in the convergently developed dermal armour of both groups without implying closer relationships between turtles and sauropterygians at all. Furthermore, 'modern analyses' are mentioned which supposedly "place all these placodonts not as their ancestors by using morphological cladistic analyses based on the bone osteology" (Diedrich 2011a, p. 4), but unfortunately these analyses are not cited here or elsewhere in the text.

Diedrich (2011a, p. 4) states that the objective of his contribution is to give a complete review of all known postcranial and cranial specimens of *Cyamodus* from the Germanic Basin – however, a brief examination of the literature (e.g. Nosotti and Pinna 1996, p. 12, Figure 14(A,B)) immediately reveals this statement to be erroneous, and that not all material has been incorporated, including previously described and published specimens. This then begs the question: why have some specimens [e.g. the postcranial armour fragment Staatliches Museum für Naturkunde Stuttgart (SMNS) 81600] from this paper and other fragmentary material (i.e. isolated osteoderms) been taken into account, while others (postcranial armour fragments SMNS 16725 and SMNS 15891c) were left out? Moreover, most of the specimens and interpretative drawings figured elsewhere in Diedrich (2011a, Figures 3–8) have already been figured in previous papers by the author (e.g. Diedrich 2010, 2011b), so one wonders what is actually novel to the present paper?

Because stratigraphy and geologic setting are so emphasised in Diedrich (2011a), several related points, especially in the 'Material and methods' (p. 4, 5), 'Geology and paleoenvironment' (p. 5) and part of the 'Systematic paleontology' sections (p. 5, 6), should be clarified:

(a) Bad Sulza, located about 20 km north of Jena in Thuringia, Germany, had a rather central instead of a marginal position in the Muschelkalk Sea; however, the basal metres of the Upper Muschelkalk, which yielded the marine reptiles in the first half of the twentieth century, are developed in a shallow water facies, indicative of a regional shoal (e.g. Hagdorn and Rieppel 1999; Seidel 2003). Diedrich (2011a, p. 5) stated that remnants of sediment were used to reconstruct the stratigraphic context of several specimens in historic collections. We would like to point out that, in general, it is not possible to conclude the exact stratigraphic origin of a specimen based on un-removed matrix, although it might occasionally be possible, if one is very familiar with a certain quarry and its stratigraphy.

(b) In several cases, Diedrich (2011a, p. 5, 17: Figure 12; see also Diedrich 2010, p. 296, 302: Figure 16) refers to and shows modified versions of Hagdorn's (2004) reconstructions of invertebrate paleocommunities, in which gastropods are drawn as browsers on indeterminate plants that are interpreted as macroalgae by Diedrich (2010, 2011a, b). However, there is no evidence for this in the fossil record and it was made clear that the paleocommunity sketches in Hagdorn (2004) were hypothetical reconstructions. The presence of plants in these reconstructions was only a possible explanation of the abundance of small browsers which could have just as easily been interpreted as epibenthic or even endobenthic faunal constituents. Furthermore, the macroalgae meadows, if present, were not 'extensive' (p. 5), and they were not hypothesised for the 'Schaumkalk Beds' (i.e. oolithic shallow water areas), but for the Wellenkalk and the Tonplatten facies (see Hagdorn 2004, p. 40: Figure 98, p. 41: Figure 103).

(c) The argumentation that *Cyamodus* disappeared during the evaporitic Middle Muschelkalk interval because there were no macroalgae meadows is not convincing, because all other large predators disappeared from the Muschelkalk Sea during this time interval (e.g. Hagdorn and Rieppel 1999, p. 671: Figure 4).

(d) There is no evidence for a relation of *Cyamodus* remains to terebratulid coquinas or to glauconitic sediments, nor are specimens usually found in bonebeds *sensu lato* (Hagdorn, pers. obs.). These

bonebeds are not just layers in which bones and teeth are found, but more or less thin condensation horizons deposited over a long period of time, yielding isolated, abraded and prefossilised vertebrate material, which are, therefore, not usable in paleoecological reconstructions (Hagdorn and Reif 1988).

(e) As noted by Gürich (1884, p. 136), *Cyamodus tarnowitzensis* was discovered in Böhm's Quarry near Tarnowitz (Silesia, now Poland), a famous locality that yielded many exceptionally well-preserved invertebrate fossils. The name of the town is now Tarnowskie Góry (Stare Tarnowice refers to 'old Tarnowitz' west of Tarnowskie Góry). Whether or not 'Tarnowice', stated by Diedrich (p. 6) as the type locality of *C. tarnowitzensis*, points to a special locality close to Tarnowskie Góry, cannot be elucidated herein.

(f) As for the type stratum of *C. tarnowitzensis*, Diedrich (2011a, p. 6) mentions a 'Terebratula Member, Karchowice Formation, middle Lower Muschelkalk (middle Pelsonian, *antecedens/balatonicus* Zone, middle Anisian, Middle Triassic)'. However, there is no formally described 'Terebratula Member' within the Karchowice Formation (= Karchowice Beds, e.g. Bodzioch 1997; Feist-Burkhardt et al. 2008, and references therein), nor does a formal '*antecedens/balatonicus* Zone' exists in this Member to our knowledge. On the other hand, the Terebratula Beds, now known as the Dziewkowice Formation, are underlying the Karchowice Formation (e.g. Kaim 1997; Niedźwiedzki 2000, 2002). However, a '*balatonicus* zone' (including a *binodosus*-, *balatonicus*- and *cuccense*-subzone) is instead found for the Pelsonian in the Triassic sequence chronostratigraphy/biochronostratigraphy chart (appendix, ammonoids column) of Hardenbol et al. (1998).

(g) In addition, lithostratigraphic and chronostratigraphic terminology are mixed up by Diedrich (2011a, p. 6) when writing 'Pelsonian Schaumkalk substage'. The Schaumkalkbank Subformation (uppermost Lower Muschelkalk) is younger, i.e. earliest Illyrian, in age. Moreover, the Schaumkalk is identified as the equivalent of the 'Saurierkalk, uppermost Lower Muschelkalk'. However, the Saurierkalk belongs to the basal Middle Muschelkalk Karlstadt Formation (*cf.* Hagdorn and Rieppel 1999).

(h) A Bad Sulza Formation of Illyrian age (p. 6, 18), an Osnabrück Formation (Illyrian/Fassanian boundary, p. 12, Figure 9), a Hegnabrunn Formation of Fassanian age (p. 12, Figure 9) or a Bindlach Formation of Illyrian (e.g. p. 7, Figure 4; p. 10, Figure 7) or Illyrian/Fassanian age (e.g. p. 8, Figure 5; p. 9, Figure 6) do not exist formally, as is expressed, for example, by the latest recommendations of the German Stratigraphic Commission (Subkommission Perm-Trias (SKPT)) on the Permian and Triassic of Central Europe (Menning et al. 2011).

Apart from these more general remarks, there are several more specific comments we wish to make concerning the data presented in the figures and the table.

In Table 1 (Diedrich 2011a, p. 15, 16), the skull No. 15855, holotype to *C. kuhnschnyderi* Nosotti and Pinna 1993, and the lower jaw No. 18380, paratype to *C. kuhnschnyderi*, are based in the collections of the SMNS not in the Senckenberg Naturhistorische Sammlungen Dresden (SNSD). The cast of the holotype skull of *C. tarnowitzensis* Gürich, 1884, is given with the No. Senckenberg Museum Frankfurt (SMF) R 5026 in Table 1, but as 'SBMF without No.' in the legend to Figure 3 (Diedrich 2011a, p. 3) and SBMF R 5026 in the 'Systematic Paleontology' section (Diedrich 2011a, p. 6; the abbreviation SBMF is not found explained in the text, so one has to assume that it is synonymous with SMF, p. 4).

The caption of the image and drawing of *C. muensteri* (Figure 6: 1a, b) in Diedrich (2011a, p. 9) is erroneous, because UMO BT 1007 cannot be the cast of the original to Meyer (1863). Meyer (1863, plate XXXI, Figures 1 and 2) figured the type specimen of *C. muensteri* (Agassiz, 1839) in Agassiz (1833–1843), which is entirely different from the cast that Diedrich referred it to. On the other hand, Meyer only described but did not figure the type of *Placodus* '*laticeps*' Owen, 1858 (= *C. muensteri*). The cast UMO BT1007 resembles the description of '*laticeps*' (compare also to Diedrich 2011a, Figure 5: 2b) in detail of the tooth formula including the presence of the little replacement tooth lingual to the second tooth on the right side of the skull; however, there are more teeth shown in the cast and also the posterior right half of the skull is present, a part which is lost in the holotype (BMNH R1644) of *C.* '*laticeps*' described by Owen (1858). The cast UMO BT 1007 might thus represent either an idealised reconstruction of the holotype BMNH R1644 (maybe done before it was sold in October 1857 to the British Museum as noted by Owen 1858, p. 170) or it might represent another skull altogether, which has since been lost. Moreover, the supposed cast UMO BT 1007 was already figured in Diedrich (2010, Figure 12: 2A–C, p. 299), with the author referring it to "*Cyamodus hildegardis* Peyer, 1931a,b [incidentally the species name is given incorrectly here; it should be "*C. hildegardis* Peyer, 1931", followed, for example, by "(Peyer 1931a)"] skull (cast) from Bindlach (Lainecker Höhenzug) near Bayreuth (Germany) from the Trochitenkalk/Meissner Fm (Illyrian/Fassanian, Anisian/Ladinian boundary)".

Similarly, the caption of the image and drawing of *C. hildegardis* (Figure 6: 2(a), (b) is erroneous, because the specimen shown is not part of the holotype of the "'*C. hildegardis* Peyer 1931' skeleton" accessioned under PIMUZ T 4763 (Diedrich 2011a, p. 9), but is a separate

skull associated with a dentary accessioned under PIMUZ T 4768 (see Pinna 1992). In addition, the tooth labelled as a 'replacement tooth' (lighter grey) in the interpretative drawing cannot be such, because the anterior edge of the enamel crown of this tooth is overlying the posterior margin of the tooth shown as the anteriorly situated 'functional tooth' (darker grey); an anatomical impossibility. It is thus more plausible to assume that the purported 'replacement tooth' is actually the old functional tooth in the process of being replaced and which was possibly displaced posteriorly during fossilisation. Re-studying the original specimen PIMUZ T 4768, the implied 'tooth eruption' of the anterior-most right premaxillary tooth could not be verified either.

The proposed illustrations of the biostratigraphy, paleobiogeography and facies relationships of the *Cyamodus* species of the Germanic Basin in Diedrich (2011a, p. 17, Figure 12) suffer from several inconsistencies and misinterpretations, some of which have been noted before by Tintori (2011):

(a) How can there be an alpine fold belt in the Middle Triassic (just north of the Monte San Giorgio point) in the 'paleobiogeographic maps' (Figure 12(A–D)), if the Alpine orogeny only started in the Cretaceous and continued mainly throughout the Cenozoic (e.g. Froitzheim et al. 2008)?
(b) Why is there a 'salt and gypsum evaporates' label, if it is not used in these maps?
(c) What exactly are 'Terrest red bed deposits'?
(d) What is the actual evidence for the 'sandy beach deposits' surrounding the hypothetical 'alpine fold belt'? (see Gaetani et al. 2000; see comment by Tintori 2011).
(e) Figure 12(C) shows the situation at the Illyrian/Fassanian boundary, that means the Anisian/Ladinian boundary.
(f) The Anisian/Ladinian boundary lies within the upper part of the Besano Fm. (Brack et al. 2005), so why is the Besano Fm. drawn in the middle of the Fassanian in Figure 12(E)?
(g) Cassina Fm. or Crocifisso Fm. are not formally used Formation names – as indicated, for example, by Sander (1989), Furrer (1995) or Furrer et al. (2008), the Besano Fm. (formerly Grenzbitumenzone) rests upon the San Salvatore Fm. (Salvatore dolomite) and is overlain by the San Giorgio Fm. (San Giorgio dolomite) and the Meride Fm. (lower and upper Meride limestones and Kalkschieferzone) – what is the basis for using these Formation names instead of commonly accepted ones? With this in mind, it is noteworthy that Monte San Giorgio should be considered as being in the 'western Tethys' not the 'northern Tethys', a mistake already mentioned in Tintori (2011). Furthermore, well-preserved reptiles at Monte San Giorgio have been found in five vertebrate beds of the Besano and Meride Formations, ranging from Late Anisian to latest Ladinian age (compare with Furrer 1995; see comment by Tintori 2011 and references therein), so the referral to 'Middle Triassic black shales from Monte San Giorgio' or 'black shales of the Monte San Giorgio' (Diedrich 2011a, p. 13, 18) is inadequate. Placodont reptiles were only found in the Besano Fm. Because fossiliferous layers crop out both on the Swiss and Italian sides of the border, references like 'Italian Monte San Giorgio site' or 'Monte San Giorgio (Switzerland)' (p. 6, 9) are not precise and should be avoided.
(h) Why are there different chronostratigraphic ages used in Figures 11 and 12(E), both based on Kozur and Bachmann (2008)? In Figure 11 the Illyrian/Fassanian boundary is dated as 241.2 Ma, whereas in Figure 12(E) the boundary is at 240 Ma. In addition, according to Kozur and Bachmann (2008, Figure 1), the base of the Anisian (Middle Triassic) is at 247 Ma, thus the Upper Buntsandstein, referred to as 'Bunter' in Figure 12(E), would be part of the Middle Triassic and not the Lower Triassic. Furthermore, the boundary between the Upper Buntsandstein and the Lower Muschelkalk would lie within the Bithynian and not at the Aegean/Bithynian boundary.
(i) How can *C. tarnowitzensis* be reconstructed with three maxillary and two premaxillary teeth (see Diedrich 2011a, p. 3, Figure 3(a)), when there are four maxillary teeth preserved on the right side of the holotype (interpretative sketch in Figure 3(b) showing six marginal teeth on the right and only five on the left side of the skull) and the premaxillary not being known at all (compare also with Nosotti and Pinna 1996)? For all we know, *C. tarnowitzensis* might have had a very pointed, elongated or even edentulous rostrum like *Psephoderma alpinum* or a very shortened rostrom with enlarged teeth similar to *C. kuhnschnyderi* – any interpretation would not be based on the fossil evidence and is thus highly speculative. As such, the reconstruction cannot be used at all to indicate a trend in tooth reduction/enlargement as is implied in Figure 12(E).
(j) Exactly the same facies models (including the misspelled gastropod '*Polygyrina*' as well as the falsely labelled gastropods '*Wortheniella*' and '*Omphalopty-cha*' in Figure 12(F)) shown in Figure 12(F–H) appear already in Diedrich (2010), in which Fürsich (1981) and Hagdorn (2004) were still cited for the paleocommunity compositions – however, in Diedrich (2011a) the only reference that is given for the same figures is the one paper of the author cited 'in review' (see comment above).

Taxonomic implications

Diedrich (2011a) brought forth several aspects of the cranial and postcranial anatomy of *C. hildegardis,* the species known from the Besano Fm. of the World Heritage Site Monte San Giorgio, as well as of the geological setting in which the findings were made, which indicate that the author has only a poor understanding of the actual fossils and their anatomy.

Synonymy of C. hildegardis and C. muensteri?

Diedrich (2011a, p. 6) considers *C. hildegardis* to be synonymous with *C. muensteri* based on similar dentition, but without discussing other cranial characters available. As such, the same skull (i.e. UMO BT 1007), for example, was referred either to *C. hildegardis* Peyer, 1931, in one paper (Diedrich 2010, p. 299, 305) or to *C. muensteri* (Agassiz, 1839) in Agassiz (1833–1843) in another (Diedrich 2011a, p. 9). However, variation found in the dentition in several specimens of different ontogenetic age of *C. hildegardis* (e.g. Kuhn-Schnyder 1959, 1974) is not taken into account. Such a synonymisation of species, in itself an important aspect of taxonomic research both in paleontology and biology, is regarded as extremely problematic when considering that diagnoses are based exclusively on tooth formulae/skull dentition without taking into consideration other cranial and postcranial characters (e.g. Rieppel 2000).

Reconstruction of* C. hildegardis *(= C. muensteri according to Diedrich 2011a)

Diedrich (2011a, p. 11, p. 13, Figure 10) proposed a new interpretative drawing of the postcranial endoskeleton and armour of *C. hildegardis* (= *C. muensteri*) based on Peyer's (1931) original description of the holotype of *C. hildegardis* (PIMUZ T 4763) and newer photographs, but without having ever seen and studied the actual fossils in person and without discussing their anatomical details (Diedrich 2011a, p. 13, Figure 10(B); see also mis-identification of the skull in Figure 6). Furthermore, the most recent comprehensive study and reconstruction of the armour and postcranium of *C. hildegardis* by Scheyer (2010) has been completely ignored. Diedrich (2011a, p. 10) noted the loss of 'dorsal spines' and 'wing-like elongated flattened lateral spines' of the vertebrae of *Cyamodus* being unique among placodonts. Assuming that the author refers to the neural spines and the transverse processes of vertebrae, respectively, we would like to point out that this condition is not unique because similar vertebrae are also present in *P. alpinum* (e.g. Pinna and Nosotti 1989; Renesto and Tintori 1995; see also Rieppel 2002b; Scheyer 2010). It is further not clear why *Placochelys* should have 'an even more strongly developed armour' (Diedrich 2011a, p. 10) than *Cyamodus*, the latter having possessed two separate armour shields covering the trunk and the pelvic region and a fully armoured tail (e.g. Pinna 1992; Scheyer 2010).

Several other skeletons of *C. hildegardis* are mentioned (specimens from an 'Italian Monte San Giorgio site' and 'Monte San Giorgio (Switzerland)') but no accession numbers are given, although these are available in the provided reference of Pinna (1992). Diedrich (2011a) further interpreted *Cyamodus* as having a single carapace shield covering the whole animal from the neck to the tip of the tail (p. 11), and which, because of its rigidity, 'precluded undulation in swimming' (p. 16). These interpretations are plainly wrong (compare with Scheyer 2010), because (a) there is no evidence for the carapace being extended over the neck region (in the holotype specimen, PIMUZ T 4763, the anterior part of the armour is dislocated; PIMUZ T 58, however, shows the nuchal region of the main carapace); (b) there are clearly two separate shields covering the trunk and the pelvic region, a similar condition is present also in *P. alpinum* (Pinna and Nosotti 1989; Renesto and Tintori 1995) and (c) the tail armour is separate from the pelvic shield and consists of four rows of dermal armour plates. In summary, there is no evidence which would preclude, at least to some degree, lateral undulation in swimming in *Cyamodus*. Given the overall well-armoured condition of the trunk and tail of the animal, we otherwise agree with the author that *Cyamodus* was probably a slow diver. In the life reconstruction of *Cyamodus*, Diedrich (2011a, p. 18, Figure 13) noted that the carapace was not visible in life because of the polygonal structure of the armour being covered by skin and also possibly being keratinous (although the reconstruction was done showing very prominent lateral spines), which is basically representing the normal condition found in reptile skin as presented in many vertebrate anatomy textbooks (e.g. Kardong 2009). There is no compelling data supporting this interpretation, however, and often the underlying osteoderm or ossicle arrangement can be directly inferred by the overlying skin or keratinous scute pattern, e.g. in crocodylian armour (e.g. Salisbury and Frey 2001). Rieppel (2002b) and Scheyer (2007) discussed epidermal scute patterns in several placodonts from Germany and Israel, based on scute sulci impressions onto the external surface of the bony armour. Neither Diedrich (2010) nor Diedrich (2011a) provides any further evidence to elucidate the possible function of the extensive armour in cyamodontoid placodonts, apart from what has been already discussed in Westphal (1976), Pinna and Nosotti (1989), Renesto and Tintori (1995), Rieppel (2002b), and Scheyer (2007), for example.

Placodonts as herbivorous macroalgae feeders?

In several papers (Diedrich 2010, 2011a, b; see also comment by Tintori 2011), the author presented his

concept of placodonts being herbivorous macroalgae feeders and analogues of modern sea cows; an interpretation not shared by other colleagues who have worked intensively on placodonts in the past (e.g. Mazin and Pinna 1993; Renesto and Tintori 1995; Tintori 1995; Nosotti and Pinna 1996; Rieppel 2002a). As pointed out by Tintori (2011), a trophic convergence cannot be completely ruled out for all species of placodonts if taking into account the spectrum of dentition and cranial morphologies within the group (e.g. Pinna and Mazin 1993). However, an osteological or functional anatomical convergence between the sauropterygian placodonts and the mammalian sea cows appears rather implausible and requires osteological evidence. In the following section, we summarise and discuss the various data which argue against the hypothesis of herbivorous placodonts as presented lately in several articles by Diedrich (2010, 2011a, b).

Both placodontoid and cyamodontoid placodonts have traditionally been regarded as durophagous aquatic reptiles (Rieppel 2002a and references therein), well adapted for feeding on hard shelled molluscs, with the exception of the problematic genus *Henodus* which shows a greatly reduced dentition and may have been adapted to some sort of scraping and/or suction feeding (Reif and Stein 1999; Rieppel 2002a). It is also noteworthy that the diversification of placodonts was roughly coeval with the development of durophagy in Osteichtyes (Tintori et al. 2006).

The postcranial skeleton of placodonts and sirenians shows functional convergences only by the fact that they share adaptations that increase body weight, thus allowing them to walk on the shallow seafloor with little effort: sirenians have pachyostotic ribs, whereas placodonts have a huge array of gastralia and, in cyamodontoids, also a single or bipartite carapace. The pachyostotic skull of *Placodus* may relate to bottom feeding as well (Rieppel 2000, p. 19). However, the sirenian-like structure of the postcranial skeleton of placodonts cannot be used as evidence of herbivory. The superficial resemblance of placodontoid placodonts [certainly not cyamodontoids – it appears that the author treats only *Cyamodus* out of this group, drawing it with a deep body, to further demonstrate the convergence of body shape of placodonts and sirenians, whereas most recent views, i.e. Pinna (1992) and Scheyer (2010), reconstruct *Cyamodus* with a much flatter 'turtle-like' appearance] with sirenians in terms of body shape only demonstrates that placodontoid placodonts were bottom walkers that needed a thick skeleton as ballast, allowing them to walk on the seafloor when feeding. However, it does not give any indication about the kind of food they ate, so any further discussion on this topic is not necessary. The same applies to cyamodontoid placodonts whose flat carapace rendered them superficially similar to some aquatic turtles such as snapping turtles (Chelydridae) or soft-shelled turtles (Trionychidae), which are also bottom dwellers (but are predators). In conclusion, the postcranial morphology of placodonts, while consistent with the hypothesis of bottom walking, does not give any particular support to the hypothesis of herbivory.

Another feature of the postcranial skeleton of placodonts speaks against herbivory, i.e. the robustness of the cervical vertebrae. These vertebrae are more indicative of durophagy than herbivory; indeed a stout neck and a robust cervical musculature may well be an adaptation for pulling molluscs off the substrate by tearing the byssus, rather than for grazing soft algae.

The placodont skull is typically a well ossified and akinetic structure, particularly so in *Placodus* (Rieppel 1995, 2002a). This genus exhibits a relatively high and narrow skull when compared with cyamodontoids, and is plesiomorphic relative to the latter in many respects, such as the structure of the braincase (Nosotti and Rieppel 2002). Rieppel (1995, 2002a) underlined a number of morphological correlates of durophagy (other than dentition) in the skull of *Placodus*, discussing the relationship between skull characters, jaw adductor musculature and jaw mechanics. He demonstrated that the robust and partly pachyostotic skull and the massive lower jaw are suitable to resist strong bending loads generated by the powerful jaw adductors during mastication. The combination of the deep and wide adductor fossa, the very high and stout coronoid process of the mandible, and the position of the posterior-most palatine and dentary tooth plates would have created a medial shift of the posterior-most bite point, and all contribute towards Rieppel's (2002a) reconstruction of the jaw adductor musculature in *Placodus* and interpretation of its jaw mechanics derived from the model by Druzinsky and Greaves (1979). The remarkably expanded upper temporal arch of *Placodus* may have restricted the extension of the superficial 1b-portion of the external adductor onto the lateral surface of the mandible. The posterodorsal orientation of muscle fibres inserted into the apex of the coronoid process (m. adductor mandibulae externus medialis) and the bodenaponeurosis (m. adductor mandibulae externus profundus) implies that the mechanical advantage of the medialis and profundus portions of the external adductor (forming the bulk of the jaw adductor musculature) would have increased with decreasing gape, reaching its maximum with the jaws near to closure (powerful crushing). By contrast, the mechanical advantage of the massive superficial pterygoideus muscle would have been greatest with the jaws wide open: because of this advantage *Placodus* could have opened the jaws to a wide extent necessary to position the prey item in between the posterior-most palatine and dentary tooth plates, thus increasing the overall efficiency of the crushing action. This way, the pterygoideus compensated the loss of

mechanical advantage of the medialis and profundus portions of the external adductor in this initial phase of crushing. Any alternative model of food processing in placodonts should give similarly precise and coherent data on musculature and osteology and also compare any interpretations with the conclusions made by Rieppel (2002a).

Besides the previously mentioned characters in osteology, dentition and myology mentioned herein and in Tintori (2011) which support shell-crushing, several other aspects argue against Diedrich's interpretation of placodonts as macroalgae feeders (it is definitely NOT a scientific 'theory' as was stated by Diedrich 2011a, p. 14):

(a) The author expresses that "the observed pattern of tooth amount reductions at all but enlargement of the surfaces of the left dentition would have never occurred in a "durophagous shell crushing animal"" (Diedrich 2011a, p. 13); however, such 'tooth reductions' as presented in Figures 11 and 12, can also be easily interpreted as feeding specialisations on specific hard-shelled prey items among the species of *Cyamodus*. Having fewer, larger and more robust teeth as seen in *C. kuhnschnyderi* might actually be very beneficial for crushing harder prey items, as stresses and stains might be more evenly distributed through the skull (compare with durophageous lizards, Dalrymple 1979; durophageous marine perciform fish, Grubich 2003; the cranial function of bone-crushing carnivorous mammals, Tseng and Binder 2010). As noted by Rieppel (2002a, p. 42), the enlargement of the posterior dentary and palatine tooth plates in cyamodontoids, when compared with *Placodus*, would also compensate for the more anterior position of the coronoid process relative to the posterior tooth plate, shifting the posterior-most bite point medially.

(b) There is no clear trend in tooth reduction in neither of the palatal teeth nor of the marginal teeth. Indeed, if all four species of *Cyamodus* from the Germanic Basin are taken into account – *C. tarnowitzensis* shows two palatinal teeth (pl), four maxillary (m) and ? premaxillary teeth (pm) summing up to at least six in total on each side of the skull; *C. rostratus* has three pl, two m and two pm (= seven in total/side); *C. muensteri* (based mainly on '*laticeps*') has two pl, three m and two pm (= seven in total/side), whereas *C. kuhnschnyderi* shows two pl, two m and one pm (= five in total/side). Note that specimen MHI 1293 (stored at the Muschelkalkmuseum Hagdorn Ingelfingen) of *C. kuhnschnyderi* from the Upper Muschelkalk of Wasselonne (Alsace, France) shows two premaxillary teeth and thus a total of six teeth per side (Rieppel and Hagdorn 1999).

(c) Using a few gastropod species – not benthic communities – as indirect evidence for large macroalgae meadows upon which the placodonts might have fed is an over-interpretation of the actual data (Diedrich 2011a, p. 5).

(d) The proposed wear stages (Diedrich 2011a, p.14), which supposedly supports macroalgae feeding might also be attributable to feeding on abrasive, tough and hard-shelled prey or, in some cases, even post-mortem erosion. In addition, we do not really know how fast and how many times placodont teeth were shed during life (see Rieppel 2001b), but in any case the lack of extensive wearing might well be due to a high frequency in replacement rather than to non-use.

(e) In modern sirenians, the feeding mode, including the crushing (the 'food-squeezing function' in Diedrich 2011a, p. 14) and chewing of plant matter, is supported by broad fleshy muzzles and cheeks, and in the case of extant manatees, perioral bristles are used in food handling (Marshall et al. 2000), for which there is no evidence in placodonts. The soft tissue of the muzzle and cheek also plays a very prominent role in the extant walrus, *Odobenus rosmarus*, whose preferred diet also consists of benthic molluscs, although this species sucks the soft tissue (i.e. the foot and siphon) out of its prey before ejecting the hard shell. Despite their preferred hard-shelled diet, walruses also often show tooth reduction (apart from the very prominent tusks) with many teeth being rudimentary in the lower and upper jaw and often do not develop at all (e.g. Fay 1985 and references therein).

Food processing

In order to be effective, any grinding action must be effected by parts in reciprocal motion. The jaw mechanics of food processing patterns associated with herbivory in non-mammalian amniotes follows two basic paths to process plant material (Reilly et al. 2001). The first is similar to the primitive jaw mechanism of all non-mammalian predatory tetrapods, that is the articulation between the lower and upper jaw is rigid and jaws move like a hinge, with the lower teeth sliding inside the upper teeth as the jaws close, in a shearing motion (Herrel and de Vree 1999; Herrel et al. 2001; Reilly et al. 2001). The second pattern implies that the morphology of the articular surfaces of the jaws allows the lower jaw to shift longitudinally with respect to the upper jaw in a propalineal (fore and aft) fashion. The first pattern, the hinge-like motion, is usually associated with leaf-like shearing teeth, but not with flattened molariform teeth. The second pattern, the propalineal movement, can be found associated with leaf-like teeth, with grinding molariform teeth or even with sharp cutting surfaces on both jaws as in turtles.

Propaliny is indeed the most effective way of chewing for non-mammalian amniotes that are unable of a transverse cycle of mastication and it is adopted by many herbivorous reptiles (Throckmorton 1980; Herrel et al. 2001). To accomplish this task, the lower jaw must be able to shift fore and aft for a considerable extent with respect to the upper dentition. This is permitted by the shape of the articular area for the lower jaw. In reptiles capable of propalineal movements, either the articular area for the quadrate is craniocaudally elongated, in order to allow the fore and aft excursion of the lower jaw (e.g. turtles, the tuatara *Sphenodon*), or the same movement is allowed by the presence of a streptostylic quadrate. The marine iguana *Amblyrhynchus cristatus*, which feeds on soft plant material in a coastal environment does not have any tooth plate or crushing device, rather, like terrestrial herbivorous iguanas, it cuts the soft plant material with its leaf-shaped teeth, and the food item is then processed by a propalineal (fore and aft) movement of the lower jaw facilitated by the streptostylic quadrate articulation. Placodonts had a rigid quadrate and their articular area for the lower jaw is short and deeply concave, allowing a rather wide gape but hindering any propalineal movement. In addition, the high and powerful coronoid rises immediately before the articular area locking the mandible in position so that only opening and closing of the jaws was possible. Placodonts thus could not have performed any kind of mastication suited for grinding or cutting plant material.

The spaced distribution of the spatulate front teeth in placodontoid placodonts speaks against grazing adaptation, since algae or any other plant material may have escaped from the wide spaces among the teeth. Grazers (artiodactyls as well as sirenians) have a continuous horny pad which is much more efficient in cutting and keeping grass (or algae) in the mouth, perissodactyls have closely spaced teeth and turtles have continuous beaks. The assumption that the wear of the chisel-shaped teeth of placodontoids is indicative of herbivory because it was caused by scraping algae from the sea floor or digging out rhizomes is invalid, since it could easily have been caused by scraping off molluscs. Furthermore, the tapering rostrum of basal cyamodontoids with small widely spaced teeth and, even more so, the narrow, beak-like edentulous rostrum of more advanced forms like *Psephoderma* were even less suited for grazing. Both rostrum types were either very probably used for picking molluscs from the substrate (Renesto and Tintori 1995) or, especially in the case of elongated edentulous rostra, for probing the sediments in search of prey items (Rieppel 2002a). Rieppel (2002a) also discussed the possibility of suction feeding for some cyamodontoids, which exhibit the latter rostrum type. Such a specialised way of searching and capturing prey items, well substantiated by the skull anatomy of some of the cyamodontoid placodonts, would not make much sense in a herbivorous animal feeding on extensive macroalgae meadows. The wide and flat teeth on the maxillae, palate and lower jaws are much more similar to the crushing plates present in a wide array of aquatic organisms with a durophagous diet, e.g. lungfishes and chimaeroids, but also many myliobatid rays than they are to those of any herbivorous animal. Diedrich suggested an alternative function for the widely spaced teeth: they would have helped to drain the sediment out of the mouth cavity preventing its ingestion during food processing. However, given that the fore and aft movement (and thus the grinding action) was impossible, it is much more probable that the tooth plates functioned as crushing devices for breaking the mollusc shell. Among extant reptiles, the teeth of the molluscivorous macroteiid lizard *Dracaena* show a similar morphology (Presch 1974; Dalrymple 1979). In contrast, extant herbivorous marine reptiles that feed on soft plant material (e.g. the marine iguana *A. cristatus* and the green turtle *Chelonia mydas*) do not possess any grinding device. The marine iguana has sharp, leaf-like, serrated teeth, whereas the green turtle has an edentulous beak with sharp cutting edges. Among extinct herbivorous amniotes (e.g. aetosaurs, dicynodonts, groups of dinosaurs; see King 1996 for a detailed survey), most had leaf-like cutting teeth, whereas some others did indeed have grinding plates or transversely elongate multicusped teeth (e.g. procolophonians, rhynchosaurs, *Trilophosaurus*; King 1996; Spielmann et al. 2008). These grinding plates, however, did not have the smooth surface of placodont teeth, but were usually formed by an array of small cusps or denticles in order to form an irregular grinding surface, useful to break down the fibres of plants. Flat teeth with a smooth surface are highly ineffective for herbivorous animals, thus the smooth palatine and dentary teeth of placodonts cannot be considered an analogue of the denticled horny pad and tongue of sirenians, being not suited for grinding, but for crushing. The shape and disposition of placodont teeth are more similar to that of durophagous teiid *Dracaena* or the sea otter *Enhydra lutris*, another, albeit less specialised, mollusc eater (Riedman and Estes 1990). Premaxillary teeth of modern sirenians (often vestigial and being resorbed during ontogeny in manatees, e.g. Husar 1978) are vertically oriented and are used to move sediment in order to better expose sea plants before consumption. There are usually no teeth at the tip of the lower jaw in modern sirenians, although occasionally small incisors (i.e. i3) have been found in the vestigial incisor sockets in mandibles of *Dugong dugon* (e.g. Lyman 1939; Lanyon and Sanson 2006 and references therein). A vast array of durophagous fishes both extant and extinct do not show extensive tooth wearing (of mandibular teeth) and the same applies to the molluscivorous reptile *Dracaena*. The assumption by Diedrich (2010, p. 301) that shell crushing was not

necessary because the flattened teeth show little wearing is thus ill founded.

The role of the upper incisors and of the padded tongue of sirenians is a functional analogue to the pad and lower incisors of artiodactyls to graze on vegetation. Arctiodactyls have stout and high molars well suited for grinding fibrous plants, while sirenians have a reduced dentition as the grinding and squeezing is performed by the action of the tongue and horny palatal pads, thus restricting their diet to soft plants. The massive and stout teeth of placodonts would have been oversized for such a diet, and their crown being smooth, lacking ridges or cusps, was also unsuitable for processing fibrous plants. Diedrich (2010, p. 301) further states that at least four of the large palatine teeth must have been in use at the same time in *Placodus*; however, the four huge teeth more likely provided a stout crushing apparatus for hard food rather than an adaptation for processing soft plant material.

Taphonomy

Diedrich (2010, p. 296; 2011a, p. 14) states that in the sites which yielded placodont remains there is no direct evidence of the presence of macroalgae, but that their presence can be deduced by the high abundance of molluscs. This obviously hardly proves that placodonts fed on macroalgae, whereas it suggests that placodonts thrived in areas where molluscs were abundant, perhaps feeding on them. In addition, Diedrich himself (2010, p. 298) states that in the Monte San Giorgio localities placodonts are found but that there were no macroalgae, which may already speak against the hypothesis of herbivory in itself. This contradiction is explained by the author by suggesting that the placodonts found in the Monte San Giorgio localities (i.e. *Paraplacodus broilii* and *C. hildegardis*) must have lived in other regions and that they must have been subjected to long transportation prior to burial. This is contradicted, however, by the fact that most placodont skeletons are nearly complete and articulated (as are those of fishes and other marine reptiles), suggesting that only little transportation occurred. It is thus more reasonable to assume that they lived nearby and fed on the abundant molluscs. The same can be assumed for the new Chinese taxa found in black micritic laminated layers, sometimes associated with bivalves remains (Jiang et al. 2009).

The absence of shell remains associated with placodont skeletal remains is further quoted by Diedrich (2010, 2011b) as evidence that placodonts did not feed on shelled molluscs. Apart being negative evidence, the absence of shell remains in the stomach and intestine of placodonts does not speak against durophagy. As it has been documented in extant durophagous reptiles (e.g. *Dracaena*), after crushing, the shell fragments are expelled from the mouth by movements of the tongue (Vanzolini 1961; Dalrymple 1979; Reilly et al. 2001) so that they are not swallowed and cannot be found in the gastric cavity. Similarly, shell fragments are also often ejected by modern durophagous fishes (see Tintori 1995 and references therein). On the other hand, large amounts of coprolites consisting of fragmented shells have been found together with *Psephoderma* remains, as well as with durophagous fishes such as *Paralepidotus* in the Norian of the Lombardian basin (Tintori 1995).

Conclusions

In retrospect, the history of science has seen multiple cases in which unorthodox ideas and hypotheses (analogous to Diedrich's interpretation of placodonts being herbivorous and feeding on macroalgae) were expressed, and in which these ideas had a hard stand prior to evoking a paradigm shift among peers. In the end, however, it was the facts, the hard evidence, which made the difference in verifying or rejecting hypotheses. Accordingly, we wish to explicitly point out that it was not the idea itself that we reject, but the sloppy style of conducting research, the lack of evidence and omission of other scientists' work, and the often unsupported over-interpretations of the data, which forced us to write this comment. A thorough re-analysis (e.g. using a stratocladistic approach) including all available data, as was hinted at by Diedrich (2011a), was unfortunately not provided; instead all interpretations are based on relatively weak data of the (often scanty) fossils and the geologic, paleobiogeographic and stratigraphic setting. Furthermore, it is deemed highly disturbing that two species can be synonymised based solely on similar tooth formulas when it is clearly apparent that ontogenetic and intraspecific variation occurs within those species. In light of the overwhelming data still being brought forth using comparative osteology and myology, cladistic analysis, as well as functional morphology, Diedrich's notion of placodonts feeding on macroalgae must, therefore, be rejected.

Acknowledgements

The colleagues at the PIMUZ are thanked for discussions and technical help. The manuscript further greatly benefited from the constructive comments of an anonymous reviewer. The study was funded by the Swiss National Science Foundation (No. 31003A 127053/1 to TMS).

References

Agassiz L. 1833–43. Recherches sur les poissons fossiles. Vol. I–V. Neuchâtel: Imprimaire de Petitpierre.

Bodzioch A. 1997. Formacja karchowicka: definicja i stratygrafia [The Karchowice formation: definition and stratigraphy; in Polish with English summary]. Geologos. 2:165–199.

Brack P, Rieber H, Nicora A, Mundil R. 2005. The global boundary stratotype section and point (GSSP) of the Ladinian Stage (Middle Triassic) at Bagolino (Southern Alps, Northern Italy) and its implications for the Triassic time scale. Episodes. 28(4):233–244.

Dalrymple GH. 1979. On the jaw mechanism of the snail-crushing lizards, *Dracaena* Daudin 1802 (Reptilia, Lacertilia, Teiidae). J Herpetol. 13(3):303–311.

Diedrich CG. 2010. Palaeoecology of *Placodus gigas* (Reptilia) and other placodontids – Middle Triassic macroalgae feeders in the Germanic Basin of central Europe – and evidence for convergent evolution with Sirenia. Palaeogeogr Palaeoclimatol Palaeoecol. 285(3–4):287–306.

Diedrich CG. 2011a. The shallow marine placodont *Cyamodus* of the central European Germanic Basin: its evolution, paleobiogeography and paleoecology Hist Biol. iFirst article, 1–19, doi: 10.1080/08912963.2011.575938.

Diedrich CG. 2011b. Fossil Middle Triassic "sea cows" – placodont reptiles as macroalgae feeders along the North-western Tethys coastline with Pangaea and in the Germanic Basin. Nat Sci. 3(1): 9–27.

Druzinsky RE, Greaves WS. 1979. A model to explain the posterior limit of the bite point in reptiles. J Morphol. 160(2):165–168.

Fay FH. 1985. *Odobenus rosmarus*. Mamm Species. 238:1–7.

Feist-Burkhardt S, Götz AE, Szulc J, Borkhataria R, Geluk M, Haas J, Hornung J, Jordan P, Kempf O, Michalík J, et al. 2008. Triassic. In: McCann T, editor. The geology of central Europe, Mesozoic and Cenozoic. Chapter 13, Vol. 2. London: The Geological Society. p. 749–821.

Fisher DC. 2008. Stratocladistics: integrating temporal data and character data in phylogenetic inference. Annu Rev Ecol Evol Syst. 39: 365–385.

Froitzheim N, Plašienka D, Schuster R. 2008. Alpine tectonics of the Alps and western Carpathians. In: McCann T, editor. The geology of central Europe, Mesozoic and Cenozoic. Chapter 18, Vol. 2. London: The Geological Society. p. 1141–1232.

Furrer H. 1995. The Kalkschieferzone (Upper Meride Limestone; Ladinian) near Meride (Canton Ticino, Southern Switzerland) and the evolution of a Middle Triassic intraplatform basin. Eclogae Geol Helv. 88(3):827–852.

Furrer H, Schaltegger U, Ovtcharova M, Meister P. 2008. U-Pb zircon age of volcaniclastic layers in Middle Triassic platform carbonates of the Austroalpine Silvretta nappe (Switzerland). Swiss J Geosci. 101(3): 595–603.

Fürsich FT. 1981. Die *Palaeonucula strigilata/Dentalium undulatum*-Faunengemeinschaft in Weichböden der mittleren alpinen Trias. In: McKerrow WS, editor. Paläoökologie. Stuttgart: Franckh. p. 138–139.

Gaetani M, Courel L, Arche A, Warrington G, Geluk M, Beutler G, Szulc J, Lozowski V, Sandulescu M, Seghedi A, et al. 2000. Early Ladinian paleogeographic map. In: Dercourt J, Gaetani M, Vrielynck B, editors. Peri-Tethys Atlas and explanatory notes. Paris: CCGM/CGMW. p. 32–40.

Grubich J. 2003. Morphological convergence of pharyngeal jaw structure in durophagous perciform fish. Biol J Linn Soc. 80(1):147–165.

Gürich GJE. 1884. Über einige Saurier des oberschlesischen Muschelkalkes. Z dt geol Ges. 36:125–144.

Hagdorn H. 2004. Muschelkalkmuseum Ingelfingen. Heilbronn: Edition Lattner. p. 87.

Hagdorn H, Reif W-E. 1988. "Die Knochenbreccie von Crailsheim" und weitere Mitteltrias-Bonebeds in Nordost-Württemberg – Alte und neue Deutungen. In: Hagdorn H, editor. Neue Forschungen zur Erdgeschichte von Crailsheim. Zur Erinnerung an Hofrat Richard Blezinger (Sonderbände der Gesellschaft für Naturkunde in Württemberg. Band 1). Stuttgart: Goldschneck-Verlag Werner K. Weidert. p. 116–143.

Hagdorn H, Rieppel O. 1999. Stratigraphy of marine reptiles in the Triassic of Central Europe. Zbl Geol Palaeont, Teil I. 1998(7–8): 651–678.

Hardenbol J, Thierry J, Farley MB, Jacquin T, de Graciansky P-C, Vail PR, editors 1998. Mesozoic and Cenozoic Sequence Stratigraphy of European Basins. SEPM Special Publication No. 60. Tulsa: SEPM (Society for Sedimentary Geology) p. 786. [ISBN 1-56576-043-3].

Herrel A, de Vree F. 1999. Kinematics of intraoral transport and swallowing in the herbivorous lizard *Uromastix acanthinurus*. J Exp Biol. 202(9):1127–1137.

Herrel A, Meyers JJ, Nishikawa KC, de Vree F. 2001. The evolution of feeding motor patterns in lizards: modulatory complexity and possible constraints. Am Zool. 41(6):1311–1320.

Husar SL. 1978. *Trichechus senegalensis*. Mamm Species. 89:1–3.

Jiang D-Y, Motani R, Hao W-C, Rieppel O, Sun Y-L, Schmitz L, Sun Z-Y. 2008. First record of Placodontoidea (Reptilia, Sauropterygia, Placodontia) from the Eastern Tethys. J Vertebr Paleontol. 28(3):904–908.

Jiang D-Y, Motani R, Hao W-C, Rieppel O, Sun Y-L, Tintori A, Sun Z-Y, Schmitz L. 2009. Biodiversity and sequence of the Middle Triassic Panxian marine reptile fauna, Guizhou Province, China. Acta Geol Sin. 83(3):451–459.

Kaim A. 1997. Brachiopod-bivalve assemblages of the middle Triassic Terebratula Beds, Upper Silesia. Poland Acta Palaeontol Pol. 42: 333–359.

Kardong KV. 2009. Vertebrates – Comparative anatomy, function, evolution. 5th ed. Boston, MA: McGraw-Hill p. 779.

King G. 1996. Reptiles and herbivory. London: Chapman & Hall p. 160.

Kozur HW, Bachmann GH. 2008. Updated correlation of the Germanic Triassic with the Tethyan scale and assigned numeric ages. In: Krystyn L, Mandl GW, editors. Upper Triassic Subdivisions, Zonations and Events: Meeting of the late IGCP 467 and STS. 28 September–2 October 2008, Vol. 76. Bad Goisern (Upper Austria): Abstracts and Excursion-Guide. Berichte der Geologischen Bundesanstalt. p. 53–58.

Kuhn-Schnyder E. 1959. Über das Gebiss von *Cyamodus*. Vierteljahresschr Naturforsch Ges Zuerich. 104(Festschrift Steiner):174–188.

Kuhn-Schnyder E. 1974. Die Triasfauna der Tessiner Kalkalpen. Neujahrsbl Naturforsch Ges Zuerich. 176:1–119.

Lanyon JM, Sanson GD. 2006. Mechanical disruption of seagrass in the digestive tract of the dugong. J Zool. 270(2):277–289.

Li C. 2000. Placodont (Reptilia: Placodontia) from Upper Triassic of Guizhou, Southwest China [in Chinese with English summary]. Vertebrata PalAsiatica. 38(4):314–317.

Li C, Rieppel O. 2002. A new cyamodontoid placodont from Triassic of Guizhou, China [in Chinese]. Chinese Sci Bull. 47(2):156–159.

Lyman CP. 1939. A vestigial lower incisor in the dugong. J Mammal. 20(2):229–231.

Marshall CD, Kubilis PS, Huth GD, Edmonds VM, Halin DL, Reep RL. 2000. Food-handling ability and feeding-cycle length of manatees feeding on several species of aquatic plants. J Mammal. 81(3): 649–658.

Massare JA. 1987. Tooth morphology and prey preference of Mesozoic marine reptiles. J Vertebr Paleontol. 7(2):121–137.

Massare JA. 1997. Introduction, Part VI: Faunas, behaviour, and evolution. In: Callaway JM, Nicholls EL, editors. Ancient marine reptiles. San Diego, CA: Academic Press. p. 401–421.

Mazin J-M. 1989. La denture et la région palatine des Placodontia (Reptilia, Trias). Implications phylogénétiques. Geobios. 22(6): 725–734.

Mazin J-M, Pinna G. 1993. Palaeoecology of the armoured placodonts. Paleontologia Lombarda N.S. 2(1):83–91.

Menning M, Schröder B, Plein E, Simon T, Lepper J, Röhling H-G, Heunisch C, Stapf K, Lützner H, Käding K-C, et al. 2011. Beschlüsse der Deutschen Stratigraphischen Kommission 1991–2010 zu Perm und Trias von Mitteleuropa [Recommendations of the German Stratigraphic Commission 1991–2010 on the Permian and Triassic of Central Europe]. Z dt Ges Geowiss. 162:1–18.

Meyer H von. 1863. Die Placodonten, eine Familie von Sauriern der Trias. Palaeontology. 11:175–221.

Niedźwiedzki R. 2000. Litostratygrafia formacji górazdzanskiej I formacji dziewkowickiej na Slasku Opolskim. Prace Geologiczno-Mineralogiczne. 71:1–72.

Niedźwiedzki R. 2002. Revision of stratigraphic ranges of selected invertebrate taxa from the Muschelkalk in Silesia. Geol Quart. 46: 219–225.

Nosotti S, Pinna G. 1993. *Cyamodus kuhn-schnyderi* n. sp., nouvelle espèce de Cyamodontidae (Reptilia, Placodontia) du Muschelkalk supérieur allemand. C.R. Acad Sci Ser 2. 317:847–850.

Nosotti S, Pinna G. 1996. Osteology of the skull of *Cyamodus kuhnschnyderi* Nosotti & Pinna 1993 (Reptilia, Placodontia). Paleontologia Lombarda N.S. 6:3–42.

Nosotti S, Rieppel O. 2002. The braincase of *Placodus* Agassiz, 1833 (Reptilia, Placodontia). Mem Soc Ital Sci Nat Mus Civ Stor Nat Milano. 31(1):3–18.

Owen R. 1858. Description of the skull and teeth of the *Placodus laticeps*, Owen, with indications of other new species of *Placodus*, and evidence of the saurian nature of that genus. Phil Trans R Soc Lond. 148:169–184.

Peyer B. 1931. Die Triasfauna der Tessiner Kalkalpen III. Placodontia. Abh Schweizer Paläontol Gesellschaft. 51:1–25.

Pinna G. 1992. *Cyamodus hildegardis* Peyer, 1931 (Reptilia, Placodontia). Mem Soc Ital Sci Nat Mus Civ Stor Nat Milano. 26(1):1–21.

Pinna G, Mazin J-M. 1993. Stratigraphy and paleobiogeography of the Placodontia. Paleontologia Lombarda N.S. 2:125–130.

Pinna G, Nosotti S. 1989. Anatomia, morfologia funzionale e paleoecologia del rettile placodonte *Psephoderma alpinum* Meyer, 1858. Mem Soc Ital Sci Nat Mus Civ Stor Nat Milano. 25(2):17–50.

Presch W. 1974. A survey of the dentition of the macroteiid lizards (Teiidae: Lacertilia). Herpetologica. 30(4):344–349.

Reif W-E, Stein F. 1999. Morphogeny and function of the dentition of *Henodus chelyops* Huene, 1936 (Placodontia, Triassic). N Jb Geol Palaeont Mh. 1999(2):65–80.

Reilly SM, McBrayer LD, White TD. 2001. Prey processing in amniotes: biomechanical and behavioral patterns of food reduction. Comp Biochem Physiol A. 128(3):397–415.

Renesto S, Tintori A. 1995. Functional morphology and mode of life of the Late Triassic placodont *Psephoderma alpinum* Meyer from the Calcare di Zorino (Lombardy, N Italy). Riv It Paleontol Strat. 101(1): 37–48.

Riedman ML, Estes JA. 1990. The sea otter (*Enhydra lutris*): behavior, ecology, and natural history. U.S. Fish and Wildlife Serv Biol Rep. 90(14):1–126, Washington, DC.

Rieppel O. 1995. The genus *Placodus*: systematics, morphology, paleobiogeography, and paleobiology. Fieldiana Geol, N.S. 31(1472):1–44.

Rieppel O. 2000. Sauropterygia I – Placodontia, Pachypleurosauria, Nothosauroidea, Pistosauroidea. Handbuch der Paläoherpetologie [Handbook of Paleoherpetology] Part 12A. Stuttgart: Schweizerbart. p. 134.

Rieppel O. 2001a. The cranial anatomy of Placochelys placodonta Jaekel, 1902, and a review of the Cyamodontoidea (Reptilia, Placodonta). Fieldiana Geol, N.S. 45(1514):1–104.

Rieppel O. 2001b. Tooth implantation and replacement in Sauropterygia. Paläont Z. 75(2):207–217.

Rieppel O. 2002a. Feeding mechanics in Triassic stem-group sauropterygians: the anatomy of a successful invasion of Mesozoic seas. J Linn Soc Lond Zool. 135(1):33–63.

Rieppel O. 2002b. The dermal armor of the cyamodontoid placodonts (Reptilia, Sauropterygia): morphology and systematic value. Fieldiana Geol, N.S. 46(1517):1–41.

Rieppel O, Hagdorn H. 1999. A skull of *Cyamodus kuhnschnyderi* Nosotti & Pinna 1993, from the Muschelkalk of Wasselonne (Alsace, France). Paläont Z. 73(3/4):377–383.

Rieppel O, Reisz RR. 1999. The origin and early evolution of turtles. Annu Rev Ecol Syst. 30:1–22.

Salisbury SW, Frey E. 2001. A biomechanical transformation model for the evolution of semi-spheroidal articulations between adjoining vertebral bodies in crocodilians. In: Grigg GC, Seebacher F, Franklin CE, editors. Crocodilian biology and evolution. Chipping Norton: Surrey Beatty & Sons. p. 85–134.

Sander PM. 1989. The pachypleurosaurids (Reptilia: Nothosauria) from the Middle Triassic of Monte San Giorgio (Switzerland) with the description of a new species. Phil Trans R Soc Lond B. 325(1230): 561–666.

Scheyer TM. 2007. Skeletal histology of the dermal armor of Placodontia: the occurrence of 'postcranial fibro-cartilaginous bone' and its developmental implications. J Anat. 211(6):737–753.

Scheyer TM. 2008. Aging the oldest turtles: the placodont affinities of *Priscochelys hegnabrunnensis*. Naturwissenschaften. 95(9): 803–810.

Scheyer TM. 2010. New interpretation of the postcranial skeleton and overall body shape of the placodont *Cyamodus hildegardis* Peyer, 1931 (Reptilia, Sauropterygia). Palaeontologia Electronica. 13(2): 15A:15p. Available from: http://palaeo-electronica.org/2010_2/232/index.html.

Seidel G, editor. 2003. Geologie von Thüringen. 2. Neubearbeitete Auflage. Stuttgart: E. Schweizerbart'sche Verlagsbuchhandlung p. 601.

Spielmann JA, Lucas SG, Rinehart LF, Heckert AB. 2008. The Late Triassic archosauromorph *Trilophosaurus*. New Mexico Museum Nat Hist Sci Bull. 43:1–177.

Throckmorton GS. 1980. The chewing cycle in the herbivorous lizard *Uromastix aegyptius* (Agamidae). Arch Oral Biol. 25(4):225–233.

Tintori A. 1995. Biomechanical fragmentation in shell-beds from the Late Triassic of the Lombardian Basin (Northern Italy). Preliminary report. Rivista Italiana di Paleontologia e Stratigrafia. 101(3):371–380.

Tintori A. 2011. Comment on "The vertebrates of the Anisian/Ladinian boundary (Middle Triassic) from Bissendorf (NW Germany) and their contribution to the anatomy, palaeoecology, and palaeobiogeography of the Germanic Basin reptiles" by C. Diedrich [Palaeogeography, Palaeoclimatology, Palaeoecology 273 (2009) 1–16]. Palaeogeogr Palaeoclimatol Palaeoecol. 300(1–4):205–207.

Tintori A, Schmitz L, Jiang D-Y, Lombardo C, Motani R. 2006. Durophagy in Triassic marine vertebrates. Ancient life and modern approaches. Paper presented at: Second International Paleontological Congress; 2006 July 17–21; Beijing, China.

Tseng ZJ, Binder WJ. 2010. Mandibular biomechanics of *Crocuta crocuta*, *Canis lupus*, and the late Miocene *Dinocrocuta gigantea* (Carnivora, Mammalia). J Linn Soc Lond Zool. 158(3):683–696.

Vanzolini PE. 1961. Notas bionomicas sóbre *Dracaena guianesis* no Pará (Sauria, Teiidae). Pap Avulsos Zool. 14(25):237–241.

Vogt C. 1983. Evolutive Palokologie der Placodontier (*Placodus*, *Henodus*; Euryapsida, Trias) [Doctoral dissertation]. [Tübingen]: Eberhard-Karls-Universität, Tübingen, Germany. p. 99.

Westphal F. 1976. The dermal armour of some Triassic placodont reptiles. In: Bellairs Ad'A, Cox CB, editors. Linnean society symposium series No. 3. Morphology and biology of reptiles. London: Academic Press. p. 31–41.

Westphal F. 1988. Pflasterzahnsaurier (Placodonten) aus dem süddeutschen Muschelkalk (Mitteltrias). In: Hagdorn H, editor. Neue Forschungen zur Erdgeschichte von Crailsheim. Zur Erinnerung an Hofrat Richard Blezinger (Sonderbände der Gesellschaft für Naturkunde in Württemberg. Band 1). Stuttgart: Goldschneck-Verlag Werner K. Weidert. p. 151–165.

Zhao L-J, Li C, Liu J, He T. 2008. A new armored placodont from the Middle Triassic of Yunnan Province, southwestern China. Vertebrata PalAsiatica. 46(3):171–177.

CHAPTER 3

THE BRAINCASE AND INNER EAR OF *PLACODUS GIGAS* (SAUROPTERYGIA, PLACODONTIA)—A NEW RECONSTRUCTION BASED ON MICRO-COMPUTED TOMOGRAPHIC DATA

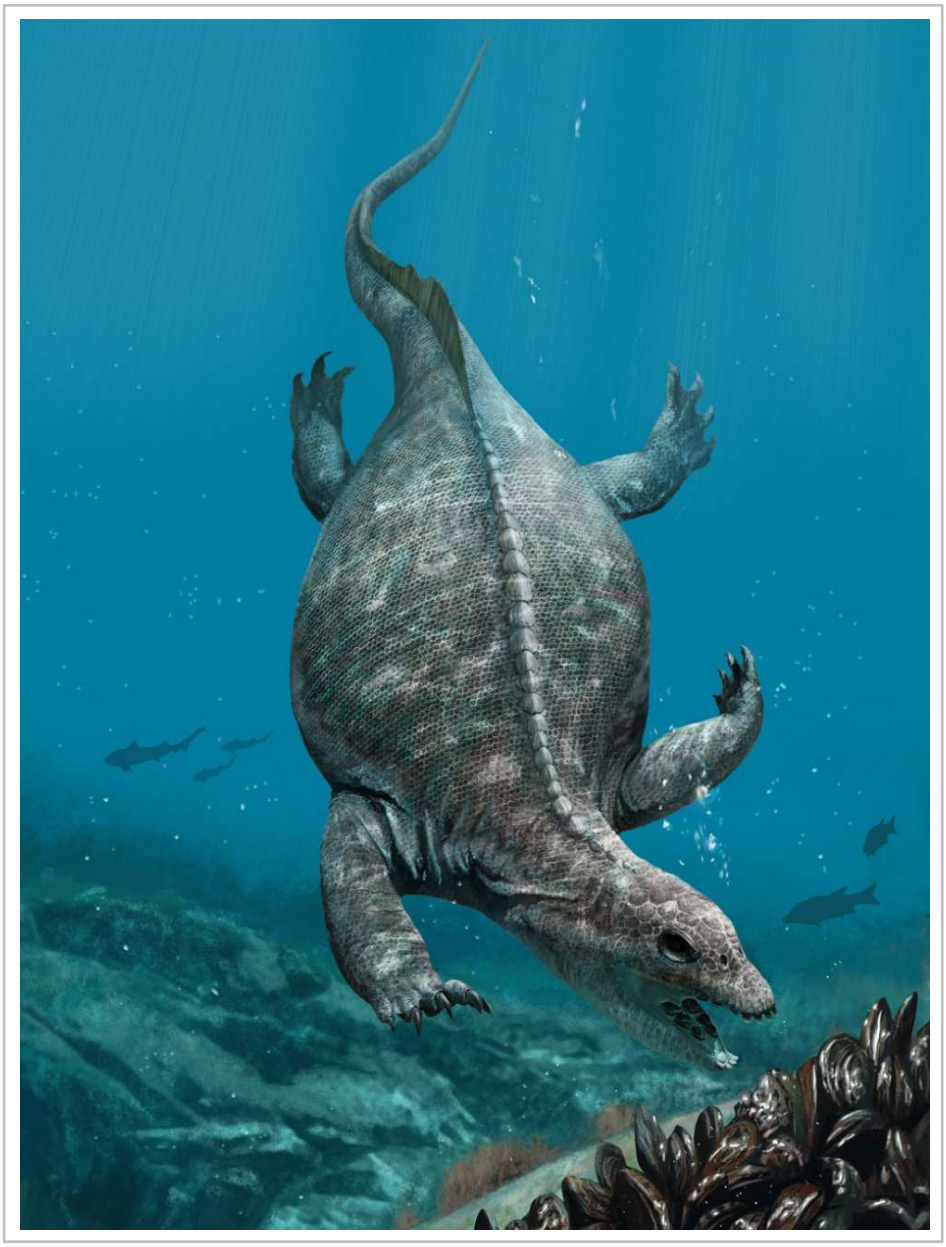

Placodus gigas by Jaime Chirinos

Journal of Vertebrate Paleontology 32(6):1350–1357, November 2012

ARTICLE

THE BRAINCASE AND INNER EAR OF *PLACODUS GIGAS* (SAUROPTERYGIA, PLACODONTIA)—A NEW RECONSTRUCTION BASED ON MICRO-COMPUTED TOMOGRAPHIC DATA

JAMES M. NEENAN* and TORSTEN M. SCHEYER
Paleontological Institute and Museum, University of Zurich, Karl-Schmid-Strasse 4, 8006 Zurich, Switzerland
james.neenan@pim.uzh.ch

ABSTRACT—*Placodus gigas* is an unarmored placodont marine reptile (Diapsida, Sauropterygia) known from the Middle Triassic of Europe, most commonly found in the shallow marine carbonate facies of the German Muschelkalk (lower Anisian to middle Ladinian, approximately 243–235 Ma). Generally, the morphology of the skull is well understood, with the exception of the braincase, which is partially obscured by dermatocranial bone. Two skulls that display well-preserved and intact chondrocranial elements were scanned using industrial micro-computed tomography (μCT), thus revealing parts of the braincase that were previously obscured and allowing a new three-dimensional reconstruction of the region to be constructed. This includes a complete osteological description, the first reconstruction of a sauropterygian vestibular apparatus, and a new virtual cranial endocast. The morphology of the braincase and sphenoid region has been revised, revealing the position of the hypophyseal pit. The enigmatic 'alisphenoid bridge' has been reinterpreted as being a dorsally extended dorsum sellae. The vestibular apparatus is shown to have strongly dorsoventrally compressed vertical semicircular canals, a commonly observed morphology of other marine reptiles, and an 'alert' head position of about 20°, indicating a highly aquatic lifestyle. Because placodonts are the sister group to all other sauropterygians, these new data are of great comparative and phylogenetic significance, providing insight into some of the morphological and functional changes that occurred on the stem leading to the more derived sauropterygians.

INTRODUCTION

Placodontia is a monophyletic group of Triassic sauropterygian marine reptiles (Fig. 1) that inhabited shallow marine environments in the eastern and western Tethys, as well as the inland epicontinental seas of Europe, with a stratigraphic range that extends from the lower Anisian to the upper Rhaetian. The clade is characterized by enlarged, 'tablet-like' teeth, particularly on the palatines and dentaries, indicating a probable durophagous diet (Scheyer et al., 2012, and references therein), and is split into the armored Cyamodontoidea and the unarmored and paraphyletic placodontoids (e.g., Mazin and Pinna, 1993; Rieppel, 2000a). These unarmored taxa consist of two genera: *Paraplacodus*, known from the Anisian–Ladinian boundary of Monte San Giorgio, Switzerland, and *Placodus*, which contains two species: *P. gigas* and *P. inexpectatus*. *P. gigas* is well known from the Middle Triassic epicontinental carbonate facies of Europe (Agassiz, 1833–1845), being most common in the German Muschelkalk, which spans approximately 243–235 Ma (Menning et al., 2011), between the Jena Formation (Bithynian, lower Anisian) and the Warburg Formation (Fassanian, middle Ladinian). *P. inexpectatus*, on the other hand, is the only known placodontoid placodont from the eastern Tethys (Jiang et al., 2008), and is currently represented by one almost complete specimen from the Pelsonian of the Guanling Formation in Guizhou, China. Because placodonts represent the most plesiomorphic clade of sauropterygians, they are particularly important for understanding how sauropterygians adapted to an increasingly secondarily aquatic lifestyle (Fig. 1).

The skull of *Placodus* has been closely studied and thoroughly described (Broili, 1912; Drevermann, 1933; Sues, 1987; Nosotti and Pinna, 1993; Rieppel, 1995, 2000b), including a detailed description of the braincase (Nosotti and Rieppel, 2002) and cranial endocast (Edinger, 1925; Hopson, 1979). However, accurate description of the chondrocranium is difficult, because dermatocranial elements such as the parietals, pterygoids, and squamosals obscure large portions of the braincase, rendering an accurate reconstruction extremely difficult using traditional methods. A solution to this problem is to utilize micro-computed tomographic (μCT) scanning, an ideal method for viewing these obscured structures without causing damage to the specimen that has been used successfully to describe the braincases of several fossil reptilian taxa, including theropod dinosaurs (e.g., Witmer and Ridgely, 2009; Smith et al., 2011), basal diapsids (Gardner et al., 2010), and metriorhynchid crocodyliforms (Fernández et al., 2011). Additionally, μCT scanning also grants the ability to reconstruct the vestibular apparatus and cranial endocast of *Placodus*, revealing information that would otherwise be unobtainable. Using this method, we present a new description of the braincase, as well as the first reconstruction of the vestibular apparatus and a new virtual cranial endocast of *Placodus*.

Institutional Abbreviations—BSP, Bayerische Staatssammlung fur Paläontologie und Historische Geologie, Munich, Germany; **SMF**, Senckenberg Museum, Frankfurt, Germany; **UMO**, Urwelt-Museum, Bayreuth, Germany.

MATERIALS AND METHODS

Two skulls from Germany were selected for this study (Fig. 2): UMO BT 13 and BSP 1968 I 75. Both show well-preserved and intact chondrocranial elements. UMO BT 13, from the Upper Muschelkalk (late Anisian/early Ladian) near Bayreuth, is the best-preserved example of a *Placodus* skull, being very complete and insignificantly deformed (Fig. 2A). In addition to this, the

*Corresponding author.

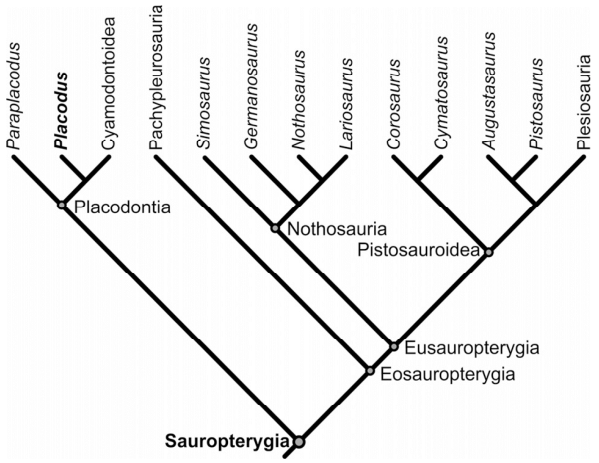

FIGURE 1. The phylogenetic relationships of Triassic Sauropterygia. The Placodontia are the most plesiomorphic members, being sister group to all other sauropterygians, the Eosauropterygia. Modified from Rieppel (2000b, 2001).

specimen has been extensively acid prepared, removing almost all of the surrounding limestone matrix, apart from a small amount in the braincase, thus making it the most comprehensively studied and best understood *Placodus* skull (e.g., Sues, 1987; Rieppel, 1995; Nosotti and Rieppel, 2002). BSP 1968 I 75 is also from the Upper Muschelkalk, but from Hegnabrunn near Kulmbach, Germany. It is missing a large portion of the rostrum, including both premaxillae (Broili, 1912; Rieppel, 1995; Fig. 2B). However, apart from this, the skull is well-preserved with little evidence of crushing or distortion—although the interior still contains a large amount of matrix, making μCT scanning the only possible method for visualizing its interior (see Supplementary Data, Figs. S1, S2; available online at www.tandfonline.com/UJVP).

The skulls were scanned at Giesserei Technologie Aalen, Hochschule Aalen in Baden-Württemberg, Germany, with a Wälischmiller RayScan 200 industrial μCT scanner with slice thicknesses of 0.2266 mm for UMO BT 13 and 0.192 mm for BSP 1968 I 75. Reconstructions were created using Avizo version 6.2.1.

DESCRIPTION

Braincase

As noted by Rieppel and Nosotti (2002), the skull of *Placodus* is a solid, robust, and akinetic structure with a well-ossified otic-occipital braincase region. The braincase is constructed from the basioccipital, supraoccipital, a pair of exoccipitals, a pair of opisthotics, and a pair of prootics (Fig. 3). The sphenoid region is unossified, apart from the basicranium, which consists almost entirely of the parabasisphenoid complex (the parasphenoid and basisphenoid are fused in *Placodus*).

The basioccipital forms the base of the foramen magnum, the entire occipital condyle, the basioccipital tubera, the ventral margin of the foramen vestibuli (oval window), and the entire braincase floor of the hindbrain (Fig. 3). The exoccipitals meet the dorsal surface of the basioccipital, forming the hypoglossal nerve foramen laterally (Fig. 3C). They also form the lateral walls of the foramen magnum, and extend laterally to form the paroccipital processes in combination with the opisthotics. The supraoccipital forms the dorsal margin of the foramen magnum, extending two flanges caudally to enclose the dorsomedial portion of the exoccipitals. It is almost entirely enclosed by the parietals.

The lateral wall of the braincase is composed of the opisthotics caudally and the prootics rostrally, both of which are partially enclosed and obscured by the parietals dorsally. The opisthotics extend laterally to contribute to the paroccipital processes, meet the basioccipital ventrally, and enclose part of the vestibular apparatus along with the prootics. They also form the dorsal margin of the jugular foramen, in conjunction with the exoccipitals, and the caudal portion of the fenestra vestibuli (Fig. 3C). The dorsal and rostral margins of the fenestra vestibuli are formed by the prootic, which also encapsulates part of the vestibular apparatus and forms a small foramen for the middle cerebral vein towards its dorsal margin (Fig. 3C). We agree with the interpretation of Nosotti and Rieppel (2002) that the prootic forms a large prootic fenestra rostrally, through which the trigeminal nerve passes (Fig. 3C).

Sphenoid Region—The sphenoid region of the braincase is not ossified in *Placodus* with the exception of the floor, which consists of the parabasisphenoid (Figs. 3A, C, 4, online Supplementary Figure 2). This element is rather short and does not extend far rostrally, lacking a cultriform process. Instead, the ethmoid cartilage was supported by a 'V'-shaped groove formed by the meeting of the palatines in a strongly dorsally projecting suture (Nosotti and Rieppel, 2002). The sphenoid region of UMO BT 13 was thoroughly described by Nosotti and Rieppel (2002), including brief descriptions of the same region from two specimens from the Senckenberg Museum in Frankfurt, SMF R 4038 and SMF R 359. With the matrix digitally removed, it has been revealed that this region in BSP 1968 I 75 is better preserved and more complete than that of UMO BT13 (Fig. 4).

The biggest difference between BSP 1968 I 75 and all other skull specimens of *Placodus* is its possession of a dorsally extended and rostrally sloping dorsum sellae (Figs. 4A, online Supplementary Figures 1, 2). This includes a pair of abducens nerve (VI) foramina, and confirms the interpretation of Hopson (1979) but contradicts Nosotti and Rieppel (2002) who maintained the presence of an 'alisphenoid bridge' based on specimen SMF R 359. Rostral to the dorsum sellae, a longitudinal, medial sagittal crest runs through the "sella turcica" (sensu Nosotti and Rieppel, 2002:7) a short distance before it bifurcates laterally (Fig. 4C). A pair of medial openings lie rostral to this, which are interpreted as the cerebral carotid foramina. These foramina are set within a deep fossa in UMO BT13 (Figs. 4D, online Supplementary Figure 3), but are not in BSP 1968 I 75 (Figs. 4C, online Supplementary Figure 1), indicating a difference in morphology, preservation, or preparation. To either side of these are a pair of laterally placed, dorsally projecting ascending processes, the function of which is unknown. However, it has previously been suggested that these structures provide the origin of the M. retractor bulbi (Nosotti and Rieppel, 2002:16) or, owing to our reconstruction of the cerebral carotid foramina being medially rather than laterally placed, may in fact have been support structures for the presumably cartilaginous lateral wall of the braincase that enclosed the forebrain.

Immediately rostral to the carotid foramina is a large, medially placed ascending process with a concave caudal surface, which probably formed the rostral surface of the hypophyseal pit (Fig. online Supplementary Figure 2A). The region directly caudal to the medial ascending process is therefore interpreted as the hypophyseal pit, owing to the presence of the cerebral carotids (e.g., Hopson, 1979). In addition, a foramen is located immediately lateral to each lateral ascending process with a medial margin composed of the parabasisphenoid and a lateral margin composed of the palatine (Fig. online Supplementary Figure 2B). These are interpreted as the foramina for the sphenoid arteries. Finally, a single medial foramen is located at the rostral-most end of the parabasisphenoid, which probably transported the palatine artery as the canal continues ventrally between the palatines. It is unusual to find an unpaired fossa in this region, and it may be autapomorphic for *Placodus*. Alternatively the foramen may indeed

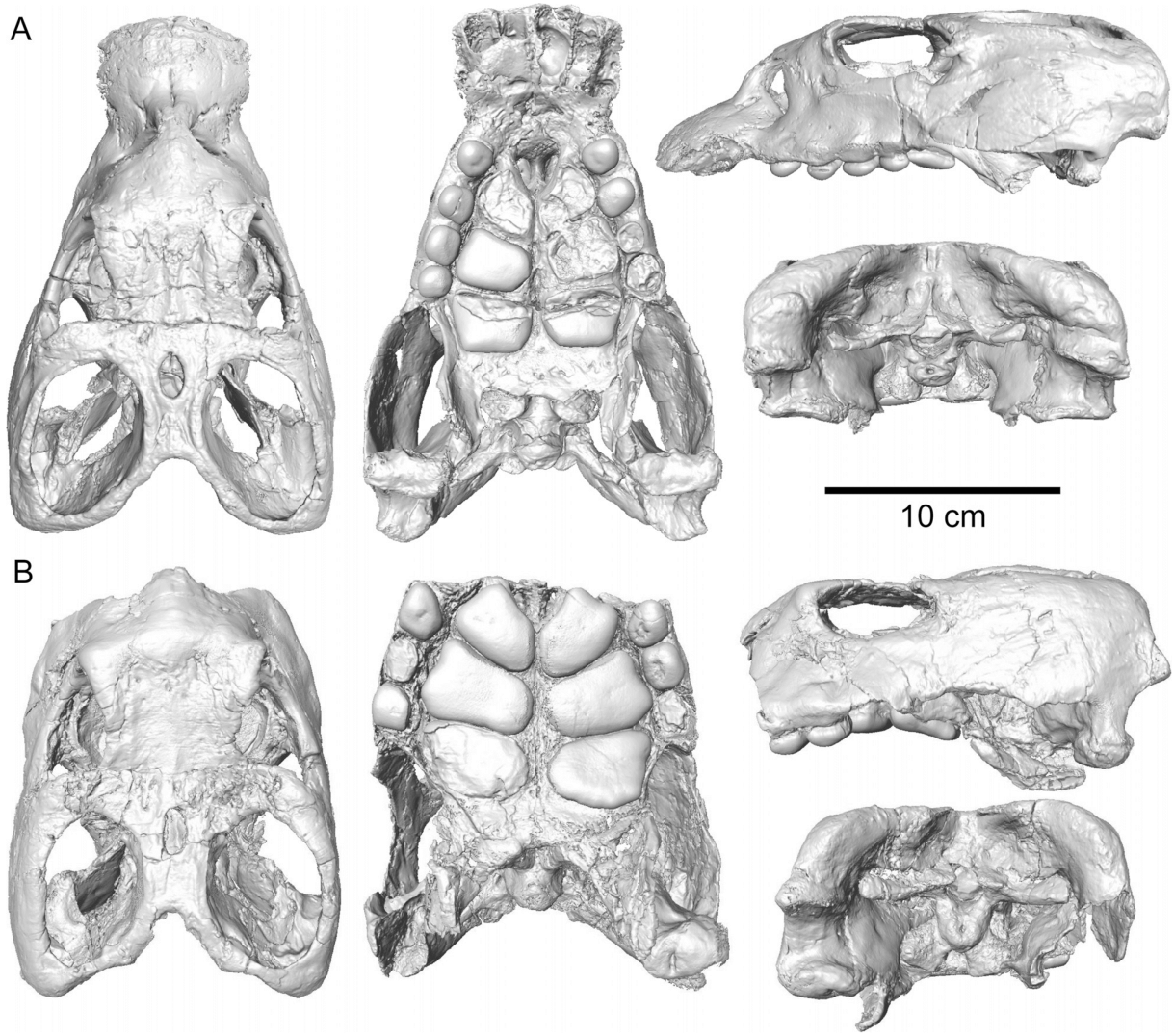

FIGURE 2. Surface rendering models of the two *Placodus gigas* skull specimens used in this study. **A**, UMO BT 13; **B**, BSP 1968 I 75. Skulls are shown in dorsal (left), palatal (middle), left lateral (upper right), and occipital (lower right) views.

have been paired, but was damaged during preservation, leaving the impression of one larger fossa.

Cranial Endocast

The paleoneurology of *Placodus* has previously been described from two specimens: SM R359, an artificial endocast, and SM R4038, a partially preserved natural one (Edinger, 1925; Hopson, 1979; Nosotti and Rieppel, 2002). Our reconstruction, based on UMO BT13 (Figs. 5A–C, online Supplementary Figure 3), represents the most complete endocast known for *Placodus*, revealing a well-preserved representation of the hindbrain cavity as well as a suite of cranial nerves and the endosseous labyrinth (see below). As the sphenoid region is not ossified in *Placodus* (see above), structures such as the olfactory bulb, hypophysis, and cranial nerves I–IV cannot be reconstructed. Despite this, the canal for the trigeminal nerve (V) can be identified because it corresponds to the prootic fenestra (Figs. 3C, 5A), as well as the abducens nerve (VI) canals that are associated with the abducens nerve foramina located in the dorsum sellae (Fig. 4A, C). The canal for the facial nerve (VII) is also revealed to be slightly ventrocaudal to nerve V and rostral to the labyrinth organ. The glossopharyngeal and vagoaccessory nerves (IX–XI) can be identified by the jugular foramen, and the hypoglossal nerve (XII) by the opening ventral to this, the hypoglossal nerve foramen (Fig. 3C). In addition, we agree with Hopson (1979) that the structure dorsocaudal to the trigeminal nerve is not the trochlear nerve as interpreted by Edinger (1925) but is in fact the vena cerebralis media (middle cerebral vein; Janensch, 1936; Fig. 5A, B).

Labyrinth Organ—μCT scanning has revealed the endosseous labyrinth in both specimens of *Placodus*, the first time that this has been fully reconstructed in a sauropterygian (Fig. 5). The organ is enclosed by the opisthotics and prootics, and is visible on

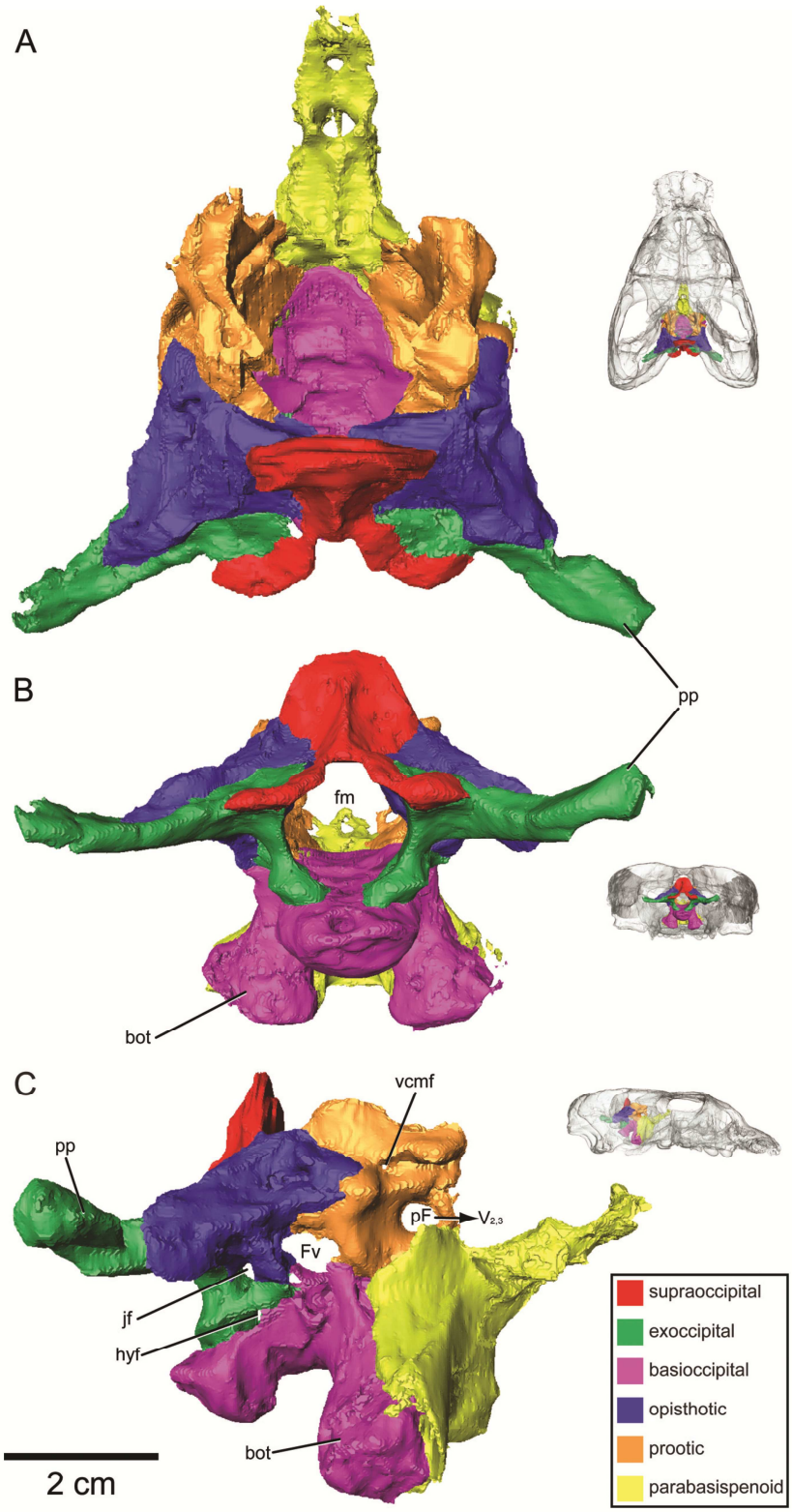

FIGURE 3. The braincase of *Placodus* specimen UMO BT 13 in dorsal (**A**), occipital (**B**), and right lateral (**C**) views. **Abbreviations**: **bot**, basioccipital tuber; **hyf**, hypoglossal nerve foramen; **jf**, jugular foramen; **fm**, foramen magnum; **Fv**, fenestra vestibuli; **pF**, prootic fenestra; **pp**, paroccipital process; **vcmf**, vena cerebralis media foramen; **$V_{2,3}$**, maxillary and mandibular branches of the trigeminal nerve.

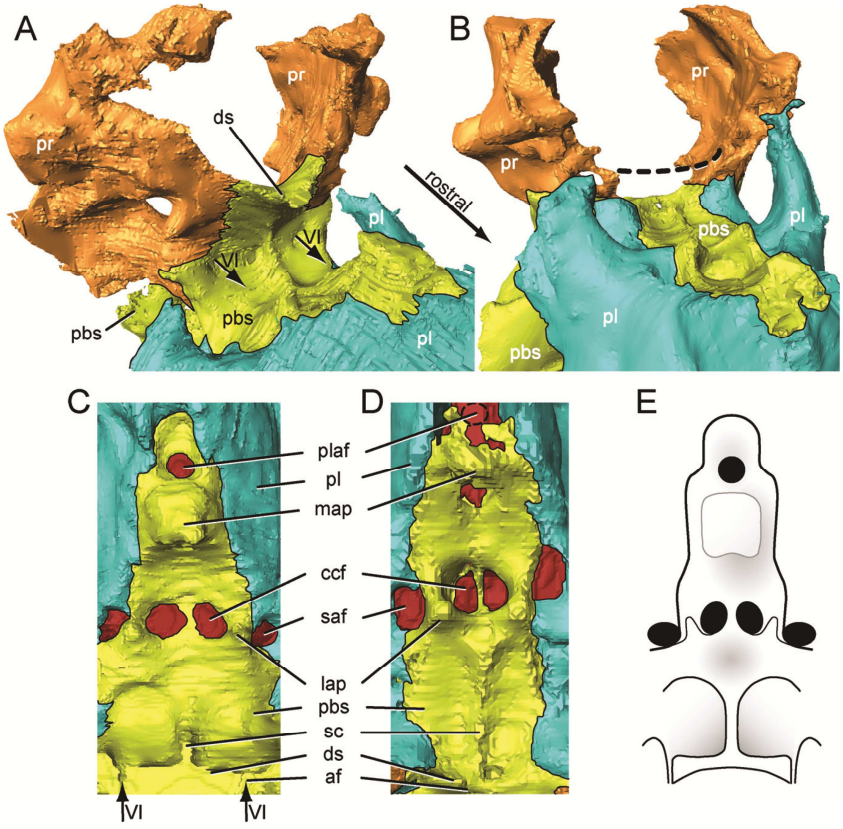

FIGURE 4. The sphenoid region of *Placodus*. **A**, Rostrolateral view of BSP 1968 I 75 showing strongly dorsally raised and rostrally sloping dorsum sellae. **B**, Rostrolateral view of UMO BT 13 showing probable position of dorsum sellae (dashed line). **C**, Basicranium dorsal surface of BSP 1968 I 75, with dorsum sellae digitally removed to expose surface. **D**, Basicranium dorsal surface of UMO BT 13. **E**, Interpretative diagram of the dorsal surface of the basisphenoid in *Placodus*, based on reconstructed μCT data. Foramina are shown as filled black spaces, whereas the medial ascending process is marked with thin gray line. Not to scale. **Abbreviations**: **af**, abducens nerve foramen; **ccf**, cerebral carotid foramina; **ds**, dorsum sellae; **lap**, lateral ascending processes; **map**, medial ascending process; **pbs**, parabasisphenoid; **pl**, palatine; **plaf**, palatine artery foramen; **pr**, prootic; **saf**, sphenoid artery foramen; **sc**, sagittal crest; **VI**, abducens nerve canal.

both sides of the skull, although not completely in BSP 1968 I 75 (online Supplementary Figure 1) and with a small portion of the left caudal semicircular canal missing in UMO BT 13 (Figs. 5B, online Supplementary Figure 3). It comprises three gracile semicircular canals, positioned perpendicular to each other, and is not reduced in size, as is the case in cetacean mammals (Spoor et al., 2002). The vertical canals are strongly dorsoventrally compressed and rostrocaudally elongated. The lagena is short and uncoiled.

DISCUSSION

Braincase

The braincase of *Placodus* is robust and somewhat shorter than those of other sauropterygians such as nothosaurs and plesiosaurs, which tend to have a relatively flat and elongate temporal region (e.g., Hopson, 1979; Rieppel, 2000b; Rieppel, 2002; Sato et al., 2011). It is fair to assume that the solid, well-ossified nature of the *Placodus* braincase is functional, and in conjunction with the akinetic palate and robust dermatocranial elements dissipated the considerable stresses and strains the skull would have endured during crushing of hard-shelled prey (e.g., Rieppel, 2002; Scheyer et al., 2012). This condition, i.e., the skull acting as a "single kinetic unit," is similar to what has been proposed for cyamodontoid placodonts such as *Protenodontosaurus italicus* (Nosotti and Pinna, 1999:5). In combination with the large abutting epipterygoids (see Nosotti and Rieppel, 2002, for more information), the braincase would thus have served as structural reinforcement for the skull, transferring stress and buttressing it to provide rigidity and stability. This is consistent with observations from other durophagous taxa such as the extant spotted hyena (*Crocuta crocuta*), which transfers a portion of the stress experienced while crushing bone through the anterior portion of the braincase (Tanner et al., 2008).

Sphenoid Region—The morphology of the dorsal surface of the parabasisphenoid differs between specimens of *Placodus* (Nosotti and Rieppel, 2002). This has been attributed to either variation due to ontogenetic change or simple variation between individuals. Although this is certainly possible, it may also be due to the state of preservation or damage from extensive acid and/or mechanical preparation, which, for example, would explain why the fragile dorsum sellae is always missing or broken. Including our new reconstruction of this region in BSP 1968 I 75, there are now four specimens known that all show slightly different morphology. However, using our new data, it is possible to interpret the region in a new light (Fig. 4E), especially with regard to the position of the internal carotid foramina. BSP 1968 I 75 clearly has this feature (Fig. 4C), as well as SMF R 4038 as described by Nosotti and Rieppel (2002). Moreover, μCT data have shown that this is also the case for UMO BT 13, contra Nosotti and Rieppel (2002), who reconstructed the basisphenoid with the carotid foramina lateral to the ascending processes and with half of their margin composed of the palatine, a condition which the authors deemed "unusual" (Nosotti and Rieppel, 2002:15). We can now show that these structures are not the carotid foramina, but are in fact the sphenoid artery foramina. Our reconstruction of UMO BT13 also shows a clear pair of foramina located within a fossa, which were partly blocked by matrix, in a position concordant with the cerebral carotid foramina seen in BSP 1968 I 75 and SMF R 4038. This would be a much more likely position for the

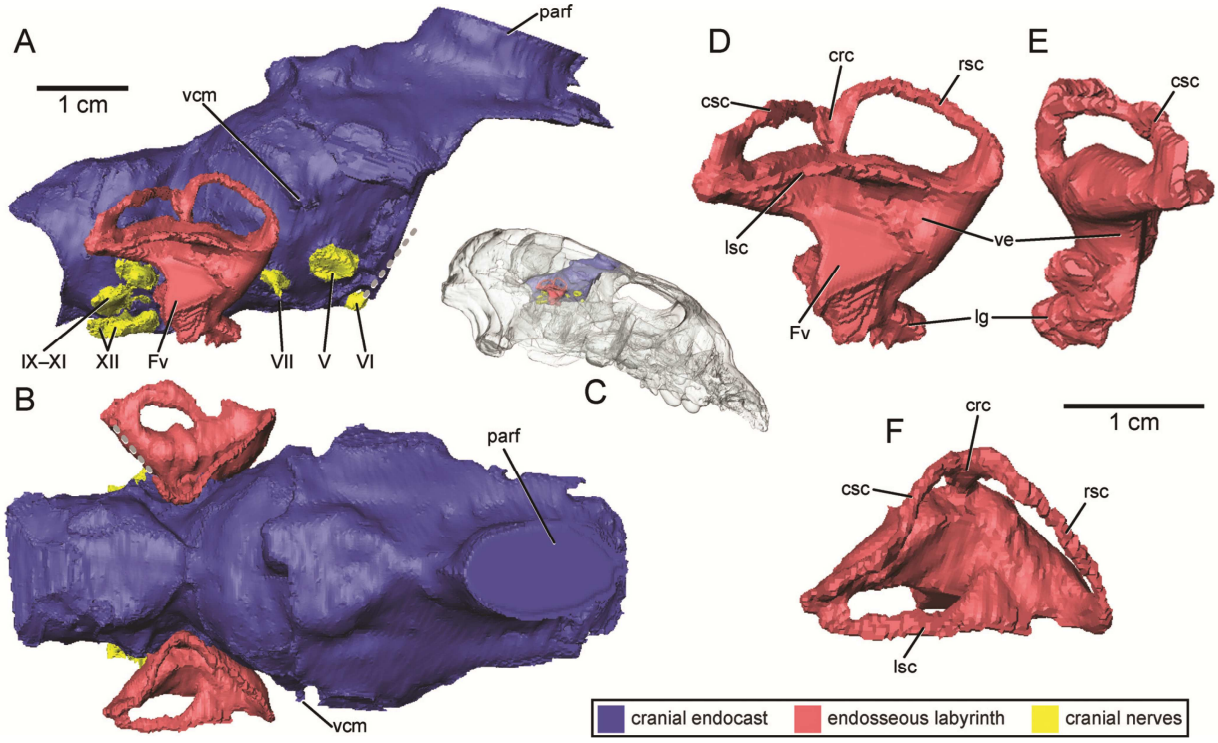

FIGURE 5. Reconstructed virtual cranial endocast and endosseous labyrinth of UMO BT 13. **A**, Endocast in right lateral view. Dashed gray line indicates position of dorsum sellae. **B**, Endocast in dorsal view. Dashed line indicates position of part of the left caudal semicircular canal, which is missing. **C**, 'Alert' head position of *Placodus*, determined by orientating the lateral semicircular canal horizontally. Not to scale. **D–F**, Right endosseous labyrinth of *Placodus* in lateral (**D**), caudal (**E**), and dorsal (**F**) views. **Abbreviations**: **crc**, crus communis; **csc**, caudal semicircular canal; **Fv**, fenestra vestibuli; **lg**, lagena; **lsc**, lateral semicircular canal; **parf**, parietal foramen; **rsc**, rostral semicircular canal; **vcm**, vena cerebralis media; **ve**, vestibuli of inner ear; **V**, trigeminal nerve canal; **VI**, abducens nerve canal; **VII**, facial nerve canal; **IX–XI**, shared canal for glossopharyngeal nerve, vagus nerve, accessory nerves, and jugular vein; **XII**, hypoglossal nerve canal.

internal carotids due to the fact that the foramina are entirely composed of the basisphenoid and are closely paired. These results also determine the position of the hypophyseal pit, which is to our knowledge always associated with the cerebral carotids and may at least be plesiomorphic for diapsids (Gardner et al., 2010). This conclusion is supported by the position of the large medial ascending process, which has a concave caudal surface that most likely formed the rostral margin of the hypophyseal pit (Fig. 4E).

It was also noted by Nosotti and Rieppel (2002) that in UMO BT13, the hypophyseal pit lies far rostral to the dorsum sellae, separated by a "sella turcica" (sensu Nosotti and Rieppel, 2002:7) that exhibits a medial, longitudinally orientated sagittal crest (Fig. 4D). This is unusual because these two structures are normally found in very close association to one another. This condition is also visible in BSP 1968 I 75, although the 'sella turcica' is somewhat shorter (Fig. 4C). The explanation of this morphology is still unknown, but could simply indicate an unusually large hypophysis in *Placodus*.

The biggest difference between BSP 1968 I 75 and all other *Placodus* specimens is the presence of a dorsally expanded and rostrally sloping dorsum sellae (Figs. 4A, online Supplementary Figure 2). This provides an explanation to the enigmatic 'alisphenoid bridge,' an autapomorphic structure described in one specimen of *Placodus* (SMF R 359; see Nosotti and Rieppel, 2002) of unknown function or affiliation. It now appears that what was once thought to be a 'bridge' of bone is in fact a damaged dorsum sellae with its ventral portion missing, an interpretation first made by Hopson (1979). Clinoid processes that emerge from the basisphenoid are expected to be present in placodonts (Rieppel, 1989, 1993) and were described in *Placodus* by Nosotti and Rieppel (2002). However, they are not visible in our CT data for either specimen (online Supplementary Figures 1, 3). In UMO BT13, what could be interpreted as clinoid processes appear to be parts of the broken dorsum sellae. Alternatively, these processes may indeed be present, but are so closely associated with the dorsum sellae that identifying them is difficult, thus explaining why they do not appear in our reconstruction of this region in BSP 1968 I 75.

From an embryological perspective, a more or less generalized condition can be seen in *Placodus* (Rieppel, 1993), with elements of the acrochordal cartilage (dorsum sellae) and the ossified hypophyseal fenestra (sella turcica and the foramina for the abducens nerves and cerebral carotids) being closely associated. Although there is no evidence of an ossified pila antotica, clinoid processes may be present but unobserved. The position of the trigeminal nerve is unusual for reptiles in that it is fully enclosed by the prootic, which would have ossified from embryonic pila metoptica. However, the plesiomorphic condition would see the trigeminal nerve pass between the pila metoptica and the dorsum sellae. This extension of the prootic may be related to the alar process seen in some lepidosaurs (Rieppel, 1993). Alternatively, it may be a functional autapomorphy of *Placodus*, providing additional support to the rostral portion of the braincase and reinforcing it from the high stresses resulting from durophagous feeding.

Vestibular System

The inner ear provides a sense of balance as well as allowing organisms to accurately coordinate body movements (Sipla and Spoor, 2008). It is therefore important to examine this structure in secondarily aquatic animals, such as *Placodus*, because aquatic habitats place different demands on the vestibular system than do terrestrial ones. Unfortunately, the structure of the inner ear is poorly understood in most extinct marine reptiles, with the exception of some work on mosasaurs (Georgi and Sipla, 2008; Polcyn, 2010), and some limited information on ichthyosaurs (McGowan, 1973). However, the vestibular apparatus from a range of extant secondarily aquatic reptiles and birds have been examined by Georgi and Sipla (2008), who observed that increasingly aquatic taxa exhibit decreased aspect ratios of the vertical semicircular canals, i.e., decreasing height and/or increasing width. The vertical semicircular canals in *Placodus* are dorsoventrally flattened and rostrocaudally extended (Fig. 5D–F), a morphology that is consistent with the results of Georgi and Sipla (2008). This would seem to indicate that despite the relatively basal position of *Placodus* within the Sauropterygia, it shows a significant amount of adaptation to life in aquatic environments. However, it is worthy of note that the basal terrestrial neodiapsid *Youngina* has also been reconstructed as having somewhat dorsoventrally compressed semicircular canals, although they do not show the same degree of rostrocaudal extension as *Placodus* (Gardner et al., 2010). This could indicate that compressed semicircular canals are basal for neodiapsids and could possibly be an exaptation in *Placodus*. Further study into this region in other placodonts and sauropterygians in general would therefore be useful.

In addition, several authors have argued that when the lateral semicircular canal is placed in a near horizontal orientation, the head is in an 'alert' position, i.e., ideally placed for the animal to be at its most alert and comfortable (Witmer and Ridgely, 2009, and references therein). When this orientation is calculated for *Placodus*, the skull inclines by about 20° (Fig. 5C). This could be interpreted as an adaptation for maximizing the efficiency of binocular vision by dipping the head to remove structures such as the snout from the field of view, as is the case in pterosaurs (Witmer et al., 2003), owls (Witmer et al., 2008), and some theropod dinosaurs (Stevens, 2006; Witmer and Ridgely, 2009). However, it is unlikely that *Placodus* would have required unobstructed binocular vision, because it most likely fed on sessile prey. An alternative interpretation is that this inclined posture would have been an adaptation for feeding in a three-dimensional aquatic environment, with the head at the level of the sea floor and the rest of the body further up in the water column at a 20° angle. This would have been aided by the partially pachyostotic skull (Nosotti and Rieppel, 2002; Rieppel, 2002), the fully pachyostotic limb bones (Buffrénil and Mazin, 1992; Ricqlès and Buffrénil, 2001), and also by the osteosclerotic armor plates (Scheyer, 2007). Thus, *Placodus* had an 'alert' head position ideally suited for feeding in an aquatic environment whilst maintaining constant vigilance for predators; further evidence of its adaptation to a highly aquatic lifestyle, despite its phylogenetic position.

CONCLUSION

The braincase of *Placodus* was a robust, well-ossified structure, and appears to have been ideally suited for supporting the skull from the stresses and strains of a durophagous diet. As one of the most plesiomorphic members of the Sauropterygia (Fig. 1), the degree of adaptation to a marine lifestyle was previously unknown. New data obtained by μCT scanning have shown that *Placodus* was probably well adapted to feeding and functioning efficiently under water.

In addition, the exact morphology of the sphenoid region has also been addressed, revising the position of the internal carotid foramina, confirming the position of the hypophyseal pit, and determining that the dorsum sellae had previously been misinterpreted as an 'alisphenoid bridge.' Given the taxonomic position of *Placodus* within Placodontia on the one hand and the sister-group relationship of the whole group with all remaining Eosauropterygia on the other, these new data will serve as valuable basis for braincase and inner ear character evolution and polarity assessment in future studies.

ACKNOWLEDGMENTS

Sincere thanks go to J. Rabold and S. Eggmaier (UMO, Bayreuth) as well as M. Moser and O. Rauhut (BSPG, Munich) for allowing access to the specimens and giving permission for them to be scanned. We are indebted to S. Nosotti, N. M. Gardner, F. R. O'Keefe, and an anonymous reviewer for their helpful comments that improved the quality of this publication. Our thanks also go to L. Rager (PIMUZ, Zurich) and A. Caromel (University of Bristol) for help with model segmentation, and the members of the PIMUZ for useful discussions and technical support. We are also grateful to W. Leis (Hochschule Aalen) for aiding us with the CT scanning itself. This study was funded by the Swiss National Science Foundation (grant no. 31003A 127053 to T.M.S.).

LITERATURE CITED

Agassiz, L. 1833–45. Recherches sur les Poissons Fossiles. Four volumes. Imprimaire de Petitpierre, Neuchâtel, 336 pp.

Broili, F. 1912. Zur Osteologie des Schädels von *Placodus*. Palaeontographica 59:149–155.

Buffrénil, V. de, and J.-M. Mazin. 1992. Contribution de l'histologie osseuse à l'interprétation paléobiologique du genre *Placodus* Agassiz, 1833 (Reptilia, Placodontia). Revue de Paléobiologie 11:397–407.

Drevermann, F. 1933. Die Placodontier. 3. Das Skelett von *Placodus gigas* Agassiz im Senckenberg-Museum. Abhandlungen der Senckenbergischen Naturforschenden Gesellschaft 38:319–364.

Edinger, T. 1925. Das Zentralnervensystem von *Placodus gigas* Ag. Abhandlungen der Senckenbergischen Naturforschenden Gesellschaft 38:311–318.

Fernández, M. S., A. Paulina Carabajal, Z. Gasparini, and G. Chong Díaz. 2011. A metriorhynchid crocodyliform braincase from Northern Chile. Journal of Vertebrate Paleontology 31:369–377.

Gardner, N. M., C. M. Holliday, and F. R. O'Keefe. 2010. The braincase of *Youngina capensis* (Reptilia, Diapsida): new insights from high-resolution CT scanning of the holotype. Palaeontologia Electronica 13(2):Article 19. Available at http://palaeo-electronica.org/2010_3/217/index.html.

Georgi, J. A., and J. S. Sipla. 2008. Comparative and functional anatomy of balance in aquatic reptiles and birds; pp. 233–256 in J. G. M. Thewissen and S. Nummela (eds.), Sensory Evolution on the Threshold: Adaptations in Secondarily Aquatic Vertebrates. University of California Press, Berkeley, California.

Hopson, J. A. 1979. Paleoneurology; pp. 39–146 in C. Gans, R. G. Northcutt, and P. Ulinski (eds.), Biology of the Reptilia, Volume 9: Neurology A. Academic Press, London.

Janensch, W. 1936. Über Bahnen von Hirnvenen bei Saurischiern und Ornithischiern, sowie einigen anderen fossilen und rezenten Reptilien. Paläontologische Zeitschrift 18:181–198.

Jiang, D.-Y., R. Motani, W.-C. Hao, O. Rieppel, Y.-L. Sun, L. Schmitz, and Z.-Y. Sun. 2008. First record of Placodontoidea (Reptilia, Sauropterygia, Placodontia) from the Eastern Tethys. Journal of Vertebrate Paleontology 28:904–908.

Mazin, J.-M., and G. Pinna. 1993. Palaeoecology of the armoured placodonts. Paleontologia Lombarda della Società Italiana di Scienze Naturali e del Museo Civico di Storia Naturale di Milano, Nuova serie 2:83–91.

McGowan, C. 1973. The cranial morphology of the Lower Liassic latipinnate ichthyosaurs of England. Bulletin of the British Museum (Natural History) Geology 24:1–109.

Menning, M., B. Schröder, E. Plein, T. Simon, J. Lepper, H.-G. Röhling, C. Heunisch, K. Stapf, H. Lützner, K.-C. Käding, J. Paul, M. Horn, H. Hagdorn, G. Beutler, and E. Nitsch. 2011. Beschlüsse der

Deutschen Stratigraphischen Kommission 1991–2010 zu Perm und Trias von Mitteleuropa. Zeitschrift der Deutschen Gesellschaft für Geowissenschaften 162:1–18.

Nosotti, S., and G. Pinna. 1993. New data on placodont skull anatomy. Paleontologia Lombarda della Società Italiana di Scienze Naturali e del Museo Civico di Storia Naturale di Milano, Nuova serie 2:109–114.

Nosotti, S., and G. Pinna. 1999. Skull anatomy of *Protenodontosaurus italicus* Pinna, 1990 (Reptilia, Placodontia). Paleontologia Lombarda della Società Italiana di Scienze Naturali e del Museo Civico di Storia Naturale di Milano, Nuova serie 11:3–17.

Nosotti, S., and O. Rieppel. 2002. The braincase of *Placodus* Agassiz, 1833 (Reptilia, Placodontia). Memoire della Società Italiana di Scienze Naturali e del Museo Civico di Storia Naturale di Milano 31:3–18.

Polcyn, M. 2010. Sensory adaptations in mosasaurs. Journal of Vertebrate Paleontology, Program and Abstracts 2010:146A.

Ricqlès, A. de, and V. de Buffrénil. 2001. Bone histology, heterochronies and the return of tetrapods to life in water: were are we?; pp. 289–310 in J.-M. Mazin and V. de Buffrénil (eds.), Secondary Adaptations of Tetrapods to Life in Water. Verlag Dr. Friedrich Pfeil, Munich.

Rieppel, O. 1989. A new pachypleurosaur (Reptilia: Sauropterygia) from the Middle Triassic of Monte San Giorgio, Switzerland. Philosophical Transactions of the Royal Society of London, Series B 323:1–73.

Rieppel, O. 1993. Patterns of diversity in the reptilian skull; pp. 344–390 in J. Hanken and B. K. Hall (eds.), The Skull, Volume 2: Patterns of Structural and Systematic Diversity. University of Chicago Press, Chicago, Illinois.

Rieppel, O. 1995. The genus *Placodus*: systematics, morphology, paleobiogeography, and paleobiology. Fieldiana: Geology, New Series 31:1–44.

Rieppel, O. 2000a. *Paraplacodus* and the phylogeny of the Placodontia (Reptilia: Sauropterygia). Zoological Journal of the Linnean Society 130:635–659.

Rieppel, O. 2000b. Sauropterygia I: Placodontia, Pachypleurosauria, Nothosauroidea, Pistosauroidea. Encyclopedia of Paleoherpetology, Volume 12A. Verlag Dr. Friedrich Pfeil, Munich, 134 pp.

Rieppel, O. 2001. The cranial anatomy of *Placochelys placodonta* Jaekel, 1902, and a review of the Cyamodontoidea (Reptilia, Placodonta). Fieldiana: Geology, New Series 45:1–104.

Rieppel, O. 2002. Feeding mechanics in Triassic stem-group sauropterygians: the anatomy of a successful invasion of Mesozoic seas. Zoological Journal of the Linnean Society 135:33–63.

Sato, T., X.-C. Wu, A. Tirabasso, and P. Bloskie. 2011. Braincase of a polycotylid plesiosaur (Reptilia: Sauropterygia) from the Upper Cretaceous of Manitoba, Canada. Journal of Vertebrate Paleontology 31:313–329.

Scheyer, T. M. 2007. Skeletal histology of the dermal armor of Placodontia: the occurrence of 'postcranial fibro-cartilaginous bone' and its developmental implications. Journal of Anatomy 211:737–753.

Scheyer, T. M., J. M. Neenan, S. Renesto, F. Saller, H. Hagdorn, H. Furrer, O. Rieppel, and A. Tintori. 2012. Revised paleoecology of placodonts—with a comment on 'The shallow marine placodont *Cyamodus* of the central European Germanic Basin: its evolution, paleobiogeogtaphy and paleoecology' by C.G. Diedrich (Historical Biology, iFirst article, 2011, 1–19, doi: 10.1080/08912963.2011.575938). Historical Biology 24:257–267.

Sipla, J. S., and F. Spoor. 2008. The physics and physiology of balance; pp. 227–232 in J. G. M. Thewissen and S. Nummela (eds.), Sensory Evolution on the Threshold: Adaptations in Secondarily Aquatic Vertebrates. University of California Press, Berkeley, California.

Smith, D. K., L. E. Zanno, R. K. Sanders, D. D. Deblieux, and J. I. Kirkland. 2011. New information on the braincase of the North American therizinosaurian (Theropoda, Maniraptora) *Falcarius utahensis*. Journal of Vertebrate Paleontology 31:387–404.

Spoor, F., S. Bajpai, S. T. Hussain, K. Kumar, and J. G. M. Thewissen. 2002. Vestibular evidence for the evolution of aquatic behaviour in early cetaceans. Nature 417:163–166.

Stevens, K. A. 2006. Binocular vision in theropod dinosaurs. Journal of Vertebrate Paleontology 26:321–330.

Sues, H.-D. 1987. On the skull of *Placodus gigas* and the relationships of the Placodontia. Journal of Vertebrate Paleontology 7:138–144.

Tanner, J. B., E. R. Dumont, S. T. Sakai, B. L. Lundrigan, and K. E. Holekamp. 2008. Of arcs and vaults: the biomechanics of bone-cracking in spotted hyenas (*Crocuta crocuta*). Biological Journal of the Linnean Society 95:246–255.

Witmer, L. M., and R. C. Ridgely. 2009. New insights into the brain, braincase, and ear region of tyrannosaurs (Dinosauria, Theropoda), with implications for sensory organization and behavior. The Anatomical Record 292:1266–1292.

Witmer, L. M., S. Chatterjee, J. Franzosa, and T. Rowe. 2003. Neuroanatomy of flying reptiles and implications for flight, posture and behaviour. Nature 425:950–953.

Witmer, L. M., R. C. Ridgely, D. L. Dufeau, and M. C. Semones. 2008. Using CT to peer into the past: 3D visualization of the brain and ear regions of birds, crocodiles, and nonavian dinosaurs; pp. 67–88 in H. Endo and R. Frey (eds.), Anatomical Imaging: Towards a New Morphology. Springer-Verlag, Tokyo.

Submitted February 21, 2012; revisions received April 12, 2012;
accepted May 7, 2012.
Handling editor: Robin O'Keefe.

SUPPLEMENTAL INFORMATION FOR:

The braincase and inner ear of *Placodus gigas* (Sauropterygia, Placodontia) – a new reconstruction based on micro-computed tomographic data

JAMES M. NEENAN[*,1] and TORSTEN M. SCHEYER[1]

[1]Paleontological Institute and Museum, University of Zurich, Karl-Schmid-Strasse 4, 8006 Zurich, Switzerland, james.neenan@pim.uzh.ch

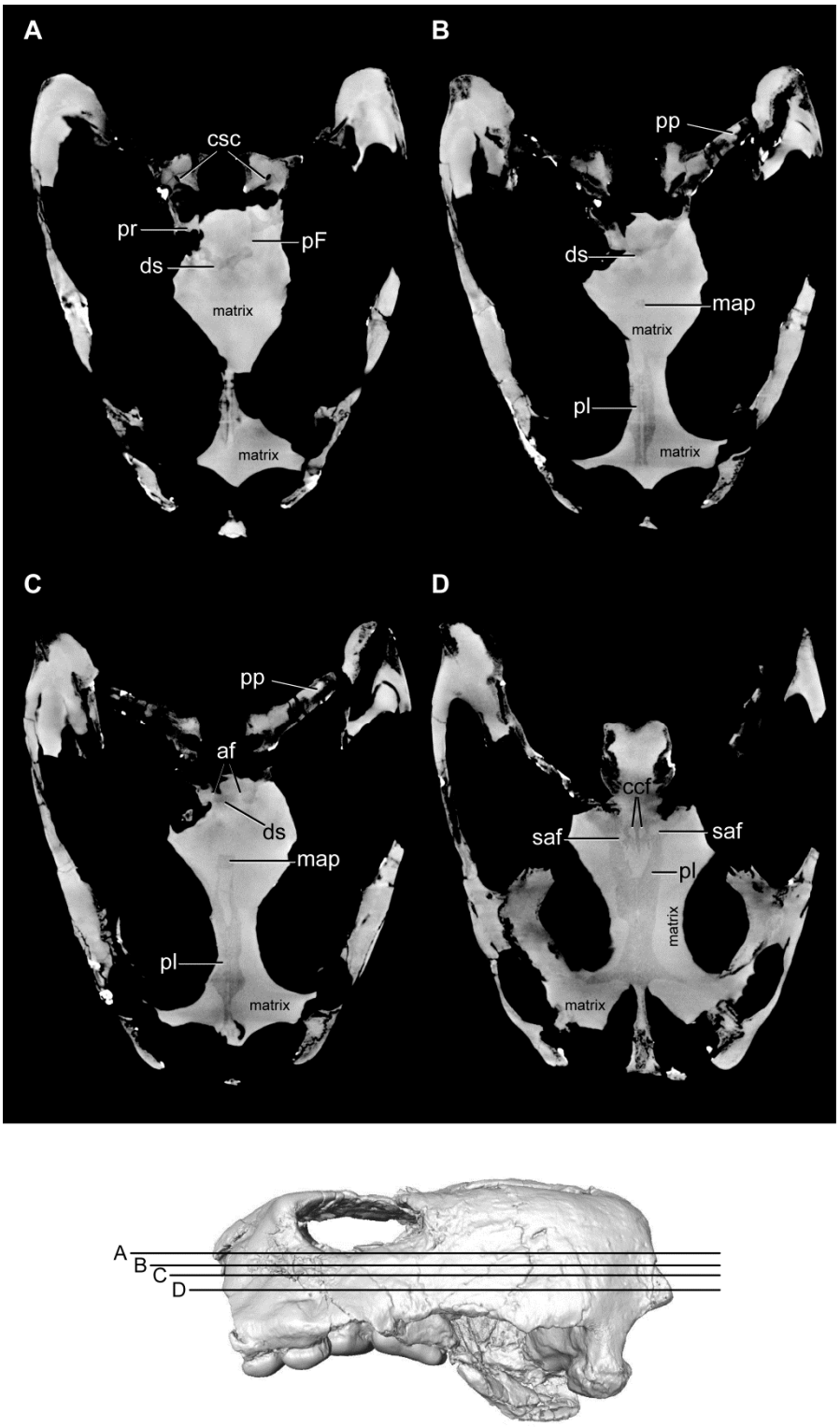

FIGURE S1. Transverse sections through BSP 1968 I 75 with areas of the sphenoid region and basicranium labeled. **A**, slice 521. **B**, slice 500. **C**, slice 486. **D**, slice 450. **Abbreviations**: **af**, abducens nerve foramen; **ccf**, cerebral carotid foramina; **csc**, caudal semicircular canal; **ds**, dorsum sellae; **map**, medial ascending process; **pl**, palatine; **pp**, paroccipital process; **pF**, prootic fenestra; **pr**, prootic; **saf**, sphenoid artery foramen.

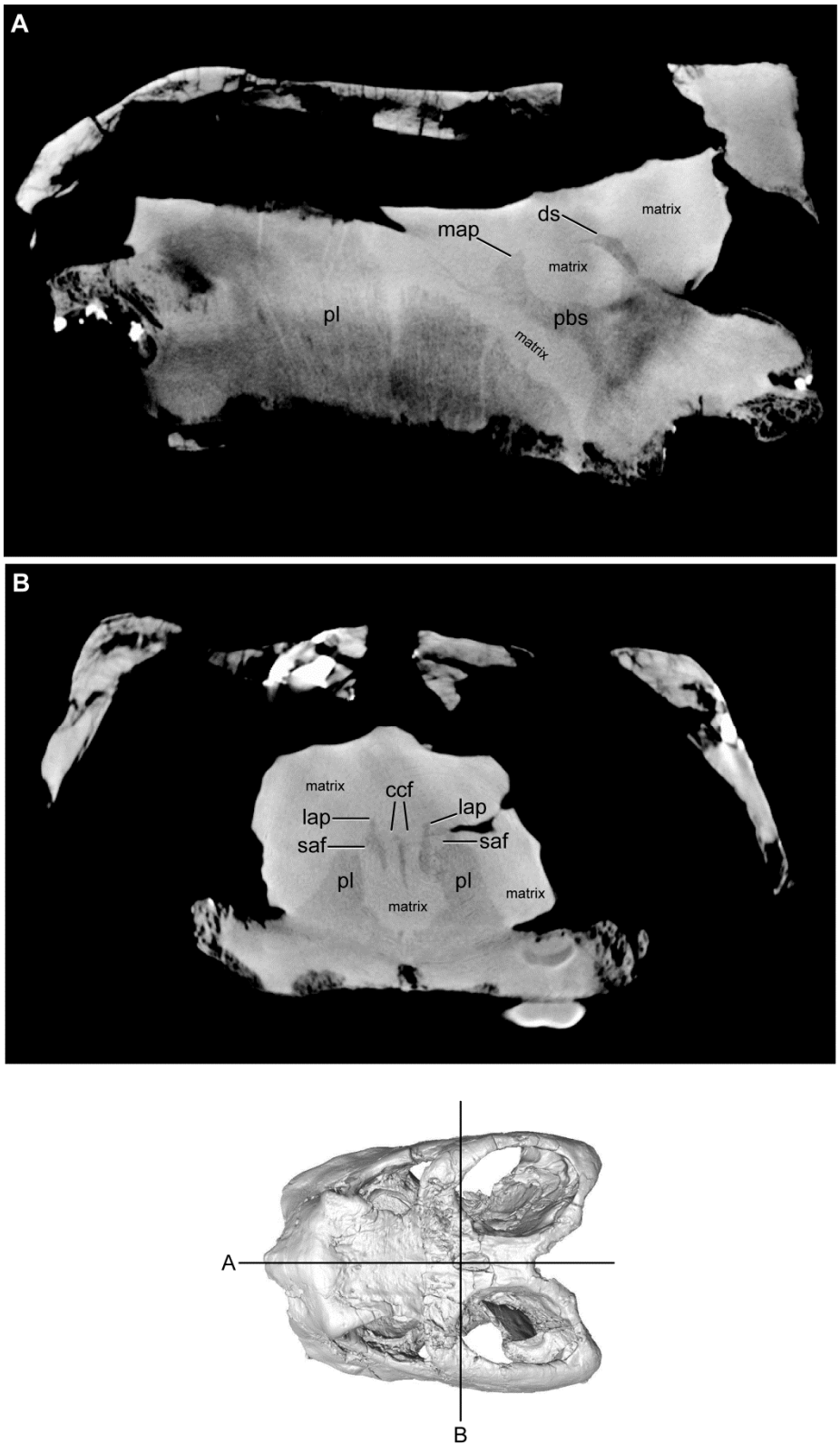

FIGURE S2. Sagittal (**A**) and coronal (**B**) slices through BSP 1968 I 75 with areas of the basicranium areas of the sphenoid region and basicranium labeled. **A**, slice 398. **B**, slice 496. Not to scale. **Abbreviations**: **ccf**, cerebral carotid foramina; **ds**, dorsum sellae; **lap**, lateral ascending process; **map**, medial ascending process; **pbs**, parabasisphenoid; **pl**, palatine; **saf**, sphenoid artery foramen.

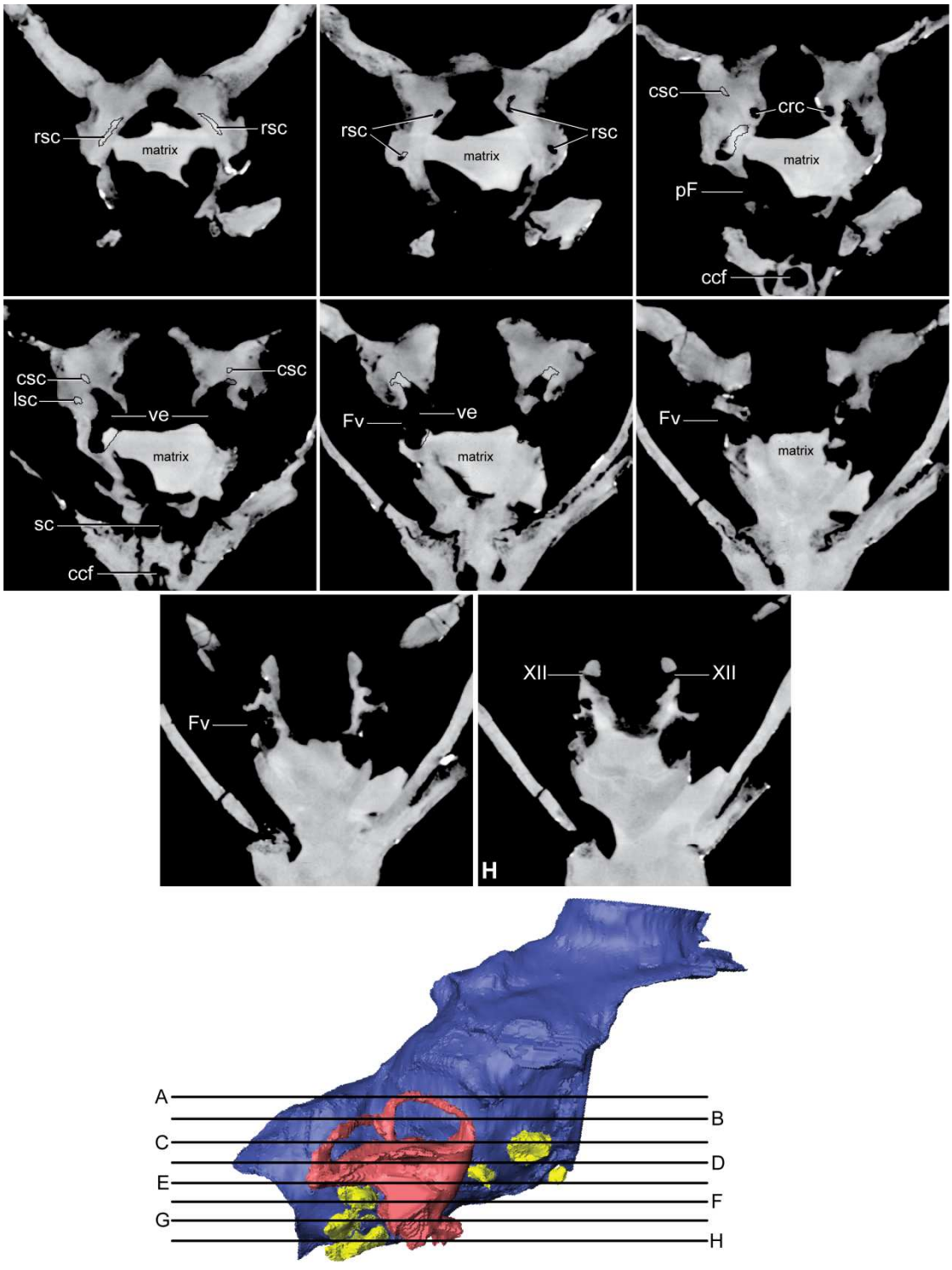

FIGURE S3. Transverse sections though the braincase of UMO BT 13 with areas of the endosseous labyrinth and basicranium labeled. Regions of the labyrinth that are infilled with matrix are outlined in black. **A**, slice 234. **B**, slice 224. **C**, slice 214. **D**, slice 204. **E**, slice 194. **F**, slice 184. **G**, slice 174. **H**, slice 164. **Abbreviations**: **ccf**, cerebral carotid foramina; **crc**, crus communis; **csc**, caudal semicircular canal; **Fv**, fenestra vestibuli; **lsc**, lateral semicircular canal; **rsc**, rostral semicircular canal; **sc**, sagittal crest; **ve**, vestibuli of inner ear; **XII**, hypoglossal nerve canal.

CHAPTER 4

EUROPEAN ORIGIN OF PLACODONT MARINE REPTILES AND THE EVOLUTION OF CRUSHING DENTITION IN PLACODONTIA

Palatodonta bleekeri by Jaime Chirinos

nature COMMUNICATIONS

ARTICLE

Received 8 Aug 2012 | Accepted 21 Feb 2013 | Published 27 Mar 2013

DOI: 10.1038/ncomms2633

European origin of placodont marine reptiles and the evolution of crushing dentition in Placodontia

James M. Neenan[1], Nicole Klein[2] & Torsten M. Scheyer[1]

Sauropterygia was the most successful marine reptile radiation in history, spanning almost the entire Mesozoic and exploiting a wide range of habitats and ecological niches. Here we report a new, exceptionally preserved skull of a juvenile stem placodont from the early Middle Triassic of the Netherlands, thus indicating a western Tethyan (European) origin for Placodontia, the most basal group of sauropterygians. A single row of teeth on an enlarged palatine supports this close relationship, although these are small and pointed instead of broad and flat, as is the case in placodonts, which demonstrate the strongest adaptation to a durophagous diet known in any reptile. Peg-like, slightly procumbent premaxillary teeth and an 'L-shaped' jugal also confirm a close relationship to basal placodonts. The new taxon provides insight into the evolution of placodont dentition, representing a transitional morphology between the plesiomorphic diapsid condition of palatal denticles and the specialized crushing teeth of placodonts.

[1] Palaeontological Institute and Museum, University of Zurich, Karl Schmid-Strasse 4, Zurich CH-8006, Switzerland. [2] Steinmann Institute for Geology, Mineralogy and Palaeontology, University of Bonn, Nussallee 8, Bonn 53115, Germany. Correspondence and requests for materials should be addressed to T.M.S. (email: tscheyer@pim.uzh.ch).

Sauropterygia is the most diverse group of marine reptiles known[1,2], with a variety of morphologies, ecologies and life history strategies that included the armoured, durophagous placodonts[3], the predatory, shallow marine pachypleurosaurs and nothosaurs[4], and the obligate swimming, viviparous plesiosaurs[5]. The group spanned around 180 myr, from the upper Lower Triassic to the Cretaceous–Palaeogene boundary (~245–65.5 mya[6,7]). Despite a global geological distribution and extensive fossil record (at least in Europe and Asia), it is still unclear where the clade originated, especially in the light of new discoveries from China[8]. Indeed, recent studies on pachypleurosaur phylogeny have suggested that despite the basalmost placodont being from Europe[9], the clade may have originated in the Eastern Tethys[10,11].

Here we present a new fossil skull of a juvenile sauropterygian from early Middle Triassic deposits of Winterswijk, the Netherlands. The fossil displays a suite of morphological characters identifying it as a stem placodont, emphasizing the role of the western Tethys (present day Europe and western Middle East) as a Middle Triassic marine reptile biodiversity hotspot (over 60 species, see compilation in Kelley *et al.*[12]). Although the skull lacks a heavily specialized dentition adapted for crushing hard-shelled prey, features such as an elongated palatine bone carrying a single row of pointed teeth strongly support that the new taxon is not only basal to all placodonts but, combined with its early stratigraphic age, also implies that the clade originated in Europe, spreading eastwards to the Eastern Tethys.

Although the placodonts have been studied since the 1830s[13], the evolutionary origin of their highly specialized durophagous dentition has, until now, remained unknown. The new fossil thus provides the unique opportunity to describe, for the first time, the dentition of a stem placodont, and enables us to pinpoint the developmental changes necessary to create the transition from a generalized piercing dentition with interlocking conical teeth to the extreme form of crushing dentition found in these reptiles.

Results

Systematic palaeontology. Sauropterygia Owen, 1860; Placodontiformes tax. nov.; *Palatodonta bleekeri* gen. et sp. nov.

Etymology. *Palato-*, from the Latin 'palatum', meaning of the palatine bone; *-donta*, from the ancient Greek 'odon', meaning tooth; *bleekeri*, after the discoverer, Remco Bleeker, Goor, the Netherlands.

Holotype. TW480000470 (Fig. 1; Supplementary Figs S1 and S2), Twentse Welle Museum, Enschede, the Netherlands.

Locality and horizon. Vossenveld Formation[14], Lower Muschelkalk (early Anisian), Winterswijk, the Netherlands. The horizon corresponds to layer 9 of Oosterink[15].

Diagnosis. Premaxilla large with distinct, narrow caudal process running between external nares and containing four blunt, peg-like, slightly procumbent teeth; a single row with at least 10 narrow, pointed teeth on the palatine; maxilla excluded from orbit and containing at least six pointed teeth; parietal with distinct caudolateral bulge located near dorsal margin of upper temporal fenestra; upper temporal fenestra laterally placed; jugal distinctly open L-shaped (boomerang-shaped); postorbital with distinct caudal process; quadratojugal absent; and excavated cheek region.

Description. The type and only known specimen is of a juvenile individual and has a high, blunt-snouted skull preserved in right lateral view, with the exception of the right parietal, the premaxillae and nasals, which are preserved in dorsal view (Fig. 1; for a detailed morphological description, see Supplementary Note 1 and Supplementary Movie). The left parietal and left splenial are disarticulated, and preserved in a position just dorsal to the skull itself. The posterior part of the maxilla was removed during preparation, and extended caudally to meet the

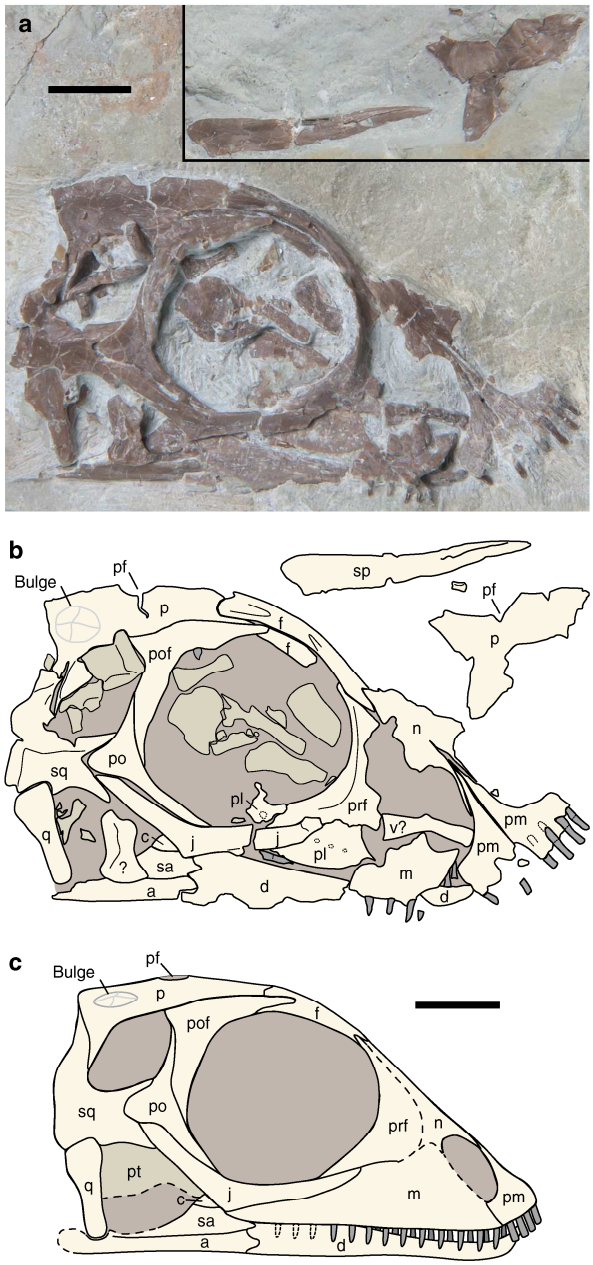

Figure 1 | *Palatodonta bleekeri* genus et species nova holotype (TW480000470). (**a**) Right lateral view of the specimen with disarticulated elements inset. (**b**) Labelled interpretation. (**c**) Reconstruction in lateral view. a, angular; c, coronoid; d, dentary; f, frontal; j, jugal; m, maxilla; n, nasal; p, parietal; pf, pineal foramen; pl, palatine; pm, premaxilla; po, postorbital; pof, postfrontal; prf, prefrontal; pt, pterygoid; q, quadrate; sa, surangular; sp, splenial; sq, squamosal; v, vomer. Scale bar, 3 mm.

jugal, containing at least six pointed teeth (Supplementary Figs S1 and S2a). *Palatodonta* can be identified as a sauropterygian, as the premaxilla forms most of the snout rostral to external nares; a lacrimal being absent; an upper temporal fenestra and a lower temporal fenestra that open ventrally; a suborbital fenestra being absent; and teeth on the pterygoid flange being absent.

Several disarticulated elements that do not belong to the skull are preserved in this specimen, mostly within the orbit. We speculate that they are mostly from the postcranium, some of which are phalanges. In addition, a disarticulated tooth is visible between the mandible and jugal, probably originating from the right dentary, but may have been from the palatine or maxilla (Supplementary Fig. S2c). However, its robust appearance would indicate a caudal position in the skull as, in the dentary at least, posterior teeth are generally more massive (Fig. 2a,e). Another disarticulated tooth is visible at the dorsal margin of the orbit, in contact with the postfrontal. The teeth are heterogeneous, with different tooth-bearing elements displaying different tooth morphologies (Supplementary Fig. S2). The premaxillary teeth are blunt, peg-like, procumbent and have long roots, roughly equal to the length of the crowns. They are somewhat similar in morphology to that of the basal placodont *Placodus*, which would have used these teeth to pick up sessile, hard-shelled prey from the sea floor[16]. In fact, several placodont taxa exhibit procumbent, elongate teeth on the premaxilla, that is, *Paraplacodus*, *Placodus*, *Protenodontosaurus* and, to a lesser degree, *Cyamodus hildegardis*[4]. However, unlike *Placodus*, the premaxillary teeth of which are almost always disarticulated from the skull owing to a presumed fibrous attachment in the large alveolar spaces, the equivalent teeth in *Palatodonta* are articulated and firmly rooted within the bone[16]. All other teeth in *Palatodonta* are of extremely different morphology to those of placodonts, and are more similar to the expected plesiomorphic condition in that they are narrow and pointed instead of flattened and rounded (Supplementary Fig. S2).

Despite these differences, the skull of *Palatodonta* shows several similarities to the basal-most placodont *Paraplacodus*. The lower temporal fossa is open ventrally, with a highly excavated cheek region, the jugal is loosely 'L-shaped' and the quadrate is a simple bar, sutured dorsally to the squamosal. However, *Palatodonta* differs from other placodonts, with the exception of *Placodus*, in that the maxilla is excluded from the orbit and the jugal directly contacts the squamosal.

Additional micro-computed tomography (μCT) scanning provided insight into structures that were not visible on the outer surface of the slab. This revealed that only the right half of the skull was preserved and the left half was lost before fossilization. Using the μCT data, it was possible to reconstruct the entire right mandible, a large portion of the right palatine carrying a row of 10 pointed teeth, a large bone fragment interpreted as the right pterygoid, part of the basisphenoid and a variety of other, less diagnostic elements that most likely pertain to the braincase and the postcranium (Fig. 2).

The morphology of the palatine is particularly noteworthy, as it shares the condition of having a single row of teeth with the placodonts, although these are narrow and pointed in *Palatodonta*, instead of the round and flat shape typical for placodonts (Supplementary Fig. S3). In addition, the portion of the basisphenoid appears to be the hypophyseal pit, as it has a clear pair of foramina that we identify as the internal cerebral carotid foramina, similar to those seen in the placodonts *Placodus* and *Placochelys*[17,18] and is consistent with the plesiomorphic condition seen in the basal diapsid *Youngina*[19]. There are two ascending processes lateral to the cerebral carotid foramina, similar to those present in *Placodus*[17]. The pterygoid is arched and edentulous, comparable to the condition seen in placodonts, providing a flange at the caudolateral margin of the palate.

Phylogenetic analysis. A phylogenetic analysis (see Methods and Supplementary Note 2 for Bremer and Bootstrap support and

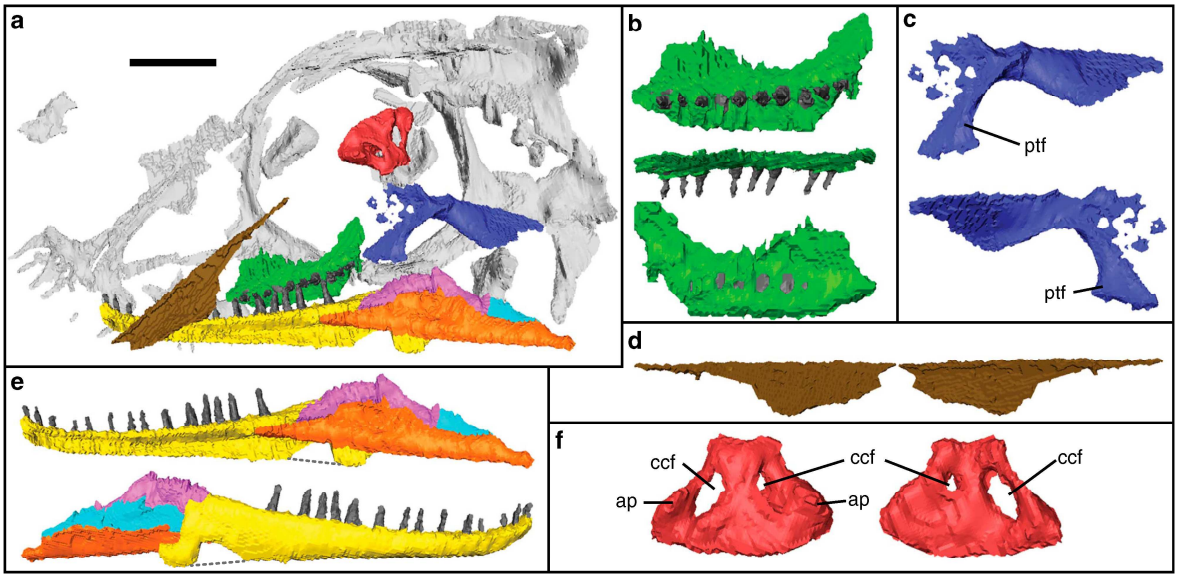

Figure 2 | Three-dimensional reconstruction of μCT data showing obscured elements. (**a**) Skull interior with obscured elements highlighted. red, basisphenoid; dark blue, pterygoid; green, palatine; brown, right splenial; yellow, dentary; pink, coronoid; light blue, surangular; orange, angular. (**b**) Palatine in ventral (top), lateral (middle) and dorsal (bottom) views. (**c**) Pterygoid in medial (top) and lateral (bottom) views. (**d**) Right splenial in lateral (left) and medial (right) views. (**e**) Right mandible in medial (top) and lateral (bottom) views. (**f**) Basisphenoid in dorsal (left) and ventral (right) views. ap, ascending process; ccf, cerebral carotid foramen; ptf, pterygoid flange. Scale bar, 3 mm, **b**–**f** not to scale.

Supplementary Note 3 for character description) revealed *Palatodonta* to be sister taxon to Placodontia, supported by a single unambiguous synapomorphy (no. 51, pterygoids are generally shorter in this group compared with the palatines) and moderate bootstrap and Bremer support values (Fig. 3; Supplementary Fig. S4; see Methods section below). On the other hand, the new taxon is clearly separated from Placodontia by missing two unambiguous synapomorphies, that is, the complete lack of durophagous dentition (no. 63) and having more than three premaxillary teeth (no. 64) (Fig. 4).

The first search run on the matrix included all taxa, which yielded three most parsimonious trees (MPTs), with the shortest tree length of 566 steps (Consistency index (CI) = 0.334, Retention index (RI) = 0.659, Rescaled consistency index (RC) = 0.220 and Homoplasy index (HI) = 0.666). The strict consensus tree (Fig. 3; Supplementary Fig. S5a) recovered a sistergroup relationship between archosauromorph taxa and the lepidosaur lineage, but a monophyletic Lepidosauromorpha (that is, Lepidosauria plus Sauropterygia) was not supported. Instead, there is a basal grade including ichthyosaurs, thalattosaurs and several other diapsid taxa leading to Sauropterygia. The proposed Placodontiformes taxon nov. is sister to a monophyletic Eosauropterygia. It is noteworthy that the pistosauroid clade, which includes the plesiosaurs, was found to be the sister taxon to the remaining eosauropterygians. Note the basal position of turtles

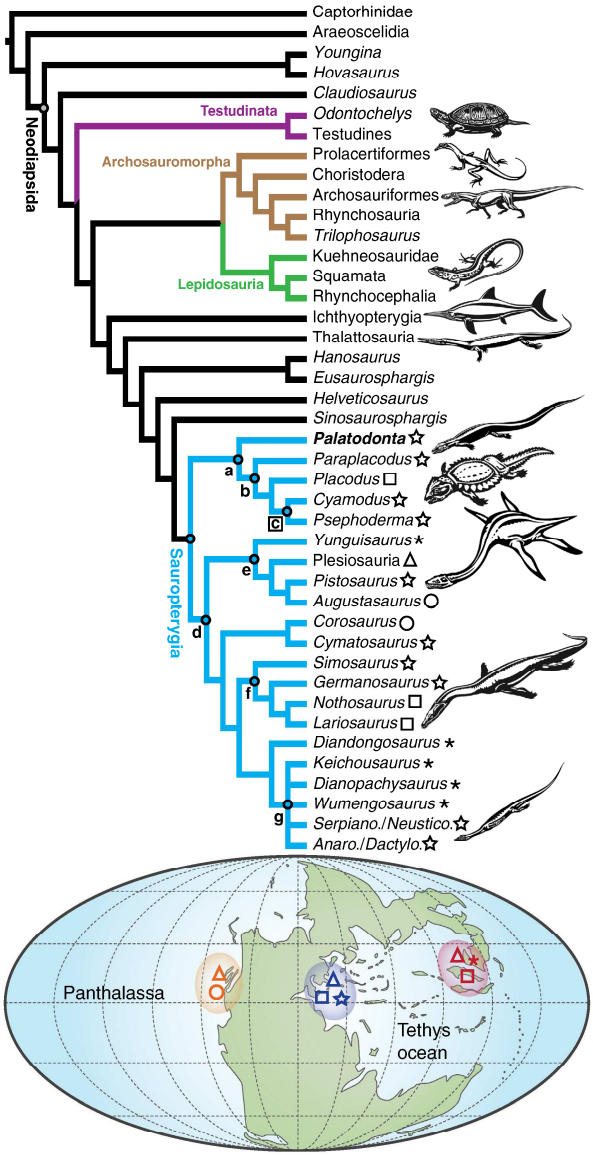

Figure 3 | Strict consensus tree showing the relationships of Sauropterygia within Diapsida combined with their geographic distribution. All scores equal 100, apart from those shown (tree description shown in Methods; Supplementary Fig. S5). (**a**) Placodontiformes (new taxon). (**b**) Placodontia. (**c**) Cyamodontoidea. (**d**) Eosauropterygia. (**e**) Pistosauroidea. (**f**) Nothosauroidea. (**g**) Pachypleurosauria. Taxa are indicated by symbols on a simplified map of the Middle Triassic (adapted from Blakey[57] and McKie and Williams[58]) with the eastern Tethyan province (red), western Tethyan province (dark blue) and eastern Panthalassic province (orange) highlighted.

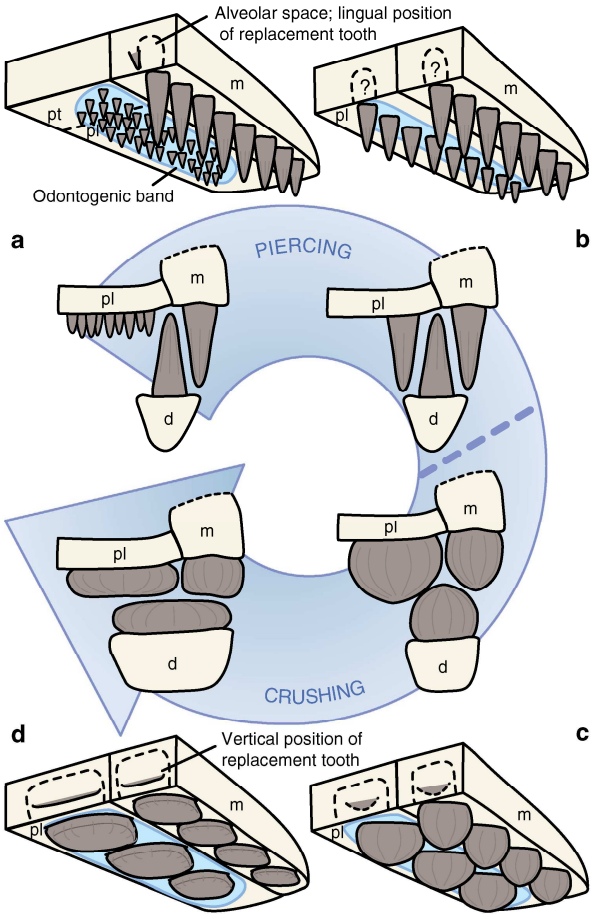

Figure 4 | Diagrammatic representation of tooth development of four taxa depicting the evolution from a pointed piercing dentition to a flattened crushing one. (**a**) Generalized stem neodiapsid showing the plesiomorphic condition of denticles on the palate. (**b**) *Palatodonta bleekeri* gen. et sp. nov., with a single row of pointed teeth on the palatine, maxilla and dentary. (**c**) The basal placodont *Paraplacodus*, with rounded teeth, more adapted for a crushing diet. (**d**) Typical dentition of *Placodus* and cyamodontoid placodonts, showing highly flattened and enlarged crushing teeth. Note that mode of tooth replacement is not known in *Palatodonta*. In *Paraplacodus*, vertical tooth replacement is inferred by presence of dentary replacement teeth in PIMUZ T2805. Abbreviations as in Fig. 1.

(*Odontochelys* and Testudines). The 50% majority rule consensus tree (Supplementary Fig. S5b) differs from the strict consensus only in the resolution within pachypleurosaurs.

The second search run on the matrix excluded Ichthyopterygia, yielding 85 MPTs, with the shortest tree length of 549 steps (CI = 0.344, RI = 0.666, RC = 0.229 and HI = 0.656). In comparison with the strict consensus tree in the first search run (Supplementary Fig. S5a), the exclusion of Ichthyopterygia led to a polytomy consisting of the archosaur and lepidosaur lineages, the turtles and the more highly nested diapsids (thalattosaurs to sauropterygians). The resolution is lower in Sauropterygia in the strict consensus compared with the first search run as well. In the 50% majority rule consensus (Supplementary Fig. S6b), *Corosaurus* is recovered as sister taxon to all remaining eosauropterygians, followed by the pistosauroid clade, with *Cymatosaurus* moving onto the stem of the latter.

The third run of the matrix excluded Ichthyopterygia and turtles (*Odontochelys* and Testudines), yielding 502 MPTs with the shortest tree length of 499 steps (CI = 0.355, RI = 0.673, RC = 0.239 and HI = 0.645). For this analysis, the number of trees retained was successively raised to 30 to acquire the shortest tree. Further increase to a 1,000 replicates and 100 retained trees per analysis led to the same topology of the strict consensus tree but differed in that all archosauromorph taxa were found in one polytomy in the 50% majority rule tree. This analysis yielded a poorly resolved strict consensus tree (Supplementary Fig. S7a) with polytomies in several sections of the cladogram. Especially, the resolution among the archosaur and lepidosaur lineages collapsed completely. The 50% majority rule consensus (Supplementary Fig. S7b) is somewhat better resolved, with sauropterygian ingroup relationships largely mirroring those shown in Supplementary Fig. S6b.

In the fourth analysis (with options set to 1,000 replicates and 100 trees retained), the all-zero ancestor, as well as Ichthyopterygia and turtles, were removed, and Captorhinidae and Araeoscelidia served as outgroups instead. Forty-seven MPTs were found with the shortest tree length of 520 (CI = 0.358, RI = 0.662, RC = 0.237 and HI = 0.642). Results were overall comparable to the outcome of the third run as indicated by the strict consensus (Supplementary Fig. S8), with relationships among Sauropterygia being slightly better resolved. Note that in this analysis, *Cymatosaurus* again moved onto the plesiosaur stem.

For the fifth analysis, the matrix was pruned to include only Sauropterygia as ingroup and *Sinosaurosphargis* as outgroup. Three MPTs were found with the shortest tree length of 315 (CI = 0.483, RI = 0.609, RC = 0.294 and HI = 0.517). Similar to the results of the first search run, a sistergroup relationship between *Corosaurus* and *Cymatosaurus* was recovered, but now this clade is sister to all remaining eosauropterygians. Ingroup relationships of the latter are not well resolved as indicated by polytomies in both the strict consensus (Supplementary Fig. S9a) and the 50% majority rule tree (Supplementary Fig. S9b).

Discussion

Palatodonta is clearly a juvenile specimen, owing to its small size (20.5 mm in length; see Supplementary Table S1 for a full list of measurements), relatively large orbit and lack of extensive bone fusion. Thus, its suitability for phylogenetic analysis was investigated using osteological comparisons with modern reptilian hatchlings and adults (turtles, non-varanoid squamate lizards and crocodylians). This lead us to the interpretation that, although overall proportions change during ontogeny and sutures might become obliterated with age, the suture patterns of this juvenile generally reflect the adult condition of the new species (see Bhullar *et al.*[20]). This is also supported by observations in pachypleurosaurs, which also do not change cranial bone configuration through ontogeny[21–23].

Palatodonta shares with the basal-most placodont *Paraplacodus* the distinctly open L-shaped jugal, as well as a ventrally open lower temporal fossa and excavated cheek region. The former character also appears convergently in *Claudiosaurus* and in some pachypleurosaurs, whereas the latter is a plesiomorphic condition for sauropterygians in general. The loss of the lower temporal fossa and closure of the cheek region is secondarily developed only among the more highly nested placodonts (*Placodus* and cyamodontoids[18,24]), the fusion of nasals found in the new skull is present only in some *Cyamodus* spp. so far, whereas the condition remains debatable in *Paraplacodus*.

Palatodonta is not a juvenile of any known placodont because juvenile specimens of *Paraplacodus* (Paläontologisches Institut und Museum Universität Zürich (PIMUZ) T2805) and the armoured cyamodontoid *Cyamodus* (PIMUZ T2797) show that, despite being of similar size, crushing dentition is already fully formed very early during ontogeny (Supplementary Fig. S3). Previous research shows that it is tooth formula that changes through placodont ontogeny, not shape[25].

Although *Palatodonta* shares several characters with *Paraplacodus*, the presence of pointed palatal teeth suggests that *Palatodonta* is a stem representative with a very different lifestyle and diet to crown group Placodontia. We hypothesize that the comb-like arrangement of blunt, peg-like premaxillary teeth in *Palatodonta* (Supplementary Fig. S2b) were used for sifting through soft sediments on the shallow ocean floor to root out small, soft prey items, whereas the more massive equivalent teeth in *Paraplacodus* and *Placodus* served to pluck hard-shelled prey from hardgrounds[3].

The palatine dentition in *Palatodonta* represents an intermediate condition between the denticles/teeth of stem neodiapsids[26], and the flattened, enlarged palatal crushing teeth seen in placodonts[4] (Fig. 4, Supplementary Note 1). An evidence-based scenario for this morphological transformation of dentition can thus be formulated.

In many Permian diapsid reptiles, clusters of small denticles or teeth are present on the vomer, palatine and pterygoid bones (Fig. 4a), thus an odontogenic band (a place of residence of stem cells active in tooth formation[27]) acting as precursor to dental lamina formation (Richman and Handrigan[28] and references therein) is assumed to be present in these ancient reptiles. In particular, the expression of *Shh* (Sonic hedgehog) and transcription factor *Pitx2* (pituitary homeobox 2) as part of a gene network with others (for example, *Wnt*- and *Bmp*-related pathways), must have had a critical role in palatal tooth formation[28,29]. These conserved pathways and proteins are not only important, for example, in patterning the central nervous system, in limb bud formation and internal organogenesis[30], but are also known to be active in tooth development from fish to mammals[31].

Compared with their Permian ancestors, the palatine of Placodontiformes increased in length and size relative to the vomer and the pterygoid, forming most of the palate, with the dentition of *Palatodonta* consisting of single row of conical palatine teeth similar to those of the maxillary tooth row (Fig. 4b). As indicated by studies of modern snakes[32], a rostral and caudal truncation of the developmental field or a suppression of growth factors by antagonistic morphogens[28] could have been responsible for the suppression of palatal teeth in the vomeral and pterygoidal regions in that taxon (Fig. 4a,b).

The dental formula was further modified in crown group Placodontia to be suited to a durophagous diet by reducing the number of ankylosed thecodont teeth[16] and allowing them to become larger and successively flattened (Fig. 4c,d), whereas at the same time, increasing the alveolar dimensions in the skull bones and the mandible. We can assume that the enamel

(=dental) organ forming placodont teeth was enlarged and flattened in the more derived placodonts in comparison with modern reptiles[28], probably filling most of the dental alveolar space, to generate the broad, sheet-like initial enamel secretion forming the top layer of the plate- or bean-shaped crushing teeth (including replacement teeth; Fig. 4). One means to achieve a size increase in teeth in mammals[33] is the suppression of apoptosis during early development (that is, suppressing *p21*, a cyclin-dependent kinase inhibitor), a mechanism associated with pathological macrodontia (anomalous enlargement of teeth). However, differences in apopotosis between reptile and mammal teeth are known, with apoptosis affecting the stellate reticulum in the former but occurring at the inner enamel epithelia in the latter[28]. A considerable increase in enamel organ dimension could then have caused a displacement of the successional dental lamina, so that tooth replacement became vertical (Fig. 4d) and not lingual to the functional tooth[16].

Although there is a general consensus that Sauropterygia are well nested within Diapsida[4,34], the exact relationships within and among groups are still debated. Our results indicate that pachypleurosaurs, together with nothosaurs, are highly nested within Sauropterygia (Fig. 3; Supplementary Fig. S4; Supplementary Notes 2 and 3). In contrast, it was previously widely accepted that the small- to medium-sized Pachypleurosauria represented the most plesiomorphic clade within Eosauropterygia, and palaeobiogeographic hypotheses favoured an origination of the whole group in the Eastern Tethyan realm[11]. This was supported, for example, by the occurrence of *Keichousaurus yuananensis* from the Jialingjiang Formation, Hubei Province, China, which is either late Early Triassic or early Middle Triassic in age[4,35]. New, yet to be described, sauropterygian material has recently been found in the Early Triassic (Spathian, Olenekian) of Chaohu, Anhui Province, however[36]. Given the fact that the geologically oldest eosauropterygians outside of Asia (*Corosaurus* from North America and Sauropterygia indet. from Europe[4]) also occur in the late Early Triassic, however, the western Tethys or the eastern Panthalassic ocean could potentially have been the site of origin for the clade as well (Fig. 3; Supplementary Fig. S4). Despite this, a robust node in all phylogenetic analyses conducted (see Supplementary Figs S5–S10) indicates that Placodontiformes originated in the Western Tethys, and from there diversified and migrated into the Eastern faunal province.

Methods

µCT scanning. Scanning was carried out with a Phoenix v tome x s (GE Phoenix X-ray; 240 kV) at the Steinmann Institute, University of Bonn, Germany, with a voltage of 170 kV and a current of 150 µA. A total of 1,501 images were taken without beam filtration, each with an exposure time of 667 ms, resulting in a voxel size of 0.055 mm. Stacks of digital CT images were produced with the VGStudio MAX 2.0 software (Volume Graphics) and served as the base for virtual three-dimensional reconstructions of the bony structures by means of the manual segmentation function of the software Avizo version 6.2.1.

Phylogenetic analysis. Analyses were run in PAUP 4.0b10 for Microsoft Windows 95/NT[37] using PaupUP[38] version 1.0.3.1. Trees resulting from the analyses were transformed using Mesquite[39] and the Adobe Photoshop Creative Suite. All analyses were run under parsimony setting using the heuristic search option, with all 140 characters being unordered and not weighted in any way. Furthermore, all characters were found to be parsimony-informative, no aspect of the tree topology was enforced and the ingroup was set to be monophyletic.

The character matrix used herein is based on the matrix of Liu *et al.*[11], which is itself based mainly on Rieppel *et al.*[40] (in return this matrix was based on Rieppel[41]). The original characters (7) and (120) were removed by Liu *et al.*[11] because they were found uninformative in their analysis, whereas two new characters (1) and (61) were added from Rieppel and Lin[10]. Note that the re-shuffling of characters by Liu *et al.*[11], in contrast to the matrices used by Li *et al.*[42], Shang *et al.*[43] or Wu *et al.*[44], is also adopted herein.

From the matrix used by Liu *et al.*[11], several character definitions of the matrix were modified and three new characters (138–140) have been introduced. On the other hand, a few of the original taxa used have been re-scored (*Cyamodus*, *Placodus*, *Wumengosaurus* and Younginiformes). Instead of Younginiformes, *Hovasaurus boulei*[45] (scoring followed mainly Currie[46] and Bickelmann *et al.*[47], as well as personal observation of specimens in the PIMUZ collections) and *Youngina capensis*[48] (scoring followed Smith and Evans[49] and Bickelmann *et al.*[47]) are used as terminal taxa, because the group was recently found to be paraphyletic[47].

On the other hand, several sauropterygian taxa new to the Liu *et al.*[11] matrix (*Diandongosaurus acutidentatus*, *Paraplacodus broilii*, *Psephoderma alpinum*; *Yunguisaurus liae* and *Palatodonta*; this paper), as well as thalattosaurs (scoring after Müller[50–52], Müller *et al.*[53], Liu and Rieppel[54], Li *et al.*[42] and personal observations of specimens in the PIMUZ collections), the stem turtle *Odontochelys semitestacea*[55], Ichthyopterygia and four additional neodiapsid taxa (*Eusaurosphargis dalsassoi*, *Sinosaurosphargis yunguiensis*, *Hanosaurus hupehensis* and *Helveticosaurus zollingeri*) have been added. The new matrix thus comprises 42 taxa (43 for those that include a hypothetical all-zero ancestor) and 140 informative characters in total. For the present study, less well-known or highly fragmentary Chinese sauropterygian taxa such as *Chinchenia*, *Kwangsisaurus*, *Sanchiaosaurus*[34,41,44] and *Largocephalosaurus*[56] were not included.

Bootstrapping and Bremer support. A first bootstrap analysis (based on 1,000 replicates) was performed on the matrix used in the first search run. This analysis shows a loss of resolution in large parts of the tree. However, the newly proposed Placodontiformes has a value of 78% (Supplementary Fig. S10a), with a Bremer support score of 3 for the clade. A second bootstrap analysis (again based on 1,000 replicates) was run on the data set of the third run (Ichthyopterygia and turtles removed), which also showed high support (75%) for Placodontiformes, while Bremer support score for the taxon remained at 3 (Supplementary Fig. S10b). Apart from these slightly different bootstrap values, the general topologies of the two trees did not change, with the exception of the all-zero ancestor and Captorhinidae forming a basal polytomy in Supplementary Fig. S10a, instead of a resolved grade in Supplementary Fig. S10b. The third bootstrap analysis (Supplementary Fig. S10c; also with 1,000 replicates) was performed on the pruned data set of the fifth analysis (Supplementary Fig. S9a). Here the bootstrap support and topology was generally similar to the previous analyses, although support for Placodontiformes is much higher at 91%, and *Wumengosaurus* now forms a clade with the European pachypleurosaurs (Supplementary Fig. S10c). Once again, the node Placodontiformes had a Bremer support score of 3.

Nomenclatural acts. This published work and the nomenclatural act it contains have been registered in ZooBank, the proposed online registration system for the International Code of Zoological Nomenclature (ICZN). The ZooBank LSIDs (Life Science Identifiers) can be resolved and the associated information viewed through any standard web browser by appending the LSID to the prefix 'http://zoobank.org/'. The LSID for this publication is: urn:lsid:zoobank.org:pub:2CC51C4F-03F2-4647-9829-99646F6DA78E.

References

1. Cheng, Y.-N., Wu, X.-C. & Ji, Q. Triassic marine reptiles gave birth to live young. *Nature* **432,** 383–386 (2004).
2. Motani, R. The evolution of marine reptiles. *Evol. Educ. Outreach* **2,** 224–235 (2009).
3. Scheyer, T. M. *et al.* Revised paleoecology of placodonts–with a comment on 'The shallow marine placodont *Cyamodus* of the central European Germanic Basin: its evolution, paleobiogeography and paleoecology' by C.G. Diedrich (Historical Biology, iFirst article, 2011, 1–19, doi:10.1080/08912963.2011.575938) *Hist. Biol.* **24,** 257–267 (2012).
4. Rieppel, O. *Handbook of Paleoherpetology* Vol 12A, 1–134 (Verlag Dr Friedrich Pfeil, Munich, 2000).
5. O'Keefe, F. R. & Chiappe, L. M. Viviparity and k-selected life history in a Mesozoic marine plesiosaur (Reptilia, Sauropterygia). *Science* **333,** 870–873 (2011).
6. Motani, R. Warm-blooded 'sea dragons'? *Science* **328,** 1361–1362 (2010).
7. Benson, R. B. J., Butler, R. J., Lindgren, J. & Smith, A. S. Mesozoic marine tetrapod diversity: mass extinctions and temporal heterogeneity in geological megabiases affecting vertebrates. *Proc. R. Soc. Lond. B* **277,** 829–834 (2010).
8. Rieppel, O. Phylogeny and paleobiogeography of Triassic Sauropterygia: problems solved and unresolved. *Palaeogeogr. Palaeoclimatol. Palaeoecol.* **153,** 1–15 (1999).
9. Rieppel, O. *Paraplacodus* and the phylogeny of the Placodontia (Reptilia: Sauropterygia). *Zool. J. Linn. Soc. Lond.* **130,** 635–659 (2000).
10. Rieppel, O. & Lin, K. Pachypleurosaurs (Reptilia: Sauropterygia) from the Lower Muschelkalk, and a review of the Pachypleurosauroidea. *Fieldiana, Geol.* **32,** 1–44 (1995).
11. Liu, J. *et al.* A new pachypleurosaur (reptilia: Sauropterygia) from the Lower Middle Triassic of Southwestern China and the phylogenetic relationships of Chinese pachypleurosaurs. *J. Vertebr. Paleontol.* **31,** 292–302 (2011).

12. Kelley, N. P., Motani, R., Jiang, D.-Y., Rieppel, O. & Schmitz, L. Selective extinction of Triassic marine reptiles during long-term sea-level changes illuminated by seawater strontium isotopes. *Palaeogeogr. Palaeoclimatol. Palaeoecol.* doi:10.1016/j.palaeo.2012.07.026 (2012).
13. Agassiz, L. *Recherches sur les Poissons Fossiles* Vol. I–V (Imprimaire de Petitpierre, 1833–1845).
14. Hagdorn, H. & Simon, T. Vossenveld formation. In LithoLex [Lithostratigraphisches Lexikon der Deutschen Stratigraphischen Kommission; online-database]. Hannover: BGR. Last updated 02.08.2010 [cited 4th March 2013], Record ID. 45. Available from: http://www.bgr.de/app/litholex/gesamt_ausgabe_neu.php?id=45 (2010).
15. Oosterink, H. W. & Winterswijk, II Geologiedeel De Triasperiode (geologie, mineralen en fossielen). *Wetenschappelijke Mededeling van de Koninklijke Nederlandse Natuurhistorische Vereniging* **178,** 1–120 (1986).
16. Rieppel, O. Tooth implantation and replacement in Sauropterygia. *Paläontol. Z* **75,** 207–217 (2001).
17. Neenan, J. M. & Scheyer, T. M. The braincase and inner ear of *Placodus gigas* (Sauropterygia, Placodontia)—a new reconstruction based on micro-computed tomographic data. *J. Vertebr. Paleontol.* **32,** 1350–1357 (2012).
18. Rieppel, O. The cranial anatomy of *Placochelys placodonta* Jaekel, 1902, and a review of the Cyamodontoidea (Reptilia, Placodonta). *Fieldiana, Geol.* **45,** 1–104 (2001).
19. Gardner, N. M., Holliday, C. M. & O'Keefe, F. R. The braincase of *Youngina capensis* (Reptilia, Diapsida): new insights from high-resolution CT scanning of the holotype. *Palaeontologia Electronica* **13,** 19A (2010).
20. Bhullar, B.-A. S. *et al.* Birds have paedomorphic dinosaur skulls. *Nature* **487,** 223–226 (2012).
21. Sander, P. A fossil reptile embryo from the Middle Triassic of the Alps. *Science* **239,** 780–783 (1988).
22. Sander, P. M. The pachypleurosaurids (Reptilia: Nothosauria) from the Middle Triassic of Monte San Giorgio (Switzerland) with the description of a new species. *Phil. Trans. R. Soc. Lond. B* **325,** 561–666 (1989).
23. Klein, N. Skull morphology of *Anarosaurus heterodontus* (Reptilia: Sauropterygia: Pachypleurosauria) from the Lower Muschelkalk of the Germanic Basin (Winterswijk, The Netherlands). *J. Vertebr. Paleontol.* **29,** 665–676 (2009).
24. Rieppel, O. The genus *Placodus*: systematics, morphology, paleobiogeography, and paleobiology. *Fieldiana, Geol.* **31,** 1–44 (1995).
25. Kuhn-Schnyder, E. Über das Gebiss von *Cyamodus. Mitteilungen aus dem Paläontologischen Institut der Universität Zürich* **1,** 174–188 (1959).
26. Romer, A. S. *Osteology of the reptiles* (University of Chicago Press, 1956).
27. Smith, M. M., Fraser, G. J. & Mitsiadis, T. A. Dental lamina as source of odontogenic stem cells: evolutionary origins and developmental control of tooth generation in gnathostomes. *J. Exp. Zool.* **312,** 260–280 (2009).
28. Richman, J. M. & Handrigan, G. R. Reptilian tooth development. *Genesis* **49,** 247–260 (2011).
29. Fraser, G. J. *et al.* An ancient gene network Is co-opted for teeth on old and new jaws. *PLoS Biol.* **7,** e1000031. doi:10.1371/journal.pbio.1000031 (2009).
30. Gilbert, S. F. *Developmental Biology* 9th edn (Sinauer Associates, Inc., 2010).
31. Fraser, G. J., Britz, R., Hall, A., Johanson, Z. & Smith, M. M. Replacing the first-generation dentition in pufferfish with a unique beak. *PNAS* **109,** 8179–8184 (2012).
32. Mahler, D. L. & Kearney, M. The palatal dentition in squamate reptiles: morphology, development, attachment, and replacement. *Fieldiana, Zool.* **108,** 1–61 (2006).
33. Kim, J.-Y. *et al.* Inhibition of apoptosis in early tooth development alters tooth shape and size. *J. Dent. Res.* **85,** 530–535 (2006).
34. Rieppel, O. The systematic status of *Hanosaurus hupehensis* (Reptilia, Sauropterygia) from the Triassic of China. *J. Vertebr. Paleontol.* **18,** 545–557 (1998).
35. Li, J.-L. A brief summary of the Triassic marine reptiles of China. *Vertebr. PalAsiat.* **44,** 99–108 (2006).
36. Jiang, D.-Y., Motani, R., Tintori, A., Rieppel, O. & Sun, Z.-Y. Two new Early Triassic marine reptiles from Chaohu, Anhui Province, South China. *J. Vertebr. Paleontol., SVP Program and Abstracts Book* 117 (2012).
37. Swofford, D. L. PAUP*. Phylogenetic Analysis Using Parsimony (*and Other Methods). Version 4 (Sinauer Associates, Sunderland, Massachusetts, 2003).
38. Calendini, F. & Martin, J.-F. PaupUP v1.0.3.1 A free graphical frontend for Paup* Dos software (2005).
39. Maddison, W. P. & Maddison, D. R. Mesquite: a modular system for evolutionary analysis. Version 2.75, http://mesquiteproject.org (2011).
40. Rieppel, O., Sander, P. M. & Storrs, G. W. The skull of the pistosaur *Augustasaurus* from the Middle Triassic of northwestern Nevada. *J. Vertebr. Paleontol.* **22,** 577–592 (2002).
41. Rieppel, O. The sauropterygian genera *Chinchenia*, *Kwangsisaurus*, and *Sanchiaosaurus* from the Lower and Middle Triassic of China. *J. Vertebr. Paleontol.* **19,** 321–337 (1999).
42. Li, C., Rieppel, O., Wu, X.-C., Zhao, L.-J. & Wang, L.-T. A new Triassic marine reptile from Southwestern China. *J. Vertebr. Paleontol.* **31,** 303–312 (2011).
43. Shang, Q.-H., Wu, X.-C. & Li, C. A new eosauropterygian from the Middle Triassic of eastern Yunnan Province, southwestern China. *Vertebr. PalAsiat.* **49,** 155–171 (2011).
44. Wu, X.-C., Cheng, Y.-N., Li, C., Zhao, L.-J. & Sato, T. New information on *Wumengosaurus delicatomandibularis* Jiang et al., 2008 (Diapsida: Sauropterygia), with a revision of the osteology and phylogeny of the taxon. *J. Vertebr. Paleontol.* **31,** 70–83 (2011).
45. Piveteau, J. Paleontologie de Madagascar, XIII.—amphibiens et reptiles permiens. *Ann. Paleontol.* **15,** 53–180 (1926).
46. Currie, P. J. *Hovasaurus boulei*, an aquatic eosuchian from the Upper Permian of Madagascar. *Palaeontol. Afr.* **29,** 99–168 (1981).
47. Bickelmann, C., Müller, J. & Reisz, R. R. The enigmatic diapsid *Acerosodontosaurus piveteaui* (Reptilia: Neodiapsida) from the Upper Permian of Madagascar and the paraphyly of 'younginiform' reptiles. *Can. J. Earth Sci.* **46,** 651–661 (2009).
48. Broom, R. A new thecodont reptile. *Proc. Zool. Soc. London Ser. B* **84,** 1072–1077 (1914).
49. Smith, R. M. H. & Evans, S. E. An aggregation of juvenile *Youngina* from the Beaufort Group, Karoo Basin, South Africa. *Palaeontol. Afr.* **32,** 45–49 (1995).
50. Müller, J. In *Recent Advances in the Origin and Early Radiation of Vertebrates*. (eds. Arratia, G., Wilson, M. V. H. & Cloutier, R.) 379–408 (Verlag Dr. Friedrich Pfeil, 2004).
51. Müller, J. The anatomy of *Askeptosaurus italicus* from the Middle Triassic of Monte San Giorgio and the interrelationships of thalattosaurs (Reptilia, Diapsida). *Can. J. Earth Sci.* **42,** 1347–1367 (2005).
52. Müller, J. First record of a thalattosaur from the Upper Triassic of Austria. *J. Vertebr. Paleontol.* **27,** 236–240 (2007).
53. Müller, J., Renesto, S. & Evans, S. E. The marine diapsid reptile *Endennasaurus* from the Upper Triassic of Italy. *Palaeontology* **48,** 15–30 (2005).
54. Liu, J. & Rieppel, O. Restudy of *Anshunsaurus huangguoshuensis* (Reptilia: Thalattosauria) from the Middle Triassic of Guizhou, China. *Am. Mus. Novit.* **3488,** 1–34 (2005).
55. Li, C., Wu, X.-C., Rieppel, O., Wang, L.-T. & Zhao, L.-J. An ancestral turtle from the Late Triassic of southwestern China. *Nature* **456,** 497–501 (2008).
56. Cheng, L., Chen, X., Zeng, X. & Cai, Y. A new eosauropterygian (Diapsida: Sauropterygia) from the Middle Triassic of Luoping, Yunnan Province. *J. Earth Sci.* **23,** 33–40 (2012).
57. Blakey, R. Global Paleogeography Maps, Library of Paleogeography, Colorado Plateau Geosystems Inc. Website. http://cpgeosystems.com/paleomaps.html (2012). [cited 4th March 2013] http://www2.nau.edu/rcb7/ (2012).
58. McKie, T. & Williams, B. Triassic palaeogeography and fluvial dispersal across the northwest European Basins. *Geol. J.* **44,** 711–741 (2009).

Acknowledgements

We are indebted to the Sibelco Europe MineralsPlus Winterswijk company and to R. Bleeker, who found the fossil and donated it to the TwentseWelle Museum so that we were able to describe it in the present paper. We thank O. Dülfer (SIPB) for preparation of the specimen, G. Oleschinski (SIPB) for photography and D. Kranz (SIPB) for providing the artwork for Supplementary Fig. S1. We also thank B. Scheffold (PIMUZ), who contributed artwork to Fig. 3, Marcelo Sánchez and the other members of PIMUZ for discussion and input, and whose assistance greatly improved the manuscript. This work was funded by the Swiss National Science Foundation (grant 31003A 127053) and the Deutsche Forschungsgemeinschaft (DFG).

Author contributions

J.M.N. and T.M.S. wrote the manuscript and prepared the figures. N.K. and J.M.N. conducted the morphological description of outwardly visible structures. N.K. carried out the CT scanning. T.M.S. and J.M.N. performed the phylogenetic analysis. J.M.N. created the three-dimensional reconstruction and conducted the morphological description of the concealed elements.

Additional information

Supplementary Information accompanies this paper at http://www.nature.com/naturecommunications

Competing financial interests: The authors declare no competing financial interests.

Reprints and permission information is available online at http://npg.nature.com/reprintsandpermissions/

How to cite this article: Neenan, J. M. *et al.* European origin of placodont marine reptiles and the evolution of crushing dentition in Placodontia. *Nat. Commun.* 4:1621 doi: 10.1038/ncomms2633 (2013).

European origin of placodont marine reptiles and the evolution of crushing dentition in Placodontia

James M. Neenan, Nicole Klein, Torsten M. Scheyer

Supplementary Information:

Supplementary Figure S1. *Palatodonta bleekeri* gen. et sp. nov. holotype TW480000470.

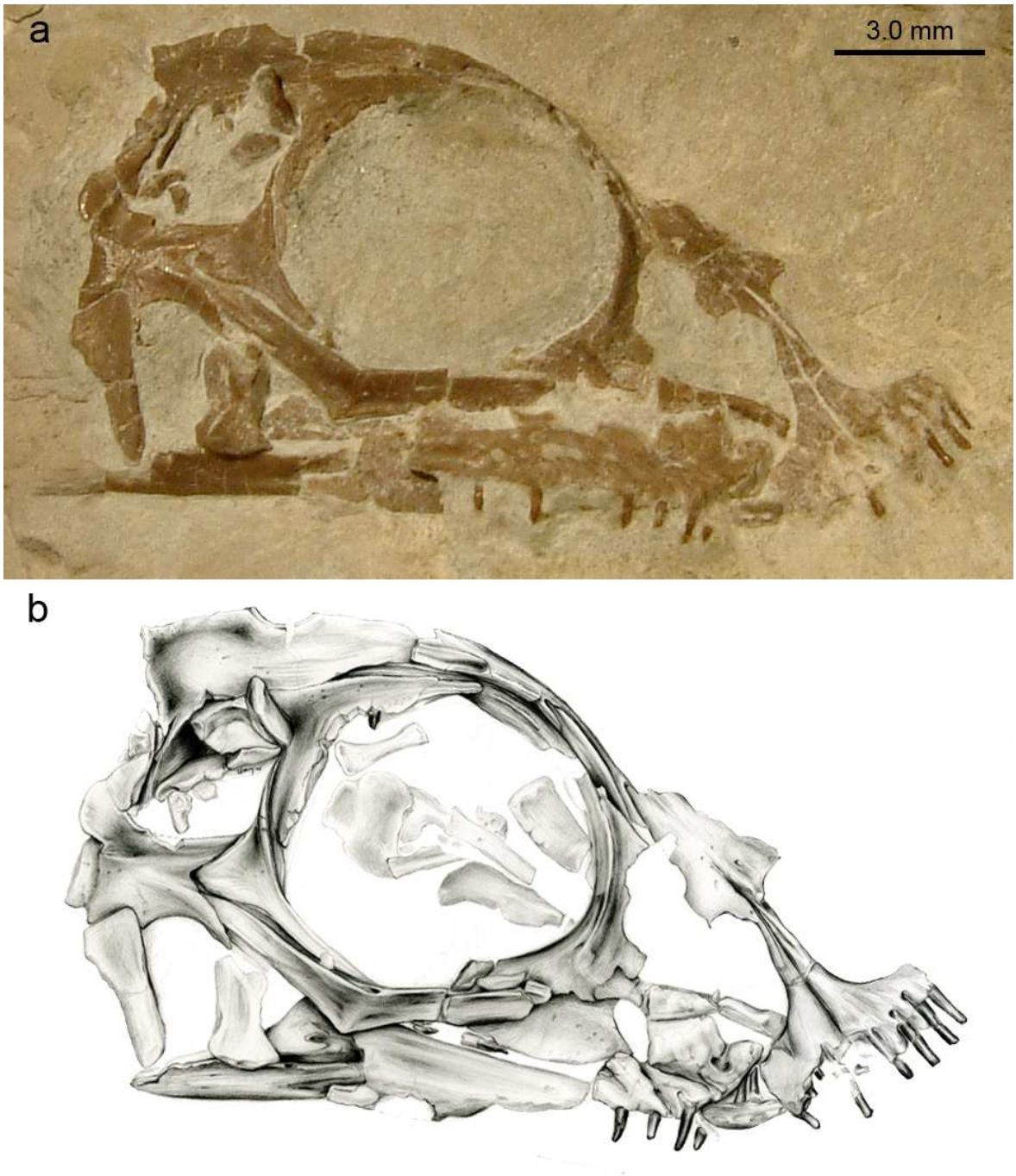

(**a**) An early stage of preparation, including the maxilla before it was broken. There are clearly at least six maxillary teeth and the maxilla extends caudally to meet the jugal. Photo credit: J. Lankamp. (**b**) Artistic drawing of the skull after preparation, with damaged maxilla. Picture credit: D. Kranz.

Supplementary Figure S2. High magnification photographs of the dentition of *Palatodonta*.

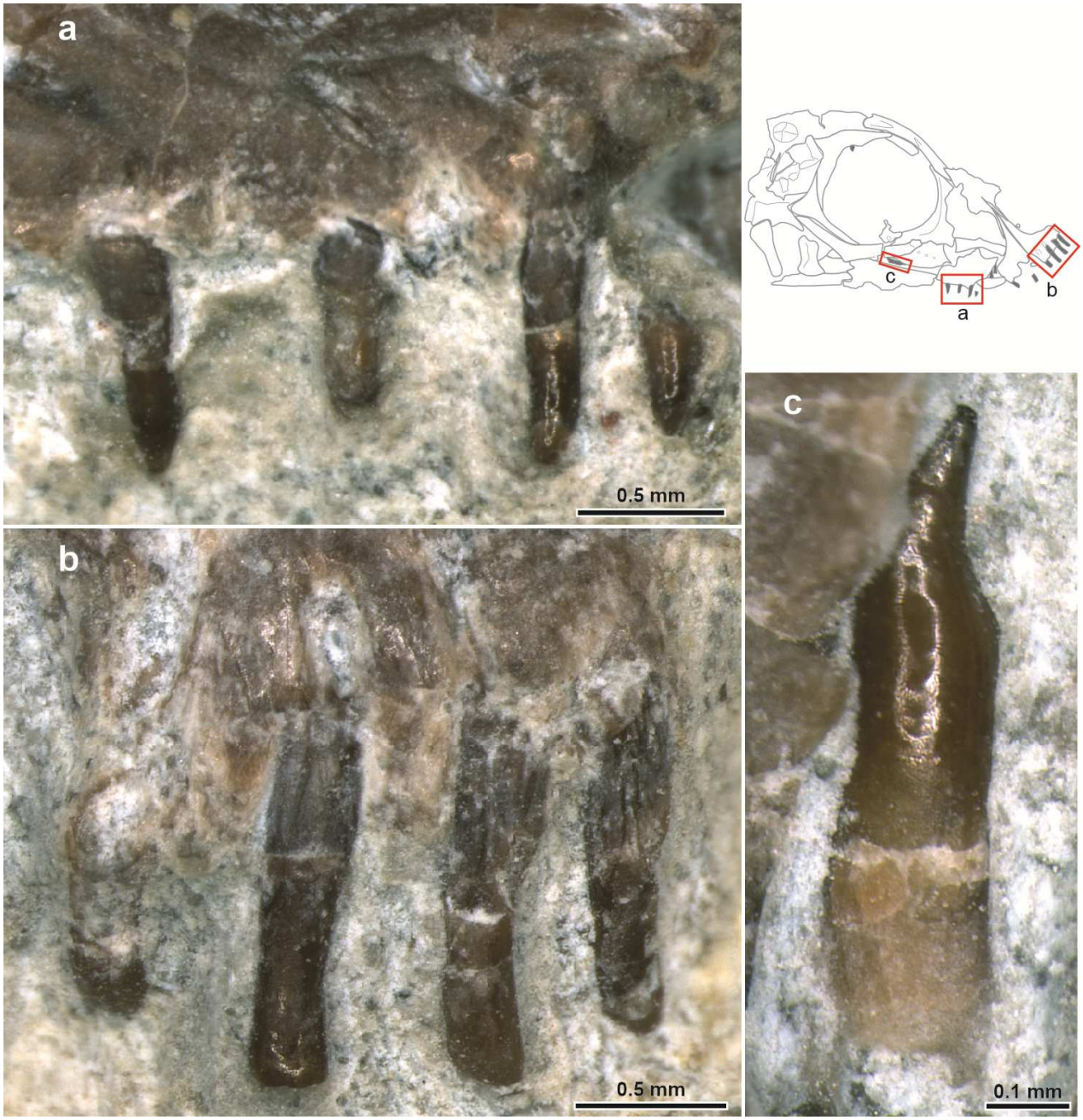

(**a**) Four pointed teeth of the maxilla. (**b**) Four blunt teeth from the left premaxilla. (**c**) Disarticulated tooth, probably from right dentary.

Supplementary Figure S3. Photographs of the dentition of juvenile placodont specimens coated with ammonium chloride (NH_4Cl).

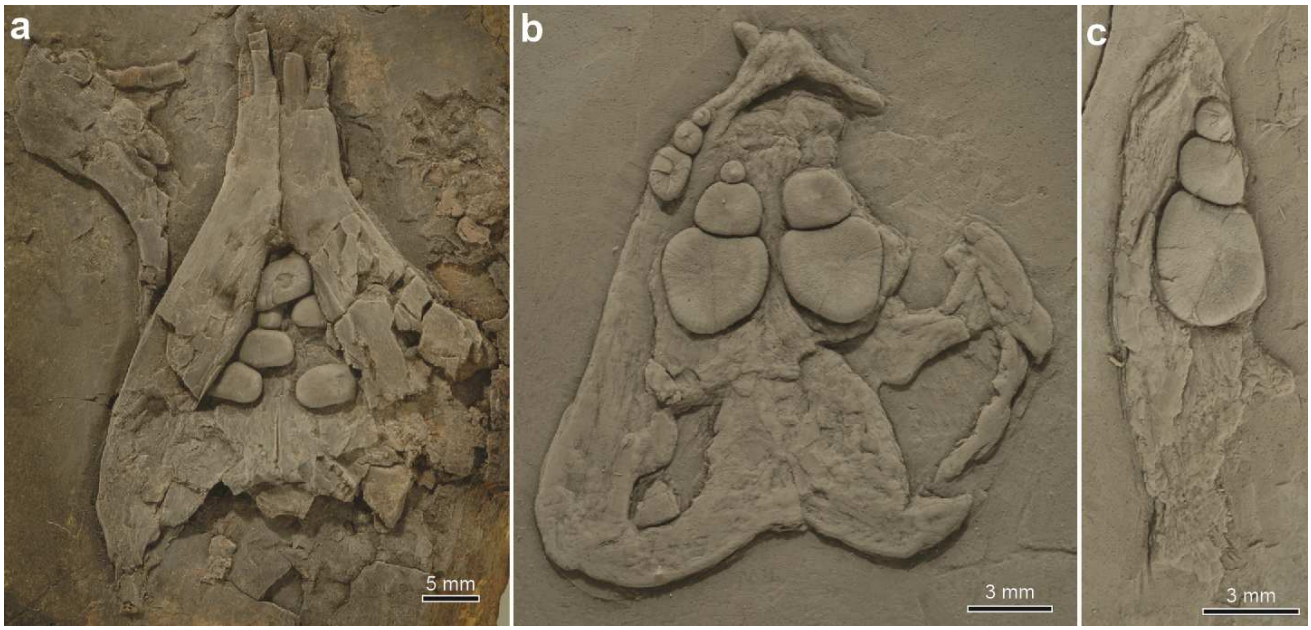

(**a**) *Paraplacodus broilii*, PIMUZ T2805. (**b**) Palatal view of *Cyamodus hildegardis,* PIMUZ T2797. (**c**) Left mandible of the same specimen of *Cyamodus hildegardis*. Despite being of a similar size to *Palatodonta*, both specimens exhibit flat, rounded teeth, very similar to that of the 'adult' placodont condition.

Supplementary Figure S4. Time-calibrated 50% majority rule cladogram (taken from Analysis 1) showing the relationships of Triassic Sauropterygia and *Sinosaurosphargis*.

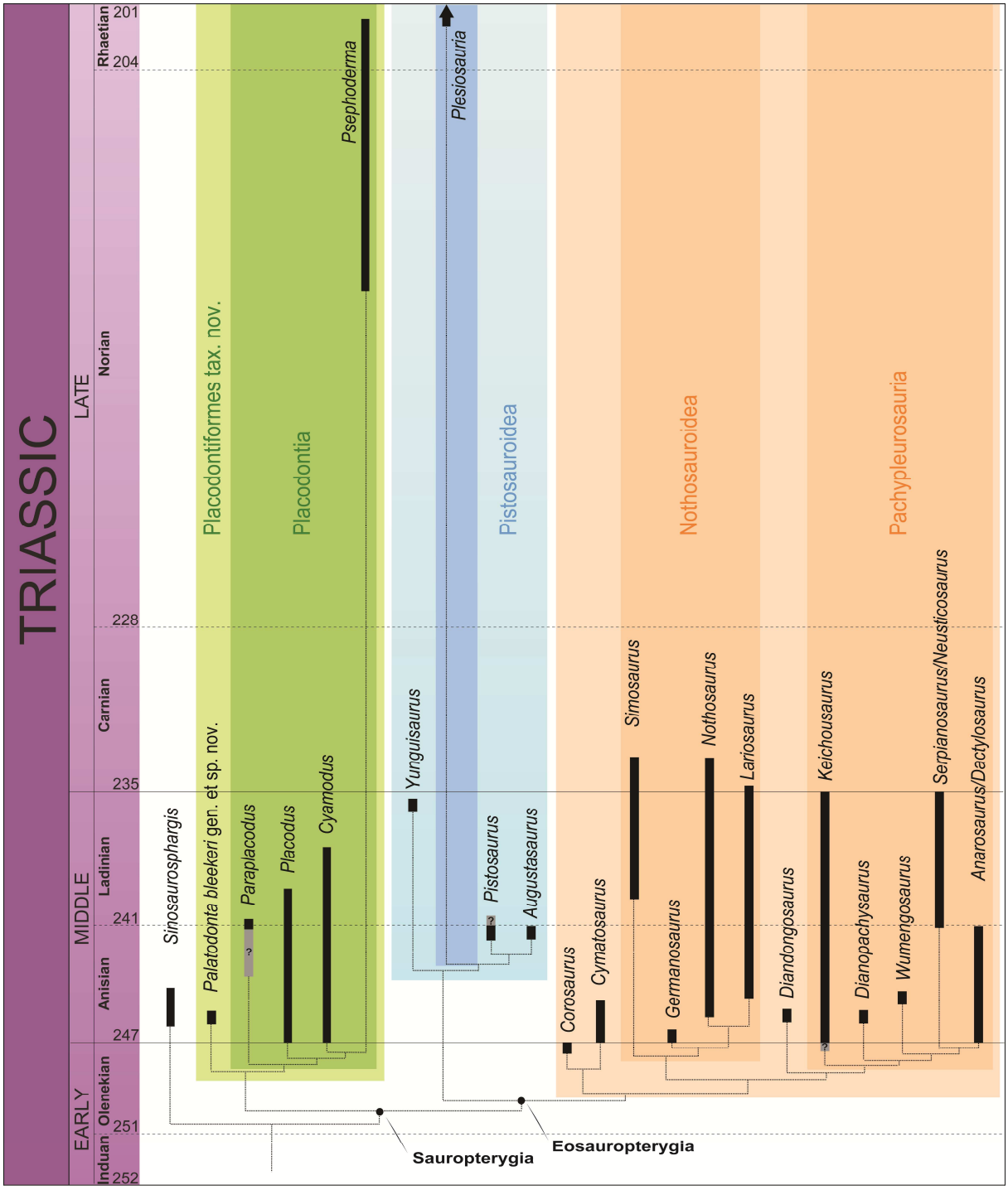

Occurrence data were taken from [1-4] and references therein

Table S1. Skull measurements of *Palatodonta bleekeri* gen. et sp. nov. holotype TW4800004.

Feature	Measurement (mm)	Comment
a, skull length	20.5	Full length from the caudal-most point of the squamosal to the rostral-most point of the 4th tooth on the premaxilla
b, skull height (including mandible)	11.0	From ventral-most point of mandible to dorsal-most part of parietal
c, diameter of naris at widest point (right / left)	3.1 / 3.5	
d, longitudinal diameter of orbit	7.1	
e, transversal diameter of orbit	6.5	
f, longitudinal diameter of upper temporal fenestra	2.7	
g, transversal diameter of upper temporal fenestra	3.3	
h, longitudinal diameter of lower temporal excavation	4.0	From ventral-most point of jugal to rostral surface of ventral-most point of quadrate
i, transversal diameter of lower temporal excavation	3.2	From the squamosal to the dorsal surface of the angular
j, length of parietal foramen	1.3	
k, length of right mandible	15.3	

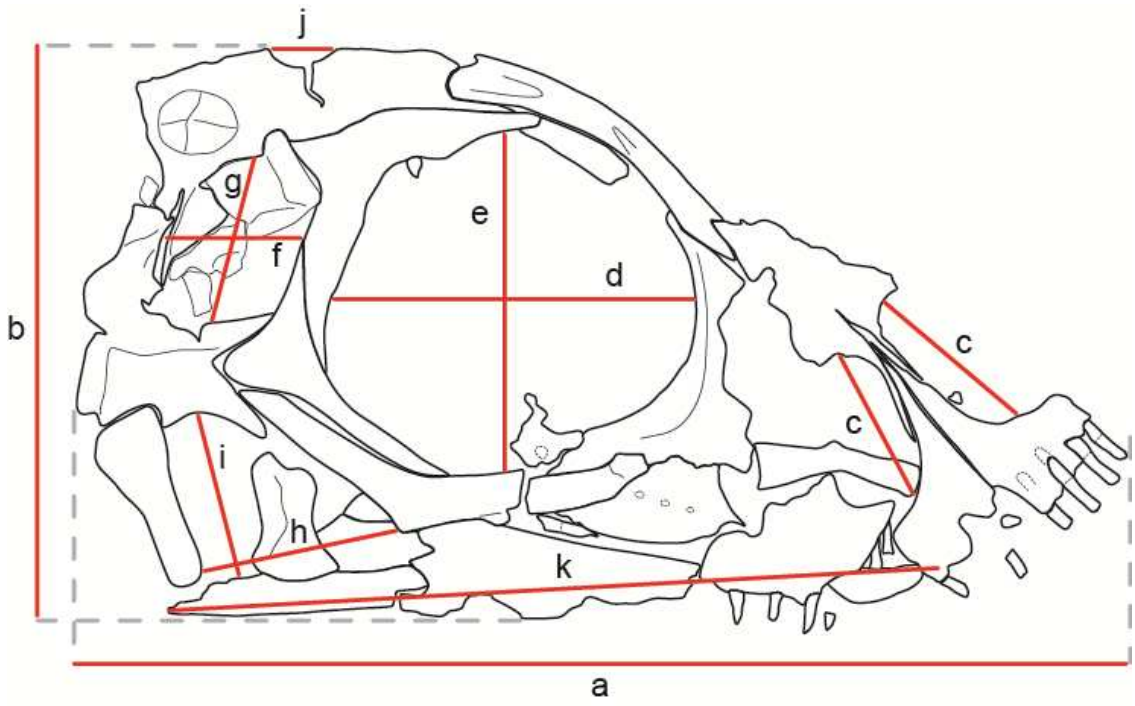

Detailed Morphological Description

Premaxilla. The premaxillae are unfused and form the rostral and ventral margins of the external naris. Mediocaudally, the premaxilla has a long tapering process, which separates the anterior third of the nasals. This posterior process borders the anterior third of the medial margin of the naris but is excluded from its upper half by a slender rostral process of the nasal. The premaxilla has three distinct round grooves/depressions, which are located directly above three articulated premaxilla teeth. Each premaxilla has four teeth. These have a blunt tip and smooth surface and are not pointed as are those from the maxilla, dentary and palatine (Supplementary Figure S2).

External naris. The large, oval external naris is dorsoventrally elongate, with the longitudinal length of the naris being nearly twice the length of the transverse length. The rostral and ventral margin is formed by the premaxilla. The lateral margin is formed by the maxilla, although the maxilla is not preserved. The dorsal margin of the naris is formed by the nasal.

Nasal. The nasals are arrowhead-shaped and appear to be fused, but split rostrally to form very narrow processes that form part of the rostral margin of the external naris. They also form the ventral margin of the naris. It is probable that the pointed caudal part of the nasal is broken, so the exact morphology of the articulation with the frontal and prefrontal is unknown.

Frontal. The frontal contributes to the dorsal margin of the orbit and has two grooves where the post- and prefrontals would have articulated in life. Ventral to the right frontal is an extension of the rostral portion of the disarticulated left frontal, which projects into the orbit. The frontal forms only a minor part of the ventral margin of the orbit, being restricted to the rostral half.

Parietal. The right parietal extends far rostrally, to about the midpoint of the orbit, and has rotated into dorsal view. The left parietal, visible in ventral view, is disarticulated

and lies slightly dorsal to the right parietal. The bones are separated along the suture line. The ventral margin of the rostral half shares a long suture with the postfrontal. The posterior portion of the parietal forms most of the dorsal margin and also a part of the caudal margin of the upper temporal fenestra. A distinct bulge is present at its caudolateral margin. The large parietal foramen is located at the centre of the parietals, slightly posterior to the narrow postorbital bridge.

Maxilla. The maxilla is incomplete, although its dorsal portion probably contributed to the caudal margin of the external nares and articulated with the prefrontal and nasal. Unfortunately the caudal portion of the maxilla was broken during preparation, but it articulated with the jugal and did not enter the margin of the orbit (Supplementary Figure S1). The maxilla bears at least 6 teeth, which are long, narrow, and unlike the premaxillary teeth, pointed. They are slightly curved and have a smooth surface (Supplementary Figure S2a). Estimating from the spacing pattern of the preserved teeth, the original number of teeth was about ten. Dorsomedial to the maxilla, a long, narrow bone is present, which may be the vomer that separated the internal nares.

Prefrontal. The prefrontal is a large, well-ossified element comprising the rostral margin of the orbit and extending rostrally at its ventral margin. The rostral portion is broken, but probably extended further rostrally to meet the nasals. The dorsalmost portion of this element would have articulated with the rostral frontal groove in life.

Postfrontal. The postfrontal is curved and forms the majority of the caudal margin of the orbit, as well as the caudal half of the dorsal margin. It forms most of the postorbital bridge, and has a small triangular caudal process that contributes to the dorsal margin of the temporal fenestra. The rostral-most portion of this element would have articulated with the caudal frontal groove in life.

Postorbital. The postorbital has a similar curved shape to the postfrontal, has a distinct caudal bulge and extends dorsally as a tapering process that forms part of

the rostral margin of the temporal fenestra. The postorbital region is short, with an excavated cheek region and lacking a quadratojugal. Its tapering dorsal process contributes to the caudal portion of the postorbital bar, as well as the majority of the rostral margin of the upper temporal fenestra. The descending process shares a long suture with the caudal process of the jugal, thus excluding it from the lower temporal opening.

Jugal. The jugal is distinctly open L-shaped (boomerang-shaped), much like the condition seen in *Paraplacodus*[5]. It forms part of the ventral margin of the orbit and its caudal process runs ventral to the postorbital, meeting the squamosal. It forms the rostral margin of the excavated lower temporal opening and excludes the maxilla from entering the margin of the orbit.

Squamosal. The squamosal forms the majority of the temporal bar, enclosing the caudal processes of the postorbital and the jugal at its rostral margin and the dorsal surface of the quadrate on its ventral surface. Caudally, the squamosal extends dorsally to meet the parietal, and also forms the dorsal margin of the lower temporal opening at its ventral margin. The squamosal has a very ventral position and is not a component of the skull roof; the main part contributes to the lateral skull and partially to the occipital region.

Quadrate. The quadrate is a simple bar, wider at its dorsal end, and has concave rostral and caudal margins. Like the jugal, it is similar in morphology to that of *Paraplacodus*[5]. The quadrate also comprises the caudal margin of the lower temporal opening, and articulates with the mandible at its ventral margin.

Mandible. The morphology of the right mandible differs from the placodont condition, being very narrow and gracile, with a low coronoid process, and a retroarticular process that is broken caudally. Neither an articular nor a prearticular was evident in the CT scan data. The dentary contains at least 14 pointed teeth (Fig. 2a, e),

comprises most of the length of the jaw, and is broken caudoventrally (marked with a dashed line in Fig. 2e). The mesial surface is concave, allowing space for Meckel's cartilage. The angular forms the ventrocaudal margin of the mandible and has a dorsal groove that houses the ventral margins of the surangular and coronoid. Medially, it extends far rostrally, tapering to a point just rostral to the caudal-most dentary tooth. The angular is broken caudally, and probably made up the majority of the retroarticular process. The surangular sits between the angular and coronoid, and has a limited exposure on the mesial surface of the jaw. The coronoid forms the dorsalmost portion of the coronoid process, and is supported mesially by an ascending process of the angular. The splenial is disarticulated, but can be seen to be a long, narrow and very thin element (Fig 1a, B; Fig. 2a, d).

Extended Results of Phylogenetic Analysis

All analyses were run in PAUP 4.0b10 for Microsoft Windows 95/NT[6] using PaupUP[7] version 1.0.3.1 under parsimony settings, using the heuristic search, tree-bisection-reconnection, and random step-wise addition options with 100 replicates and holding 10 trees at each step if not indicated otherwise. All 140 characters were unordered and not weighted in any way.

Analysis 1: The first search run on the matrix included all taxa, which yielded three most-parsimonious trees (MPTs), with a shortest tree length of 566 steps (CI=0.334, RI=0.659, RC=0.220, HI=0.666).

The strict consensus tree (Fig. S5a) recovered a sistergroup relationship between archosauromorph taxa and the lepidosaur lineage, but a monophyletic Lepidosauromorpha (i.e., Lepidosauria plus Sauropterygia) was not supported. Instead there is a basal grade including ichthyosaurs, thalattosaurs and several other diapsid taxa leading to Sauropterygia. The proposed Placodontiformes taxon nov. is sister to a monophyletic Eosauropterygia. It is noteworthy that the pistosauroid clade, which includes the plesiosaurs, was found to be the sister taxon to the remaining eosauropterygians. Note the basal position of turtles (*Odontochelys* and Testudines). The 50% majority rule consensus tree (Fig. S5b) differs from the strict consensus only in the resolution within pachypleurosaurs.

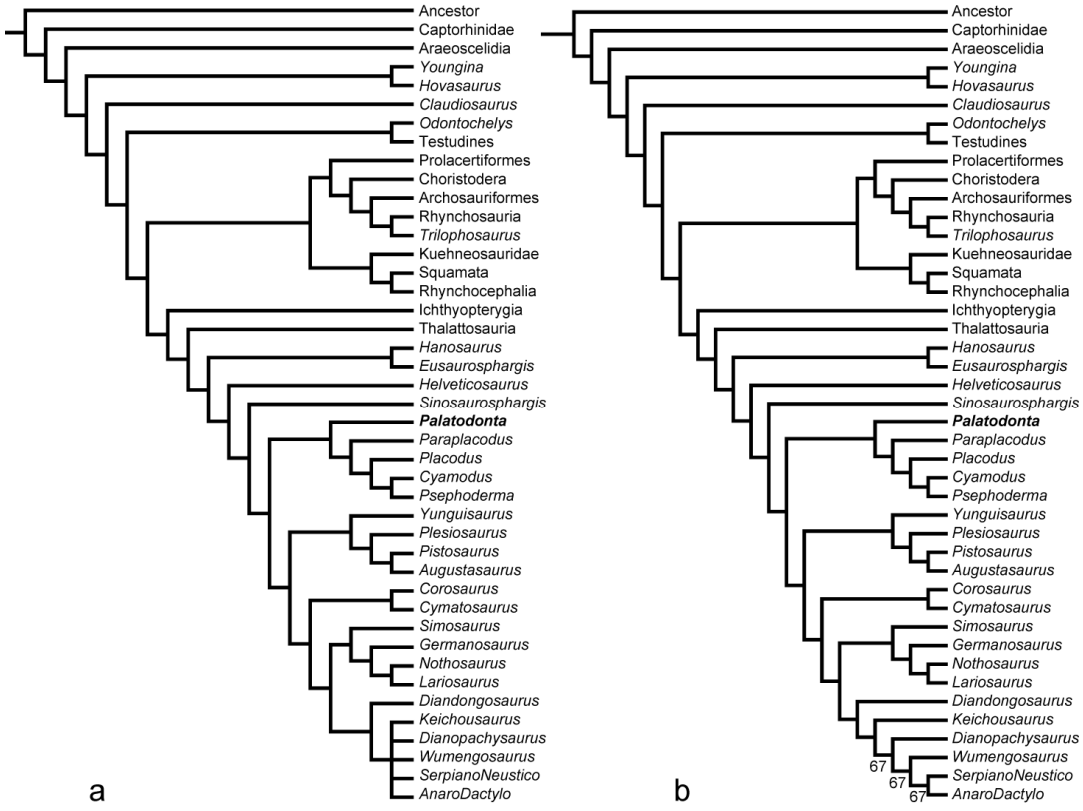

Fig. S5. Resulting trees of Analysis 1. (**a**) Strict consensus tree, (**b**) 50% majority rule consensus tree. Only percentages diverging from 100 are given.

Analysis 2: The second search run on the matrix excluded Ichthyopterygia, yielding 85 MPTs, with a shortest tree length of 549 steps (CI=0.344, RI=0.666, RC=0.229, HI=0.656).

In comparison to the strict consensus tree in Analysis 1 (Fig. S5a), the exclusion of Ichthyopterygia led to a polytomy consisting of the archosaur and lepidosaur lineages, the turtles, and the more highly nested diapsids (thalattosaurs to sauropterygians). The resolution is lower in Sauropterygia in the strict consensus compared to Analysis 1 as well. In the 50 % majority rule consensus (Fig. S6b), *Corosaurus* is recovered as sister taxon to all remaining eosauropterygians, followed by the pistosauroid clade, with *Cymatosaurus* moving onto the stem of the latter.

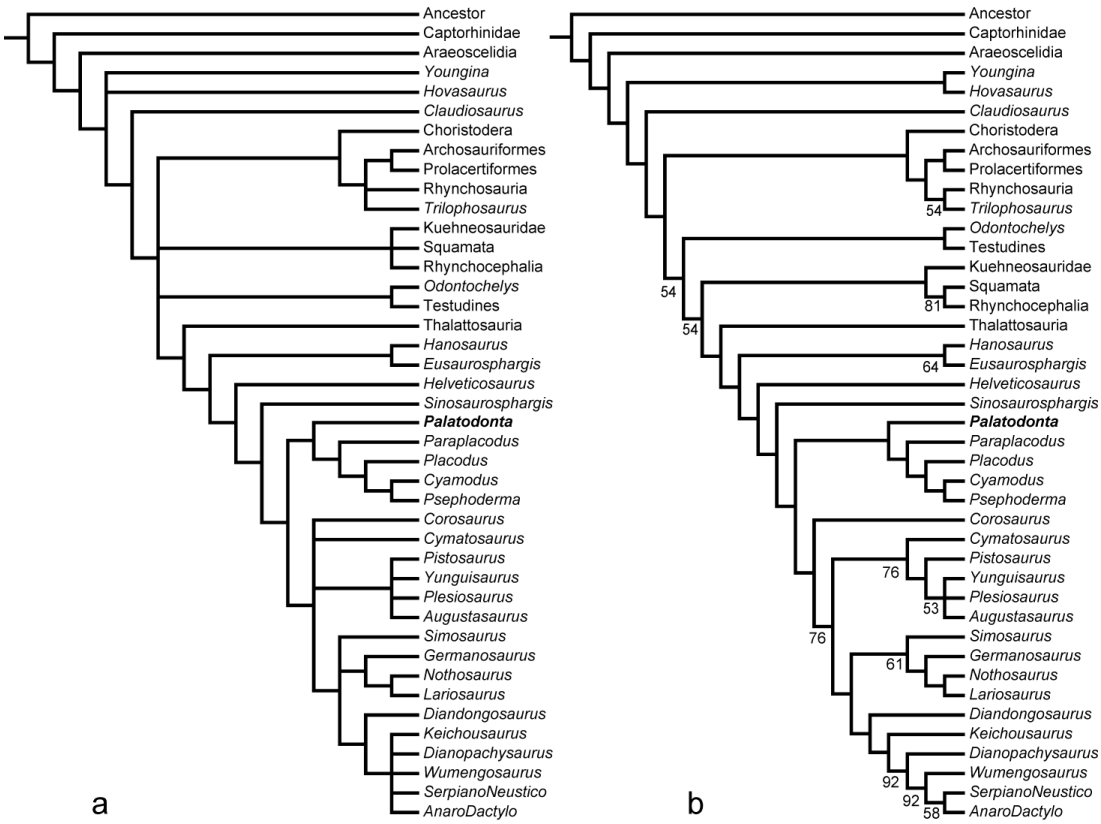

Fig. S6. Resulting trees of Analysis 2. (**a**) Strict consensus tree, (**b**) 50% majority rule consensus tree. Only percentages diverging from 100 are given.

Analysis 3: The third run of the matrix excluded Ichthyopterygia and turtles (*Odontochelys* and Testudines), yielding 502 MPTs with a shortest tree length of 499 steps (CI=0.355, RI=0.673, RC=0.239, HI=0.645). For this analysis the number of trees retained was successively raised to 30 to acquire the shortest tree. Further increase to a 1000 replicates and 100 retained trees per analysis led to the same topology of the strict consensus tree but differed in that all archosauromorph taxa were found in one polytomy in the 50% majority rule tree.

This analysis yielded a poorly resolved strict consensus tree (Fig. S7a) with polytomies in several sections of the cladogram. Especially the resolution among the archosaur and lepidosaur lineages collapsed completely. The 50 % majority rule

consensus (Fig. S7b) is somewhat better resolved, with sauropterygian ingroup relationships largely mirroring those shown in Fig. S6b.

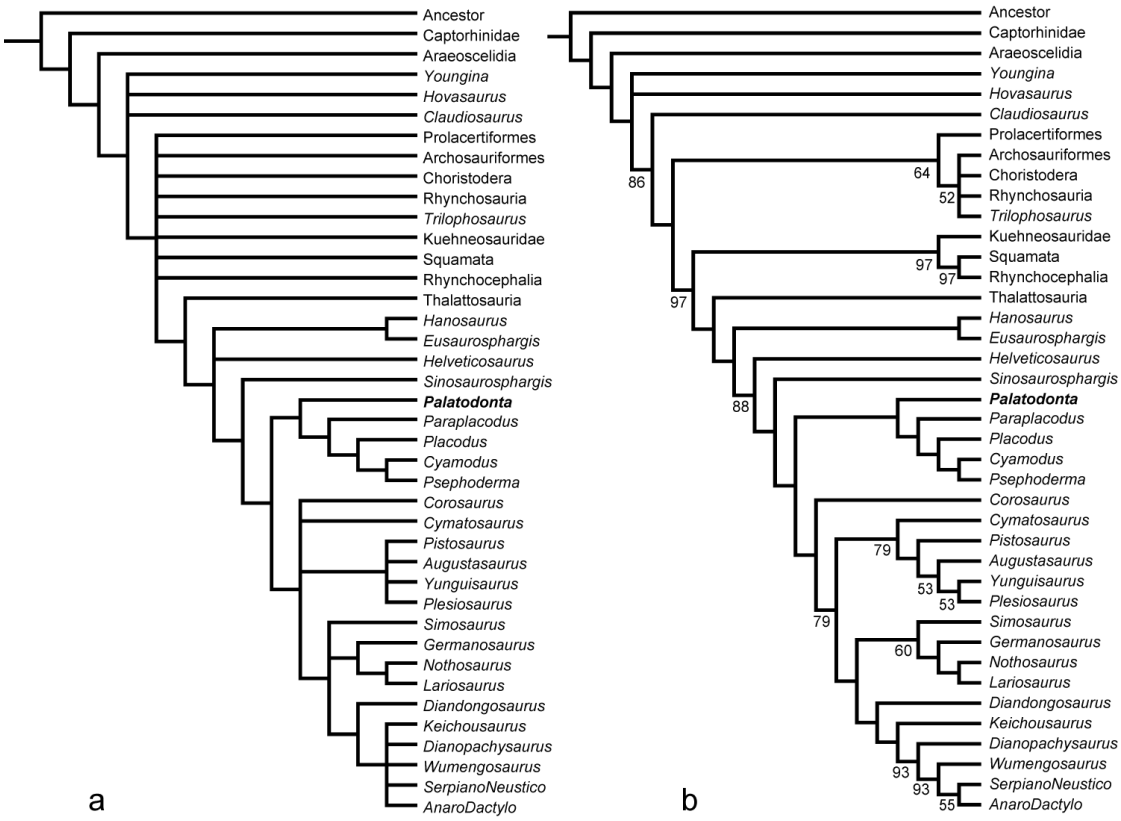

Fig. S7. Resulting trees of Analysis 3. (**a**) Strict consensus tree**,** (**b**) 50% majority rule consensus tree. Only percentages diverging from 100 are given.

Analysis 4: In the fourth analysis (with options set to 1000 replicates and 100 trees retained), the all-zero-ancestor, as well as Ichthyopterygia and turtles were removed, and Captorhinidae and Araeoscelidia served as outgroups instead. 47 MPTs were found with a shortest tree length of 520 (CI= 0.358, RI= 0.662, RC=0.237, HI=0.642). Results were overall comparable to the outcome of Analysis 3 as indicated by the strict consensus (Fig. S8), with relationships among Sauropterygia being slightly better resolved. Note that in this analysis, *Cymatosaurus* again moved onto the plesiosaur stem.

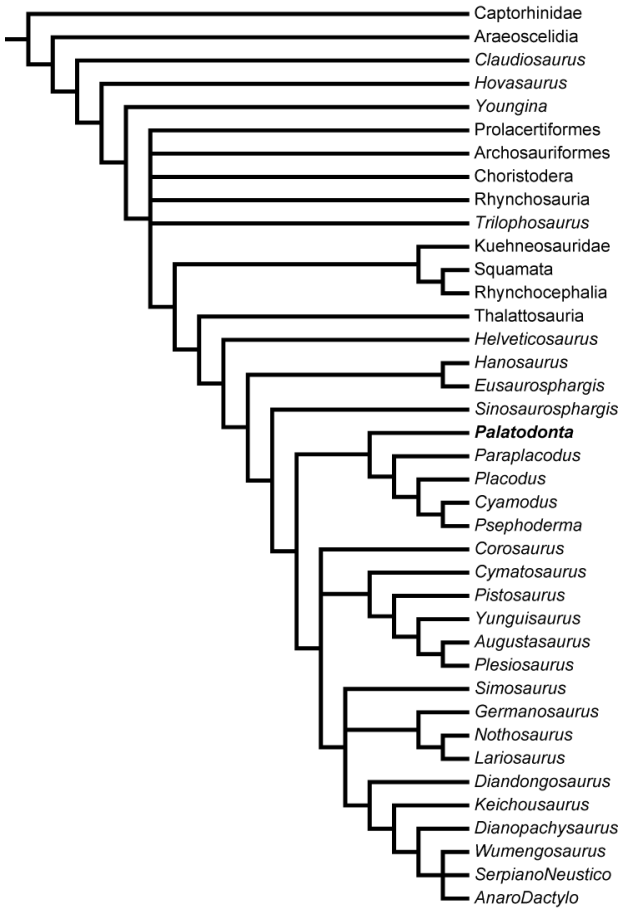

Figure S8. Resulting strict consensus tree of Analysis 4.

Analysis 5: For this analysis, the matrix was pruned to include only Sauropterygia as ingroup and *Sinosaurosphargis* as outgroup. Three MPTs were found with a shortest tree length of 315 (CI=0.483, RI=0.609, RC=0.294, HI=0.517).

Similar to the results of Analysis 1, a sistergroup relationship between *Corosaurus* and *Cymatosaurus* was recovered, but now this clade is sister to all remaining eosauropterygians. Ingroup relationships of the latter are not well resolved as indicated by polytomies in both the strict consensus (Fig. S9a) and the 50% majority rule tree (Fig. S9b).

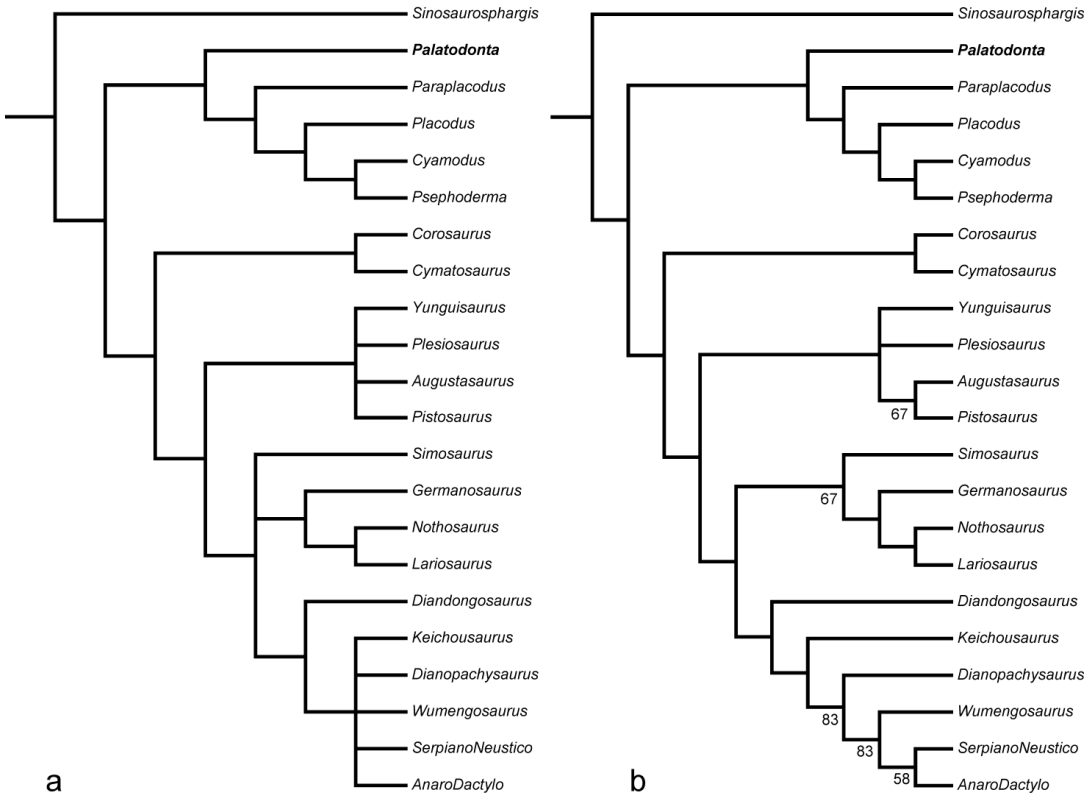

Fig. S9. Resulting trees of Analysis 5. (**a**) Strict consensus tree, (**b**) 50% majority rule consensus tree. Only percentages diverging from 100 are given.

Bootstrapping and Bremer support: A first bootstrap analysis (based on 1000 replicates) was performed on the matrix used in Analysis 1. This analysis shows a loss of resolution in large parts of the tree. However, the newly proposed Placodontiformes has a value of 78 % (Fig. S10a), with a Bremer support score of 3 for the clade. A second bootstrap analysis (again based on 1000 replicates) was run on the data set of Analysis 3 (Ichthyopterygia and turtles removed), which also showed high support (75%) for Placodontiformes, while Bremer support for the taxon remained at 3 (Fig. S10b). Apart from these slightly different bootstrap values, the general topologies of the two trees did not change, with the exception of the all-zero ancestor and Captorhinidae forming a basal polytomy in Fig.S10a, instead of a resolved grade in Fig. S10b.

The third bootstrap analysis (Fig. S10c; also with 1000 replicates) was performed on the pruned dataset of Analysis 5 (Fig. S9a). Here the bootstrap support and topology was generally similar to the previous analyses, although support for Placodontiformes is much higher at 91 %, and *Wumengosaurus* now forms a clade with the European pachypleurosaurs (Fig. S10c). Once again, the node Placodontiformes had a Bremer support of 3.

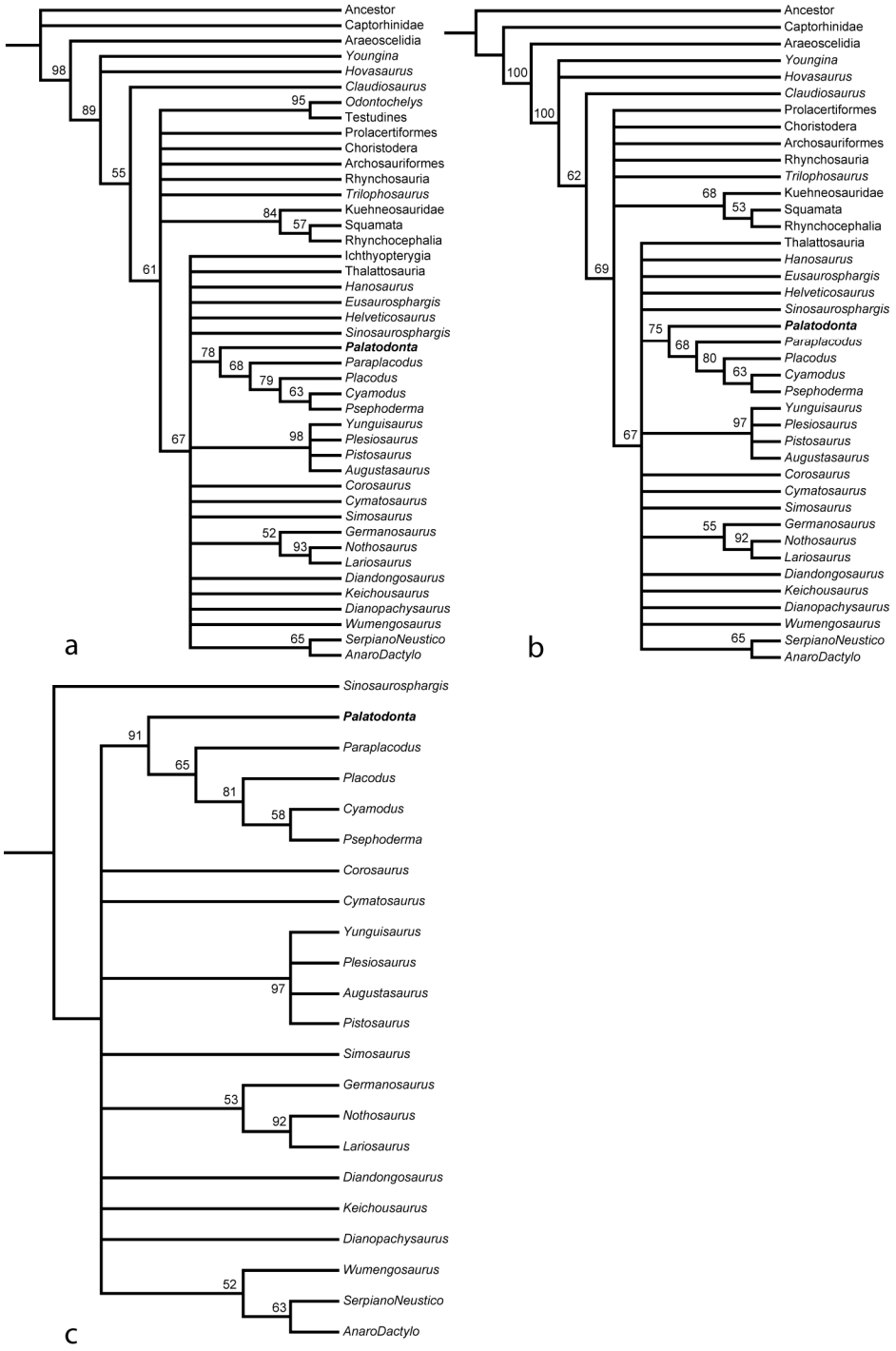

Fig. S10. Bootstrap strict consensus trees of data sets used in (**a**) Analysis 1, (**b**) Analysis 3, and (**c**) Analysis 5. Bootstrap values >50% are given above the branches.

In conclusion, although overall support is low, a monophyletic Placodontiformes was recovered in each of the analyses, with reasonable Bremer

and Bootstrap support values. *Sinosaurosphargis* consistently emerged as direct sister taxon to Sauropterygia, with the ingroup relationships of the latter changing little between analyses, with the exception of the position of *Cymatosaurus*. Our results also argue against a close relationship between thalattosaurs and *Sinosaurosphargis*, which was initially indicated by the analysis in the original description of the latter taxon[8].

It is worthy of note that in Analysis 1, lepidosaurs form a clade with Archosauromorpha, instead of a closer relationship to Sauropetrygia as in the other analyses. In addition, *Eusaurosphargis* and *Sinosaurosphargis* never form a monophyletic group, with *Eusaurosphargis* plotting closer to *Hanosaurus* in analyses 1-4. Indeed, *Hanosaurus* is never resolved within the Sauropterygia, as was proposed previously[9], but rather appears on the stem.

Given that the various analyses conducted vary little from Analysis 1, we chose this as our preferred tree owing to its high resolution and taxon inclusion. Our preferred tree agrees with the study of Liu et al.[10] by having the European pachypleurosaurs nested within the Chinese ones. However, it was recently suggested that the European pachypleurosaur *Anarosaurus* may in fact be the least adapted to the marine environment, as well being the one of the oldest members of the clade[11]. Therefore, future studies may reconstruct the position of this taxon as being more plesiomorphic. Conversely, our tree differs significantly in the position of *Corosaurus* and *Cymatosaurus*, which cluster more closely with nothosaurs and pachypleurosaurs, and, importantly, in pachypleurosaurs not being the basal-most group within Eusauropterygia.

Phylogenetic Character Descriptions

Characters were adopted from Liu et al.[10] with original character order used in Rieppel et al.[12] given in parentheses (e.g. R3). The scoring of Ichthyopterygia generally follows Li et al.[8]; notes and deviations from previous character definitions are marked in the text where applicable.

(1) Bones in dermatocranium: distinctly sculptured (0); relatively smooth (1). (From Rieppel and Lin[13]).

(2) Preorbital and postorbital region of skull: of subequal length (0); preorbital region distinctly longer (1); postorbital region distinctly longer (2). (R12)

(3) Snout: relatively short (0); elongated with broad anterior termination (1); elongated and tapering anteriorly (2). (R132); Thalattosauria: this character has been partly adapted from character 132 of Li et al.[8]; see character 4 below.

(4) Distinct snout constriction in adult: absent (0); present (1). (R3); “Younginiformes”: scoring changed from (0) to *Youngina* (0) and *Hovasaurus* (?); *Yunguisaurus*: Sato et al.[14] (p.190) noted "to regard the *Yunguisaurus* specimen as a juvenile, or at least not reaching the full adult stage", and therefore the taxon is strictly scored as (?) here; Thalattosauria: scored as (0) now - it was scored as (2) in Nosotti and Rieppel[15] and Li et al.[8], because character state (2) was “snout tapering/pointed" therein; in Liu et al.[10], however, the state (2) was removed from character 4 and added to character 3 instead ("elongated and tapering anteriorly (2)").

(5) Premaxillae: small (0); large, forming most of snout in front of external nares (1). (R1)

(6) Postnarial process of premaxilla: absent (0); present, excluding maxilla from posterior margin of external naris (1). (R2)

(7) External nares: not retracted (0); retracted with a longitudinal diameter approaching or exceeding half the longitudinal diameter of orbit (1); retracted, narrow, and with a longitudinal diameter distinctly less than half the longitudinal diameter of orbit (2). (R133); *Wumengosaurus*: following Wu et al.[16], score was changed from (2) to (1); *Sinosaurosphargis* and *Eusaurosphargis*: note that this character was not used by Li et al.[8].

(8) Nasal(s): shorter than frontal(s) (0); longer than frontal(s) (1). (R5)

(9) Nasal(s): not reduced (0); reduced (1); absent (2). (R6)

(10) Nasal(s): meeting in dorsomedial suture (0); fused (1); seperated from one another by nasal processes of premaxillae extending back to frontal(s) (2). (R8)

(11) Lacrimal: present, entering external naris (0); present, excluded from external naris (1); (2) absent. (R9); *Psephoderma*: scored as (2), contra Pinna and Nosotti[17].

(12) Dorsal exposure of prefrontal: large (0); reduced (1). (R11)

(13) Prefrontal: without slender anteromedial process (0); with slender anteromedial process entering between maxilla and premaxilla (1). (R121)

(14) Frontal: participating in the formation of dorsal margin of orbit (0); excluded from dorsal margin of orbit by a contact of prefrontal and postfrontal (1). (R10)

(15) Frontal(s) in adult: paired (0); fused (1). (R14); *Yunguisaurus*: following Sato et al.[14], character has been rescored with (?) instead of (0), due to dorsoventral crushing of holotype skull

(16) Distinct posterolateral processes of frontal(s): (0) absent; (1) present. (R15)

(17) Frontal: widely separated from upper temporal fossa (0); narrowly approaching upper temporal fossa (1); entering the anteromedial margin of upper temporal fossa (2). (R16)

(18) Postfrontal: large and plate-like (0); with distinct lateral process overlapping the dorsal tip of postorbital (1); with reduced lateral process and hence more of an elongate shape (2). (R26); Ichthyopterygia: scored (1,2) instead of (0) by Li et al.[8].

(19) Jugal: extending anteriorly along the ventral margin of orbit (0); restricted to a position behind orbit but entering the latter's posterior margin (1); restricted to a position behind orbit without reaching the latter's posterior margin (2). (R23)

(20) Jugal: extending backwards no farther than to the middle of cheek region (0); extending nearly to the posterior end of skull (1). (R24)

(21) Jugal: excluded from upper temporal arch (0); entering upper temporal arch (1). (R25)

(22) Parietal(s) in adult: paired (0); fused in their posterior part only (1); fully fused (2). (R17); *Wumengosaurus*: following Wu et al.[16], score changed from (2) to (0), as parietals are paired in adults and not fully fused.

(23) Parietal skull table: broad (0); weakly constricted (1); strongly constricted (at least posteriorly) (2); forming a sagittal crest (3). (R19); Ichthyopterygia: scored (0,1,3) following Motani[18] as there are definitely crested forms, contra Li et al 2011[8].

(24) Pineal foramen: close to the middle of skull table (0); weakly displaced posteriorly (1); strongly displaced posteriorly (2); displaced anteriorly (3); absent (4). (R18); Changed definition: following Li et al. (2011), the fourth character state was introduced.

(25) Postparietals: present (0); absent (1). (R20); *Paraplacodus*: scoring changed from (?) in Li et al.[8] to (1), because no postparietals were visible in CT scan data of the well-preserved Munich specimen (BSP 1953 XV5).

(26) Tabulars: present (0); absent (1). (R21); *Paraplacodus*: scoring changed from (?) in Li et al.[8] to (1), because no tabulars were visible in CT scan data of the well-

preserved Munich specimen (BSP 1953 XV5); “Younginiformes”: following Bickelmann et al.[19] scoring changed from (0&1) to *Youngina* (0) and *Hovasaurus* (0).

(27) Supratemporals: present (0); absent (1). (R22); *Paraplacodus*: scoring changed from (?) in Li et al.[8] to (1), because no supratemporals were visible in CT scan data of the well-preserved Munich specimen (BSP 1953 XV5).

(28) Temporal region of skull: relatively high (0); strongly depressed (1). (R4)

(29) Upper temporal fossa: absent (0); present and subequal in size or slightly larger than orbit (1); present and distinctly larger than orbit (2); present and distinctly smaller than orbit (3); secondarily closed (4). (R13); Changed definition: this character has been modified following Li et al.[8] by adding the forth character state; which in that study turned out to be a synapomorphy between Thalattosauria and *Sinosaurosphargis*; we keep the forth character state here to indicate the difference from state (0).

(30) The anteromedial corner of upper temporal fossa: not (0); partially (1); (2) fully floored by a descensus from postorbital, which together with neighbouring elements (postfrontal, parietal) separates it from orbit. (R122); *Wumengosaurus*: following Wu et al.[16], score changed from (0) to (1).

(31) Lower temporal fossa: absent (0); present and closed ventrally (1); present but open ventrally (2). (R27); *Psephoderma*: scored with (0) to underscore difference to the condition seen in *Paraplacodus* and the new skull from Winterswijk; “Younginiformes”: following Bickelmann et al.[19], *Hovasaurus* shares with *Acerosodontosaurus* a present but ventrally open lower temporal fossa.

(32) Squamosal: descending to ventral margin of skull (0); broadly separated from ventral margin of skull (1). (R28)

(33) A box-like suspensorium of squamosal: absent (0); present (1). (R123)

(34) Distinct notch of squamosal to receive distal tip of paroccipital process: absent (0); present (1). (R32)

(35) Quadratojugal: present (0); absent (1). (R29); *Cyamodus*, *Paraplacodus*, *Placodus* and *Psephoderma*: note that Rieppel[5] erroneously inverted the character scoring - accordingly *Paraplacodus* and *Placodus* should be scored as (1), whereas *Cyamodus* and *Psephoderma* should be scored (0); note that this character was scored (?) for *Paraplacodus* in Li et al.[8].

(36) Anterior process of quadratojugal: present (0); absent (1). (R30); *Paraplacodus*: scored as (1) following Rieppel[5] (personal observations); *Placodus*: contra to Liu et al.[10] and Li et al.[8] who scored it (0), we score this character (1).

(37) Quadrate: covered by squamosal and quadratojugal in lateral view (0); exposed in lateral view (1). (R38)

(38) Posterior margin of quadrate: straight (0); concave (1). (R37); *Paraplacodus*: scored as (0) here, based on CT scan data on Munich skull (BSP 1953 XV5) and in agreement with Li et al.[8], but contra Rieppel[5].

(39) Lateral conch on quadrate: absent (0); present (1). (R40)

(40) Dorsal wing of epipterygoid: approximately as broad as its base (0); narrower than its base (1). (R39)

(41) Braincase: located at posterior end (0); deeply recessed below parietal skull roof (or parietal sagittal crest) (1). (R124)

(42) Occipital crest: absent (0); present but squamosals not meeting behind parietal (1); present and squamosals meeting behind parietal (2). (R36); *Paraplacodus*: contra Li et al.[8] scored as (?) instead of (0), because the occipital region is not sufficiently known for this taxon.

(43) Occiput: with paroccipital process forming the lower margin of posttemporal fossa and extending laterally (0); paroccipital processes trending posteriorly (1);

plate-like with no distinct paroccipital process and with strongly reduced posttemporal fossae (2). (R31)

(44) Mandibular articulations: approximately at level with occipital condyle (0); displaced to a level distinctly behind occipital condyle (1); positioned anterior to occipital condyle (2). (R33)

(45) Supraoccipital: exposed more or less vertically on occiput (0); exposed more or less horizontally at posterior end of parietal skull table (1); U-shaped (2). (R35); Ichthyopterygia: scored (0,1,2) instead of (0) by Li et al.[8].

(46) Contact between exoccipitals and basioccipital condyle: present (0); absent (1). (R34)

(47) Basioccipital tubera: free (0); in complex relation to pterygoid, as they extend ventrally (1); in complex relation to pterygoid, as they extend laterally (2). (R42)

(48) Palate: kinetic (0); akinetic (1). (R41); *Paraplacodus*: based on CT scan data of new, undescribed cranial material (PIMUZ T2805), the palate is akinetic; scored as (?) in Li et al.[8].

(49) Premaxillae: entering internal naris (0); excluded from internal naris (1). (R45); Ichthyopterygia: scored (0,1) instead of (0) in Li et al.[8].

(50) Posterior palatine vacuities: absent (0); present (1). (R125); *Paraplacodus*: based on CT scan data of new, undescribed cranial material (PIMUZ T2805), posterior palatine vacuities are absent; scored as (?) in Li et al.[8].

(51) Pterygoids: longer than palatines (0); shorter than palatines (1). (R130); *Paraplacodus*: based on CT scan data of new, undescribed cranial material (PIMUZ T2805), pterygoids are shorter than palatines; scored as (?) in Li et al.[8].

(52) Pterygoid flanges: well developed and transversely oriented (0); well developed and longitudinally oriented (1); strongly reduced (2). (R44)

(53) Ectopterygoid: present (0); absent (1). (R46)

(54) Suborbital fenestra: absent (0); present (1). (R43); *Paraplacodus*: based on CT scan data of new, undescribed cranial material (PIMUZ T2805), suborbital fenestra is absent; was scored (1) in Li et al.[8].

(55) Internal carotid passage: entering basicranium (0); entering quadrate ramus of pterygoid (1). (R47); Ichthyopterygia: scored (0) following Sollas[20] and Romer[21] instead of (?) in Li et al.[8].

(56) Splenial bone: entering mandibular symphysis (0); excluded therefrom (1). (R52)

(57) Distinct coronoid process of lower jaw: absent (0); present (1). (R49)

(58) Strongly projecting lateral ridge of surangular defining the insertion area for superficial adductor muscle fibers on the lateral surface of lower jaw: absent (0); present (1). (R50)

(59) Mandibular symphysis: short (0); somewhat enforced (1); elongated and 'scoop-like' (2). (R51); *Paraplacodus*: based on new, undescribed cranial material (PIMUZ T2805), scored as (2); was scored (?) in Li et al.[8].

(60) Retroarticular process of lower jaw: absent (0); present (1). (R48); Thalattosauria: following Müller[4,22] and personal observations of specimens stored in the PIMUZ collections, this character is scored (0&1), because although most thalattosaurs have a retroarticular process, *Askeptosaurus* does not; Ichthyopterygia: scored (0,1) instead of (0) in Li et al.[8].

(61) Trough on dorsal surface of retroarticular process: absent (0); present (1). (From Rieppel and Lin[13]); *Diandongosaurus*: Shang et al.[23] noted fossa on retroarcticular process, therefore this character is scored as (1); *Sinosaurosphargis*: as this taxon does not have a retroarticular process, this character was scored as (?) accordingly here – note that this character is not used in Li et al.[8] or Wu et al.[16]; Thalattosauria: in those taxa which have a retroarticular process, there seems to be no trough on dorsal surface so it is scored (0) here; *Wumengosaurus*: following Wu et al.[16] scoring

changed from (?) to (0), as on p. 76 it is noted that there is no deep concavitiy or trough but a thick ridge on the retroarticular process; *Yunguisaurus*: neither Cheng et al.[24] nor Sato et al.[14] noted a trough and no such structure was visible in the accompanying images, therefore it was scored as (0).

(62) Teeth: setting in shallow or deep sockets (0); superficially attached to bone (1). (R53)

(63) Durophagous dentition: absent (0); present (1). (R128); Changed definition: the additional part “including much enlarged palatine tooth plates” was removed here, and a new character (140) was introduced.

(64) Number of premaxillary teeth: four or more (0); three or less (1). (R129)

(65) Anterior (premaxillary and dentary) teeth: upright or only sightly procumbent (0); strongly procumbent (1). (R54); *Keichousaurus*: following Wu et al.[16], the character would have to be scored with (0&1) instead of (1) as in Holmes et al.[25].

(66) Premaxillary and anterior dentary fangs: absent (0); present (1). (R55)

(67) One or two enlarged teeth on maxilla: present (0); absent (1). (R56); *Diangongosaurus*: changed from (1) to (0), as an enlarged maxillary tooth is clearly present; compare to Shang et al.[23] (figure 2); *Sinosaurosphargis*: Li et al.[8] scored this character with (0) although on p. 308 the authors state: "The size of the exposed teeth, and tooth morphology, remains constant along the margins of the upper and lower jaws.", and therefore it should be scored (1).

(68) Maxillary tooth row: restricted to a level in front of the posterior margin of orbit (0); extending backwards to a level below the posterior corner of orbit and/or the anterior corner of upper temporal fossa (1); extending backwards to a level below the anterior one third to one half of upper temporal fossa (2). (R57)

(69) Teeth on pterygoid flange: present (0); absent (1). (R58); *Paraplacodus*: based on CT scan data of new, undescribed cranial material (PIMUZ T2805), it was scored (1); was scored (?) in Li et al.[8].

(70) Vertebrae: notochordal (0); non-notochordal (1). (R59)

(71) Vertebrae: amphicoelous (0); platycoelous (1); or other (2). (R60); *Yunguisaurus*: scored with (0&1) in Cheng et al.[24] and Sato et al.[14], but only amphicoelous vertebrae are described and figured; we here score the taxon with (0) only.

(72) Vertebral centrum: distinctly constricted in ventral view (0); with parallel lateral edges (1). (R67)

(73) Subcentral foramina: absent (0); present (1). (R127)

(74) Zygosphene-zygantrum articulation: absent (0); present (1). (R64)

(75) Zygapophyseal pachyostosis: absent (0); present (1). (R69); *Cyamodus*: was scored (?) in Liu et al.[10] and Li et al.[8].

(76) Number of cervical vertebrae: less than 30 (0); more than 30 (1). (R134); *Sinosaurosphargis*: even though not all cervical vertebrae are visible in the specimen, the neck region is still rather short and thus scored with (0).

(77) Cervical centra: rounded ventrally (0); keeled ventrally (1). (R63)

(78) Parapophysis: not shifting backwards on centrum along cervical vertebral column (0); shifting backwards on centrum along cervical vertebral column (1). (R135)

(79) Cervical intercentra: present (0); absent (1). (R62)

(80) Distal articular surface on transverse processes of dorsal vertebrae: oblong (0); evenly rounded (1). (R136); Ichthyopterygia: scored (?) instead of (1) in Li et al.[8], based on the absence of transverse processes of dorsal vertebrae.

(81) Transverse processes of neural arches in dorsal region: relatively short (0); distinctly elongated (1). (R66)

(82) Distal end of transverse processes of dorsal vertebrae: not increasing in diameter (0); distinctly thickened (1). (R68); Ichthyopterygia: scored (?) based on the absence of transverse processes of dorsal vertebrae.

(83) Sutural facets receiving pedicels of neural arch on dorsal surface of centrum in dorsal region: narrow (0); expanded into a cruciform or 'butterfly-shaped' platform (1). (R65); *Paraplacodus*: although a weak "butterfly-shaped" platform was noted in Rieppel[5] (p. 642); we agree with Li et al.[8] that this character should be scored as (0)

(84) Dorsal intercentra: present (0); absent (1). (R61)

(85) Anteroposterior trend of increasing inclination of pre- and postzygapophyses within dorsal and sacral region: absent (0); present (1). (R70)

(86) A distinct free anterior process of cervical ribs: absent (0); present (1). (R71)

(87) Pachyostosis of dorsal ribs: absent (0); present (1). (R72); *Yunguisaurus*: was scored (?) in Cheng et al.[24] and Sato et al.[14]; no apparent pachyostosis is visible though.

(88) Number of sacral ribs: two (0); three (1); four or more (2). (R73); *Serpiano-Neustico*: changed from (1) to (1&2), because these taxa can have 3 or 4 sacrals (*N. edwardsii* has only 3 sacrals); *Sinosaurosphargis*: although Li et al.[8] noted the presence of broadened pachyostotic dorsal ribs, this is difficult to assess without looking at the microstructures to see if the cortical bone is indeed thickened - therefore we use a conservative approach and score it (?).

(89) Distinct expansion of distal head of sacral ribs: present (0); absent (1). (R74); *Cyamodus*: changed from (?) in Liu et al.[10] to (0); *Wumengosaurus*: following Wu et al.[16] scoring changed from (0) to (1).

(90) Sacral (and caudal) ribs or transverse processes and their respective centrum: sutured (0); fused (1). (R75); *Cyamodus*: changed from (?) in Liu et al.[10] to (0);

Paraplacodus: changed from (?) in Li et al.[8] to (0); “Younginiformes”: scoring changed from (0&1) to (?) in *Youngina* (?) and (0) in *Hovasaurus*.

(91) Mineralized sternum: absent (0); present (1). (R118); *Cyamodus*: changed from (?) in Liu et al.[10] to (0).

(92) Median gastral element: angulated (0); straight (1). (R131)

(93) The medial gastral rib element: with a single lateral process (0); with two-pronged lateral process (1). (R119); *Cyamodus*: changed from (?) in Liu et al.[10] to (0); *Paraplacodus*: changed from (?) in Li et al.[8] to (0).

(94) Cleithrum: present (0); absent (1). (R76); “Younginiformes”: changed from (0&1) to (?) in *Youngina* and (0) in *Hovasaurus*.

(95) Clavicles: broad medially (0); narrow medially (1). (R77); *Wumengosaurus*: scoring with (?) is following Liu et al.[10] - note that Wu et al.[16] (p. 78) noted that there occurred some flattening of the bone during fossilisation.

(96) Clavicles: not meeting in front of interclavicle (0); meeting in an interdigitating anteromedial suture (1). (R79)

(97) Anterolaterally expanded corners of clavicles: absent (0); present (1). (R80)

(98) Clavicle: applied to anterior (lateral) surface of scapula (0); applied to medial surface of scapula (1). (R81); *Psephoderma*: scoring follows Rieppel[26].

(99) Relationship between clavicles and interclavicle: in simple overlapping contact (0); anteromedioventral end of clavicle embracing lateral tip of interclavicle in a complex contact (1). (R78)

(100) Interclavicle: rhomboidal (0); T-shaped (1). (R82); “Younginiformes”: changed from (0&1) to (1) in *Youngina* and (1) in *Hovasaurus*; Ichthyopterygia: scored (0,1) based on the diverse shapes indicated by Motani[18] instead of (1) in Li et al.[8].

(101) Posterior process on (T-shaped) interclavicle: elongate (0); short (1); rudimentary or absent (2). (R83)

(102) Scapula: represented by a broad blade of bone (0); with a constriction separating a ventral glenoidal portion from a posteriorly directed dorsal wing (1); rod-like (2). (R84); Following Li et al.[8], character description was changed to include state (2). *Paraplacodus*: a distinct constriction is present (see Rieppel[5]) so we score it (1); was scored (0) in Li et al.[8]; Ichthyopterygia: scored as (?), not with (2) as in Li et al.[8].

(103) Dorsal wing or process of eosauropterygian scapula: tapers to a blunt tip (0); ventrally expanded at its posterior end (1). (R85)

(104) Supraglenoid buttress: present (0); absent (1). (R86); *Youngina* and *Hovasaurus*: scoring follows Müller[27] and Liu et al.[10] who scored "Younginiformes" with (1); Currie[28] (p. 137) also noted absence of supraglenoid ridge in *Hovasaurus.*

(105) Number of coracoid ossifications: one (0); two (1). (R87)

(106) Coracoid: of rounded contours (0); slightly waisted (1); strongly waisted (2); with expanded medial symphysis and ridge-like thickening of the bone extending from glenoid facet posteriorly along lateral edge of the bone, coracoid foramen not enlarged (3); with expanded medial symphysis and ridge-like thickening of the bone extending from glenoid facet transversely through the bone, coracoid foramen much enlarged (4). (R88); *Cyamodus*: based on Pinna[29] and Scheyer[30] scored as (0); note it was changed (?) in Li et al.[8] and Liu et al.[10]; *Psephoderma*: scored as (1) following Pinna and Nosotti[17].

(107) Coracoid foramen: enclosed by coracoid ossification (0); between coracoid and scapula (1). (R89); "Younginiformes": following Bickelmann et al.[19], changed from (0) to (?) in *Youngina* and (0) in *Hovasaurus.*

(108) Pectoral fenestration: absent (0); present (1). (R90)

(109) Limbs: short and stout (0); long and slender (1). (R91)

(110) Foot: short and broad (0); long and slender (1). (R112); *Psephoderma*: scoring based on Renesto and Tintori[31]; Ichthyopterygia: scored (0,1) instead of (0) in Li et al., 2011; *Plesiosaurus*: score changed from (0) in Liu et al.[8] to (1).

(111) Humerus: rather straight (0); 'curved' (1). (R92)

(112) Deltopectoral crest: well developed (0); reduced (1); absent (2). (R93); *Paraplacodus*: following Rieppel[5] this is scored (0) – was scored (1) in Li et al.[8]; *Psephoderma*: scoring follows Renesto and Tintori[31]; *Youngina*: scoring also based on juvenile material pictured in Smith and Evans[32].

(113) Insertional crest for latissimus dorsi muscle: prominent (0); reduced (1). (R94); *Psephoderma*: scored as (1) following Renesto and Tintori[31], who noted traces of the insertion of the muscle latissimus dorsi being visible; "Younginiformes": changed from (0) to (?) in *Youngina* and (0) in *Hovasaurus.*

(114) Epicondyles of humerus: prominent (0); reduced (1). (R95)

(115) Ectepicondylar groove: open and notched anteriorly (0); open without anterior notch (1); closed (2); absent (3). (R96); "Younginiformes": changed from (0&2) to (0) in *Youngina* and (2) in *Hovasaurus.*

(116) Entepicondylar foramen: present (0); absent (1). (R97); Ichthyopterygia: scored (1) instead of (0) in Li et al.[8].

(117) Radius: shorter than ulna (0); longer than ulna (1); approximately of same length (2). (R98); "Younginiformes": changed from (0&1) to (?) in *Youngina* and (2) in *Hovasaurus*; Ichthyopterygia: scored (1,2) instead of (?) in Li et al.[8].

(118) Distal end of ulna: not expanded (0); distinctly expanded to at least the width of the proximal part (1). (R126); Changed description: description of original character state 2 ("distinctly expanded") used in Liu et al.[10] was amended; *Keichousaurus*: the ulna is not distally expanded, thus the scoring (?) of Liu et al.[10] is changed to (0); *Paraplacodus*: scored with (1), based on personal observation of the specimens in

the PIMUZ and on Rieppel[5] (figure 8b), although in the latter, the proximal part of ulna is cut off in the image; scored as (0) in Li et al.[8]; *Plesiosaurus*: following Li et al.[8] the condition in plesiosaurs is treated as (?); *Sinosaurosphargis*: the distal end of ulna is expanded, although not as much as the proximal part and is thus scored (0) as in Li et al.[8].

(119) Total number of carpal ossifications: more than three (0); three (1); two (2). (R137); *Wumengosaurus*: following Wu et al.[16] scoring changed from (2) to (1).

(120) Iliac blade: well developed (0); reduced but projecting beyond level of posterior margin of acetabular portion of ilium (1); reduced and no longer projecting beyond posterior margin of acetabular portion of ilium (2); (3) absent, i.e., reduced to simple dorsal stub; (4) elongated shaft. (R99); Changed description: following Sato et al.[14], the fourth character state "elongated shaft" was introduced, so *Yunguisaurus* and *Plesiosaurus* are scored (4); *Cyamodus*: changed from (?) in Liu et al.[10] to (1); Ichthyopterygia: scored as (4).

(121) Pubis: with convex ventral (medial) margin (0); with concave ventral (medial) margin (1). (R100)

(122) Obturator foramen in adult: closed (0); open or absent (1). (R101); Changed description: in the original state 1 (“open”) was amended. *Yunguisaurus*: we keep the original scoring of Liu et al.[10] (same scoring as in Rieppel et al.[12]) on which our matrix is based; Sato et al.[14] (p.195) introduced a new character state (2) (“foramen absent”) instead for *Yunguisaurus* and *Plesiosaurus*; some inconsistencies were encountered however in the article, because on p. 188 Sato et al.[14] state "there is no obturator foramen in the pubis" (of *Yunguisaurus*); whereas in table 1 on p. 190 "Obturator foramen open (101, "2")" is mentioned for "*Yunguisaurus* and Pistosauria/Pistosauridae" instead.

(123) Thyroid fenestra: absent (0); present (1). (R102); *Eusaurosphargis*: according to Nosotti and Rieppel[15], the thyroid fenestra could either be reduced or absent, thus we scored it (?); *Paraplacodus*: Note that character 102 (“Thyroid fenestra absent (0), present (1), reduced (3)") of Li et al.[8] and Nosotti and Rieppel[15] is rather unconventional, missing a character score (2) - in both their matrices *Paraplacodus* was scored (3), we instead score it with (1) here, thus following Rieppel[5] (p. 647), who noted the presence of a "more distinct thyroid fenestra in *Paraplacodus*"; Thalattosauria: Müller[22] noted that there is no thyroid fenestra present in *Askeptosaurus*; also scored as (0) in Müller[27]; Liu and Rieppel[33] also noted absence in *Anshunsaurus* and further mention a similar condition in *Hescheleria* - therefore scoring is (0); Ichthyopterygia: scored (0,1) instead of (1) in Li et al.[8]; *Helveticosaurus*: is scored as (0) herein, contra Nosotti and Rieppel[15].

(124) Acetabulum: oval (0); circular (1). (R103)

(125) Femoral shaft: stout and straight (0); slender and sigmoidally curved (1). (R104); *Cyamodus*: scoring changed from (?) in Liu et al.[10] and Li et al.[8] to (0) herein; *Helveticosaurus*: based on personal observation of holotype specimen (PIMUZ T 4352) scored as (0), thus following Rieppel[34] but contra Nosotti and Rieppel[15].

(126) Internal trochanter: well developed (0); reduced (1). (R105)

(127) Intertrochanteric fossa: deep (0); distinct but reduced (1); rudimentary or absent (2). (R106)

(128) Distal femoral condyles: prominent (0); not projecting markedly beyond shaft (1). (R107); *Cyamodus*: changed scoring from (?) in Liu et al.[10] and Li et al.[8] to (1).

(129) Anterior femoral condyle relative to posterior condyle: larger and extending further distally (0); smaller/equisized and of subequal extent distally (1). (R108); *Cyamodus*: changed scoring from (?) in Liu et al.[10] and Li et al.[8] to (1).

(130) Total number of tarsal ossifications: four or more (0); three (1); two or less (2). (R115); Note character definition state (2) was changed from “two” to “two or less” herein. *Helveticosaurus*: note that taxon was scored (3) in Nosotti and Rieppel[15], although the character description allowed only for (0, 1 and 2). We refrain from creating a character state (3) for a single tarsal ossification only, because it would be an autapomorphy of *Helveticosaurus* in the analysis.

(131) Perforating artery: passes between astragalus and calcaneum (0); between distal heads of tibia and fibula proximal to astragalus (1). (R109)

(132) Proximal concavity of astragalus: absent (0); present (1). (R110); Ichthyopterygia: scored (0) instead of (?) in Li et al.[8].

(133) Calcaneal tuber: absent (0); present (1). (R111)

(134) Distal tarsal 1: present (0); absent (1). (R113); Ichthyopterygia: scored (0,1) instead of (?) in Li et al.[8].

(135) Distal tarsal 5: present (0); absent (1). (R114)

(136) Metatarsal 5: long and slender (0); distinctly shorter than other metatarsals and with a broad base (1). (R116)

(137) Metatarsal 5: straight (0); ‘hooked’ (1). (R117); Ichthyopterygia: scored (1) instead of (?) in Li et al.[8].

New characters:

(138) Dermal armour ("osteoderms"): absent (0); present (1); forming carapace, excluding endoskeletal elements (2); forming carapace, including endoskeletal elements (3). **Note**: This character was adapted from character (1) of Rieppel and Zanon[35], but modified as used, e.g., in Rieppel[36], with only a combined, simplified state (2); character description has further been modified following Scheyer[37] to acknowledge the peculiar nature of placodont armour plates.

(139) Distinctly open L-shaped (boomerang-shaped) jugal: absent (0); present (1). **Note**: character has been revised from Rieppel[5,38] (and references therein), who noted that the L-shaped/boomerang-shaped jugal in *Paraplacodus* is connected with the temporal bar being formed only by the postorbital and squamosal and the absence of a quadratojugal.

(140) Palatine dentition: multiple rows with small numerous teeth/denticles (0); single row with four or more teeth (1), single row with three to one teeth/tooth (2); absent (3). **Note**: character was introduced due to the changed definition of character (63) above.

Supplementary References

1 Nicholls, E. L. & Brinkman, D. B. New thalattosaurs (Reptilia: Diapsida) from the Triassic Sulphur Mountain Formation of Wapiti Lake, British Columbia. *J. Paleontol.* **67**, 263-278 (1993).

2 Nicholls, E. L. A reexamination of *Thalattosaurus* and *Nectosaurus* and the relationships of the Thalattosauria (Reptilia: Diapsida). *PaleoBios* **19**, 1-29 (1999).

3 Rieppel, O. Handbook of Paleoherpetology Vol. 12A, 1-134 (Verlag Dr Friedrich Pfeil, Munich, 2000).

4 Müller, J. First record of a thalattosaur from the Upper Triassic of Austria. *J. Vertebr. Paleontol.* **27**, 236-240 (2007).

5 Rieppel, O. *Paraplacodus* and the phylogeny of the Placodontia (Reptilia: Sauropterygia). *J. Linn. Soc. Lond., Zool.* **130**, 635-659 (2000).

6 Swofford, D. L. PAUP*. Phylogenetic Analysis Using Parsimony (*and Other Methods). Version 4. Sinauer Associates, Sunderland, Massachusetts. (2003).

7 Calendini, F. & Martin, J.-F. PaupUP v1.0.3.1 A free graphical frontend for Paup* Dos software. (2005).

8 Li, C., Rieppel, O., Wu, X.-C., Zhao, L.-J. & Wang, L.-T. A new Triassic marine reptile from Southwestern China. *J. Vertebr. Paleontol.* **31**, 303-312 (2011).

9 Rieppel, O. The systematic status of *Hanosaurus hupehensis* (Reptilia, Sauropterygia) from the Triassic of China. *J. Vertebr. Paleontol.* **18**, 545-557 (1998).

10 Liu, J. *et al.* A new pachypleurosaur (Reptilia: Sauropterygia) from the Lower Middle Triassic of Southwestern China and the phylogenetic telationships of Chinese pachypleurosaurs. *J. Vertebr. Paleontol.* **31**, 292-302 (2011).

11 Klein, N. Postcranial morphology and growth of the pachypleurosaur *Anarosaurus heterodontus* (Sauropterygia) from the Lower Muschelkalk of Winterswijk, The Netherlands. *Paläontol. Z*., **86**, 389-408 (2012).

12 Rieppel, O., Sander, P. M. & Storrs, G. W. The skull of the pistosaur *Augustasaurus* from the Middle Triassic of northwestern Nevada. *J. Vertebr. Paleontol.* **22**, 577-592 (2002).

13 Rieppel, O. & Lin, K. Pachypleurosaurs (Reptilia: Sauropterygia) from the Lower Muschelkalk, and a review of the Pachypleurosauroidea. *Fieldiana, Geol.* **32**, 1-44 (1995).

14 Sato, T., Cheng, Y.-N., Wu, X.-C. & Li, C. Osteology of *Yunguisaurus* Cheng et al., 2006 (Reptilia; Sauropterygia), a Triassic pistosauroid from China. *Paleontological Research* **14**, 179-195 (2010).

15 Nosotti, S. & Rieppel, O. *Eusaurosphargis dalsassoi* n. gen. n. sp., a new, unusual diapsid reptile from the Middle Triassic of Besano (Lombardy, N Italy). *Mem. Soc. Ital. Sci. Nat. Mus. Civ. Stor. Nat. Milano* **31**, 3-33 (2003).

16 Wu, X.-C., Cheng, Y.-N., Li, C., Zhao, L.-J. & Sato, T. New information on *Wumengosaurus delicatomandibularis* Jiang et al., 2008 (Diapsida: Sauropterygia), with a revision of the osteology and phylogeny of the taxon. *J. Vertebr. Paleontol.* **31**, 70-83, (2011).

17 Pinna, G. & Nosotti, S. Anatomia, morfologia funzionale e paleoecologia del rettile placodonte *Psephoderma alpinum* Meyer, 1858. *Mem. Soc. Ital. Sci. Nat. Mus. Civ. Stor. Nat. Milano* **25**, 17-50 (1989).

18 Motani, R. On the evolution and homologies of ichthyopterygian forefins. *J. Vertebr. Paleontol.* **19**, 28-41 (1999).

19 Bickelmann, C., Müller, J. & Reisz, R. R. The enigmatic diapsid *Acerosodontosaurus piveteaui* (Reptilia: Neodiapsida) from the Upper Permian of Madagascar and the paraphyly of “younginiform” reptiles. *Can. J. Earth Sci.* **46**, 651-661 (2009).

20 Sollas, W. J. The skull of *Ichthyosaurus*, studied in serial sections. *Phil. Trans. of the R. Soc. Lond. Series B, containing Papers of a Biological Character* **208**, 63-65+67-126 (1918).

21 Romer, A. S. *Osteology of the reptiles*. (University of Chicago Press, 1956).

22 Müller, J. The anatomy of *Askeptosaurus italicus* from the Middle Triassic of Monte San Giorgio and the interrelationships of thalattosaurs (Reptilia, Diapsida). *Can. J. Earth Sci.* **42**, 1347-1367 (2005).

23 Shang, Q.-H., Wu, X.-C. & Li, C. A new eosauropterygian from the Middle Triassic of eastern Yunnan Province, southwestern China. *Vertebr. PalAsiat.* **49**, 155-171 (2011).

24 Cheng, Y.-N., Sato, T., Wu, X.-C. & Li, C. First complete pistosauroid from the Triassic of China. *J. Vertebr. Paleontol.* **26**, 501-504 (2006).

25 Holmes, R., Cheng, Y.-N. & Wu, X.-C. New information on the skull of *Keichousaurus hui* (Reptilia: Sauropterygia) with comments on sauropterygian interrelationships. *J. Vertebr. Paleontol.* **28**, 76-84 (2008).

26 Rieppel, O. The dermal armor of the cyamodontoid placodonts (Reptilia, Sauropterygia): morphology and systematic value. *Fieldiana, Geol.* **46**, 1-41 (2002).

27 Müller, J. in *Recent Advances in the Origin and Early Radiation of Vertebrates* (eds G. Arratia, M. V. H. Wilson, & R. Cloutier) 379-408 (Verlag Dr. Friedrich Pfeil, 2004).

28 Currie, P. J. *Hovasaurus boulei*, an aquatic eosuchian from the Upper Permian of Madagascar. *Palaeontol. Afr.* **29**, 99-168 (1981).

29 Pinna, G. Lo scheletro postcraniale di *Cyamodus hildegardis* Peyer, 1931 descritto su un esemplare del Triassico Medio Lombardo (Reptilia Placodontia). *Atti Soc. it. Sci. nat. Museo civ. Stor. nat. Milano* **121**, 275-306 (1980).

30 Scheyer, T. M. New interpretation of the postcranial skeleton and overall body shape of the placodont *Cyamodus hildegardis* Peyer, 1931 (Reptilia, Sauropterygia). *Palaeontologia Electronica* **13**, 1-15 (2010).

31 Renesto, S. & Tintori, A. Functional morphology and mode of life of the Late Triassic placodont *Psephoderma alpinum* Meyer from the Calcare di Zorino (Lombardy, N Italy). *Rivista Italiana di Paleontologia e Stratigrafia* **101**, 37-48 (1995).

32 Smith, R. M. H. & Evans, S. E. An aggregation of juvenile *Youngina* from the Beaufort Group, Karoo Basin, South Africa. *Palaeontol. Afr.* **32**, 45-49 (1995).

33 Liu, J. & Rieppel, O. Restudy of *Anshunsaurus huangguoshuensis* (Reptilia: Thalattosauria) from the Middle Triassic of Guizhou, China. *Am. Mus. Novit.* **3488**, 1-34 (2005).

34 Rieppel, O. *Helveticosaurus zollingeri* Peyer (Reptilia, Diapsida) skeletal paedomorphosis, functional anatomy and systematic affinities. *Palaeontogr. Abt. A* **208**, 123-152 (1989).

35 Rieppel, O. & Zanon, R. T. The interrelationships of Placodontia. *Hist. Biol.* **12**, 211-227 (1997).

36 Rieppel, O. The cranial anatomy of *Placochelys placodonta* Jaekel, 1902, and a review of the Cyamodontoidea (Reptilia, Placodonta). *Fieldiana, Geol.* **45**, 1-104 (2001).

37 Scheyer, T. M. Skeletal histology of the dermal armor of Placodontia: the occurrence of ‘postcranial fibro-cartilaginous bone’ and its developmental implications. *J. Anat.* **211**, 737-753 (2007).

38 Rieppel, O. The genus *Placodus*: systematics, morphology, paleobiogeography, and paleobiology. *Fieldiana, Geol.* **31**, 1-44 (1995).

```
#NEXUS
[written Fri Oct 26 17:23:21 CEST 2012 by Mesquite  version 1.12 (build h66)]

BEGIN TAXA;
        TITLE Untitled_Block_of_Taxa;
        DIMENSIONS NTAX=43;
        TAXLABELS
                Ancestor Captorhinidae Araeoscelidia Claudiosaurus Youngina
Rhynchosauria Trilophosaurus Prolacertiformes Choristodera Archosauriformes
Kuehneosauridae Rhynchocephalia Squamata Corosaurus Cymatosaurus Augustasaurus
Pistosaurus Plesiosaurus Simosaurus Germanosaurus Nothosaurus Lariosaurus
Wumengosaurus SerpianoNeustico AnaroDactylo Keichousaurus Dianopachysaurus
Hovasaurus Eusaurosphargis Thalattosauria Yunguisaurus Diandongosaurus
Psephoderma Cyamodus Placodus Paraplacodus Sinosaurosphargis WinterswijkSkull
Testudines Helveticosaurus Odontochelys Hanosaurus Ichthyopterygia
        ;

END;


BEGIN CHARACTERS;
        TITLE  'Matrix modified from "Liuetal. suppl data 1.nex.nex", part of
Liu et al., 2011 (JVP, Vol 31:292-302)';
        DIMENSIONS  NCHAR=140;
        FORMAT DATATYPE = STANDARD GAP = - MISSING = ? SYMBOLS = "  0 1 2 3 4";
        CHARSTATELABELS
                1 Bones_in_the_dermatocranium, 2
Preorbital_and_postorbital_region_of_skull, 3 Snout_, 4
Distinct_snout_constriction_in_adult, 5 Premaxillae, 6
Postnarial_process_of_premaxilla, 7 External_nares, 8 'Nasal(s)', 9 'Nasal(s)',
10 'Nasal(s)', 11 Lacrimal, 12 Dorsal_exposure_of_prefrontal, 13 Prefrontal_,
14 Frontal, 15 'Frontal(s) in adult', 16 'Distinct posterolateral processes of
frontal(s)', 17 Frontal, 18 Postfrontal, 19 Jugal, 20 Jugal, 21 Jugal, 22
'Parietal(s) in adult', 23 Parietal_skull_table, 24 Pineal_foramen, 25
Postparietals_, 26 Tabulars, 27 Supratemporals, 28 Temporal_region_of_skull, 29
Upper_temporal_fossa, 30 The_anteromedial_corner_of_the_upper_temporal_fossa,
31 Lower_temporal_fossa, 32 Squamosal, 33 'A box-like suspensorium of the
squamosal', 34
Dstinct_notch_of_squamosal_to_receive_distal_tip_of_paroccipital_process_, 35
Quadratojugal, 36 Anterior_process_of_quadratojugal, 37 Quadrate, 38
Posterior_margin_of_quadrate, 39 Lateral_conch_on_quadrate, 40
Dorsal_wing_of_epipterygoid, 41 Braincase_, 42 Occipital_crest, 43 Occiput, 44
Mandibular_articulations, 45 Supraoccipital, 46
Contact_between_exoccipitals_and_the_basioccipital_condyle, 47
Basioccipital_tubera, 48 Palate, 49 Premaxillae, 50
Posterior_palatine_vacuities, 51 Pterygoids_, 52 Pterygoid_flanges, 53
Ectopterygoid, 54 Suborbital_fenestra, 55 Internal_carotid_passage_, 56
Splenial_bone, 57 Distinct_coronoid_process_of_lower_jaw, 58
Strongly_projecting_lateral_ridge_of_surangular_defining_the_insertion_area_for
_superficial_adductor_muscle_fibers_on_the_lateral_surface_of_the_lower_jaw_,
59 Mandibular_symphysis, 60 Retroarticular_process_of_lower_jaw, 61
Trough_on_dorsal_surface_of_retroarticular_process, 62 Teeth, 63
Durophagous_dentition, 64 Number_of_premaxillary_teeth, 65 'Anterior
(premaxillary and dentary) teeth', 66 Premaxillary_and_anterior_dentary_fangs,
67 One_or_two_enlarged_teeth_on_maxilla, 68 The_maxillary_tooth_row, 69
Teeth_on_pterygoid_flange, 70 Vertebrae_, 71 Vertebrae_, 72 Vertebral_centrum,
73 Subcentral_foramina, 74 'Zygosphene-zygantrum articulation', 75
Zygapophyseal_pachyostosis, 76 Number_of_cervical_vertebrae, 77
Cervical_centra, 78 Parapophysis_, 79 Cervical_intercentra, 80
Distal_articular_surface_on_transverse_processes_of_dorsal_vertebrae, 81
Transverse_processes_of_neural_arches_of_the_dorsal_region_, 82
Distal_end_of_transverse_processes_of_dorsal_vertebrae, 83
Sutural_facets_receiving_the_pedicels_of_the_neural_arch_on_the_dorsal_surface_
of_the_centrum_in_the_dorsal_region, 84 Dorsal_intercentra, 85 'Anteroposterior
trend of increasing inclination of pre- and postzygapophyses within the dorsal
and sacral region', 86 A_distinct_free_anterior_process_of_cervical_ribs, 87
```

```
Pachyostosis_of_dorsal_ribs, 88 The_number_of_sacral_ribs, 89
Distinct_expansion_of_distal_head_of_sacral_ribs, 90 'Sacral (and caudal) ribs
or transverse processes and their respective centrum', 91 Mineralized_sternum,
92 Median_gastral_element, 93 The_medial_gastral_rib_element, 94 Cleithrum_, 95
Clavicles, 96 Clavicles_, 97 Anterolaterally_expanded_corners_of_clavicles_, 98
Clavicle_, 99 The_relationship_between_clavicles_and_interclavicle, 100
Interclavicle_, 101 'Posterior process on (T-shaped) interclavicle', 102
Scapula_, 103 The_dorsal_wing_or_process_of_the_eosauropterygian_scapula, 104
Supraglenoid_buttress, 105 Number_of_coracoid_ossifications, 106 Coracoid_, 107
Coracoid_foramen, 108 Pectoral_fenestration, 109 Limbs_, 110 Foot_, 111
Humerus_, 112 Deltopectoral_crest, 113
Insertional_crest_for_latissimus_dorsi_muscle, 114 Epicondyles_of_humerus_, 115
Ectepicondylar_groove, 116 Entepicondylar_foramen, 117 Radius_, 118
Distal_end_of_ulna, 119 Total_number_of_carpal_ossifications, 120 Iliac_blade,
121 Pubis_, 122 Obturator_foramen_in_adult, 123 Thyroid_fenestra, 124
Acetabulum_, 125 Femoral_shaft, 126 Internal_trochanter, 127
Intertrochanteric_fossa, 128 Distal_femoral_condyles, 129
Anterior_femoral_condyle_relative_to_posterior_condyle, 130
Total_number_of_tarsal_ossifications, 131 Perforating_artery, 132
The_proximal_concavity_of_astragalus_, 133 Calcaneal_tuber, 134
Distal_tarsal_1, 135 Distal_tarsal_5, 136 Metatarsal_5, 137 Metatarsal_5, 138
'new_character_Dermal_armour_("osteoderms")', 139
'new_character_Distinctly_open_L-shaped_jugal', 140
'new_character_Palatine_dentition' ;
        MATRIX
        Ancestor
0000000000000000000000000000000000000000000000000000000000000000000000000000000000000000
0000000000000000000000000000000000000000000000000000000000000000000000000000
        Captorhinidae
0000000000000000?000000(0,2)0100000000000000000000?000000100000000000000?000000000
0000000?0000000000?000000?0?0100000000000000000000000000000000000000
        Araeoscelidia
1100000000000000101000000000030(0,1)00000000?000001000000001010000000000000000000
0100000?000000010000000100?0100011000000000000000000000000000000(0,1)
        Claudiosaurus
0100000000100001010000001110302000001000?00000?00000201010?00000000100?000000100
000?0010001?00110000100?1000001011110000000011011100000000010
        Youngina
1100000000100001010000000000301000001l0?000001000000010?1001000000100000000010O
0000000000?100?10000100?1000?1100?000?000000110101000000010000
        Rhynchosauria
1000110000100000001010133111010110000110100100000100001001001000?01011000000100
000?0(0,1)00000?00110000100?100(0,1)011000001000000011010101010111003
        Trilophosaurus
11001?0000?00100110?003311?0100?000?11000?120?000000010?10010000?01011(1,2)?000
0100000?001000??0?110000100?10000l100?0010000000110101000101110003
        Prolacertiformes
1100110100100000(0,1)010(0,1)0(0,1)0(0,1)0(2,3)11(0,1)0302100(0,1)1110?001001000000010
1(0,1)00100000010(0,1)1(0,2)0000010(0,1)000?(0,1)0100011001100000?0?10000110000
01(1,2)00000(0,1)110101000(0,1)(0,1)11(0,1)00(0,3)
        Choristodera
1200110100100000001000013111010l100(0,1)0110?0111010?10000101000100000010011000O
0100000110101007?0?110001100?10000110000(0,2)120000001101110?01011100(0,3)
        Archosauriformes
(0,1)(0,1)001101001000(0,1)(0,1)(0,1,2)1010(0,1)(0,2)(0,3,4)11(0,1)030110000110
?0(0,1)(0,1)(0,1,2)010(0,1)(0,1)000(0,1)101(0,1)00100000010(0,1)1(0,1,2)0000010
(0,1)0100(0,1)(0,1)10(0,2)0(0,1)100110000100?100(0,1)011000(0,1)010000000110(1,
2)(0,1)10001(0,1)11110(0,3)
        Kuehneosauridae
1000000000100001010000021110102100111l1?01000100?000?10?000100000001011000000101
010?11?0001?0?????????1?100001?000021200000111010l??0?????00(0,1)
        Rhynchocephalia
1000000000(1,2)000(0,1)(0,1)01(0,1)10(0,1)(0,2)(0,2)11(0,1)010(1,2)0000111(0,1)
10(0,1)(0,1)0010000000101100l010000101(0,1)0001001000000(0,1)000001100110000100
?100001100002000000011101010100(0,1)111001
```

Squamata
1(0,1,2)00000000(1,2)00(0,1)(0,1)001(0,1)00(0,1)(0,2)(0,2,3,4)11(0,1)0102100?1
1110(0,1)0(0,1,2)(0,1)(0,1)00(0,1)0000101100101010000101 1(0,2)00(0,1)0010000001(0
,1)0000110?1(0,1)00001(0,1)0?10000110000(0,2)10(0,1)0000111010101001111 1(0,1)(0
,1,2,3)
Corosaurus
0010101000200000111?000101110102001??100101110 1?1?00000??111100001101110001001 01
0011111010100111011111111011100111100201101111011111000 11??000
Cymatosaurus
0211101022200(0,1)01(1,2)1100(1,2)(2,3)011102120011?100?0(0,1)110??110000011 0?2
?000011011110 01????100111??0??00001??????????0???0?000000?0??011110111????????0
03
Augustasaurus
0020102?222010012100103311102220 1?1?100012112111110000??012100000102111 01?01111
10111?10???00?10?011??10?03?10?12113121 1??????????????????003
Pistosaurus
0020102022201001 21?011331110222 01?1?10011211???1?00000??????000110111101100?1?
0011??10???00?1??????? 11103??0?1?113121 10????11???????????003
Plesiosaurus
0000100?(1,2)220000001001033111022201 01?100112112111110200??010100000011111 0100
1101101110101000 0?101011??101041101(0,1)110312?04?111012110?001000003
Simosaurus
0200100012200010010002111110202000011000002101210002001101010000101211100 100101
0001111010000110111111110102110010111120121011112111110 1100003
Germanosaurus
0211101002210001112 0?111111120200???100?00?????1?00??????????0001111????0??????
??????????00?1?????????? 0???????????? 0???????????????????003
Nothosaurus
021110100(0,2)2100110(1,2)(1,2)002(2,3)21111202000(0,1)11000012(0,1)1121100(0,2
)0011012100001102111101(0,1)01010001101(0,1)11(0,1)0011(0,1)1111(0,1)2101021100
1(0,1)(0,1)1(0,1)0201210111121111101100003
Lariosaurus
021110100(0,2)21001102(1,2)002211111(1,2)02000??10000120 1??1?00100??01210000110
211110?10101000?101(0,1)2100001011 1??10102110011111020(0,1)3(0,1)1111121101101
100003
Wumengosaurus
0120101000?0000??1???00011103 12?0???11??0??0???????????0??100000010?10?0?00?0?
000???11110?0?1??11???1?10???0011?10010100?1?1??1121101100013
SerpianoNeustico
110010000(0,2)2000(0,1)10(1,2)0000001110302000011101002 01??1000210??00011000001
0110101101010001101 1(1,2)10000101011(0,1)2101021100101(0,1)(0,1)0(1,2)0(1,2)3(0
,1)(0,1)111121121101100013
AnaroDactylo
1100100000200001010000001110302000??110100201??1000210??000110000010110101101 01
0001101011000010111 1??10102110?10100010130011?1?????0?????013
Keichousaurus
1000100012200011010(0,1)0203110030210001100?002011?10002?0?010011000(0,1)000110
101101?100011011(0,1)10000101111121010211001(0,1)(0,1)1111002001111211110011000
03
Dianopachysaurus
1200100000200011110002001110302 00?0?100?00?0???????????00?1?0000000??????10???
?0????11110???10??1???101????001111102002 01??1121121001100 01?
Hovasaurus
?1???????????00101000000??0030200???100?00020100?0???1?????1?00????000000000100
0000000000010001000010 0?10000110000202000000110101001 00?10?0?
Eusaurosphargis
?10010?????????????????003???030??0????????0????????????????0??0000010?1110?0????
?10?1?10????011100?0??0??001?0?0??0?100?001??11211????????1??
Thalattosauria
1(0,1)2010(1,2)0(0,1)220000(0,1)?10(0,1)000(0,3)?10040210 01?110?0011??00100(0,2
)01??110(0,1)0000(0,1)010(0,1)?000?001???00?1?10000000110000100?10000000111?(0,
1)20000001111 11(0,1)?10(0,1)100003
Yunguisaurus
001?1020122000?0(1,2)1?0??33????2220??1?20?????1??2??1?2000010210000 1??11101010
10?110?11?10100????????1??111?3??01111131212 4?11?01?1?0100??00003

```
        Diandongosaurus
011010100220011111000110111031200001110?0??????????????????00?1100011102?1?00100101
000110101100001111?102???02110011111?1102?011111111121001100017
        Psephoderma
022110201221000?0100020311102001000011 0?00100??1001110???????011?0101?00??001??
??10?10101000101???1???0??01?10010102100?10111101111?101100202
        Cyamodus
021110100(0,1)20000(0,1)0100120311102001000001000011 0(0,1)01101110 0?10210011001
01?000000101?10010101000101?0011?20???0?10?1110??20110111 0??11????????202
        Placodus
02111011002001(0,1)101001(0,2)00111020010011111010010011110110000102100111010100
000001011100111010001011001111 0?10011001110012021001110111121001100102
        Paraplacodus
001?102?0?20?1???1000???111010210?11100?0??0???1?01??0??112110111010110000?00???
11001?10100?101100?0??1??011?001010?121(0,1)3011?101111?10????011
        Sinosaurosphargis
0010102000?0?001?000120011104?20001?0?0???11???0?0020??10?10?00000101?000?100??
?11?0??1????00110100 1?1??001?0?1211??100??????????????????213
        WinterswijkSkull
0?1?10?00120?0?101000?001110?0210?11110?0??0??????1?????1??1?0001010 1?????????
??????????????????????????????????????????????????????????????11
        Testudines
0(0,2)00000000100(0,1)00??00000311(0,1)0000100001100000(0,2)000(0,1)(0,1)000110
1000(0,1)0?00????0(0,1)(0,2)0000010(0,1)0000100000000?100000100??001000000(0,1)
(0,2)1000(1,2)0010000110100(0,1)111303
        Helveticosaurus
?000100????00???1?????????01?????????????0???????????1??1?0000010??000?00?0?
010?1?10???0101100001 00?100100011 1?1102101 0?012112?1?11000??
        Odontochelys
1200000000?0??????????04???00???0???????0??0??00?000?????00??0000100100000010100
00001??00000???0???0??2??0110000000??0100?00?1001?01000?1?30?
        Hanosaurus
0000???100200011 0?0001031110 3?2000????0?00?11?????????????????00???10??010?????
0???1??1????011100???????02??00??????????010?112111110110000??
        Ichthyopterygia
0120102100(0,1)00(0,1)00(0,1,2)(1,2)0000(0,1,3)(0,3)1100(1,3)021000111 0?0001(0,
1,2)10?(0,1)002?000001(0,1)?0(0,1)0001011010000 1?0???01?00???0??111000(0,1)0??1
02?00(0,1)011131(1,2)004??(0,1)?01211??0?(0,1)??10(0,1)3

;

END;
```

CHAPTER 5

UNIQUE METHOD OF TOOTH REPLACEMENT IN DUROPHAGOUS PLACODONT MARINE REPTILES, WITH NEW DATA ON THE DENTITION OF CHINESE TAXA

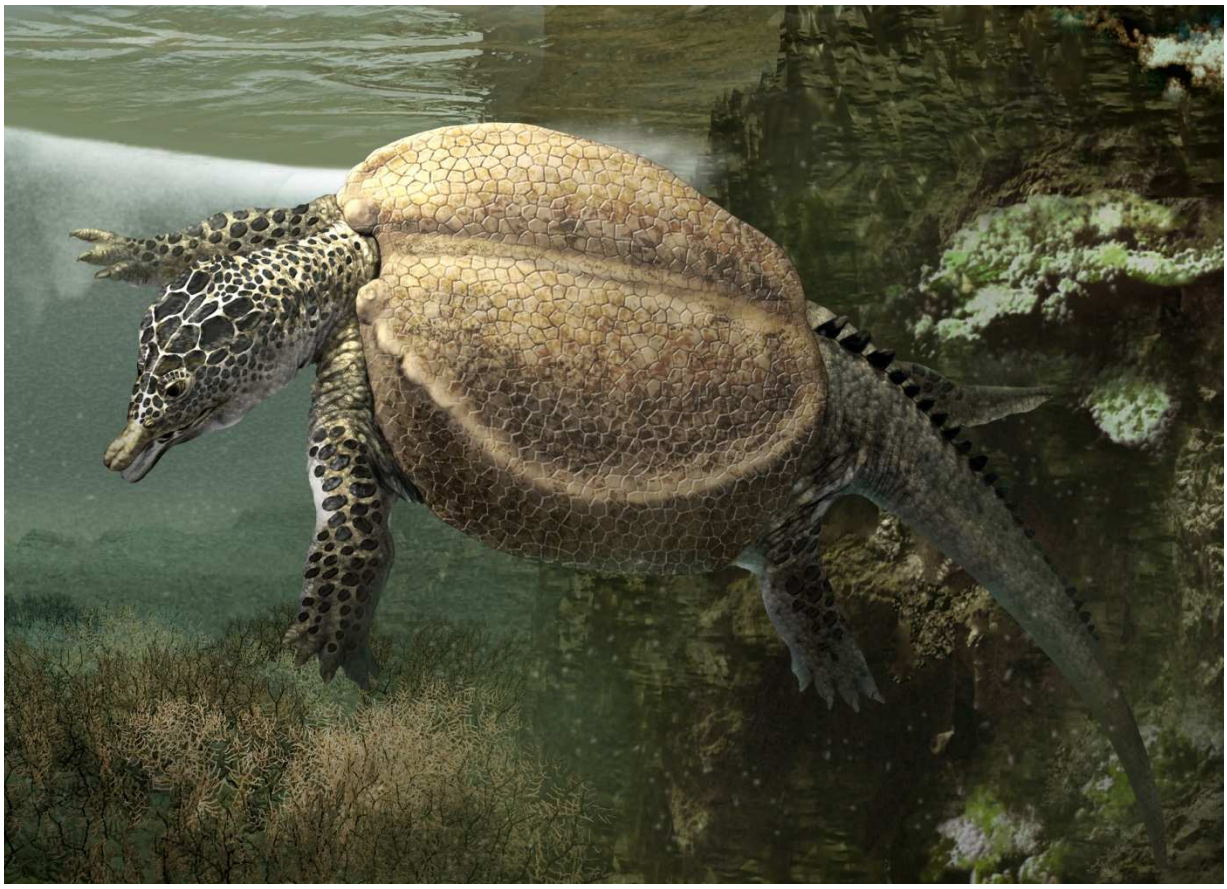

Psephochelys polyosteoderma by Jaime Chirinos

Journal of Anatomy

J. Anat. (2014) **224**, pp603–613 doi: 10.1111/joa.12162

Unique method of tooth replacement in durophagous placodont marine reptiles, with new data on the dentition of Chinese taxa

James M. Neenan,[1] Chun Li,[2] Olivier Rieppel,[3] Federico Bernardini,[4] Claudio Tuniz,[4] Giuseppe Muscio[5] and Torsten M. Scheyer[1]

[1]*Palaeontological Institute and Museum, University of Zurich, Zurich, Switzerland*
[2]*Institute of Vertebrate Paleontology and Paleoanthropology, Chinese Academy of Sciences, Beijing, China*
[3]*The Field Museum, Chicago, IL, USA*
[4]*The 'Abdus Salam' International Centre for Theoretical Physics, Trieste, Italy*
[5]*Museo Friulano di Storia Naturale, Udine, Italy*

Abstract

The placodonts of the Triassic period (~252–201 mya) represent one of the earliest and most extreme specialisations to a durophagous diet of any known reptile group. Exceptionally enlarged crushing tooth plates on the maxilla, dentary and palatine cooperated to form functional crushing areas in the buccal cavity. However, the extreme size of these teeth, combined with the unusual way they occluded, constrained how replacement occurred. Using an extensive micro-computed tomographic dataset of 11 specimens that span all geographic regions and placodont morphotypes, tooth replacement patterns were investigated. In addition, the previously undescribed dental morphologies and formulae of Chinese taxa are described for the first time and incorporated into the analysis. Placodonts have a unique tooth replacement pattern and results follow a phylogenetic trend. The plesiomorphic *Placodus* species show many replacement teeth at various stages of growth, with little or no discernible pattern. On the other hand, the more derived cyamodontoids tend to have fewer replacement teeth growing at any one time, replacing teeth unilaterally and/or in functional units, thus maintaining at least one functional crushing area at all times. The highly derived placochelyids have fewer teeth and, as a result, only have one or two replacement teeth in the upper jaw. This supports previous suggestions that these taxa had an alternative diet to other placodonts. Importantly, all specimens show at least one replacement tooth growing at the most posterior palatine tooth plates, indicating increased wear at this point and thus the most efficient functional crushing area.

Key words: durophagy; Placodontia; tooth replacement; Triassic marine reptiles.

Introduction

Placodontia are a clade of Triassic sauropterygian marine reptiles that inhabited the margins of the Tethys Ocean in present day Europe, Middle East and China (Hagdorn & Rieppel, 1999; Li, 2000; Rieppel, 2000; Li & Rieppel, 2002; Jiang et al. 2008; Zhao et al. 2008; Scheyer et al. 2012). The clade is composed of two main groups: the more plesiomorphic, non-armoured 'placodontoid' genera (*Paraplacodus* and *Placodus*), and the more derived, heavily armoured Cyamodontoidea. They are characterised by their highly specialised crushing dentition which, when combined with features such as an akinetic skull, robust braincase and heavily reinforced cranial bones, represent one of the most extreme examples of reptilian durophagy known (Sander, 1999; Rieppel, 2000; Neenan & Scheyer, 2012). Placodont teeth are extremely enlarged, and are located on the palatine, as well as the marginal tooth-bearing elements, i.e. maxilla, dentary and, in most cases, premaxilla. It has recently been shown that placodont palatine dentition originally evolved for feeding on soft prey, and was later adapted for crushing (Neenan et al. 2013). Placodont dentitions have been extensively studied (Jaekel, 1907; Peyer, 1931; Kuhn-Schnyder, 1959; Vogt, 1983; Mazin, 1989; Rieppel, 1995, 2000; Sander, 1999; Neenan et al. 2013), with sauropterygian tooth replacement and implantation being described in detail by Rieppel (2001). However, this study only utilised one placodont taxon, *Placodus gigas*, in the form of four

Correspondence
James M. Neenan, Palaeontological Institute and Museum, University of Zurich, Karl Schmid-Strasse 4, 8006 Zurich, Switzerland.
E: james.neenan@pim.uzh.ch

Accepted for publication *2 January 2014*
Article published online *11 February 2014*

fragmentary specimens and some cross-sections [not computed tomography (CT)] of the skull and dentary. While this did shed light on the process of placodont dental replacement, it did not reveal data on replacement patterns, nor was it conclusive for all placodont taxa. Indeed, four new taxa have been described from China since: *Sinocyamodus xinpuensis* (Li, 2000); *Psephochelys polyosteoderma* (Li & Rieppel, 2002); *Placodus inexpectatus* (Jiang et al. 2008); and *Glyphoderma kangi* (Zhao et al. 2008).

The inclusion of these relatively new Chinese taxa in this study is vital, owing to our comparatively poor understanding of their morphology (including dentition), and for obtaining a complete record of placodont tooth evolution on both the eastern and western margins of the Tethys Ocean (i.e. present-day South China and Europe/Middle East). We thus provide in this paper a description of the dentition of these taxa (with the exception of *Glyphoderma*, see below), as well as including them in the tooth replacement analysis.

Tooth replacement in reptiles

Reptiles generally replace teeth constantly throughout life (polyphyodonty) and, as a consequence, show replacement teeth in several stages of development within the jaw/skull (Owen, 1840–1845). Teeth are implanted in various ways (Edmund, 1960, 1969), with the ancestral condition of subthecodonty (socketed teeth with some ankylosis by cementum) being present in parareptiles and some early synapsids, such as pelycosaurs. Most lizards and snakes show pleurodont attachment (ankylosed to the inner side of the labial wall of the tooth-bearing bone), while many marine reptiles, most archosaurs and mammals exhibit thecodont implantation (the tooth sits in a deep socket and is affixed by uncalcified connective tissue). Teeth are replaced in an alternating manner, i.e. even numbered teeth are coordinated in one wave of replacement from posterior to anterior, while the odd numbered teeth do the same but at roughly the opposite phase of replacement. These waves of replacement, first described by Woerdeman (1921), are known as Zahnreihen and are a phenomenon that has been confirmed subsequently (in adult specimens at least) for fossil and extant taxa by several authors (e.g. Edmund, 1960, 1969; Hopson, 1980; DeMar & Bolt, 1981; de Ricqlès & Bolt, 1983; Kieser et al. 1993; Small, 1997; Delgado et al. 2003), but see a review by Whitlock & Richman (2013) for other hypotheses. In most reptiles, replacement teeth develop directly lingually to the corresponding functional teeth and lie in resorption pits at the bases of the latter, whereupon the attachment is resorbed, the functional tooth is lost and the replacement tooth takes its place. This can be seen clearly in squamates such as *Iguana* (termed the 'iguanid' method), but also occurs in crocodilians (Edmund, 1960, 1969) and ichthyosaurs (Maxwell et al. 2012). There are exceptions to this, however, such as in varanid and anguimorph lizards (McDowell & Bogert, 1954; Edmund, 1960; Cooper, 1966; Rieppel, 1978) where the replacement tooth grows in an apparently interdental position, posterior and lingual to the functional tooth (termed the 'varanid' method by Edmund, 1960); and in some agamid lizards that show both acrodont and pleurodont tooth attachment (Cooper et al. 1970). In squamates with palatal dentition, such as many iguanids, lacertids, anguids and snakes, palatal teeth are usually replaced in the same way as marginal ones, but the replacement tooth is situated labially rather than lingually (Mahler & Kearney, 2006).

In sauropterygians such as *Nothosaurus* and *Simosaurus*, tooth replacement occurs in a similar way to other reptiles, i.e. in waves of Zahnreihen. Unique to Sauropterygia, however, replacement teeth grow in distinct alveolar spaces located disto-lingual to each functional tooth (Burckhardt, 1895; Edinger, 1921; Rieppel, 2001). Here, once a replacement tooth reaches full size, the bone separating the alveolus from the functional tooth is resorbed, and the replacement migrates horizontally and labially. The ankylosed base of the old functional tooth is resorbed, thus expelling it, and the new replacement tooth takes its place. Placodonts are the exception to this general rule, however. Despite their polyphyodont condition, it has already been suggested that they might not replace their teeth in an alternating order (Rieppel, 2001) and, owing to the extreme size of the functional teeth, spatial constraints prevent horizontal tooth replacement. This issue is overcome by instead utilising a vertical mode of replacement, with new teeth growing directly below the functional ones in a large alveolar space (Fig. 1; Jaekel, 1907; Vogt, 1983; Rieppel, 2001).

Placodont teeth act together in groups to create functional 'crushing areas' (*sensu*; Mazin & Pinna, 1993); regions between palatine, maxillary and dentary tooth plates that generate maximum force in order to crush hard-shelled prey. However, if placodonts replaced their teeth like most other reptiles/sauropterygians, i.e. in alternating waves, these 'areas' would potentially be rendered inert, preventing the animal from efficiently feeding. We therefore hypothesise that placodonts modified the plesiomorphic condition of alternate tooth replacement to compensate for this feeding strategy. Because replacement teeth are not usually visible in external view in placodonts, as they are located under the functional teeth, a large dataset of 11 micro (μ)-CT scans, including all placodont morphotypes, was used to reveal *in situ* replacement teeth at their various stages of development.

Materials and methods

The skulls of all valid placodont species, including at least one specimen of each, were scanned using μCT, with the exception of *Placochelys placodonta*, a specimen of which the authors were unable to obtain. *Paraplacodus broilii*, *Cyamodus hildegardis*, *Henodus*

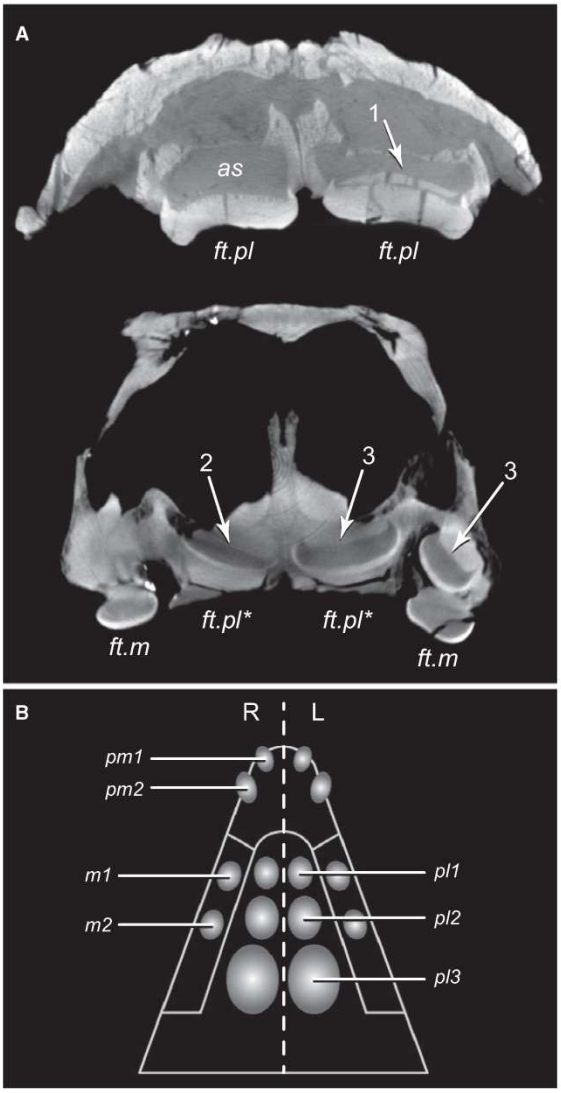

Fig. 1 Visualisation of the tooth replacement stages (A) and dental formula nomenclature (B) used in this paper. (a) Coronal sections revealing replacement teeth in the armoured placodont *Psephoderma alpinum* PIMUZ A/III 1491 (top), and the unarmoured *Placodus gigas* BSP 1968 I 75 (bottom). Stage 1, the replacement tooth is little more than a thin layer of enamel and does not resemble a functional tooth. Stage 2, the replacement tooth begins to resemble a functional tooth, but has not reached full size. Stage 3, the replacement tooth has reached approximately full size and is ready to replace the functional one. (b) Schematic representation of a placodont palate to demonstrate the dental nomenclature used in this paper. as, alveolar space; ft.m, maxillary functional tooth; ft.pl, palatine functional tooth; ft.pl*, broken palatine functional tooth; m1 and m2, 1st and 2nd maxillary teeth; pl1–pl3, 1st to 3rd palatine teeth; pm1 and pm2, 1st and 2nd premaxillary teeth.

chelyops and the Chinese *Glyphoderma kangi* were excluded from this study owing to excessive scan artefacts and/or poor state of preservation that prevented the observation of replacement teeth. However, it should be noted that *Henodus* is not considered to be durophagous but rather a filter feeder (Rieppel, 2002). Details of the specimens used herein, as well as the scan parameters, are provided in Table 1. All German specimens were scanned at Giesserei Technologie Aalen, Hochschule Aalen, Germany with a Wälischmiller RayScan 200; all Chinese specimens at the Institute of Vertebrate Paleontology and Paleoanthropology, Beijing, P. R. China with a specially constructed 2D scanner commissioned by the IVPP; *Protenodontosaurus* was scanned at the 'Abdus Salam' International Centre for Theoretical Physics, Trieste, Italy with a special machine of their own construction, described by Tuniz et al. (2013); and *Psephoderma* was scanned at the Steinmann-Institute for Geology, Mineralogy and Palaeontology, University of Bonn, Germany using a Phoenix v tome x s. μCT slice data were reconstructed into 3D volumes using the manual segmentation function of Avizo 6.2. Replacement teeth were identified by the presence of enamel which, owing to its high density, made them relatively simple to locate and segment.

Replacement teeth were categorised into three stages of development (Fig. 1A), based mostly on the state of growth of the enamel cap, as dentine is not always visible in our scan data. Stage 1 replacement teeth are at the earliest stage and are much smaller than functional teeth, consisting mainly of a thin enamel layer with very little or no dentine. Stage 2 replacement teeth resemble a functional tooth more closely, but have not yet reached full size, having a thinner enamel cap and less dentine than a functional tooth. Finally, stage 3 replacement teeth are approximately full size, with fully developed enamel and dentine components, and are ready to erupt and become functional.

Owing to the frequent mention of specific teeth in the current paper, they will be referred to throughout the text in the following manner: right or left side of the skull (R or L), followed by the tooth-bearing element (pm, premaxilla; m, maxilla; pl, palatine; d, dentary), and then by the number of the tooth position, where 1 is the most anterior (palatal dentition) or mesial (marginal dentition; Fig. 1B). For example, the second palatine tooth on the right side will be referred to as Rpl2.

Institutional abbreviations used in this paper are: BSP; Bayerische Staatssammlung fur Paläontologie und Historische Geologie, Munich, Germany; IVPP, Institute of Vertebrate Paleontology and Paleoanthropology, Beijing, P. R. China; MFSN, Museo Friulano di Storia Naturale di Udine, Italy; PIMUZ, Palaeontological Institute and Museum, University of Zurich, Switzerland; SMNS; Staatliches Museum für Naturkunde Stuttgart, Germany; UMO, Urwelt-Museum Oberfranken, Bayreuth, Germany.

Results

All specimens scanned revealed replacement teeth at varying stages of growth (Figs 1 and 2, and Figs S1–S11), and in all cases a maximum of one replacement tooth is present per functional tooth, with the exception of *Cyamodus kuhnschnyderi*, which has two replacement teeth for Rpm1 (Fig. S3b).

All *Placodus* specimens show multiple replacement teeth at various stages of growth (Figs 1 and 2, and Figs S1, S2 and S9). The UMO BT 13 specimen of *Placodus gigas* is missing all premaxillary teeth, a common state of preservation in this taxon owing to these teeth being attached by soft tissue (Rieppel, 2001), as well as Rm4. Because the latter shows no sign of a replacement tooth, it is assumed that it

Table 1 Information regarding the taxa included in this study.

Taxon	Specimen number	Locality and stratum	μCT slice thickness, mm	μCT voltage, kV	μCT current, μA
Placodus gigas Agassiz (1833)	UMO BT 13	Hegnabrunn, Bavaria, Germany. Upper Muschelkalk, Anisian, Middle Triassic	0.227	210	130
Placodus gigas Agassiz (1833)	BSP 1968 I 75	Near Bayreuth, Bavaria, Germany. Upper Muschelkalk, Anisian, Middle Triassic	0.192	210	120
Placodus inexpectatus Jiang et al. (2008)	IVPP V 14996 new specimen	Yangjuan Village, Guizhou Province, China. Falang Formation, Anisian, Middle Triassic	0.200	190	100
Sinocyamodus xinpuensis Li (2000)	IVPP V 11872 holotype	Guanling, Guizhou Province, China. Guanling Formation, Carnian, Upper Triassic	0.194	190	100
Cyamodus kuhnschnyderi Nosotti & Pinna (1993)	SMNS 15855 holotype	Tiefenbach, Baden-Württemberg, Germany. Upper Muschelkalk, lower Ladinian, Middle Triassic	0.227	210	120
Cyamodus muensteri Agassiz (1839)	BSP AS VII 1210 holotype	Near Bayreuth, Bavaria, Germany. Upper Muschelkalk, Anisian, Middle Triassic	0.139	215	150
Cyamodus rostratus Münster (1839)	UMO BT 748 holotype	Near Bayreuth, Bavaria, Germany. Upper Muschelkalk, Anisian, Middle Triassic	0.155	210	120
Protenodontosaurus italicus Pinna (1990)	MFSN 1819GP holotype	Chiout Zuguin, Udine, Italy. Carnian, Upper Triassic	0.040	149	201
Macroplacus raeticus Schubert-Klempnauer (1975)	BSP 1967 I 324 holotype	Hinterstein, Bavaria, Germany. Kössen Formation, Rhaetian, Upper Triassic	0.213	210	120
Psephoderma alpinum Meyer (1858)	PIMUZ A/III 1491 new specimen	Schesaplana Mountain, Switzerland. Rhaetian, Upper Triassic	0.166	130	130
Psephochelys polyosteoderma Li & Rieppel (2002)	IVPP V 12442 holotype	Xinpu, Guizhou Province, China. Falang Formation, Carnian, Upper Triassic	0.200	190	100

is missing due to taphonomic reasons. All other teeth are preserved and are paired with a replacement tooth, with the exception of Lpl2. BSP 1968 I 75 is missing part of the rostrum, and consequently the premaxillary and first maxillary teeth have not been preserved. Similar to UMO BT 13, the m4 is missing, but on the left side rather than the right, and has no replacement. However, unlike the other two *Placodus* specimens, all palatine teeth have a replacement tooth that is at least at stage 2, and only has one maxillary tooth with a replacement tooth present. *Placodus inexpectatus* is the Chinese representative of the genus (Figs 2b and 3) and, similar to its European counterpart, appears to also easily lose the premaxillary teeth during fossilisation, although one is still preserved *in situ*. All other teeth are preserved in the skull, despite the heavily damaged right side. Similar to UMO BT 13, all maxillary teeth save one have a replacement tooth at some stage of growth. Palatine tooth plates 1 and 3 on both sides have replacement teeth; however, neither pl2 has one. The mandible of *Placodus inexpectatus* shows a much more homogeneous pattern of tooth replacement, in that three of the four anterior teeth (Ld1, Rd1, Rd2) have replacement teeth at stage 2, the second and third dentary tooth plates of both sides (Ld4, Ld5, Rd4, Rd5) have stage 3 replacement teeth, and the first and fourth tooth plates have no detectable replacement teeth (Ld3, Ld6, Rd3, Rd6). It should be noted, however, that extensive damage on the right side of the skull as well as poor preservation below Ld6 could account for the lack of observed replacement teeth here (Fig. S9). The only missing tooth in the mandible is Ld4, which has a stage 3 replacement tooth. Thus, the functional tooth may have been lost prior to death.

Three of the four valid species of *Cyamodus* were included (Rieppel, 2000; Fig. 2a, and Figs S3–S5), *C. hildegardis* only being excluded due to its poor state of preservation. *Cyamodus kuhnschnyderi* is unique among our sample of taxa in that Rpm1 has two replacement teeth: a stage 3 immediately followed by a stage 1. With the exception of

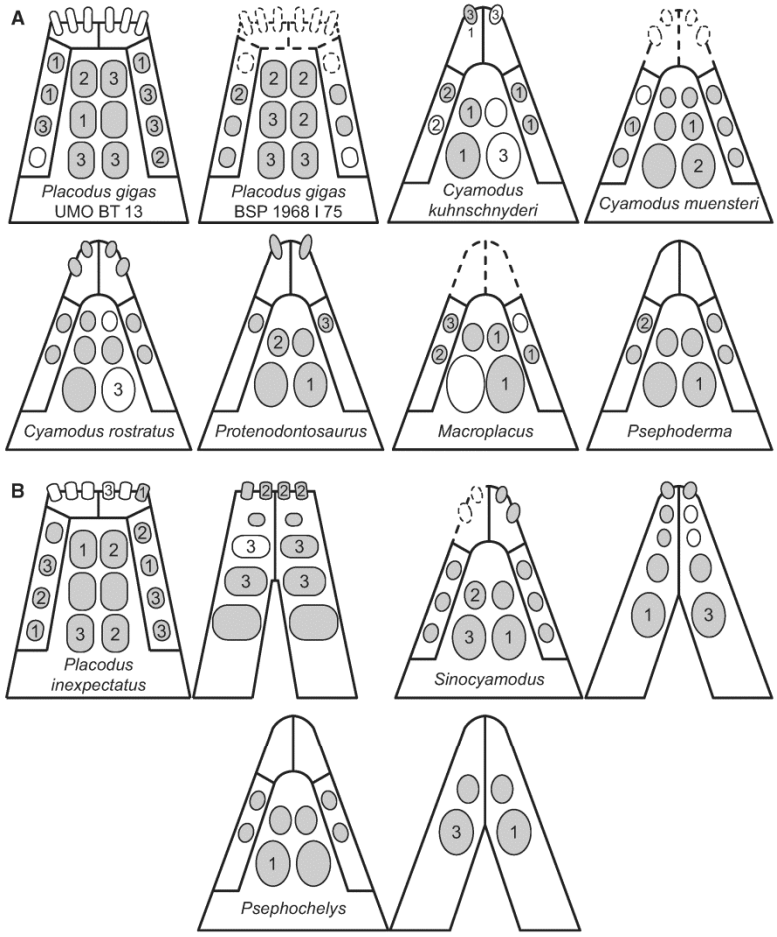

Fig. 2 Simplified reconstructions of placodont skulls and mandibles showing functional dentition and replacement tooth stages. (a) Palatal view of European placodont skulls. (b) Palatal view of Chinese placodont skulls with dorsal view of each corresponding mandible. Preserved teeth are shown in grey and missing teeth in white. Dashed lines indicate broken parts of specimens that have not been preserved. The numbers indicate tooth replacement stages and correspond to Fig. 1.

Lpl1, all teeth in the skull have corresponding replacement teeth in all phases of development. In total, four teeth are missing in this specimen (Lpm1, Rm2, Lp1 and 2), with only Lpm1 and Lpl2 exhibiting a stage 3 replacement tooth. This skull also features a fairly uniform replacement pattern with all teeth in a specific element being at the same stage, with the exception of the left palatine. The holotype of *Cyamodus muensteri* is damaged and extensively reconstructed, with the rostrum and all premaxillary teeth missing. Rm1 is also missing and lacks a replacement tooth. Of the preserved teeth, only Rm2, Lpl2 and Lpl3 have replacement teeth, all at either stage 1 or 2 of growth. *Cyamodus rostratus* contains even fewer replacement teeth, with only one stage 3 being present (Lpl3), the corresponding functional tooth of which is missing and may have been in the process of replacement before death. The dentition of *Sinocyamodus* (Figs 2b and 4, and Fig. S10) supports a close relationship with *Cyamodus* (see below). The right premaxilla is missing in this specimen, but all other teeth in the skull are present. The dentary is missing two teeth (Rd2 and 3), neither of which have replacement teeth. The majority of teeth have no replacement, with the exceptions being Rpl1, Rpl2, Lpl2, Rd5 and Ld5. Importantly, the pl2 and their corresponding d5 teeth are at exactly the same stage of replacement (stage 1 on the left and stage 3 on the right).

Protenodontosaurus is characterised by its uniquely elongated and procumbent premaxillary teeth, as well as the presence of only one tooth on each maxilla (Fig. 2a, and Fig. S6). All functional teeth are preserved in this specimen, with only three featuring replacement teeth (Lm1, Rpl1, Lpl2).

Macroplacus (Fig. 2a, and Fig. S7) shares many features with the placochelyid taxa *Placochelys*, *Psephoderma* and *Psephochelys* (and possibly *Glyphoderma*); however, the lack of a preserved rostrum prevents certain assignment into this clade, which is characterised by edentulous rostra. This taxon features enormous pl2 teeth, by far the largest of any placodont, although the right one is missing and lacks a replacement tooth (as is Lm1). This was probably lost due to taphonomic factors. However, the remaining Lpl2 forms a functional unit with the surrounding Lpl1 and Lm2 teeth, all of which have a replacement tooth at stage 1 of growth, thus indicating a degree of modularity in this taxon.

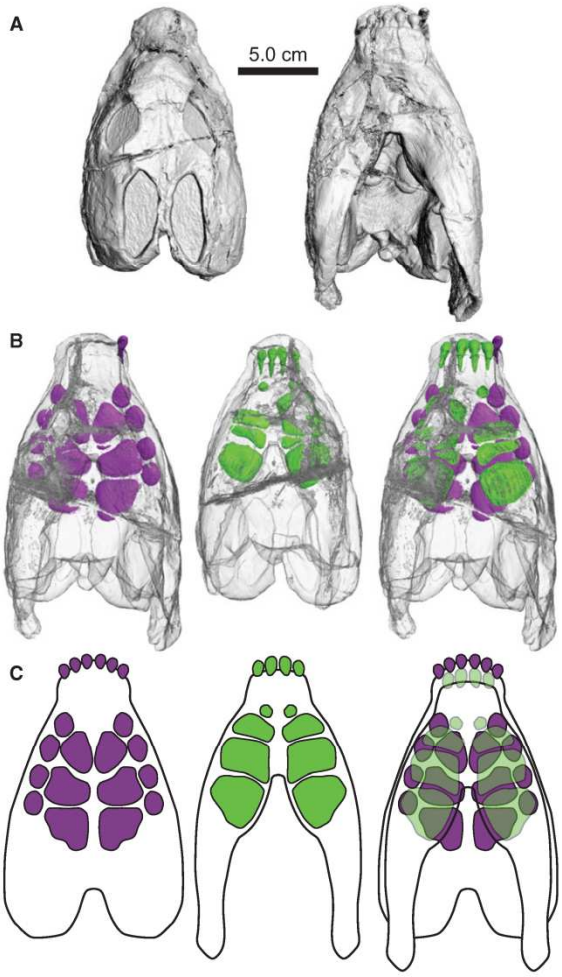

Fig. 3 The skull and functional dentition of the Chinese placodont *Placodus inexpectatus* IVPP V 14996. (a) Surface renderings of the skull in dorsal (left) and palatal (right) views. (b) Transparent surfaces revealing the dentition of the skull in palatal view (left), the dentary in dorsal view (middle) and occluding in palatal view (right). (c) Reconstructions of the complete dentition that correspond to (b). Purple, teeth in upper jaw (premaxilla, maxilla and palatine); green, teeth in dentary.

Psephoderma represents the only European placochelyid in our sample, and is characterised by two tooth plates on the maxilla and palatine, with a long, narrow edentulous rostrum (Fig. 2a, and Fig. S8). While all functional teeth have been preserved in this specimen, only two have replacement teeth (Rm1 and Lpl2). A similar condition can be found in the Chinese placochelyid, *Psephochelys* (Figs 2b and 5, and Fig. S11), which shares the same tooth formula as *Psephoderma*. In contrast, however, there is only one replacement tooth in the skull (Rpl2) and two in the dentary (Ld2 and Rd2). Rpl2 and the corresponding Rd2 both have stage 1 replacement teeth, whereas Ld2 has a stage 3, while its palatine counterpart has none.

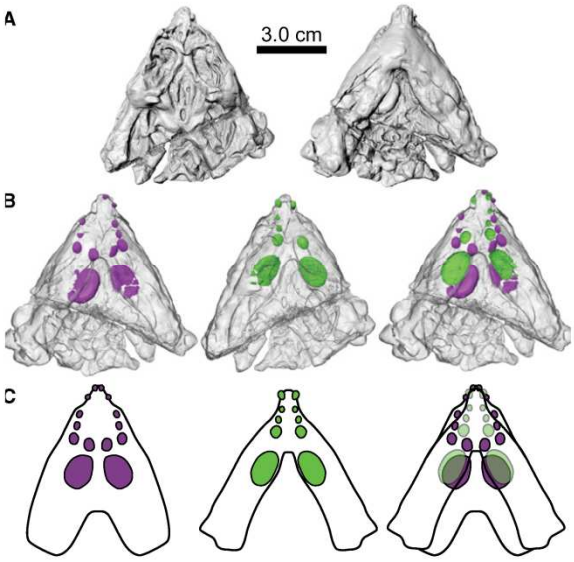

Fig. 4 The skull and functional dentition of the Chinese placodont *Sinocyamodus xinpuensis* IVPP V 11872. (a) Surface renderings of the skull in dorsal (left) and palatal (right) views. (b) Transparent surfaces revealing the dentition of the skull in palatal view (left), the dentary in dorsal view (middle) and occluding in palatal view (right). (c) Reconstructions of the complete dentition that correspond to (b). Colour scheme as in Fig. 3.

The dentition of Chinese placodonts

The dentitions of Chinese placodonts have not previously been described in any detail owing to the fact that specimens are usually embedded in a block of matrix and/or the mandibles are still articulated with the skull, thus obscuring the teeth. However, our μCT scans have revealed them for the first time, providing valuable morphological data for future comparative and phylogenetic analyses (Figs 3–5). A new specimen of *Placodus* (IVPP V 14996) is almost certainly synonymous with the holotype specimen of *Placodus inexpectatus* described by Jiang et al. (2008), and is a solitary skull with articulated jaw that is three-dimensionally preserved (Fig. 3, and Fig. S9). There is a large crack running through the entire specimen which, in dorsal view, begins below the right orbit and travels posteriorly past the posterior margin of the left orbit, also passing through the right and left pl3 and Rd6. There is also a smaller crack that runs anterior to the orbits and through both pl1 and d5 teeth. Our μCT data show the entire right side of the skull to be damaged, including most of the teeth. However, almost all of the teeth are preserved, with the exception of the premaxillary ones, which are all missing apart from Lpm3. The dentition of *Placodus inexpectatus* is very similar to that of its European counterpart, *Placodus gigas*, in that there are three premaxillary, four maxillary (although this ranges from three to five in *Placodus gigas*, but four is by far the most common condition; see Rieppel, 1995 for an

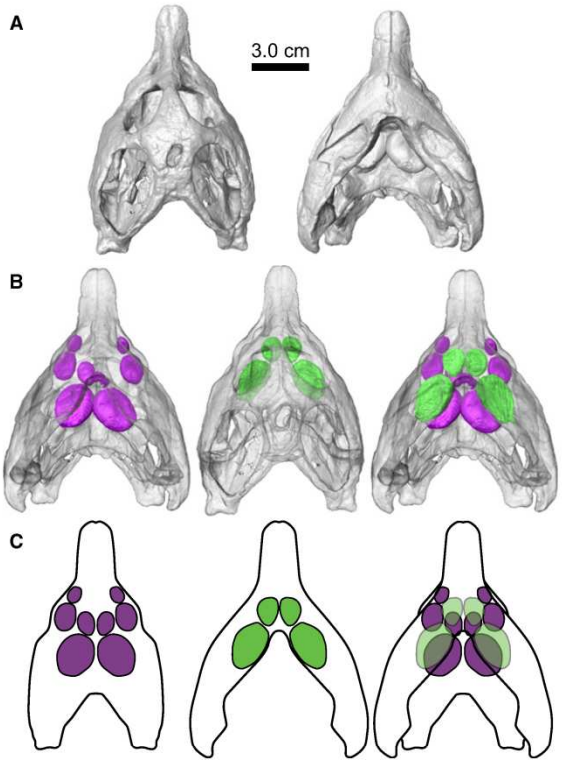

Fig. 5 The skull and functional dentition of the Chinese placodont *Psephochelys polyosteoderma* IVPP V 12442. (a) Surface renderings of the skull in dorsal (left) and palatal (right) views. (b) Transparent surfaces revealing the dentition of the skull in palatal view (left), the dentary in dorsal view (middle) and occluding in palatal view (right). (c) Reconstructions of the complete dentition that correspond to (b). Colour scheme as in Fig. 3.

overview), three palatine and two anterior, procumbent dentary teeth. However, the anterior premaxillary and dentary teeth are much shorter and more rounded than those of *Placodus gigas*, indicating a possible functional difference. These teeth also feature extended roots that are over double the length of the crown. In addition, there are four tooth plates on the dentary in *Placodus inexpectatus*, whereas only three is the most common condition found in *Placodus gigas*, although some specimens do exhibit four (Rieppel, 1995). This 'extra' tooth in *Placodus inexpectatus*, as well as in a minority of *Placodus gigas* jaws, is the anteriormost crushing tooth, and is much smaller and rounder than the others (Fig. S9d), occluding slightly anterior to the first maxillary and palatine teeth of the skull (Fig. 3b,c). The dentary crushing plates are also somewhat larger than those on the palatine, and are located slightly more labially. This allows them to not only occlude with the palatine teeth, but with the maxillary ones too, forming functional crushing areas.

The holotype specimen of *Sinocyamodus* (IVPP V 11872) was described by Li (2000) and consists of an almost complete skeleton prepared in dorsal view. The skull and articulated mandible (which have been prepared out of the slab) are three-dimensionally preserved but somewhat crushed, with several cervical vertebrae still being attached (Fig. 4, and Fig. S10). Both pl2 and the left d5 teeth have been damaged due to the crushing, but do not appear to have moved. A large crack runs through the anterior of the right upper temporal fossa and through the posterior of the left one, although this does not contact the teeth. A large part of the right premaxilla is missing, as are its associated teeth, and Rd2 and 3 have also been lost. The functional teeth of *Sinocyamodus* are numerous, generally small and widely spaced. There are two blunt and rounded premaxillary, three maxillary, two palatine and five dentary teeth. With the exception of the posteriormost tooth plates, none of the teeth occlude to create functional crushing areas, but fit alongside one another. The tooth formula is similar to that of the subadult *Cyamodus hildegardis* specimen PIMUZ T 2796 (Fig. S12; Kuhn-Schnyder, 1959) which, when combined with the small size of the specimen, would suggest that this animal was not yet fully grown. The lack of functional crushing areas in both specimens may also indicate a softer diet at earlier ontogenetic stages in these placodonts.

The holotype specimen of *Psephochelys* was first described by Li & Rieppel (2002), and consists of an exquisitely preserved skull with articulated jaw and some postcranial material including the dorsal armour, gastralia, parts of the shoulder and pelvic girdle, and a few vertebrae. The skull is almost complete, with only some posterior elements of the braincase missing. However, the right palatine teeth have taphonomically shifted ventrally, with Rpl1 having rotated as well. This could account for the lack of replacement teeth in this element. Like the European placodonts *Placochelys* and *Psephoderma*, *Psephochelys* lacks any anterior teeth in the premaxilla or dentary, and was thus suggested by Li & Rieppel (2002) to form a clade with these genera (Placochelyidae). All of its teeth are enlarged crushing plates, with the maxilla, palatine and dentary each bearing two teeth (Fig. 5, and Fig. S11).

Discussion

Our results follow a clear phylogenetic trend (Fig. 6), with notably different patterns of tooth replacement being observed between the more plesiomorphic 'placodontoids' (i.e. *Placodus*) and the derived cyamodontoid taxa. However, we acknowledge at this point that the results are based on a limited sample, because in many cases only a single specimen per species is known or available, and thus we were unable to test for intraspecific variation.

The basal *Placodus gigas* and *Placodus inexpectatus* show many replacement teeth at various stages of growth, with little or no discernable pattern (Fig. 2). Indeed, teeth of the various tooth-bearing elements are not replaced in functional units, and no maintenance of functional crushing

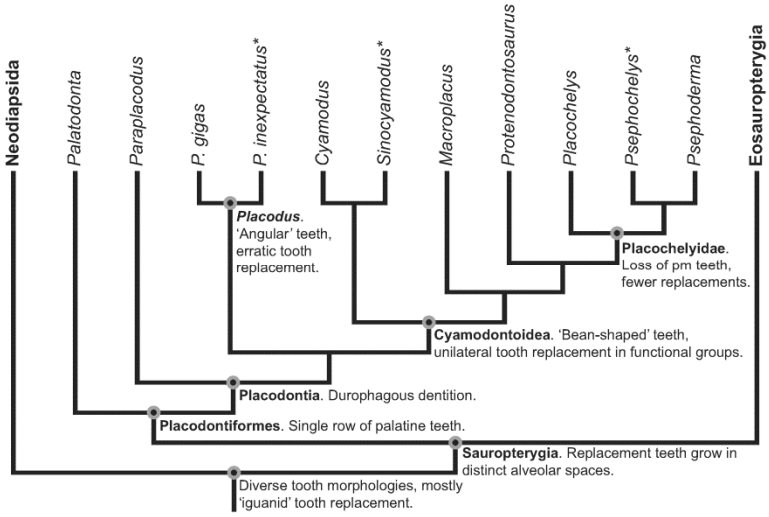

Fig. 6 Composite phylogeny of placodont relationships with the evolution of dental formula, morphology and replacement highlighted. Based on Rieppel (2000), Jiang et al. (2008) and Neenan et al. (2013). The phylogenetic position of *Placodus inexpectatus* was recovered by Jiang et al. (2008), whereas the positions of *Sinocyamodus* and *Psephochelys* are hypothetical, based on dental and gross morphological features provided in this paper as well as previously published data (Li, 2000; Li & Rieppel, 2002). Asterisked taxa are Chinese, all other placodonts are from Europe. pm, premaxilla.

areas is apparent. However, most, if not all, of the palatine tooth plates always have replacement teeth, with the posteriormost ones always featuring at least one at stage 3 of growth. The skull of both species of *Placodus* is particularly robust, reinforced with pachyostotic bone, a highly ossified and load-bearing braincase, with evidence of massive jaw musculature (Rieppel, 2002; Neenan & Scheyer, 2012). The frequent replacement of the palatine teeth, combined with this skull morphology suggests that these teeth were being subjected to high strains, and would indicate that *Placodus* was eating particularly tough food items. It is also important to note that despite the apparently disordered replacement pattern of the teeth in the upper jaw, the dentary teeth in *Placodus inexpectatus* show a highly organised bilateral pattern of replacement, with teeth on each element corresponding to their opposite number (with the exception of d2), a condition seen in some lizards (e.g. *Anguis*; Cooper, 1966). Why tooth replacement in the dentary should follow such a clear bilateral pattern while the condition of the upper jaw is so unpredictable is unclear.

The three species of *Cyamodus* as well as *Sinocyamodus* have the most teeth of the cyamodontoid taxa, and also show the most variation in tooth replacement (Fig. 2). The skulls of *C. muensteri* and *C. rostratus* are quite damaged, and many of the replacement teeth appear to be missing. However, *C. kuhnschnyderi* not only has a wealth of replacement teeth, but shows a high degree of modularity and uniformity in that each tooth-bearing element has a replacement tooth at the same stage of growth, with the exception of the left palatine that is probably missing a replacement tooth (Fig. S3). This is the only example in our sample that grows replacement teeth in this fashion; however, the palatine teeth are at opposite phases of replacement, meaning that a functional crushing area is preserved at all times. This is also the case for *Sinocyamodus*, which only has a few replacement teeth. However, a clear pattern is visible at the posteriormost palatine and dentary teeth, which correlate to each other in terms of replacement tooth stage. The advantage of having a mandible in this specimen has revealed that, in cyamodontoids at least, corresponding teeth of the upper and lower jaws are replaced in unison on individual sides in order to preserve functional crushing areas. This is also the case in *Psephochelys*, although damage to the left palatine teeth means that this pattern is only visible for the right half of the skull.

Macroplacus exhibits a strong pattern in that it clearly replaces its teeth in unilateral functional units. The left palatine teeth worked in unison with Lm2 (Lm1 is missing in this specimen along with its replacement tooth) and the corresponding dentary tooth/teeth to form functional crushing areas, and were all replaced at the same time. During replacement, the equivalent unit on the right side would have been used for feeding.

Placochelyid placodonts such as *Psephoderma* and *Psephochelys* lack anterior dentition (i.e. premaxillary and anterior dentary teeth), and it has been suggested that, instead of feeding on epibenthic sessile prey like most placodonts, they would have fed on endobenthic non-sessile hard-shelled invertebrates (Pinna & Nosotti, 1989; Mazin & Pinna, 1993; Rieppel, 2002). The elongate rostra of these taxa would have been used to probe sediments to find buried prey items, much like extant eagle rays, and possibly would have fed more on crustaceans than bivalve molluscs (Stefani et al. 1992). Our results support these predictions. The number of replacement teeth in *Psephoderma* and *Psephochelys* is heavily reduced, with very little tooth replacement occurring anterior to the posteriormost palatine and dentary tooth plates (Fig. 2). Like other placodonts, it is likely that the majority of crushing occurred at this point, thus requiring more replacement.

Some specimens exhibit replacement teeth that are inverted or strongly angled: *Placodus gigas* (Figs S1a–d and S2a);

C. kuhnschnyderi (Fig. S3a,c); and *C. muensteri* (Fig. S4a). Because the majority of placodont replacement teeth grow in a horizontal or near-horizontal position, we suggest that these occurrences are purely taphonomic in origin. As previously mentioned, replacement teeth grow in a large alveolar space, so it is logical to assume that as the tissues in this space decomposed, some teeth may have moved from their original positions.

All placodont specimens share one characteristic in common: at least one replacement tooth is always present for the posteriormost palatine and dentary tooth plates (with the exception of the posterior dentary teeth of *Placodus inexpectatus*, which are probably missing due to poor preservation). We suggest that this is the case for functional reasons. Rieppel (2002) used morphological and biomechanical analyses to determine the feeding methods of placodonts. He found that in both *Placodus* and cyamodontoids (with the exception of *Henodus*), the position of the coronoid process compared with the mandibular articulation and reconstructed jaw musculature would have placed the most efficient centre of crushing at the posterior tooth plates. It is logical then that these teeth would be subjected to increased stresses and wear, requiring constant replacement. It is also worth noting that large alveolar spaces directly below functional teeth that are experiencing high crushing loads represent a structural weakness. Future research planned by JMN and TMS aims to clarify how stress and strain is distributed though the placodont skull despite this.

A characteristic common to all cyamodontoid placodonts is that tooth replacement is always unilateral (apart from the premaxillae of *C. kuhnschnyderi*). This is once again for functional reasons, preserving functional crushing areas on at least one side of the mouth.

Chinese taxa

The dental morphology of the Chinese taxa has provided valuable data for future comparative and phylogenetic analyses. While no comprehensive placodont phylogeny exists (this work is currently in preparation elsewhere), we can draw some conclusions regarding the phylogenetic position of these taxa (Fig. 6). Judging by tooth shape, formula and replacement patterns, *Placodus inexpectatus* is confirmed as a separate species to the European *Placodus gigas*, in agreement with the phylogenetic analysis of Jiang et al. (2008). The procumbent anterior teeth of the premaxilla and dentary are much shorter and more bulbous in *Placodus inexpectatus*, indicating a dietary and/or functional difference between the two taxa. Tooth formula and shape also indicate a close relationship between the European *Cyamodus* and *Sinocyamodus*. The *Sinocyamodus* holotype is also interpreted to be a subadult, judging by its small size, the similar tooth formula to a subadult *C. hildegardis* (Fig. S12) and the low number of replacement teeth (Fig. 2b). The small teeth that do not occlude (with the exception of the pl2 and corresponding d5 teeth) indicate that juvenile placodonts may have consumed softer prey before adulthood. In agreement with Li & Rieppel (2002), tooth formula and replacement patterns also support the placement of *Psephochelys* within the Placochelyidae, owing to its striking similarity with *Psephoderma*.

Tooth replacement rates

While we have demonstrated the patterns of placodont tooth replacement in this paper, the rate at which this occurred remains unclear. It has been observed that in many extant reptiles replacement teeth require approximately 3 months to grow (e.g. *Heloderma*, *Iguana* and *Varanus*; Edmund, 1969). However, it is important to note that they also tend to replace their teeth at progressively slower rates as they age (Cooper, 1966; Cooper et al. 1970; Kline & Cullum, 1984), especially in *Alligator* (Erickson, 1996). Owing to the posterior–anterior replacement pattern seen in most reptiles, this can mean that posterior teeth are replaced at a slower rate than anterior ones, or can even stop being replaced altogether, as seen in agamid lizards (Cooper et al. 1970). Placodonts appear to have the opposite condition, however, with cyamodontoid specimens frequently lacking anterior replacement teeth, but always having posterior ones. This is probably due to the method of feeding employed, as the posterior teeth are experiencing the most stress and thus wear. It is also possible that placodonts simply stopped replacing teeth after a certain age, at least in the anterior part of the mouth. Heterodontosaurid dinosaurs for example, which had a high degree of tooth wear, are known to completely stop tooth replacement in mature individuals (Hopson, 1975, 1980). In addition, it has recently been shown that sauropod dinosaurs show strong interspecific variation in tooth replacement rates, depending on the feeding method employed (D'Emic et al. 2013), which could also be the case for placodonts – particularly when explaining the differences observed between the 'placodontoid' and cyamodontoid taxa.

Concluding remarks

Placodonts have a unique and highly specialised dentition for duraphagous feeding, and the methods of tooth replacement required for this are equally unique. By combining evidence gleaned from individual specimens in our sample, we can show that placodonts did not replace their teeth in Zahnreihen waves as is the case with most reptiles. In *Placodus*, a diet of particularly hard-shelled prey caused increased wear, especially in the posterior dentition. As a consequence, tooth replacement was relatively frequent and occurred in no discernable pattern. However, in the more derived cyamodontoids, multiple teeth worked in unison as efficient functional units on opposite sides of the

skull, and were replaced together and unilaterally in order to maintain this functionality. The highly-derived placochelyids show very little tooth replacement anterior to the posteriormost crushing plates, thus suggesting a slightly softer diet, i.e. crustaceans.

Tooth formula, shape and replacement patterns can also be used to make phylogenetic conclusions regarding the Chinese placodonts, pending future analyses (Fig. 6). *Placodus inexpectatus* is supported as a member of the genus *Placodus,* while *Sinocyamodus* shares similarities with *Cyamodus,* and *Psephochelys* closely resembles *Psephoderma*.

Acknowledgements

J. Rabold and S. Eggmaier (UMO, Bayreuth, Germany), M. Moser and O. Rauhut (BSPG, Munich, Germany), and R. Schoch (SMNS, Stuttgart, Germany) are thanked for providing access to specimens and allowing them to be scanned. L. Rager (SMNS, Stuttgart, Germany) and C. Bickelmann (MNHUB, Berlin, Germany) are also thanked for their help with labelling and segmentation, and O. Strauss (PIMUZ, Zurich, Switzerland) for conducting the pilot study. Additionally, we are grateful to N. Klein (SIPG, Bonn, Germany), W. Leis (Hochschule Aalen, Germany), Hou Yemao (IVPP, Beijing, P. R. China), L. Mancini, D. Dreossi and N. Sodini (all Elettra-Sincrotrone Trieste S.C.p.A, Italy) for their help and support while CT scanning specimens. We also thank M. Sánchez-Villagra, E. Maxwell and all the members of PIMUZ, Zurich for useful discussions and advice, as well as B.-A. S. Bhullar and two anonymous reviewers, whose helpful comments improved the manuscript. This work was funded by the Swiss National Science Foundation (grant 31003A 146440 to TMS).

Author contributions

TMS and JMN designed the research. JMN carried out the segmentation, analysis and wrote the manuscript. OR and CL provided expert knowledge and insight. CL enabled and supported scanning of the Chinese material at the IVPP. GM made the specimen of *Protenodontosaurs* available for scanning and transported it to Trieste, where FB and CT carried out the scan.

References

Agassiz L (1833–1843) *Recherches sur les Poissons Fossiles*, Vol. I–V. Neuchâtel: Imprimaire de Petitpierre.

Burckhardt R (1895) Das Gebiss der Sauropsiden. *Morphol Arb* **5**, 341–385.

Cooper JS (1966) Tooth replacement in the Slow worm (*Anguis fragilis*). *J Zool* **150**, 235–248.

Cooper JS, Poole DFG, Lawson R (1970) The dentition of agamid lizards with special reference to tooth replacement. *J Zool* **162**, 85–98.

Delgado S, Davit-Beal T, Sire JY (2003) Dentition and tooth replacement pattern in *Chalcides* (Squamata; Scincidae). *J Morphol* **256**, 146–159.

DeMar R, Bolt JR (1981) Dentitional organization and function in a Triassic reptile. *J Paleontol* **55**, 967–984.

D'Emic MD, Whitlock JA, Smith KM, et al. (2013) Evolution of high tooth replacement rates in sauropod dinosaurs. *PLoS ONE* **8**, e69235.

Edinger T (1921) Über Nothosaurus II. Zur Gaumenfrage. *Senckenbergiana* **3**, 193–205.

Edmund AG (1960) *Tooth Replacement Phenomena in the Lower Vertebrates*. Toronto: University of Toronto Press.

Edmund AG (1969) Dentiton. In: *Biology of the Reptilia*. (eds Gans C, Bellairs A, Parsons TS), pp. 117–200. London: Academic Press.

Erickson GM (1996) Daily deposition of dentine in juvenile *Alligator* and assessment of tooth replacement rates using incremental line counts. *J Morphol* **228**, 189–194.

Hagdorn H, Rieppel O (1999) Stratigraphy of marine reptiles in the Triassic of Central Europe. *Zent Geol Paläontol Teil I* **1998**, 651–678.

Hopson JA (1975) On the generic separation of the ornithischian dinosaurs *Lycorhinus* and *Heterodontosaurus* from the Stormberg Series (Upper Triassic) of South Africa. *S Afr J Sci* **71**, 302–305.

Hopson JA (1980) Tooth function and replacement in early Mesozoic ornithischian dinosaurs: implications for aestivation. *Lethaia* **13**, 93–105.

Jaekel O (1907) *Placochelys placodonta* aus der Obertrias des Bakony. Resultate der Wissenschaftlichen Erforschung des Balatonsees, 1. Band 1. Teil. Paläontologischer Anhang III. Band 1–91.

Jiang D-Y, Motani R, Hao W-C, et al. (2008) First record of Placodontoidea (Reptilia, Sauropterygia, Placodontia) from the Eastern Tethys. *J Vertebr Paleontol* **28**, 904–908.

Kieser JA, Klapsidis C, Law L, et al. (1993) Heterodonty and patterns of tooth replacement in *Crocodylus niloticus*. *J Morphol* **218**, 195–201.

Kline LW, Cullum D (1984) A long term study of the tooth replacement phenomenon in the young green iguana, *Iguana iguana*. *J Herpetol* **18**, 176–185.

Kuhn-Schnyder E (1959) Über das Gebiss von *Cyamodus*. *Mitt Paläontol Inst Univ Zür* **1**, 174–188.

Li C (2000) Placodont (Reptilia: Placodontia) from Upper Triassic of Guizhou, Southwest China. *Vertebr PalAsiat* **38**, 314–317.

Li C, Rieppel O (2002) A new cyamodontoid placodont from Triassic of Guizhou, China. *Chin Sci Bull* **47**, 156–159.

Mahler DL, Kearney M (2006) The palatal dentition in squamate reptiles: morphology, development, attachment, and replacement. *Fieldiana (Zool) N Ser* **108**, 1–61.

Maxwell EE, Caldwell MW, Lamoureux DO (2012) Tooth histology, attachment, and replacement in the Ichthyopterygia reviewed in an evolutionary context. *Paläontol Z* **86**, 1–14.

Mazin J-M (1989) La denture et la région palatine des Placodontia (Reptilia, Trias). Implications phylogénétiques. *Geobios* **22**, 725–734.

Mazin J-M, Pinna G (1993) Palaeoecology of the armoured placodonts. *Paleontol Lomb N. S.* **2**, 83–91.

McDowell SB, Bogert CM (1954) The systematic position of *Lanthanotus* and the affinities of the anguinomorphan lizards. *Bull Am Mus Nat Hist* **105**, 1–142.

Meyer HV (1858) *Psephoderma alpinum* aus dem Dachsteinkalke der Alpen. *Palaeontographica* **6**, 246–252.

Münster G (1839) *Beiträge zur Petrefaktenkunde, mit XVIII Nach der Natur Gezeichneten Tafeln der Herren Hermann v. Meyer und Professor Rudolph Wagner*. Bayreuth: Buchner'sche Buchhandlung.

Neenan JM, Scheyer TM (2012) The braincase and inner ear of *Placodus gigas* (Sauropterygia, Placodontia) – a new

reconstruction based on micro-computed tomographic data. *J Vertebr Paleontol* **32**, 1350–1357.

Neenan JM, Klein N, Scheyer TM (2013) European origin of placodont marine reptiles and the evolution of crushing dentition in Placodontia. *Nat Commun* **4**, 1621.

Nosotti S, Pinna G (1993) *Cyamodus kuhn-schnyderi* n. sp., nouvelle espèce de Cyamodontidae (Reptilia, Placodontia) du Muschelkalk supérieur allemand. *C R Acad Sci Paris Sér I* **317**, 847–850.

Owen R (1840–1845) *Odontography, or, a Treatise on the Comparative Anatomy of the Teeth; Their Physiological Relations, Mode of Development, and Microscopic Structure in the Vertebrate Animals*. London: Hippolyte Bailliere.

Peyer B (1931) Die Triasfauna der Tessiner Kalkalpen III. Placodontia. *Abh Schweiz Paläontol Ges* **51**, 1–25.

Pinna G (1990) *Protenodontosaurus italicus* n.g., n.sp., un nuovo placodonte del Carnico italiano. *Atti Soc Ital Sci Nat Museo Civ Storia Nat Milano* **131**, 5–12.

Pinna G, Nosotti S (1989) Anatomia, morfologia funzionale e paleoecologia del rettile placodonte *Psephoderma alpinum* Meyer, 1858. *Mem Soc Ital Sci Nat Museo Civ Storia Nat Milano* **25**, 17–50.

de Ricqlès A, Bolt JR (1983) Jaw growth and tooth replacement in *Captorhinus aguti* (Reptilia: Captorhinomorpha): a morphological and histological analysis. *J Vertebr Paleontol* **3**, 7–24.

Rieppel O (1978) Tooth replacement in anguinomorph lizards. *Zoomorphologie* **91**, 77–90.

Rieppel O (1995) The genus *Placodus*: systematics, morphology, paleobiogeography, and paleobiology. *Fieldiana: Geol, N Ser* **31**, 1–44.

Rieppel O (2000) Sauropterygia I – Placodontia, Pachypleurosauria, Nothosauroidea, Pistosauroidea. In: *Encyclopedia of Paleoherpetology*. (ed. Wellnhofer P), pp. 134. Munich: Verlag Dr. Friedrich Pfeil.

Rieppel O (2001) Tooth implantation and replacement in Sauropterygia. *Paläontol Z* **75**, 207–217.

Rieppel O (2002) Feeding mechanics in Triassic stem-group sauropterygians: the anatomy of a successful invasion of Mesozoic seas. *Zool J Linn Soc* **135**, 33–63.

Sander PM (1999) The microstructure of reptilian tooth enamel: terminology, function, and phylogeny. *Münch Geowiss Abh: Reihe A, Geol Paläontol* **38**, 1–102.

Scheyer TM, Neenan JM, Renesto S, et al. (2012) Revised paleoecology of placodonts – with a comment on 'The shallow marine placodont *Cyamodus* of the central European Germanic Basin: its evolution, paleobiogeography and paleoecology' by C.G. Diedrich (Historical Biology, iFirst article, 2011, 1–19, doi: 10.1080/08912963.2011.575938). *Hist Biol*, **24**, 257–267.

Schubert-Klempnauer H (1975) *Macroplacus raeticus* n.g., n. sp. - ein neuer Placodontier aus dem Rät der Bayerischen Alpen. *Mitt Bayer Staatssamml Paläontol Hist Geol* **15**, 33–55.

Small BJ (1997) A new procolophonid from the Upper Triassic of Texas, with a description of tooth replacement and implantation. *J Vertebr Paleontol* **17**, 674–678.

Stefani M, Arduini P, Garassino A, et al. (1992) Paleoenvironment of extraordinary fossil biotas from the Upper Triassic of Italy. *Atti Soc Ital Sci Nat Mus Civ Stor Nat Milano* **132**, 309–335.

Tuniz C, Bernardini F, Cicuttin A, et al. (2013) The ICTP-Elettra X-ray laboratory for cultural heritage and archaeology. *Nucl Instrum Methods Phys Res Sect A* **711**, 106–110.

Vogt C (1983) Evolutive Palökologie der Placodontier (*Placodus, Henodus*; Euryapsida, Trias). Geowissenschaftliche Fakultät, pp. 99. Tübingen: Eberhard-Karls-Universität.

Whitlock JA, Richman JM (2013) Biology of tooth replacement in amniotes. *Int J Oral Sci* **5**, 66–70.

Woerdeman MW (1921) Beiträge zur Entwicklungsgeschichte von Zähnen und Gebiss der Reptilien. Beitrag IV: Über die Anlage und Entwicklung der Zähne. *Arch Mikrosk Anat* **95**, 265–395.

Zhao L-J, Li C, Liu J, et al. (2008) A new armored placodont from the Middle Triassic of Yunnan Province, southwestern China. *Vertebr PalAsiat* **46**, 171–177.

Supporting Information

Additional Supporting Information may be found in the online version of this article:

Fig. S1 Coronal slices in anterior view through six planes in the skull of *Placodus gigas* UMO BT 13, showing replacement teeth at various stages of growth (red).

Fig. S2 Coronal slices in anterior view through three planes in the skull of *Placodus gigas* BSP 1968 I 75, showing replacement teeth at various stages of growth (red).

Fig. S3 Coronal slices in anterior view through six planes in the holotype skull of *Cyamodus kuhnschnyderi* SMNS 15855, showing replacement teeth at various stages of growth (red).

Fig. S4 Coronal slices in anterior view through three planes in the holotype skull of *Cyamodus muensteri* BSP AS VII 1210, showing replacement teeth (red).

Fig. S5 Coronal slice in anterior view through the holotype skull of *Cyamodus rostratus* UMO BT 748, showing replacement tooth (red).

Fig. S6 Coronal slices in anterior view through three planes in the holotype skull of *Protenodontosaurus italicus* MFSN 1819GP, showing replacement teeth at various stages of growth (red).

Fig. S7 Coronal slices in anterior view through four planes in the holotype skull of *Macroplacus raeticus* BSP 1967 I 324, showing replacement teeth at various stages of growth (red).

Fig. S8 Coronal slices in anterior view through two planes in the new skull of *Psephoderma alpinum* PIMUZ A/III 1491, showing replacement teeth (red).

Fig. S9 Coronal slices in anterior view through eight planes in the skull of the Chinese placodont *Placodus inexpectatus* IVPP V 14996, showing replacement teeth at various stages of growth.

Fig. S10 Coronal slices in anterior view through three planes in the holotype skull of the Chinese placodont *Sinocyamodus xinpuensis* IVPP V 11872, showing replacement teeth at various stages of growth.

Fig. S11 Coronal slice in anterior view through the holotype skull of the Chinese placodont *Psephochelys polyosteoderma* IVPP V 12442, showing replacement teeth.

Fig. S12 Reconstruction of the dentition of a subadult specimen of *Cyamodus hildegardis* PIMUZ T 2796, showing the dentition of the skull in palatal view (top left), the dentary in dorsal view (top right) and tooth occlusion in palatal view (bottom).

Supplementary Information for:

Unique method of tooth replacement in durophagous placodont marine reptiles, with new data on the dentition of Chinese taxa

James M. Neenan, Chun Li, Olivier Rieppel, Federico Bernardini, Claudio Tuniz, Giuseppe Muscio and Torsten M. Scheyer

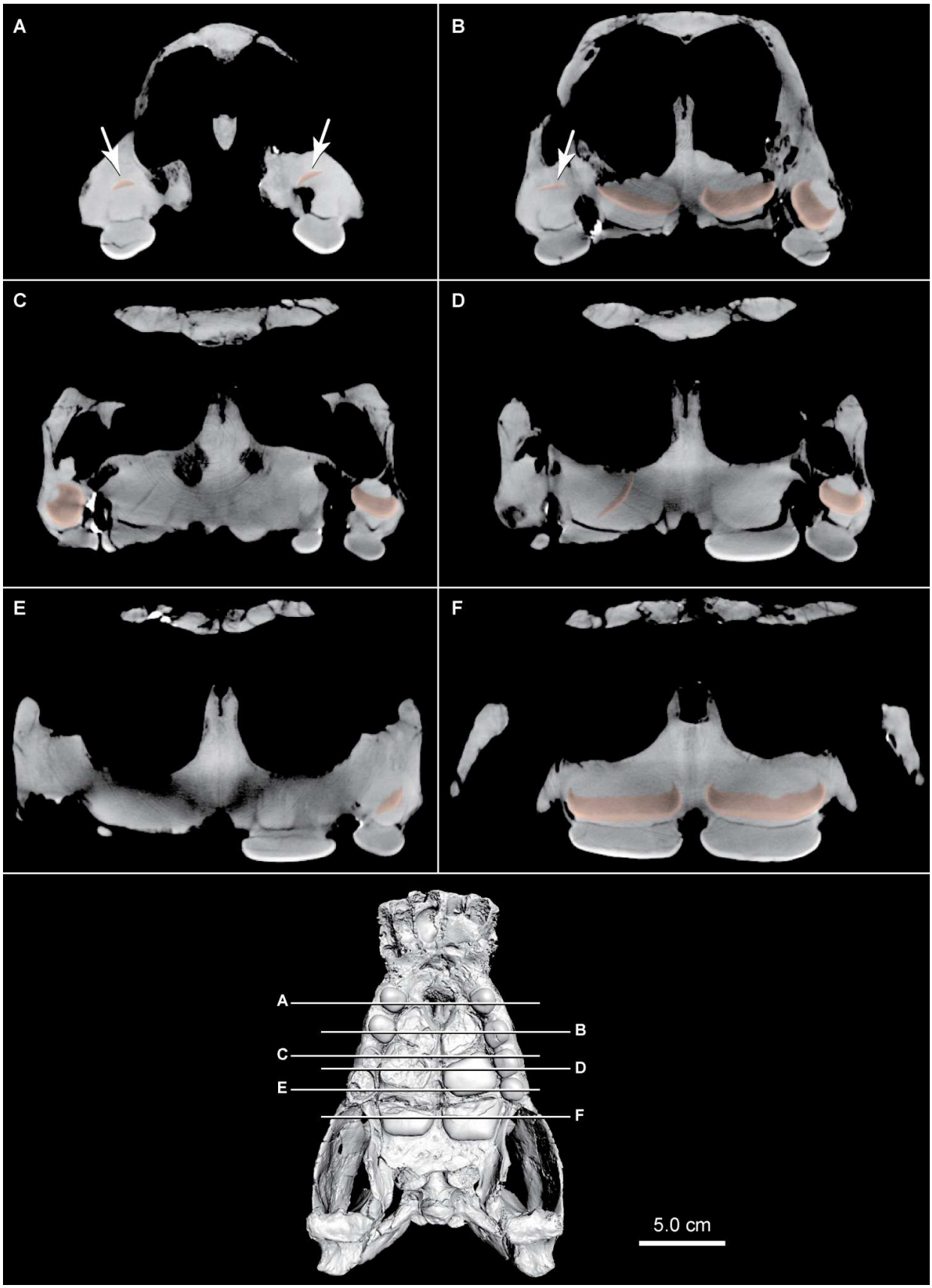
A
B
C
D
E
F
A
B
C
D
E
F
5.0 cm

Supplementary Fig. S1 (previous page) Coronal slices in anterior view through six planes in the skull of *Placodus gigas* UMO BT 13, showing replacement teeth at various stages of growth (red). (A) slice 675 showing both m1 teeth that have stage 1 replacements. Note that these replacements have been preserved in an inverted orientation. (B) slice 610 showing both m2 and pl1 replacement teeth. Once again, note the inverted Rm2. (C) slice 549 showing the m3 replacements. (D) slice 524 showing the stage 1 replacement of Rpl2, as well as a repetition of Lm3 (as seen in C). (E) slice 469 showing the replacement at Lm4. (F) slice 405 showing both pl3 replacements.

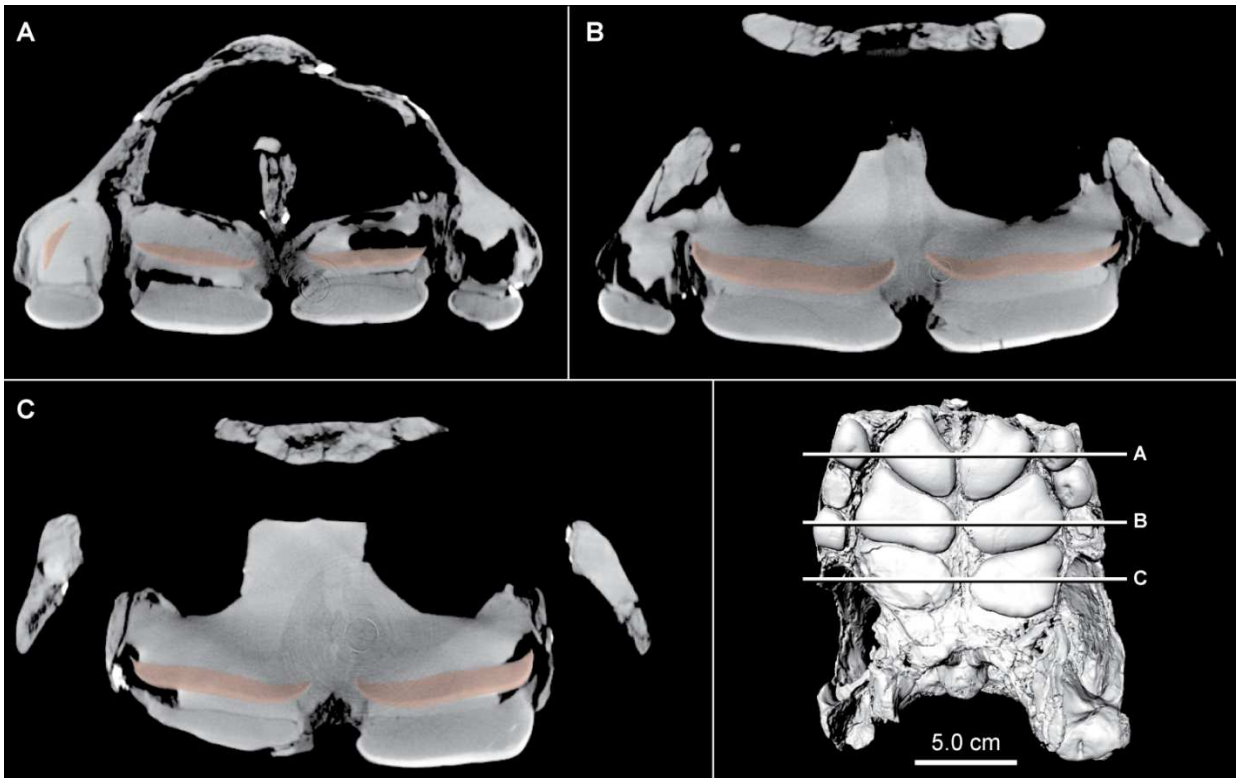

Supplementary Fig. S2 Coronal slices in anterior view through three planes in the skull of *Placodus gigas* BSP 1968 I 75, showing replacement teeth at various stages of growth (red). (A) slice 100 showing replacement teeth for Rm2 and both pl1 teeth. Similar to the UMO specimen, this maxillary replacement tooth has an unusual orientation. (B) slice 258 showing both pl2 replacements. (C) slice 380 showing both pl3 replacements.

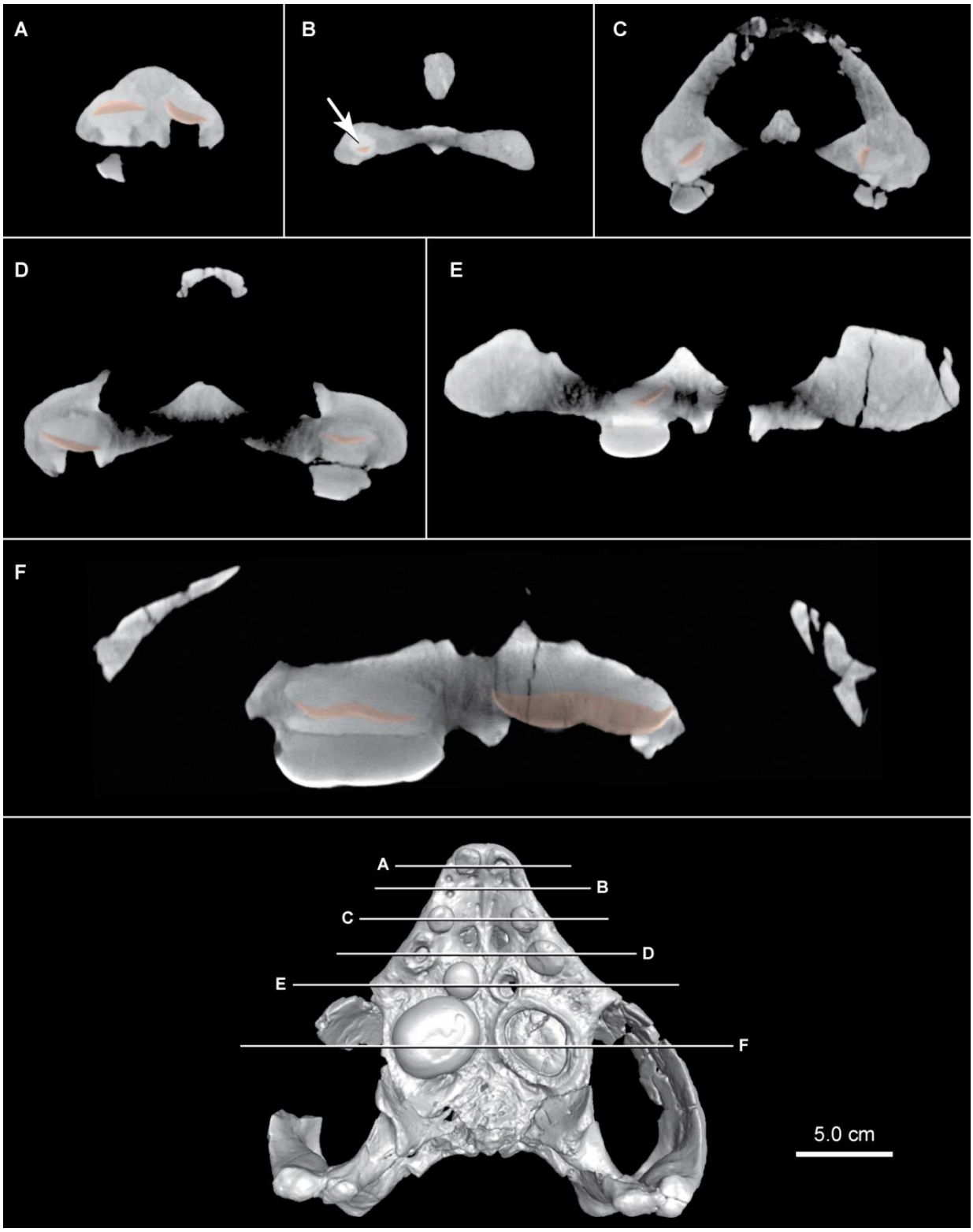
A
B
C
D
E
F
A
B
C
D
E
F
5.0 cm

Supplementary Fig. S3 (previous page) Coronal slices in anterior view through six planes in the holotype skull of *Cyamodus kuhnschnyderi* SMNS 15855, showing replacement teeth at various stages of growth (red). (A) slice 773 showing both stage 3 pm1 replacement teeth. Note that the right replacement tooth is inverted. (B) slice 719 showing the second replacement tooth of Rpm1. This is the only example of a second replacement tooth in all placodont taxa in our sample. (C) slice 650 showing both m1 replacement teeth. Both are orientated medially. (D) slice 588 showing both m2 replacements. (E) slice 528 showing the replacement at Rpl1. (F) slice 404 showing both pl2 replacements. Note that Lpl2 appears to be in the process of eruption.

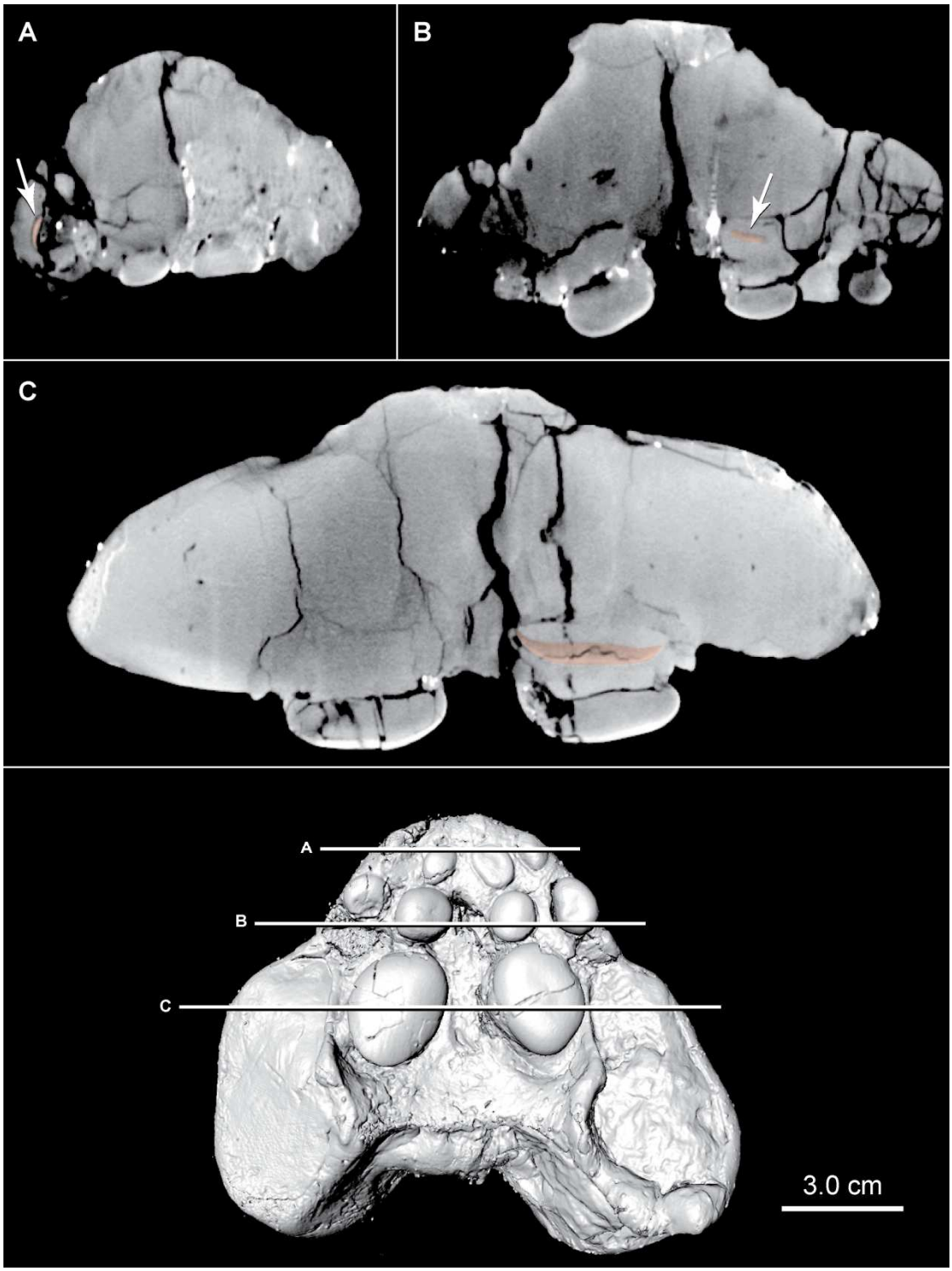

Supplementary Fig. S4 Coronal slices in anterior view through three planes in the holotype skull of *Cyamodus muensteri* BSP AS VII 1210, showing replacement teeth (red). (A) slice 170 showing the laterally shifted stage 1 Rm2 replacement. (B) slice 275 showing the Lpl1 replacement. (C) slice 403 showing the Lpl2 replacement.

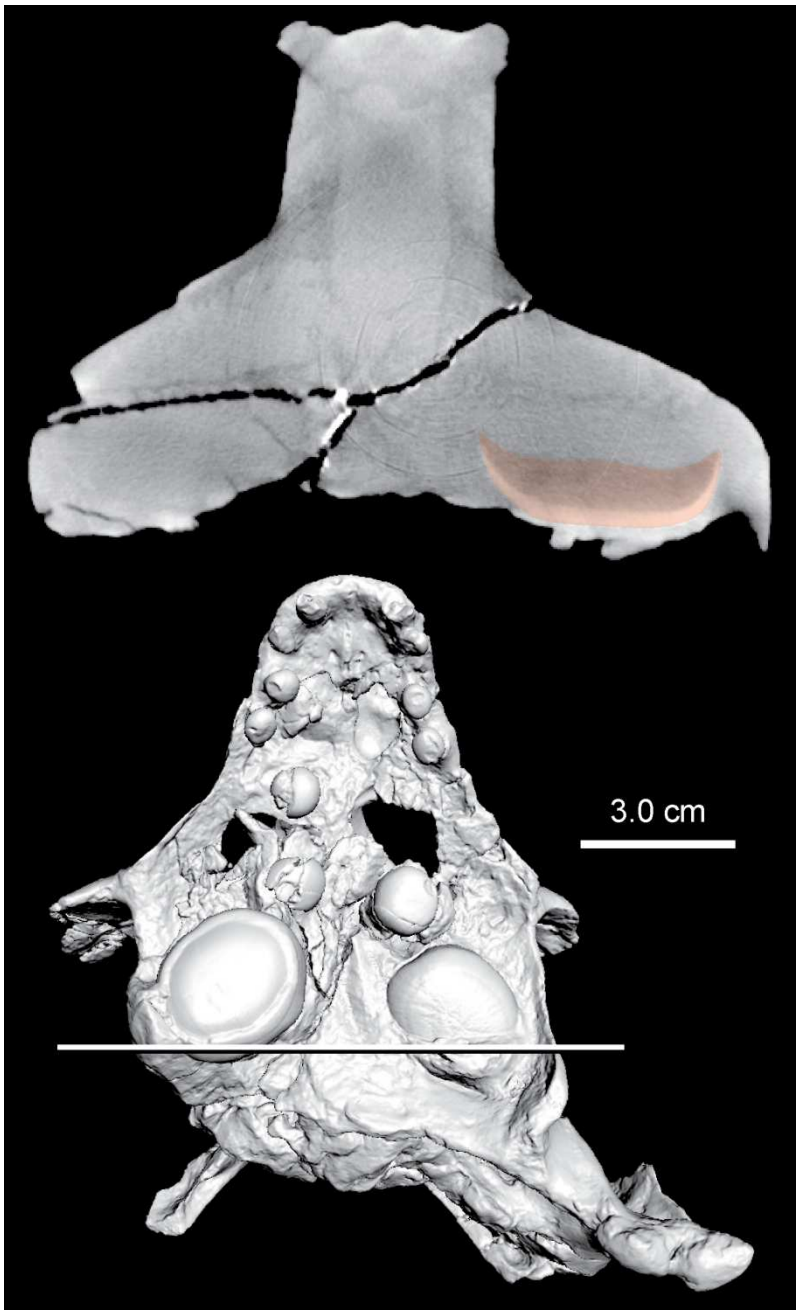

Supplementary Fig. S5 Coronal slice in anterior view through the holotype skull of *Cyamodus rostratus* UMO BT 748, showing replacement tooth (red). Slice 384 shows the skull's only preserved replacement tooth, which is a stage 3 at the Lpl3 position.

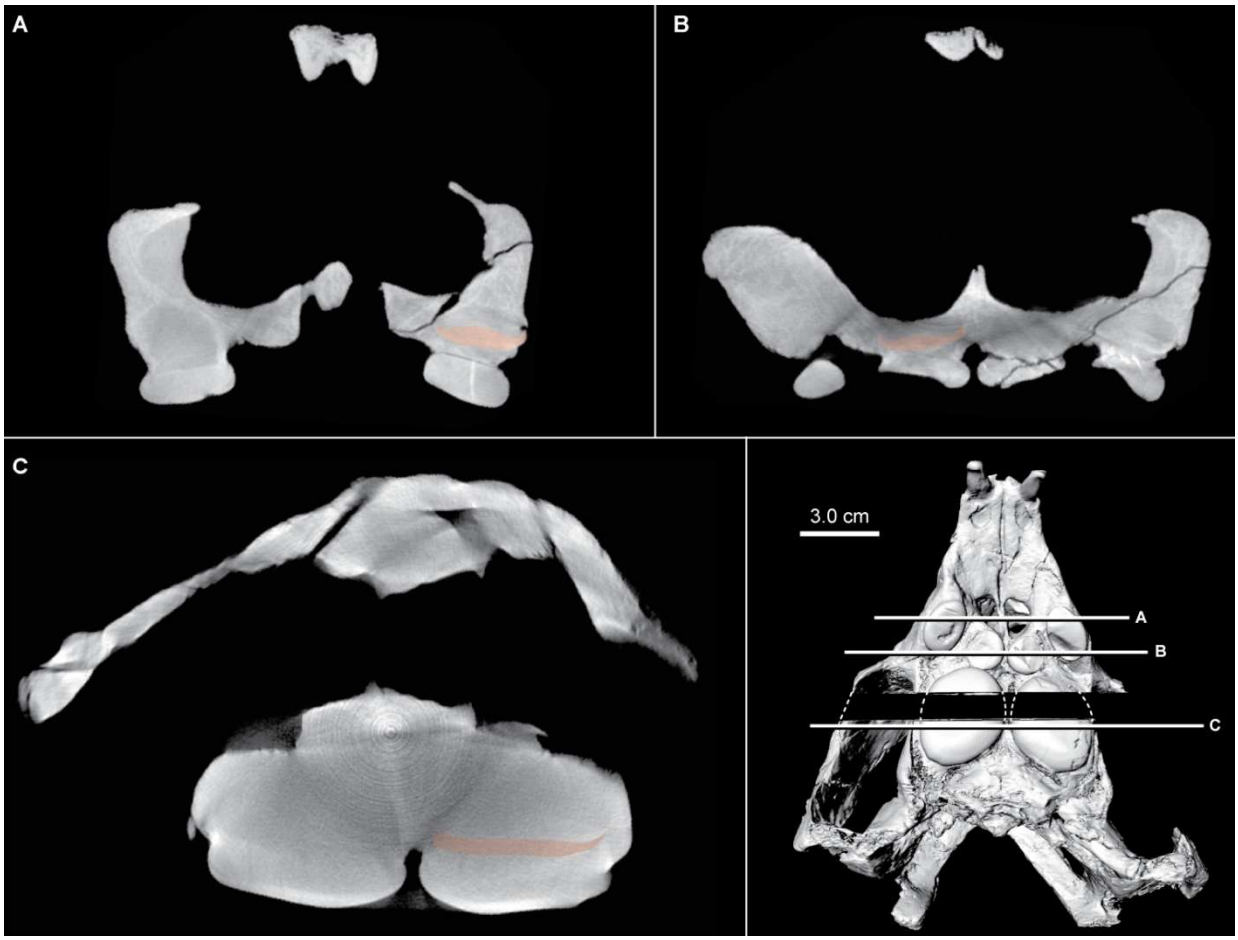

Supplementary Fig. S6 Coronal slices in anterior view through three planes in the holotype skull of *Protenodontosaurus italicus* MFSN 1819GP, showing replacement teeth at various stages of growth (red). Note that this specimen was scanned in two parts and a small portion of the middle of the skull is missing. (A) slice 1440 showing the Lm1 replacement. (B) slice 1335 showing the Rpl1 replacement. (C) slice 1021 showing the Lpl2 replacement.

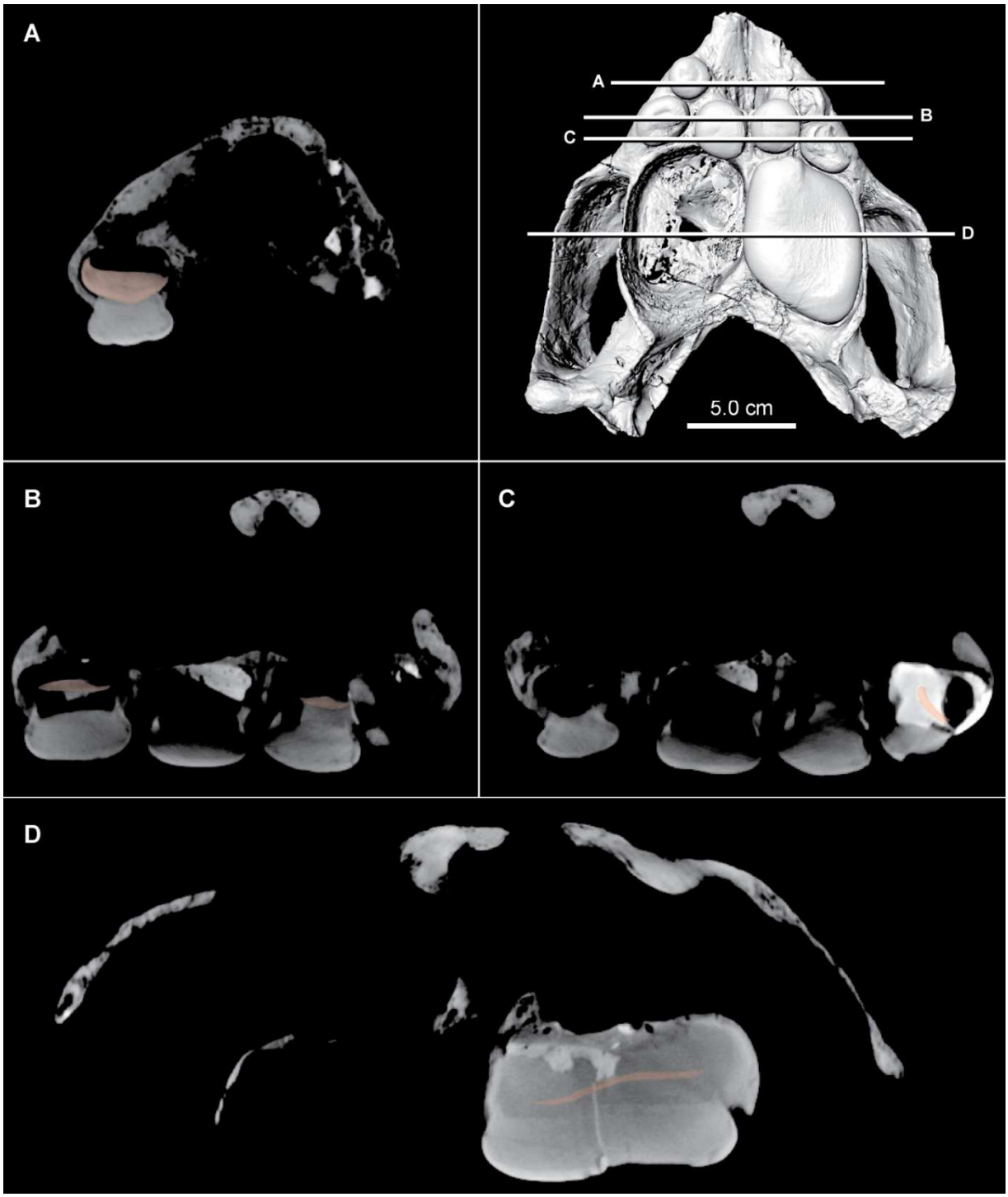

Supplementary Fig. S7 Coronal slices in anterior view through four planes in the holotype skull of *Macroplacus raeticus* BSP 1967 I 324, showing replacement teeth at various stages of growth (red). (A) slice 736 showing the Rm1 replacement tooth. (B) slice 660 showing the Rm2 and Lpl1 replacements. (C) slice 633 showing the slightly displaced Lm2 replacement. (D), slice 439 showing the Lpl2 replacement.

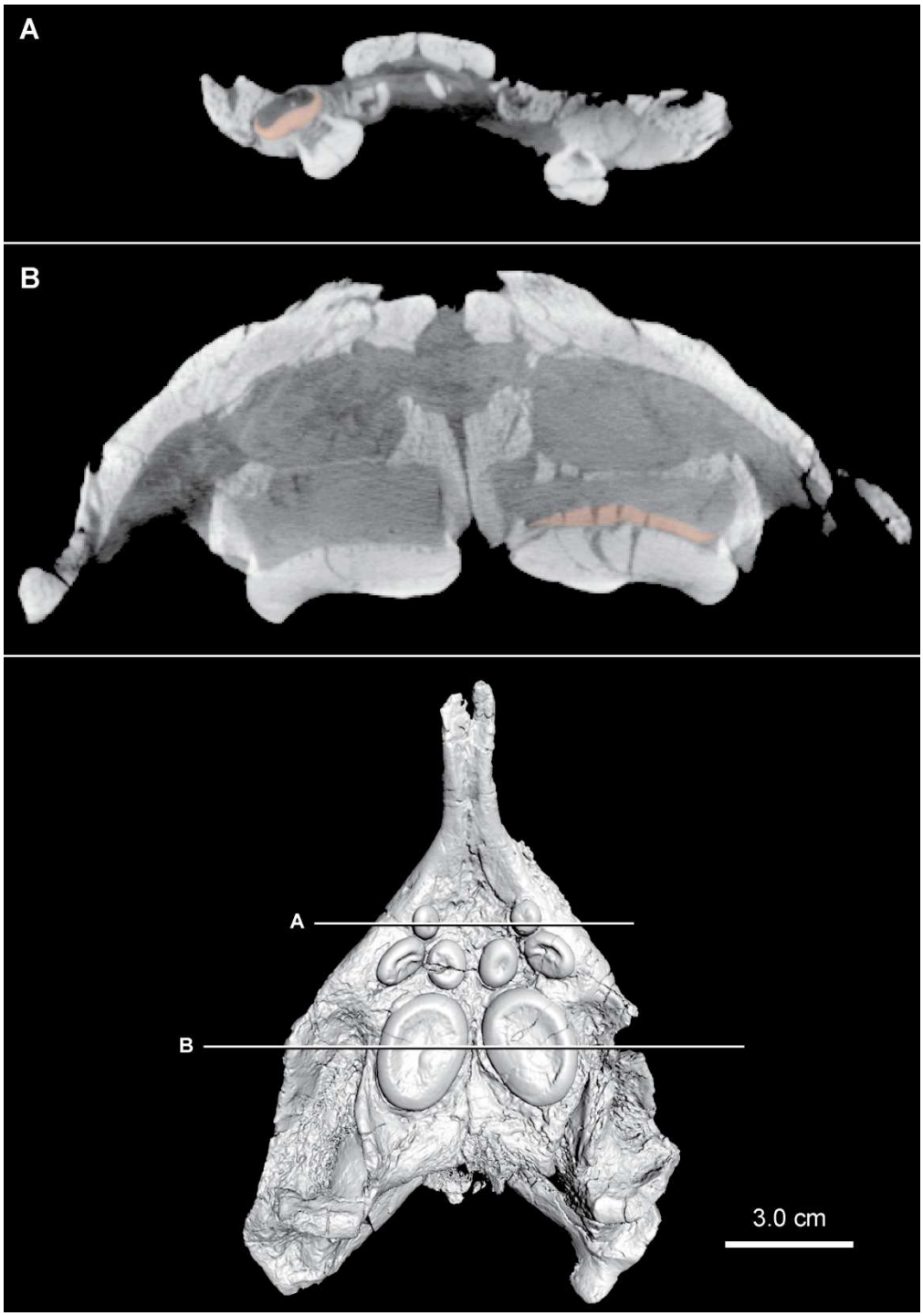

Supplementary Fig. S8 Coronal slices in anterior view through two planes in the new skull of *Psephoderma alpinum* PIMUZ A/III 1491, showing replacement teeth (red). (A) slice 573 showing the Rm1 replacement. (B) slice 411 showing the Lpl2 replacement.

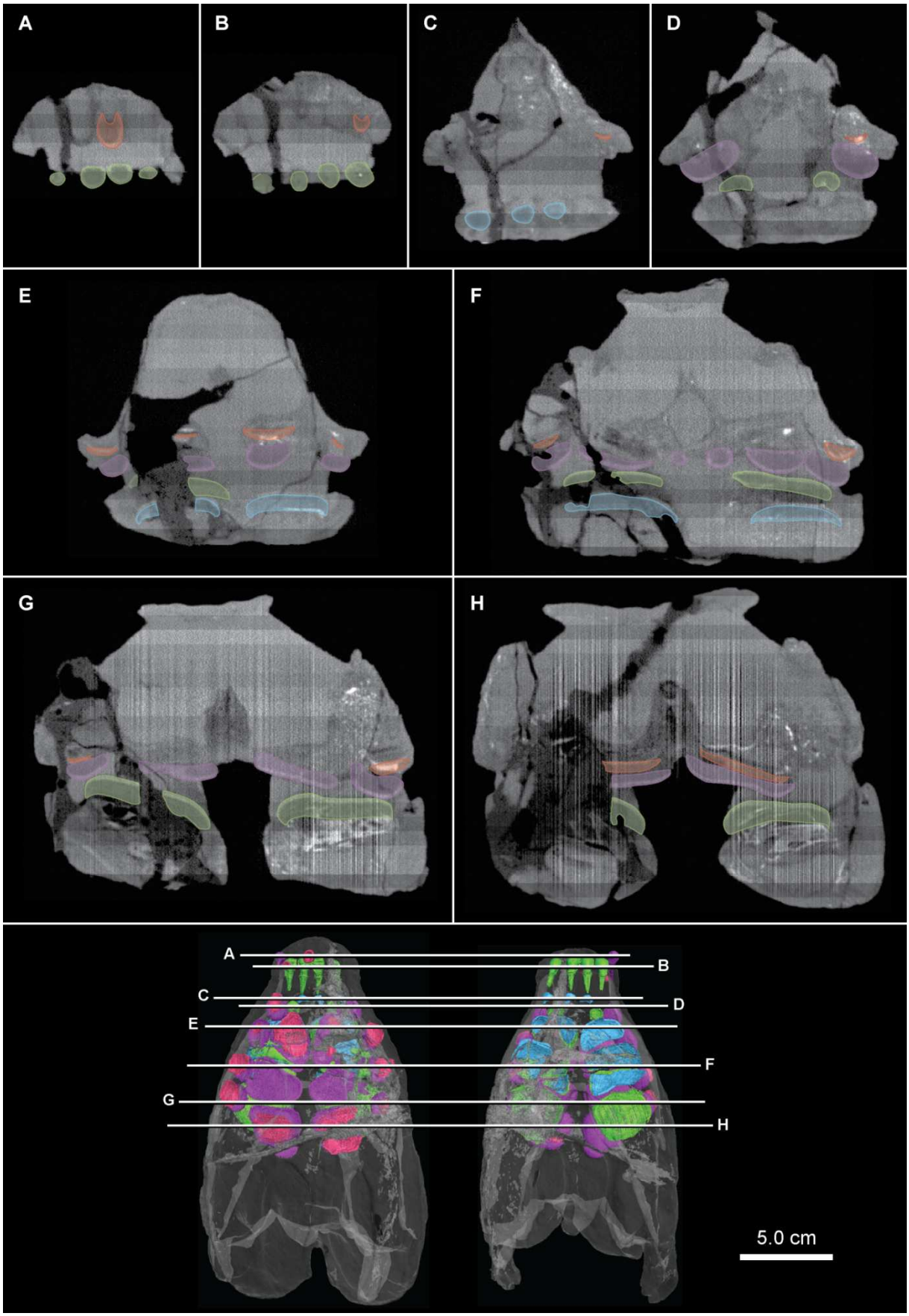
A
B
C
D
E
F
G
H
A
B
C
D
E
F
G
H
5.0 cm

Supplementary Fig. S9 (previous page) Coronal slices in anterior view through eight planes in the skull of the Chinese placodont *Placodus inexpectatus* IVPP V 14996, showing replacement teeth at various stages of growth. (A) slice 544 showing the Rpm1 replacement tooth (B) slice 627 showing the Rpm3 replacement tooth (C) slice 660 showing the replacements for Ld1, Rd1 and Rd2, as well as a small amount of Lm1. (D) slice 708 showing the full sized Lm1 replacement tooth. (E) slice 733 showing replacements for both the left and right m2, pl1 and d4 teeth. (F) slice 833 showing replacements for both the left and right m3 and d5 teeth. (G) slice 921 showing replacements for both m4 teeth. (H) slice 975 showing replacement teeth for both pl3 teeth. Purple, functional teeth in upper jaw (premaxilla, maxilla and palatine); green, functional teeth in dentary; red, replacement teeth in upper jaw; blue, replacement teeth in dentary.

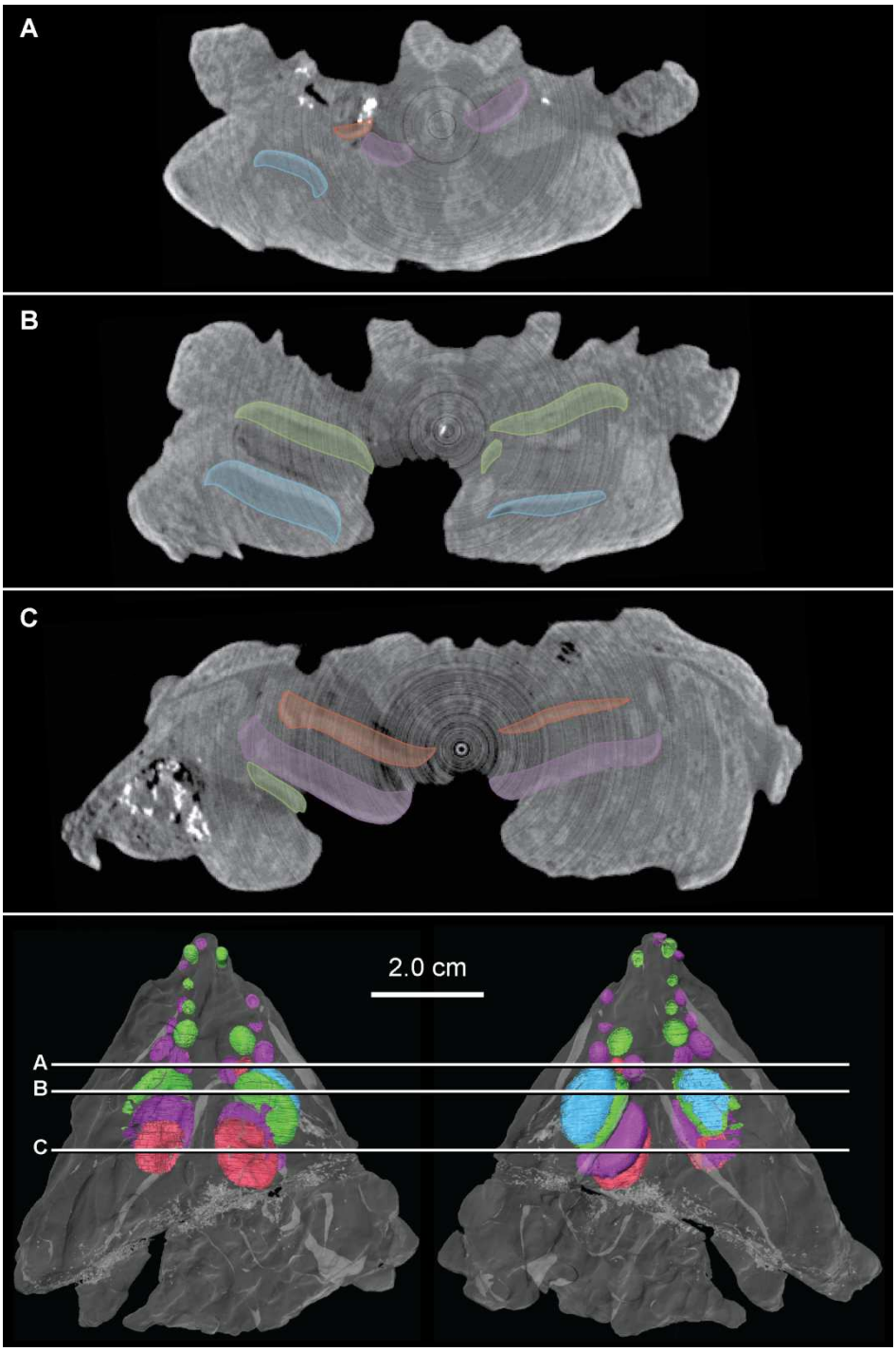

Supplementary Fig. S10 Coronal slices in anterior view through three planes in the holotype skull of the Chinese placodont *Sinocyamodus xinpuensis* IVPP V 11872, showing replacement teeth at various stages of growth. (A) slice 511 showing the replacement tooth for Rpl1 and the anterior portion of Rd5(B) slice 597 showing the

replacements for both d5 teeth (C) slice 763 showing the replacements for both pl2 teeth. Colour scheme as in Supplementary Fig. S9.

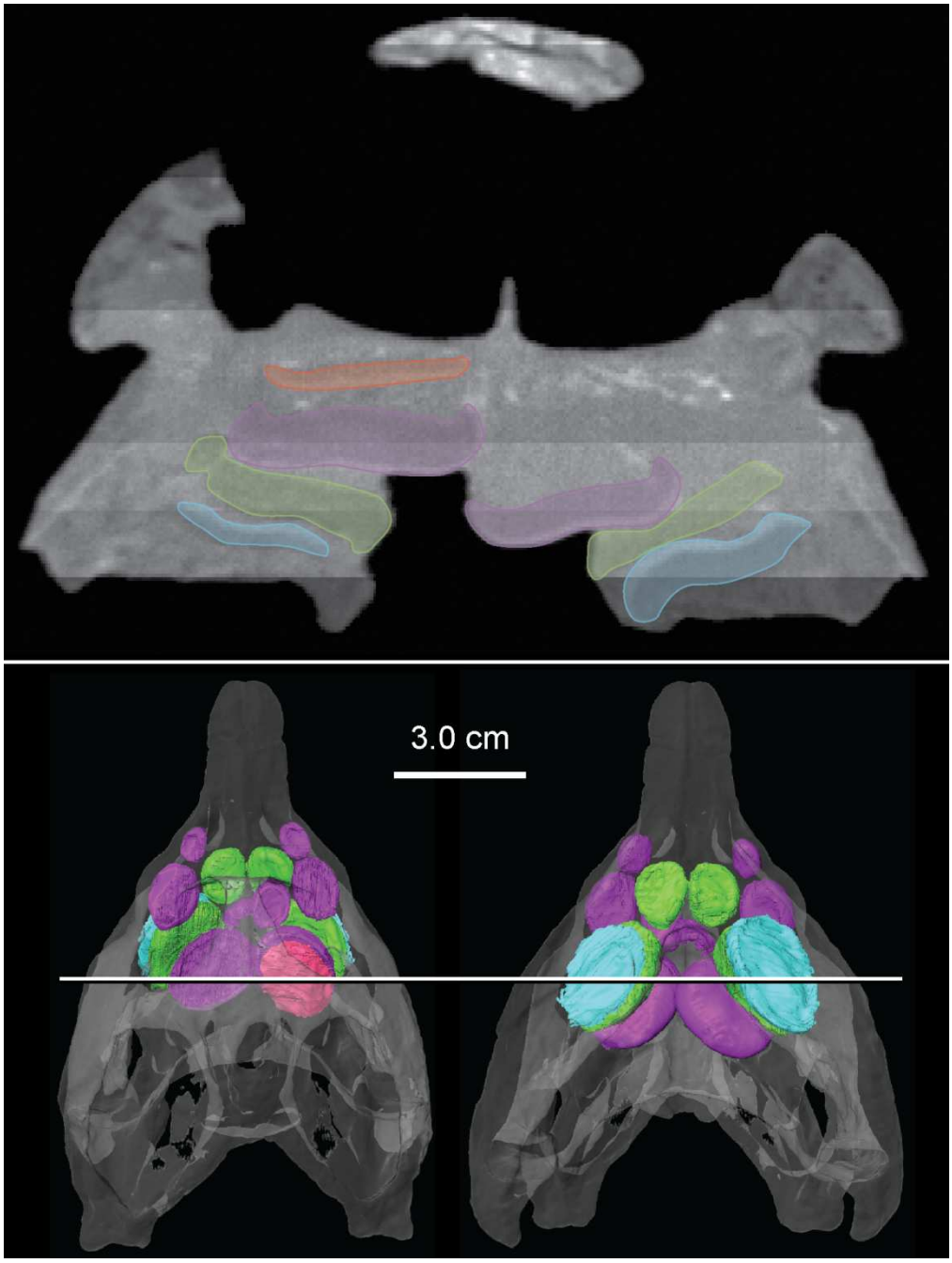

Supplementary Fig. S11 Coronal slice in anterior view through the holotype skull of the Chinese placodont *Psephochelys polyosteoderma* IVPP V 12442, showing replacement teeth. Slice 435 showing all three of the replacement teeth in the skull: Rpl2, Rd2 and Ld2. Colour scheme as in Supplementary Fig. S9.

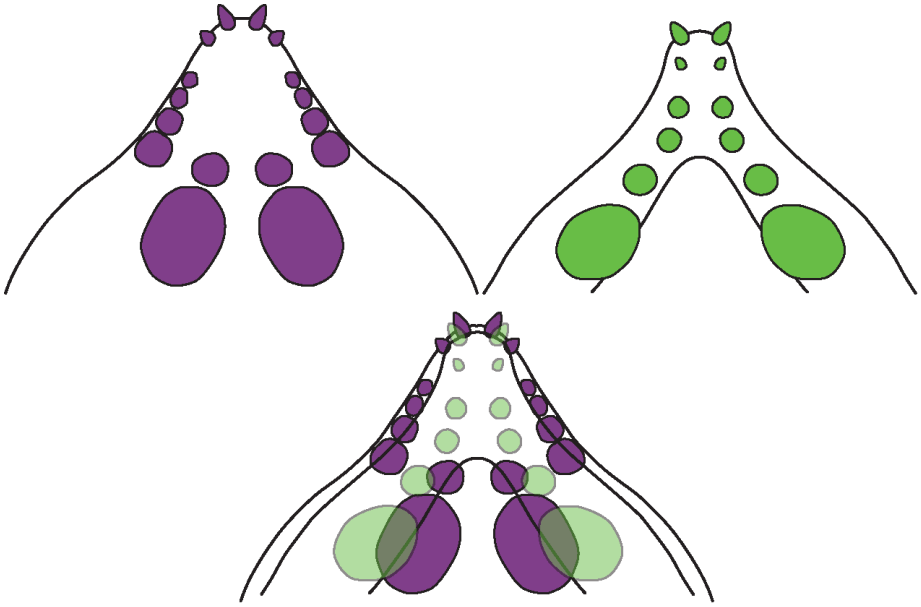

Supplemental Fig. S12 Reconstruction of the dentition of a subadult specimen of *Cyamodus hildegardis* PIMUZ T 2796, showing the dentition of the skull in palatal view (top left), the dentary in dorsal view (top right) and tooth occlusion in palatal view (bottom). Redrawn and modified from Kuhn-Schnyder (1959). Colour scheme as in Fig. 3.

CHAPTER 6

THE CRANIAL ANATOMY OF CHINESE PLACODONTS AND THE PHYLOGENY OF PLACODONTIA

Glyphoderma kangi by Jaime Chirinos

The cranial anatomy of Chinese placodonts and the phylogeny of Placodontia

James M. Neenan[1*], Chun Li[2], Da-Yong Jiang[3], Olivier Rieppel[4], Torsten M. Scheyer[1]

[1] Palaeontological Institute and Museum, University of Zurich, Karl Schmid-Strasse 4, 8006 Zurich, Switzerland.[*] james.neenan@pim.uzh.ch

[2] Institute of Vertebrate Paleontology and Paleoanthropology, Chinese Academy of Sciences, Beijing 100044, P. R. China.

[3] Department of Geology and Geological Museum, Peking University, Beijing 100871, P. R. China.

[4] The Field Museum, 1400 South Lake Shore Drive, Chicago, IL, 60605-2496, USA.

1. ABSTRACT

Placodonts are Triassic marine reptiles that inhabited the eastern and western margins of the Tethys Ocean (modern South China and Europe/Middle East). While the crania of European taxa are relatively well understood, those of Chinese taxa have not been extensively studied, nor have most of them been incorporated into a comprehensive phylogeny. Here we present the first reconstructions of all Chinese placodont holotype skulls using micro-computed tomography (µCT) and/or detailed anatomical study. We also present the first phylogenetic analyses that incorporate all placodont genera using a general diapsid matrix that includes postcranial characters, and a placodont only, cranial matrix. Results vary between matrices, but both support a monophyletic Placodontia with eastern taxa interspaced throughout, indicating no major separation between the eastern and western Tethyan realms. Support is strong for a western Tethyan origin of Placodontia, although the highly nested Placochelyidae first appear in the upper Middle Triassic of the eastern Tethys. Thus all placodont clades appear to have originated in a period of intense speciation during the Middle Triassic.

2. INTRODUCTION

Placodontia is a clade of mostly durophagous Triassic sauropterygians that inhabited the eastern and western margins of the Tethys Ocean, which correlate to present day South China and Europe/Middle East respectively (e.g. Neenan et al. 2013). While western taxa are relatively well studied, especially with regard to crania (e.g., Huene, 1956; Sues, 1987; Pinna and Nosotti, 1989; Nosotti and Pinna, 1996; Reif and Stein, 1999; Rieppel, 2000a; 2001), including some braincase and inner ear data (Edinger, 1925; Nosotti and Rieppel, 2002; Neenan and Scheyer, 2012), Chinese specimens have only recently come to light, with the first valid species, *Sinocyamodus xinpuensis*, being described by Li (2000). Since then, three additional taxa have been described: *Psephochelys polyosteoderma*, Li and Rieppel (2002), *Placodus inexpectatus*, Jiang et al. (2008), and *Glyphoderma kangi*, Zhao et al. (2008).

Since placodonts are considered to be the most plesiomorphic group of sauropterygians, these discoveries are important, as they have the potential to shed light on the palaeogeographic origins of Sauropterygia; the largest and most diverse group of marine reptiles known (Motani, 2009). It has previously been suggested that the clade initially evolved in the eastern Tethys and moved westwards (e.g. Rieppel and Hagdorn, 1997; Rieppel, 1999), although more recent evidence suggests a western origin (Neenan et al. 2013). A comprehensive placodont phylogeny that includes all European and Chinese taxa would thus be important to shed light on this. However, due to often unclear external morphology and the concealment of important structures within sediment matrix, no Chinese placodont has yet been incorporated into a phylogenetic analysis (with the exception of *Placodus inexpectatus*, which was included in a matrix with European taxa, Jiang et al. 2008). Nor have any of the Chinese holotypes had interpretational reconstructions of cranial morphology published, with the exception of *Placodus inexpectatus* and a single dorsal skull

reconstruction of *Psephochelys*. Recent examination of specimens at the GMPKU and IVPP (see below for institutional abbreviations), as well as µCT scanning at the IVPP have revealed a wealth of new morphological data that were previously undescribed. These data have allowed us to reconstruct the cranial morphology of the holotypes of these taxa for the first time in most cases, as well as carry out the first comprehensive placodont phylogeny that includes all European and Chinese placodont genera.

Institutional abbreviations: GMPKU: Geological Museum, Peking University, Bejing, P. R. China. **IVPP**: Institute of Vertebrate Paleontology and Paleoanthropology, Beijing, P. R. China. **ZMNH**: Zhejing Museum of Natural History, Hangzhou, P. R. China.

3. MATERIALS AND METHODS

Of the four Chinese placodont holotypes, only two crania were suitable for micro-computed tomographic (µCT) scanning: *Sinocyamodus* IVPP V 11872 and *Psephochelys* IVPP V 12442 (Fig. 6.1). Scanning was conducted at the IVPP with a slice thickness of 0.194 mm and 0.200 mm respectively, both having a voltage of 190 kV and a current of 100 µA. Slice data were reconstructed using the manual segmentation tool in Avizo 6.2.1. *Placodus inexpectatus* GMPKU-P-1054 (Fig. 6.2A) and *Glyphoderma* ZMNH M 8729 (Fig. 6.3) are both embedded in a matrix slab, and thus could not be scanned. However both specimens were examined in detail by JMN and TMS in August 2010, with an additional examination of *P. inexpectatus* in March 2012. Chinese specimens were compared to European taxa that have already been described in detail by Rieppel (1995, 2000a, 2000b, 2001) and to personal observations from specimens JMN and TMS have studied and CT scanned (see Neenan et al. (2014) for full details, scan parameters etc.).

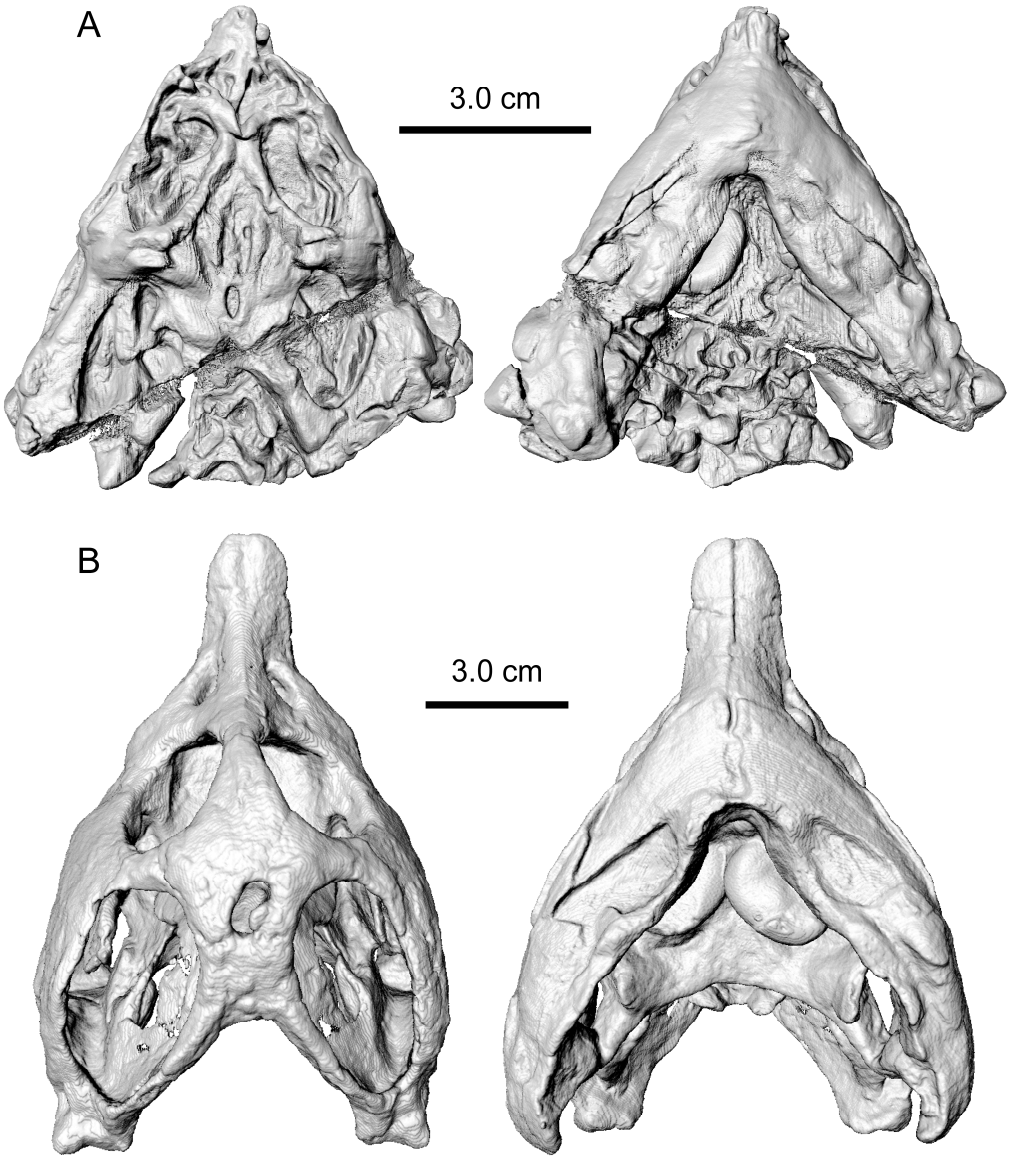

Figure 6.1. The two Chinese placodont holotype crania that were µCT scanned for this study. **A**, *Sinocyamodus*, IVPP V 11872. **B**, *Psephochelys*, IVPP V 12442. Dorsal view is on the left and palatal view on the right.

Phylogenetic analyses were conducted in PAUP 4.0b10 for Microsoft Windows 95/NT (Swofford, 2003) using PaupUP version 1.0.3.1 (Calendini and Martin, 2005). Trees were modified with Mesquite (Maddison and Maddison, 2011) and the Adobe Creative Suite. All analyses were run with the heuristic search option, with all characters being unordered and unweighted, and with an all-zero ancestor as an outgroup taxon. Two analyses were conducted in this study using two separate

matrices: Analysis 1, the comprehensive diapsid analysis, was based on the matrix of Neenan et al. (2013), which in turn was based on that of Liu et al. (2011). The new unarmoured placodont *Pararcus*, which was coded by Klein and Scheyer (in press), was included; as were the European genera that were excluded by Neenan et al. (2013) (i.e. *Henodus*, *Macroplacus*, *Protenodontosaurus* and *Placochelys*). Analysis 2, The placodont-only cranial analysis, was based on the character matrix of Rieppel (2001), but with some additional characters from Rieppel (2000b) and Jiang et al. (2008). *Pararcus* was not included in this analysis due to a lack of cranial material, but the placodontiform *Palatodonta* (Neenan et al. 2013) was.

4. RESULTS

4.1 Description of Cranial Osteology

***Placodus inexpectatus* Jiang, Motani, Hao, Rieppel, Sun, Schmitz and Sun, 2008.**

Holotype specimen: GMPKU-P-1054 (Fig. 6.2A). Owing to the fact that the skull of this specimen is embedded in matrix, it was unsuitable for scanning.

Other known specimen: IVPP V 14996. A detailed account of the dental morphology and tooth replacement patterns of this skull was given by Neenan et al. (2014), including a detailed account of the dental morphology and tooth replacement patterns. This specimen will be described in detail elsewhere, and will thus not be used in the current paper.

The skull of GMPKU-P-1054 was thoroughly described by Jiang et al. (2008), however further examination combined with initial observations from IVPP V 14996 have led us to an alternative interpretation of the cranial osteology of the holotype skull (Fig. 6.2B). The most important of these is that the posterior portion of the external naris is actually broken in this specimen, and the prefrontal does not enter its

posterior margin. We have also defined the sutures for the following elements that were not identified by Jiang et al (2008): maxilla, jugal, postorbital, dentary, surangular, and angular.

Premaxilla – A large, paired element that forms the majority of the rostrum and the anterior margin of the external naris. Contains 3 bulbous, procumbent teeth that are shorter than those of *P. gigas*.

Maxilla – This element contains 4 rounded crushing tooth plates, and has a dorsal process that contributed to about half of the posterior margin of the external naris. It is excluded from the margin of the orbit by an anterior process of the jugal. There is a small anterior process that enters the rostrum.

Nasal – This element is fused, and forms the dorsal margin of the external naris. It is much the same as described by Jiang et al. (2008).

Prefrontal – The prefrontal is most likely excluded from the external naris, owing to the posterior margin being broken in the latter. The element forms the anterior half of the dorsal margin of the orbit as well as the dorsal half of the anterior margin. It does not form the entire anterior margin of the orbit as described by Jiang et al. (2008).

Frontal – The frontal is fused and is once again very similar to the reconstruction of Jiang et al. (2008).

Postfrontal – Unlike the reconstruction of Jiang et al. (2008), this element forms a large part of the posterior margin of the orbit by means of a tapering descending process. The postfrontal is also appears to be excluded from the upper temporal fenestrae by a narrow process of the postorbital.

Postorbital – Similar to Jiang et al. (2008), our reconstruction shows that this element forms a great deal of the lateral margin of the upper temporal fenestra, although we can show that this was a relatively narrow posterior process. It also

enters the lower half of the posterior margin of the orbit, but is excluded from the ventral margin by the jugal.

Jugal – The jugal nests the entire ventral margin of the orbit, as well as the ventral half of the anterior margin. There is a narrow anterior process that terminates in a flared projection between the orbit and external naris. The element extends as far posteriorly as the postorbital, and appears to be broken in its posterior part

Parietal – The parietal is also fused and has a similar shape to that of the interpretation of Jiang et al. (2008), although we do not consider it to have quite as much of a posterior projection.

Squamosal – We reconstruct the right squamosal as being somewhat larger than Jiang et al. (2008), especially in its ventral margin. This element forms the margin of the posterior portion of the upper temporal fenestra and mostly obscures the quadrate in lateral view.

Quadrate – We reconstruct this element as being much smaller than Jiang et al. (2008), only being exposed a small amount in lateral view where it articulates with the articular.

Mandible – The dentary is narrow in lateral aspect, and contains 4 crushing teeth and 2 procumbent anterior teeth similar to those in the premaxilla (Neenan et al. 2014). It also constitutes a large amount of the coronoid process. The angular and suragular form the posterior portion of the lateral ramus, and both taper anteriorly to meet the dentary. We reconstruct the retroarticular process as being slightly wider than Jiang et al. (2008), and have identified the prearticular running along the dorsal surface.

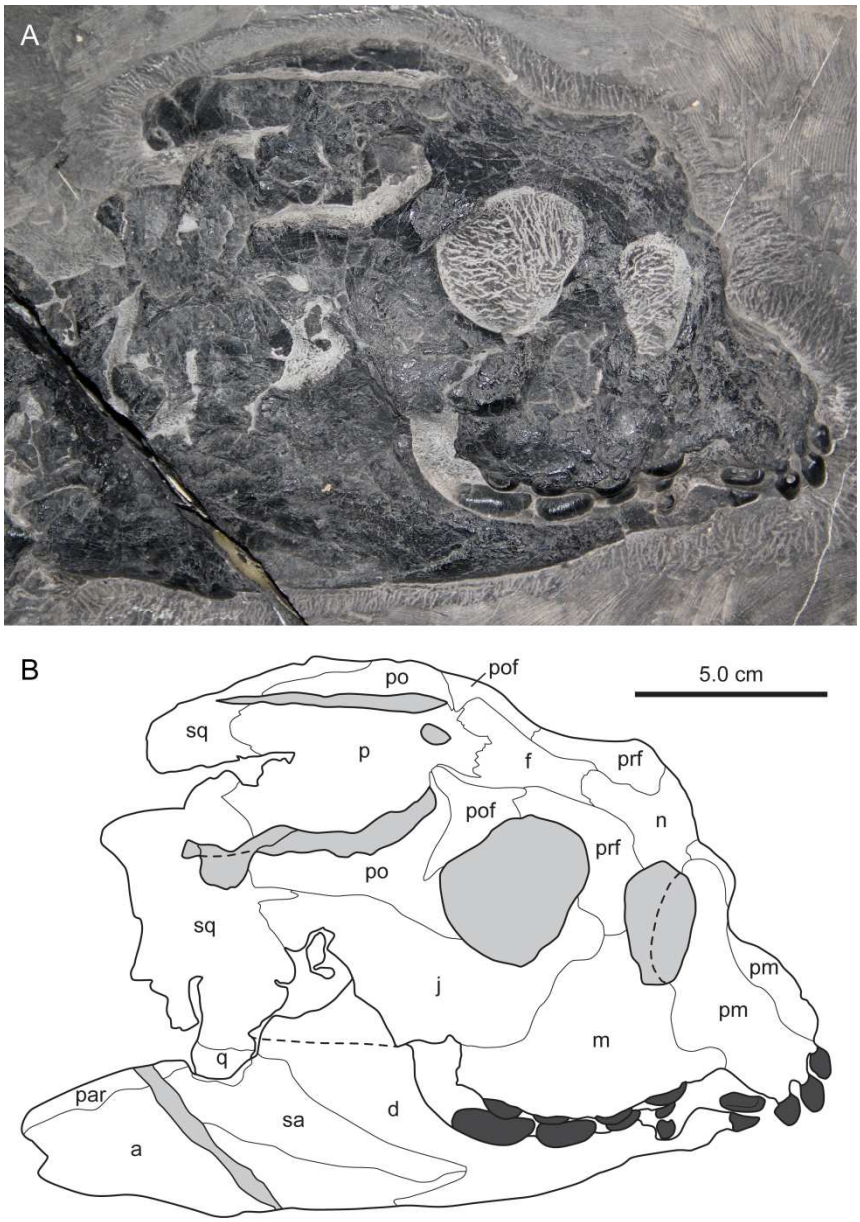

Figure 6.2. The cranium of the holotype specimen of *Placodus inexpectatus*, GMPKU-P-1054 **A**, photograph of the skull in right lateral view. **B,** revised reconstruction. Dashed lines indicate broken elements – note broken posterior margin of external naris. Abbreviations: a, angular; d, dentary; f, frontal; j, jugal; m, maxilla; n, nasal; p, parietal; par, prearticular; pm, premaxilla; po, postorbital; pof, postfrontal; prf, prefrontal; q, quadrate; sa, surangular; sq, squamosal.

Sinocyamodus xinpuensis Li, 2000

Holotype specimen: IVPP V 11872. The skull of this specimen has been prepared out from the matrix, so is therefore suitable for scanning (Fig. 6.1A).

This skull has been removed from a ventrally preserved specimen with almost complete postcranial remains. It can be identified as a subadult as the dentition corresponds to that of a subadult specimen of *Cyamodus hildegardis* (see Neenan et al. 2014). As a result, many of the skull elements are not completely fused, and have become somewhat disarticulated. The skull is dorsoventrally crushed, has a large crack running through the right temporal region, is articulated with the mandible and has a few postcranial elements attached to the posterior portion, obscuring most of the occipital region and some of the palate. µCT scanning has revealed several previously obscured structures, however (Fig. 6.3).

Premaxilla – Only the left premaxilla remains intact, the right one is mostly missing, revealing a dentary tooth. The remaining element contains 2 small, round teeth (not 3 as described by Li, 2000) and forms half of a short rounded rostrum. The premaxilla has a posterolateral process that meets the maxilla and forms part of the ventral margin of the external naris. On the dorsal surface of the anterior margin of the remaining premaxilla is a concavity, which may represent a rostral nerve foramen (see description of *Glyphoderma* below).

Maxilla –The left maxilla has an ascending process that would in life articulate with a notched surface of the prefrontal, however crushing has separated these elements. The maxilla would also form part of the posterior margin of the external naris, but distortion has once again made this unclear. It also forms the ‘floor’ of the external naris. The maxilla supports 3 small, round teeth.

Nasal – The left nasal remains intact and would meet the right nasal in a midline suture between the external nares. The element is long and narrow and forms the entire medial wall of the external naris, however a small lateral projection also forms part of the anterior margin as well. Part of the right nasal remains, but the posterior

portion has been lost. It is unclear where the posterior margin lies, as this is obscured by the prefrontals.

Prefrontal – The prefrontal is a relatively large element which forms the anterior margin of the orbit and part of the posterior margin of the external naris. There is a notched structure on its ventral margin that held the ascending process of the maxilla. Although it appears the prefrontals meet in a medial suture, this is merely an artefact of crushing. In life these elements were separated by the nasals and frontals.

Frontal – Although the anterior margin of this element cannot be distinguished, it forms the majority of the dorsal margin of the orbit and runs almost all the way posteriorly to the pineal foramen. It is a long, narrow element that meets in a medial suture. The posterior margin is in contact with the parietal, while the posterolateral margin is in contact with the postfrontal.

Postfrontal – The postfrontal is a somewhat 'Y-shaped' element which has a descending process, which forms the posterior margin of the orbit, a posterior process, which meets the parietlal and postorbital just posterior to the anterior margin of the supratemporal fenestra, and a smaller anterior process, which forms part of the dorsal margin of the orbit.

Postorbital – This is a large element which receives the descending process of the postfrontal and forms part of the posteroventral orbital margin. It forms most of the anterior margin, as well as about half of the lateral margin of the supratemporal fenestra. It is held by the jugal anteriorly, and meets the quadratojugal for most of its lateral margin. The medial process is framed by the postfrontal anteriorly and the parietal posteriorly.

Jugal – The jugal has a long and narrow dorsal anterior process that forms part of the ventral margin of the orbit. The left jugal extends to a point around the posterior margin of the orbit, where it meets the quadratojugal. However the right element only

appears to extend posteriorly a short distance, possibly indicating this element is broken.

Parietal – This is fused, broad, heavily ornamented and encloses a pineal foramen towards the anterior margin. The lateral margins are concave, and the element forms the entire medial margin of the supratemporal fenestrae. These processes continue far posteriorly, meeting the squamosals near the posterior margin of the skull.

Quadratojugal – This forms a large portion of the temporal bar, and extends far anteriorly, at least until a level with the posterior margin of the orbit. Only a small amount enters the lateral margin of the supratemporal fenestra, being prevented from doing so further anteriorly by a posterior process of the postorbital.

Squamosal – This element has a relatively small dorsal exposure and forms part of the posterior margin of the supratemporal fenestra. It is interpreted as containing up to 4 osteoderms both on the posterodorsal and posterolateral surfaces.

Quadrate – The right quadrate can be seen to articulate with the mandible, but apart from this not much can be defined.

Palatine – The palatine is a large, element that contains 2 crushing tooth plates (Neenan et al, 2014). It is unclear if it is fused or not. There is a posterior dental lamina foramen posterior to the larger crushing tooth.

Pterygoid – The left pterygoid is more exposed than the right, and had a flange at its posterolateral boundary. It forms the posterior margin of the posterior dental lamina foramen and appears to meet in a medial suture, although the precise outline of this is unclear.

Mandible – Each dentary contains 5 teeth: 1 anterior bulbous tooth, and 4 crushing teeth. The anterior-most 2 are very small and rounded, with the third being slightly larger, and the fourth being a large, flat crushing plate (see Neenan et al. 2014). Like the left premaxilla, a concavity is visible on the right dentary, which is possibly a

nerve foramen. The splenials meet in a medial suture and separate the dentary from the medial ramus margin. The angular contains at least 2 osteoderms and has an anterior process that separates the dentary from the splenial for roughly half their length. A prearticular is visible on the right ramus. The coronoid process is visible dorsally through the upper temporal fenestra.

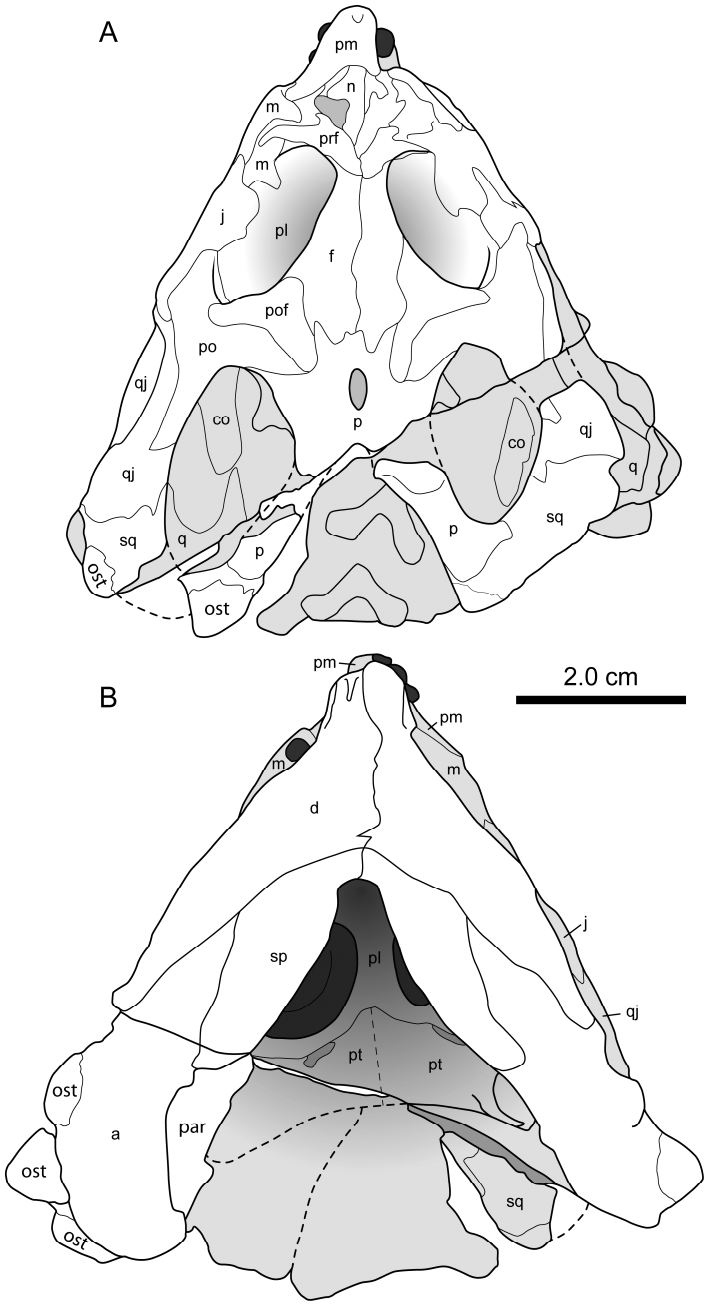

Figure 6.3. Reconstruction of the cranium of the *Sinocyamodus* holotype, IVPP V 11872, in dorsal (A) and palatal (B) views. Abbreviations as in Fig. 2 and: co, coronoid; ost, osteoderm; pl, palatine; pt, pterygoid; qj, quadratojugal; sp, splenial.

***Glyphoderma kangi* Zhao, Li, Liu and He, 2008**

Holotype specimen: ZMNH M 8729 (Fig. 6.4). Owing to the fact that the skull of this specimen is embedded in matrix, it was unsuitable for scanning. This is an apparently complete, although flattened skull that has large portions obscured by matrix. A large mineral vein runs through the right temporal region, which has destroyed the specimen here.

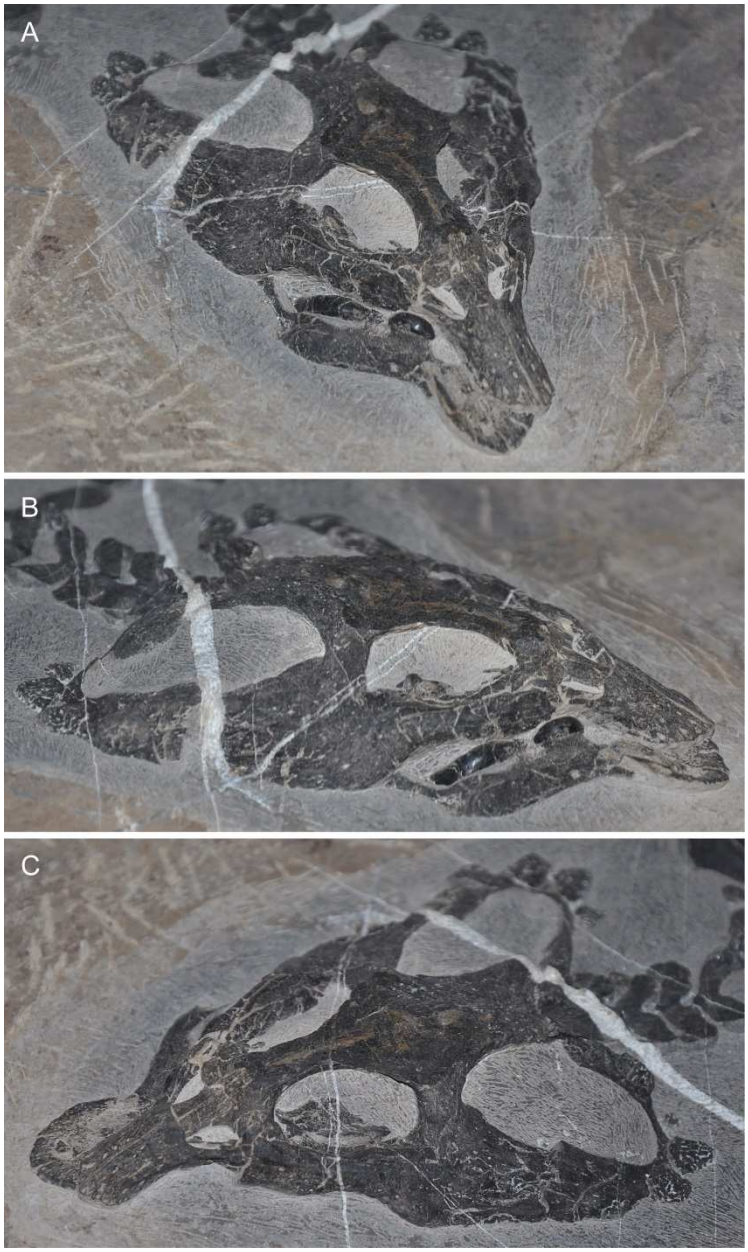

Figure 6.4. Photographs of the holotype skull of *Glyphoderma*, ZMNH M 8729, highlighting previously undescribed features. **A**, angled view of anterodorsal and right lateral side. **B**, Angled view of right lateral side. **C**, Angled view of left dorsolateral side. Note nerve canals on premaxilla. Not to scale.

Premaxilla – The premaxilla is edentulous and spatulate (shorter and more rounded than in *Psephochelys*), and contains several (at least 8) small fossae, probably for rostral nerves to aid in prey detection (Figs. 6.4, 5). There is a narrow posterolateral process that forms the ventral margin of the external naris although, due to crushing, it appears that it is the maxilla that forms this margin, but it is in fact the floor of the external naris.

Maxilla – These are long, extending almost as far as the posterior margin of the orbits. There is an ascending process that forms the posterior margin of the external naris, and an anterior process medial to the premaxilla that forms at least part of the ventral margin of the external naris. As mentioned previously, the maxilla appears to form the entirety of this margin, but this is an artefact due to crushing and is actually the floor of the external naris. The maxilla enters the ventral margin of the external naris, but is mostly restricted from doing so by an anterior process of the jugal.

Nasal – Unlike *Pspehochelys* and *Psephoderma* but similar to *Placochelys*, the nasals meet in a medial suture. The nasal is narrow and forms a large portion of the dorsal margin of the external naris.

Prefrontal – The prefrontal forms the anterior portion the orbit, and has a pointed posterolateral process that defines the anterior portion of the ventral margin as well. It does not enter the external naris.

Frontal – The frontal is long and slender and forms the dorsal margin of the orbit. It does not extend far posteriorly, only to the posterior margin of the orbit. The frontal meets the nasal in an interdigitated suture.

Postfrontal – This element forms the posterior margin of the orbit and also a portion of the posteroventral margin. It is excluded from the upper temporal fenestra by a narrow medial process of the postorbital, where it meets the palatine.

Postorbital – The postorbital does not extend far ventrally on the temporal arch, rather remaining in a dorsal position, where it forms the anterior third/half of the lateral margin of the upper temporal fenestra. It also has a narrow medial process that envelops the anterior end of the fenestra, preventing the postfrontal from entering its margin.

Jugal – The jugal forms the anterior portion of the temporal arch, much like in *Psephochelys*. There is an anteromedial process that travels along the ventral margin of the orbit. It meets the quadratojugal at about the level of the anterior margin of the upper temporal fenestra.

Quadratojugal – Along with the jugal, the quadratojugal forms the posterior remainder of the temporal arch. It also enters the posterior half of the lateral margin of the upper temporal fenestra.

Parietal – This is a fused element that contains a small pineal foramen in a fairly anterior position, about level with the anterior margin of the upper temporal fenestra. As in *Psephochelys* and *Sinocyamodus*, the parietal extends far caudally, forming the majority of the medial margin of the upper temporal fenestra. The parietal is heavily ornamented, along with the postfrontals and part of the frontals.

Squamosal – As in *Psephochelys* and *Sinocyamodus*, this element is reduced in size compared to other cyamodontoids. There are at least 3 osteoderms on the posterodorsal margin, but examination of the left squamosal indicates that there may have been 4. The squamosal also forms the posterior-most margin of the upper temporal fenestra. A squamosal buttress cannot be seen in this specimen without further preparation.

Palatine – Little of this element can be seen, but there are at least two crushing teeth.

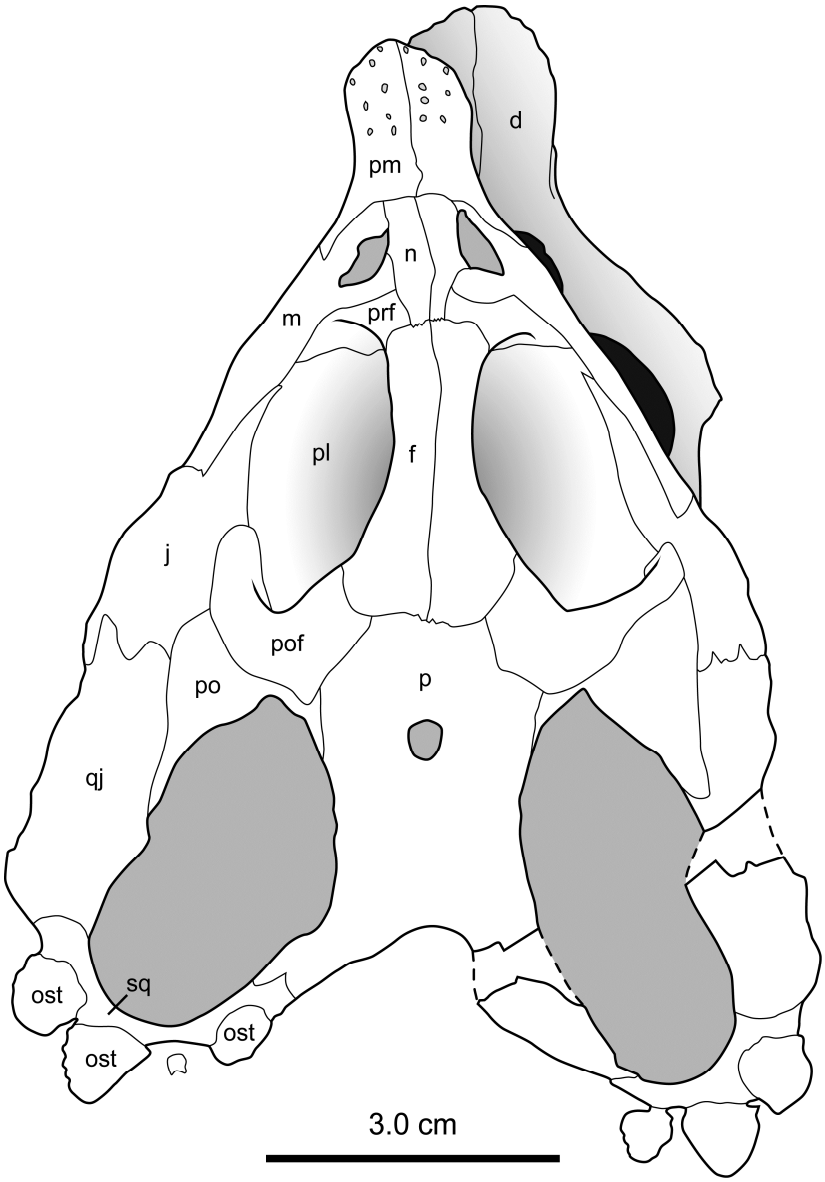

Figure 6.5. Reconstruction of the holotype skull of *Glyphoderma*, ZMNH M 8729, in dorsal view. Abbreviations as in Figs. 2 and 3.

Psephochelys polyosteoderma Li and Rieppel, 2002

Holotype specimen: IVPP V 12442 (Fig. 6.1B). This specimen was originally described in Chinese (Li and Rieppel, 2002a), but was later described in English (Li and Rieppel, 2002b). Owing to the excellent preservation of the skull and full preparation of the specimen, it was ideal for scanning, and revealed several discrepancies from the interpretation of the original description by Li and Rieppel (2002a, b) (Fig. 6.6).

The holotype skull is articulated with the mandible and is almost complete, with the exception of the posterior region of the braincase, i.e. exoccipitals, basioccipital condyle, prootics and opisthotics. The supraoccipital and lateral portions of the paroccipital processes are present however.

Premaxilla – The paired premaxillae form a long, narrow (but not as narrow as *Psephoderma*), edentulous rostrum and extend far posteromedially to form the anterodorsal margin of the external nares. There is also a posterolateral process that extends about half the length of the external naris (not further than this as in Li and Rieppel (2002a, b).

Maxilla – Forming the posterior half of the ventral margin of the external naris, the maxilla has an ascending process that also forms part of the posterior margin as well. A small medial process enters the orbit at approximately the middle of its ventral margin. The maxilla contains two rounded crushing teeth (see Neenan et al., 2014 for more information on the dentition).

Nasal – Similar to *Psephoderma*, *Macroplacus* and *Henodus*, the nasals do not meet medially and are separated by extended processes of the premaxillae and frontals. The nasal is a small, fairly rectangular element and forms the posterior half of the dorsal margin of the external naris.

Prefrontal – This is a narrow element which forms the anterior margin of the orbit, as well as part of the anterior portion of its ventral margin. The prefrontal is elongate, and prevents the maxilla from entering the margin of the orbit until its approximate mid-point. The prefrontal does not enter the external naris, as reconstructed by Li and Rieppel (2002a, b), nor does it have such a long posterolateral process.

Frontal – The frontal is narrow and elongate, forming the majority of the ventral margin of the orbit. It has an extended anterior process which separates the nasals. It is similar in proportions to the interpretation of Li and Rieppel (2002a, b).

Postfrontal – The anterior portion of this element is similar in shape to the interpretation of Li and Rieppel (2002a, b), however it does not extend as far posteriorly. It does not enter the upper temporal fenestra, being prevented from doing so by narrow processes of the postorbital and parietal. Nor does it enter the pineal foramen.

Postorbital – This element is similar to the interpretation of Li and Rieppel (2002a, b), although the extent to which it enters the posterior margin of the orbit was over estimated. There is a long, narrow posterior process that forms the anterior half of the upper temporal fenestra, as well as a smaller medial process that forms most of its anterior margin.

Jugal – Similar to *Glyphoderma*, the jugal forms the anterior portion of the temporal arch. It enters the posterior half of the ventral orbital margin, and has a narrow ventral process that extends posteriorly along the temporal arch. In dorsal view it is similar to the reconstruction of Li and Rieppel (2002a, b).

Quadratojugal – A large element that forms the posterior portion of the temporal arch. There is descending process that obscures the majority of the quadrate in lateral view, and the lateral-most portion of the quadrate in occipital view. The quadratojugal forms roughly the posterior half of the medial upper temporal fenestra margin.

Parietal – The parietal is fused and extends far posteriorly to form the majority of the medial margins of the upper temporal fenestrae, which are highly curved. It meets the squamosal quite far posteriorly, articulates with the supraoccipital, and has a descending process that meets the epipterygoid. The anterior margin is located far more anteriorly than the interpretation of Li and Rieppel (2002a, b), encompassing the entire pineal foramen. The latter is apparently large and placed relatively

anteriorly. However, owing to its non-symmetrical shape, it is apparently broken, so its true size and exact position is unclear.

Squamosal – As with other Chinese cyamodontoids, the squamosal is reduced in *Psephochelys*, forming a small portion of the posterior margin of the upper temporal fenestra. Each squamosal contains two osteoderms at their posterodorsal extremity, and in occipital view, forms a squamosal buttress that supports the distal portion of the paroccipital processes (a character shared by all placochelyids). It forms a portion of the posterior posttemporal fossa.

Quadrate – In occipital view, the quadrate forms a clear suture with the pterygoid at its medial margin that runs almost vertically towards the remains of the paroccipital processes. As expected, the quadrate is exposed mostly in occipital view and articulates with the mandible.

Palatine – The palatal contains two crushing teeth on each element, although the posterior left tooth has become disarticulated, but remains attached to the specimen by matrix. From dorsal view, the palatines can be seen to form a broad flat element that meet medially in a raised, dorsally-projecting suture. At the posterior portion of this projection is nestled a small basisphenoid (similar to that of *Placochelys* and *Placodus*, see Rieppel, 2001; Neenan and Scheyer, 2012), which extends posteriorly between the epipterygoids.

Pterygoid – The pterygoids are not fused and contribute a small amount to the posterior part of the palate, less so than in *Placochelys*, where they meet the palatines and form the posterior margins of the caudal dental lamina foramina. There is a large pterygoid flange on each element and, in occipital view, the pterygoid expands laterally to meet the quadrate very close to the quadrate-articular articulation. The pterygoid also forms the anterior portion of the ventral margin of the posttemporal fossa and extends anteriorly to meet the epipterygoid and palatine. The

dorsal exposure of the pterygoid contact is obscured by the remains of the basioccipital.

Epipterygoid – This element forms the anterior portion of the braincase wall, meets the parietal dorsally, and mostly articulates with the palatine ventrally, although it also meets the pterygoid posteriorly. The basisphenoid is located between these elements.

Basisphenoid – This small element is similar to that of *Placochelys*, but is poorly preserved and neither the internal carotid foramina nor the hypophyseal seat can be seen externally or with our CT data. It is almost entirely supported by the palatines, and it runs posteriorly between the epipterygoids, meeting the basioccipital at its posterior margin.

Basioccipital – This element is broken, and does not have a condyle or tubera. It is almost cylindrical in shape, and runs medially from the posterior margin of the basisphenoid until the posterior margin of the pterygoids.

Supraoccipital – The supraoccipital would have formed the dorsal margin of the foramen magnum and would have articulated with the lost exoccipitals. It articulates entirely with the parietal dorsally, and is distinctly ‘n-shaped’ in occipital view.

Mandible – The mandible is of a typical cyamodontoid shape, with and extremely large coronoid process and a short retroarticular process. The rostrum is elongate and edentulous and the dentary contains two crushing tooth plates that meet those in the palatine. In lateral view, the coronoid extends far ventrally, causing the posterior process of the dentary and the anterior process of the surangular to taper. The articular is obscured by the quadrate, but a prearticular can be seen, as can the splenial, which forms a large part of the medial margin of the jaw ramus.

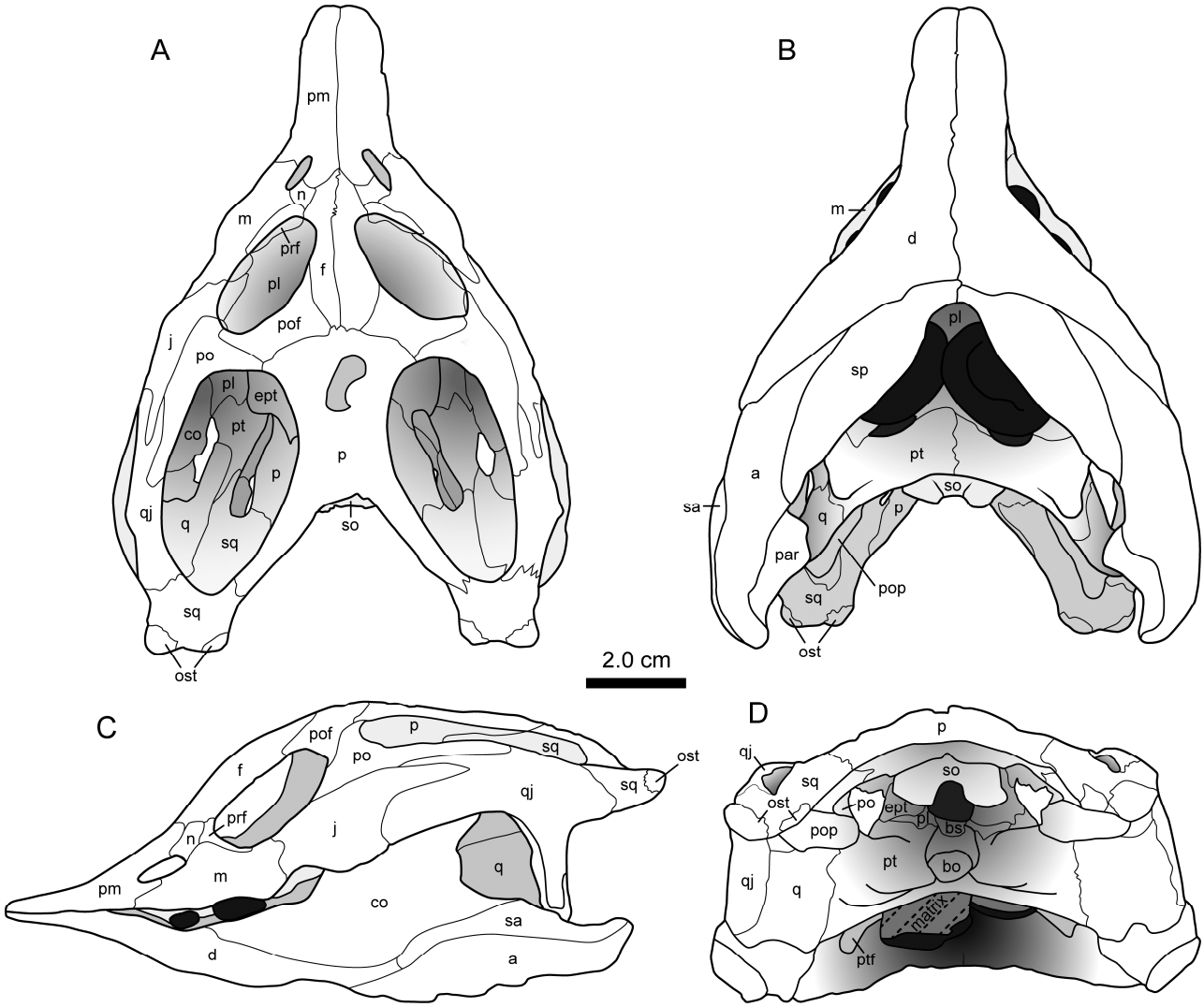

Figure 6.6. Reconstruction of the holotype skull of *Psephochelys*, IVPP V 12442, in dorsal (A), palatal (B), left lateral (C) and occipital (D) views. Abbreviations as in Figs. 2 and 3, and: bo, basioccipital; bs, basisphenoid, ept, epipterygoid; pop, paroccipital process; ptf, pterygoid flange; so, supraoccipital.

4.2 Phylogenetic analyses

Analysis 1: comprehensive diapsid analysis

This analysis yielded 24 most parsimonious trees (MPTs), with a shortest tree length of 613 steps (consistency index (CI) = 0.315, Retention index (RI) = 0.687, rescaled consistency index (RC) = 0.216, and homoplasy index (HI) = 0.685). Placodontia are recovered as sister group to the remaining sauropterygians (Eosauropterygia), with a paraphyletic ‘Placodontoidea’ and a monophyletic Cyamodontoidea (Fig. 6.7).

Chinese placodonts are spaced throughout the tree, and do not form a monophyletic group, which would indicated geographic separation from the western Tethys. Unlike the results of Jiang et al. (2008), *Placodus inexpectatus* does not form a clade with *Placodus gigas*, the former instead forming a more basal polytomy with the newly-described *Pararcus* from the Netherlands. *Sinocyamodus* forms a clade with the European *Cyamodus*. *Glyphoderma* and *Psephochelys* cluster among the Placochelyidae, with the former nesting with *Placochelys* and the latter with *Psephoderma*. Unusually, *Henodus* and *Macroplacus*, which are not usually considered as being highly-nested (Rieppel, 2001), are also recovered amongst the Placochelyidae, between *Glyphoderma* and *Psephochelys* (Fig. 6.7E)

It is also worthy of note that unlike the results of Neenan et al. (2013), pachypleurosaurs are recovered as plesiomorphic within Eosauropterygia, which is the more traditional interpretation (e.g. Rieppel, 2000a).

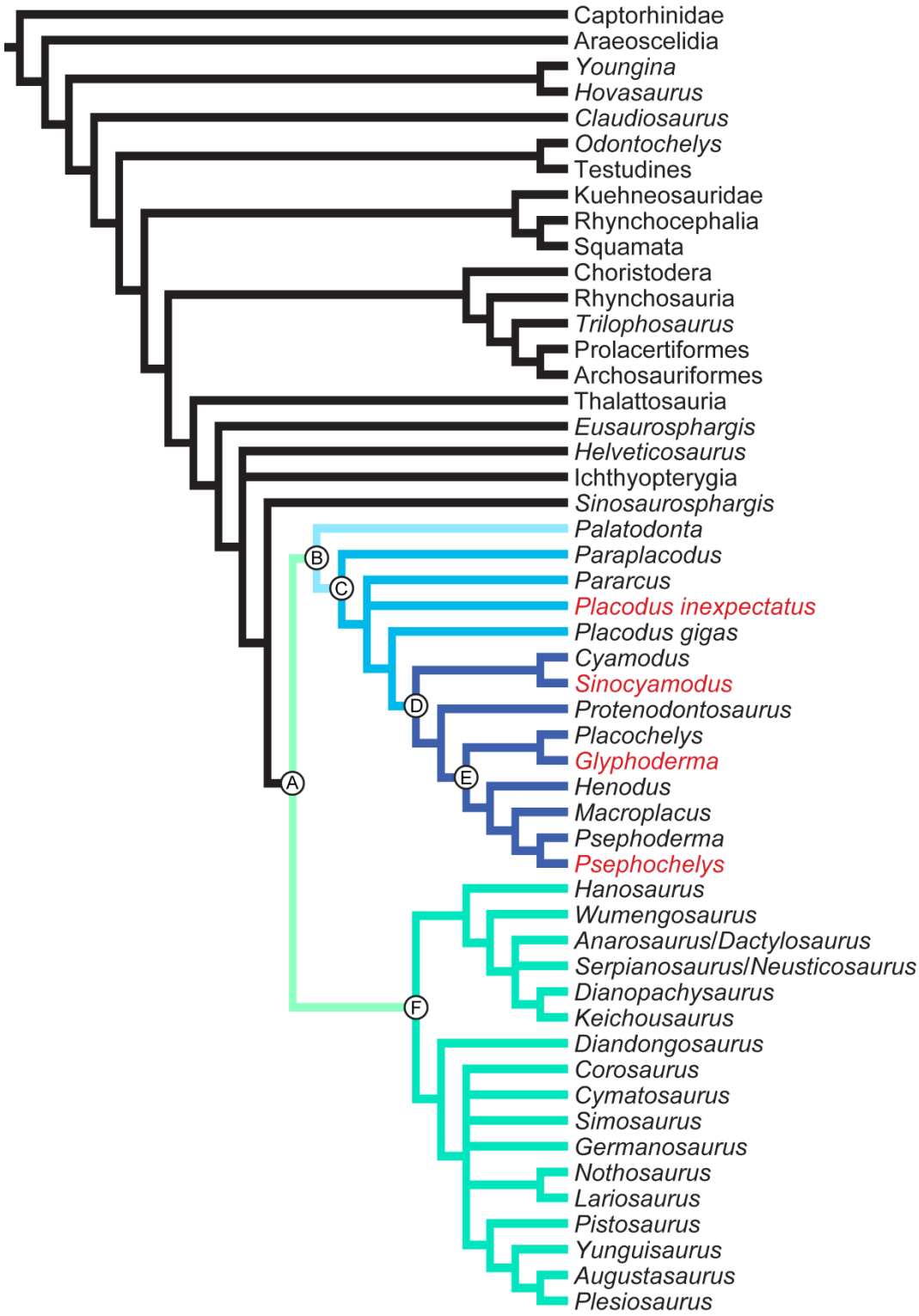

Figure 6.7. Strict consensus tree of diapsid relationships (Analysis 1), with special emphasis on Sauropterygia (A), based on a combination of cranial and postcranial characters from the matrix of Neenan et al. (2013). **A**, Sauropterygia. **B**, Placodontiformes. **C**, Placodontia. **D**, Cyamodontoidea. **E**, Placochelyidae. **F**, Eosauropterygia. Chinese placodont taxa shown in red.

Analysis 2: placodont cranial analysis

This analysis yielded 4 most parsimonious trees (MPTs), with a shortest tree length of 133 steps (CI = 0.579, RI = 0.646, RC = 0.374, HI = 0.421). Unlike Analysis 1 and the results of Rieppel (2001), Placodontoidea are recovered as a monophyletic group (Fig. 6.8C). Cyamodontoidea are once again monophyletic, however the Cyamodontida (Fig. 6.8E) show a polytomy between *Henodus*, *Sinocyamodus*, *Cyamodus hildegardis*, and a clade of the remaining two *Cyamodus* species (but see Supplementary Fig. S6.1). The topology for the European Placochelyida is similar to that of Rieppel (2001), however *Macroplacus* is now more highly nested than *Protenodontosaurus*, *Glyphoderma* has moved *Psephoderma* into a more plesiomorphic position, while *Psephochelys* appears as the most basal member of Placochelyidae.

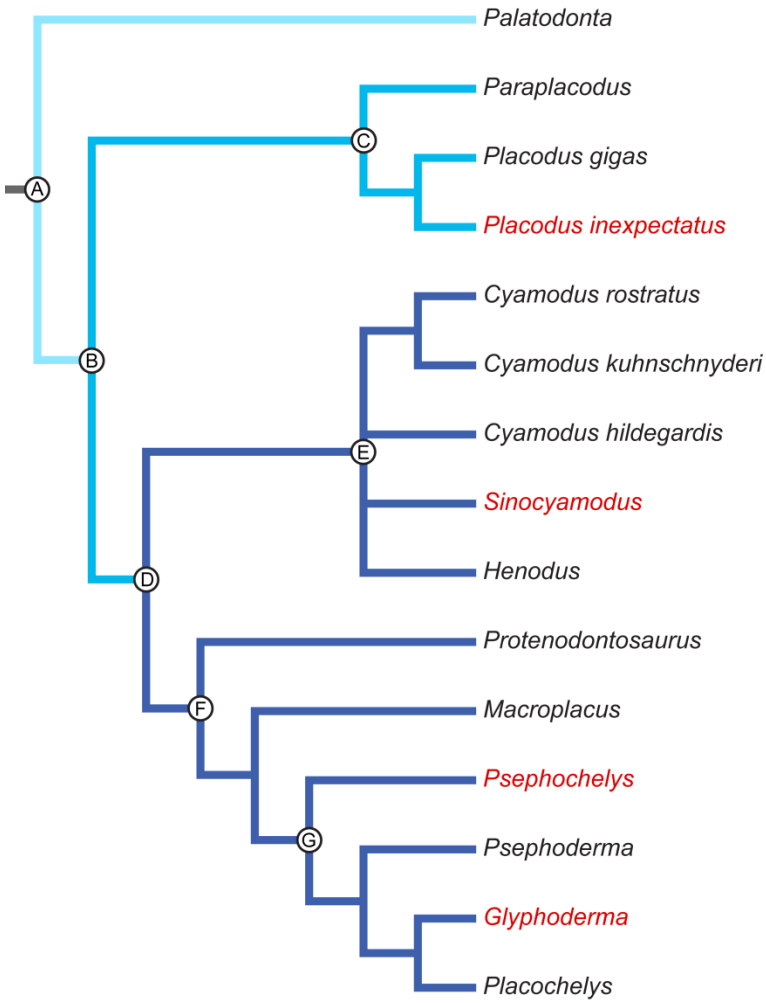

Figure 6.8. Strict consensus tree of placodont relationships (Analysis 2), based on cranial characters of Rieppel (2001), but with some additional characters from Rieppel (2000b) and Jiang et al. (2008). **A**, Placodontiformes. **B**, Placodontia. **C**, Placodontoidea. **D**, Cyamodontoidea. **E**, Cyamodontida. **F**, Placochelyida. **G**, revised Placochelyidae Chinese taxa shown in red.

5. DISCUSSION

Analyses 1 and 2 show considerably different placodont in-group relationships from each other, not to mention from the most recent published phylogenies by Rieppel (2000b, 2001) and Jiang et al. (2008). Analysis 1 shows a polyphyletic 'Placodontoidea', *Psephoderma* and *Psephochelys* to be the most highly-nested taxa, and *Henodus* and *Macroplacus* as members of the Placochelyidae. On the other hand, Analysis 2 shows a monophyletc Placodontoidea, *Glyphoderma* and *Placochelys* as the most highly nested taxa, and *Henodus* as a member of the

Cyamodontida. However the positions of the Chinese cyamodontoids *Sinocyamodus*, *Psephochelys* and *Glyphoderma* in both analyses corroborate the predictions of the authors' original descriptions: with *Sinocyamodus* clustering with *Cyamodus*, and *Psephochelys* and *Glyphoderma* with members of the Placochelyidae. Indeed, the position of *Placodus inexpectatus* as sister species to *Placodus gigas* is also supported in our analyses as well as the original one by Jiang et al. (2008). This has important palaeobiogeographic implications, as it shows that there was clear interchange of populations throughout the Middle and Late Triassic. The Placodontiformes can be interpreted to have initially evolved in the Germanic Basin and Alpine Triassic of the western Tethys (see Neenan et al. 2013 for further discussion), and then spread to the eastern Tethys. Cyamodontoid placodonts appear to have first appeared in the west as well, with *Cyamodus rostratus* and *Cyamodus hildegardis* both being known from the Anisian (early Middle Triassic) and *Sinocyamodus* not being known until the Carnian (early Late Triassic). The recovery of *Glyphoderma* (from the Ladinian, Middle Triassic) as a member of the Placochelyidae in both analyses is important, as the clade had only previously been known from the Late Triassic. This indicates that every known placodont clade originated at a time of intense speciation in the Middle Triassic, with only two genera surviving until the Rhaetian (latest Triassic): *Macroplacus* and *Psephoderma*. However it is important to note that the date of the Zhuganpo Formation (the locality from which *Glyphoderma* was found) has been argued to be at least partly Carnian (see Benton et al. 2013, for further discussion). This relatively early stratigraphic age also indicated a Chinese origin of the Placochelyidae.

The Placochelyidae was first defined by Romer (1956), with the definition being refined by Rieppel (2000a), who characterised the group as a "monophyletic taxon including the genera *Placochelys* and *Psephoderma*" (Rieppel, 2000a; pp. 34).

This was due to several cranial characteristics, but most importantly being the presence of an elongate, edentulous rostrum, and a squamosal buttress. Indeed, these features led Li and Rieppel (2002a, b) and Zhao et al. (2008) to assign *Psephochelys* and *Glyphoderma* to this clade (although it is still unclear whether the latter has a squamosal buttress). Our analyses support these conclusions, and we therefore suggest a revised Placochelyidae (Fig. 6.8G) as recovered in Analysis 2 that contains *Psephochelys*, *Psephoderma*, *Glyphoderma* and *Placochelys.* We exclude *Henodus*, despite its recovery as a member of this clade in Analysis 1, as it not only lacks these characters, but we also consider its position to be an artefact of a convergent morphology with some members of the Placochelyidae that have separated nasals (i.e. *Psephoderma* and *Psephochelys*).

The position of *Macroplacus* is of particular interest, as in both cases it clusters closer to the Placochelyidae than in previous analyses. This is not surprising, as it shares considerable morphological similarities to the clade, such as the aforementioned separated nasals, as well as a narrow rostrum with a ventral groove, similar to that seen in *Placochelys* and *Psephoderma* (this remains unclear in *Psephochelys* and unknown in *Glyphoderma*). Not to mention similar dental morphology, formula and replacement patterns to the Placochelyidae (Rieppel, 2001; Neenan et al. 2014). Although the rostrum in the only known specimen is broken, it seems highly likely that it would also be edentulous, although this remains uncertain until more specimens are described. *Macroplacus* is also the only placodont known entirely from the Rhaetian (latest Triassic), with the morphologically similar *Psephoderma* being contemporaneous, thus adding weight to the argument of a close relationship.

In Analysis 2, the polytomic relationship between *Henodus*, *Sinocyamodus*, *Cyamodus hildegardis* and the clade of remaining *Cyamodus* species in figure 6.8 is

an artefact of unclear/unknown morphology and, in the case of *Henodus* at least, highly derived morphology. However, the four most parsimonious trees on which the strict consensus tree is based are resolved in this region (Supplementary Fig. S6.1).

Judging by the different topologies, as well as the polytomies, resulting from analyses 1 and 2, it is clear that further work needs to be conducted on placodont phylogeny. µCT scanning of more specimens is necessary to clarify unclear morphology, especially in 'wildcard' taxa such as *Henodus.* New specimens of *Placodus inexpectatus* and *Glyphoderma* are also pending description by Chinese colleagues, which will increase our understanding of these taxa and thus eventually lead to a more robust placodont phylogeny in the framework of Sauropterygia.

6. CONCLUSION

In this paper we have presented the first cranial reconstructions of all Chinese placodonts, as well as thorough osteological descriptions for each holotype specimen. We also carried out the first comprehensive placodont phylogenetic analyses that include taxa from both the eastern and western Tethys. Our analyses still support a monophyletic Placodontiformes which is sister group to Eosauropterygia, however the ingroup relationships of Placodontia are still somewhat unresolved. Our results favour a sauropterygian origin in the western Tethys, with both the 'placodontoid' and cyamodontoid placodonts first appearing here. However Chinese taxa are interspersed throughout placodont phylogeny, indicating no major separation between the eastern and western faunal provinces of the Tethys. The revised Placochelyidae are the most highly nested and geologically most long-lived placodont clade, having first appeared in the Middle Triassic, and not the Late Triassic as previously thought. The early stratigraphic position of *Glyphoderma* supports a Chinese placochelyid origin.

The use of µCT data has complemented gross anatomical observations in this study, particularly with the Chinese holotypes of *Psephochelys* and *Sinocyamodus*, where unclear/obscured morphologies were revealed. Future work should focus on using µCT scanning on the remaining Chinese placodont taxa to strengthen phylogenetic relationships.

7. AUTHOR CONTRIBUTIONS

TMS and JMN designed the research and examined specimens in China together. JMN carried out model segmentation, osteological descriptions, skull reconstructions, phylogenetic analyses and wrote the manuscript. TMS, CL, D-YJ and OR provided expert knowledge and advice. CL and DY-J provided permission and access for the examination of specimens, and CL facilitated the CT scanning process at the IVPP. TMS supervised the project.

8. ACKNOWLEDGEMENTS

We are very grateful to Dr. Zhao Li-Jun (ZMNH) for allowing access to specimens and hosting us in Hangzhou, as well as Hou Yemao (IVPP) for assisting with CT scanning. TMS and JMN are also thankful for the hospitality of both the IVPP and Peking University during their research stays in China. Additional thanks to Prof. Dr. Marcelo Sánchez and all the members of PIMUZ, Zurich for useful discussions and advice. This work was funded by the Swiss National Science Foundation (grant 31003A 146440 to TMS).

9. REFERENCES

Benton, M. J., Q.-Y. Zhang, S. Hu, Z.-Q. Chen, W. Wen, J. Liu, J. Huang, C.-Y. Zhou, T. Xie, J. Tong, and B. Choo. 2013. Exceptional vertebrate biotas from the Triassic of China, and the expansion of marine ecosystems after the Permo-Triassic mass extinction. *Earth Science Reviews*. (doi:10.1016/j.earscirev.2013.05.014).

Calendini, F., and J.-F. Martin. 2005. PaupUP v1.0.3.1 A free graphical frontend for Paup* Dos software.

Edinger, T. 1925. Das Zentralnervensystem von *Placodus gigas* Ag. *Abhandlungen der Senckenbergischen Naturforschenden Gesellschaft* 38:311-318.

Huene, F. v. 1956. *Paläontologie und Phylogenie der Niederen Tetrapoden*. Gustav Fisher Verlag, Jena, 716 pp.

Jiang, D.-Y., R. Motani, W.-C. Hao, O. Rieppel, Y.-L. Sun, L. Schmitz, and Z.-Y. Sun. 2008. First record of Placodontoidea (Reptilia, Sauropterygia, Placodontia) from the Eastern Tethys. *Journal of Vertebrate Paleontology* 28:904-908.

Klein, N., and T. M. Scheyer. In press. A new placodont sauropterygian from the Middle Triassic of the Netherlands. *Acta Palaeontologica Polonica*. (doi:10.4202/app.2012.0147).

Li, C. 2000. Placodont (Reptilia: Placodontia) from Upper Triassic of Guizhou, Southwest China. *Vertebrata PalAsiatica* 38:314-317.

Li, C., and O. Rieppel. 2002a. A new cyamodontoid placodont from Triassic of Guizhou, China. *Chinese Science Bulletin* 47(2):156-159.

Li, C., and O. Rieppel. 2002b. A new cyamodontoid placodont from Triassic of Guizhou, China. *Chinese Science Bulletin* 47(5):403-407.

Liu, J., O. Rieppel, D.-Y. Jiang, J. C. Aitchison, R. Motani, Q.-Y. Zhang, C.-Y. Zhou, and Y.-Y. Sun. 2011. A new pachypleurosaur (Reptilia: Sauropterygia) from the Lower Middle Triassic of Southwestern China and the phylogenetic telationships of Chinese pachypleurosaurs. *Journal of Vertebrate Paleontology* 31:292-302.

Maddison, W. P., and D. R. Maddison. 2011. Mesquite: a modular system for evolutionary analysis. Version 2.75 http://mesquiteproject.org.

Motani, R. 2009. The evolution of marine reptiles. *Evolution: Education and Outreach* 2:224-235.

Neenan, J. M., and T. M. Scheyer. 2012. The braincase and inner ear of *Placodus gigas* (Sauropterygia, Placodontia) – a new reconstruction based on micro-computed tomographic data. *Journal of Vertebrate Paleontology* 32:1350-1357.

Neenan, J. M., N. Klein, and T. M. Scheyer. 2013. European origin of placodont marine reptiles and the evolution of crushing dentition in Placodontia. *Nature Communications* 4:1621. (doi:10.1038/ncomms2633).

Neenan, J. M., C. Li, O. Rieppel, F. Bernardini, C. Tuniz, G. Muscio, and T. M. Scheyer. 2014. Unique method of tooth replacement in durophagous placodont marine reptiles, with new data on the dentition of Chinese taxa. *Journal of Anatomy* 224:603-613.

Nosotti, S., and G. Pinna. 1996. Osteology of the skull of *Cyamodus kuhnschnyderi* Nosotti & Pinna 1993 (Reptilia, Placodontia). *Paleontologia Lombarda N. S.* 6:1-42.

Nosotti, S., and O. Rieppel. 2002. The braincase of *Placodus* Agassiz, 1833 (Reptilia, Placodontia). *Memoire della Società Italiana di Scienze Naturali e del Museo Civico di Storia Naturale di Milano* 31:3-18.

Pinna, G., and S. Nosotti. 1989. Anatomia, morfologia funzionale e paleoecologia del rettile placodonte *Psephoderma alpinum* Meyer, 1858. *Memoire della Società Italiana di Scienze Naturali e del Museo Civico di Storia Naturale di Milano* 25:17-50.

Reif, W.-E., and F. Stein. 1999. Morphogeny and function of the dentition of *Henodus chelyops* Huene, 1936 (Placodontia, Triassic). *Neues Jahrbuch für Geologie und Paläontologie, Monatshefte* 2:65-80.

Rieppel, O. 1995. The genus *Placodus*: systematics, morphology, paleobiogeography, and paleobiology. *Fieldiana: Geology, New Series* 31:1-44.

Rieppel, O. 1999. Phylogeny and paleobiogeography of Triassic Sauropterygia: problems solved and unresolved. *Palaeogeography, Palaeoclimatology, Palaeoecology* 153:1-15.

Rieppel, O. 2000a. Sauropterygia I - Placodontia, Pachypleurosauria, Nothosauroidea, Pistosauroidea; pp. 134 in P. Wellnhofer (ed.), *Encyclopedia of Paleoherpetology*. Verlag Dr. Friedrich Pfeil, Munich.

Rieppel, O. 2000b. *Paraplacodus* and the phylogeny of the Placodontia (Reptilia: Sauropterygia). *Zoological Journal of the Linnean Society* 130:635-659.

Rieppel, O. 2001. The cranial anatomy of *Placochelys placodonta* Jaekel, 1902, and a review of the Cyamodontoidea (Reptilia, Placodonta). *Fieldiana: Geology, New Series* 45:1-104.

Rieppel, O., and H. Hagdorn. 1997. Paleobiogeography of Middle Triassic Sauropterygia in central and western Europe; pp. 121-144 in J. M. Callaway and E. L. Nicholls (eds.), *Ancient Marine Reptiles*. Academic Press, San Diego, California.

Romer, A. S. 1956. Osteology of the reptiles. University of Chicago Press, Chicago, 772 pp.

Sues, H.-D. 1987. On the skull of *Placodus gigas* and the relationships of the Placodontia. *Journal of Vertebrate Paleontology* 7:138-144.

Swofford, D. L. 2003. PAUP*. Phylogenetic Analysis Using Parsimony (*and Other Methods). Version 4. Sinauer Associates, Sunderland, Massachusetts.

Zhao, L.-J., C. Li, J. Liu, and T. He. 2008. A new armored placodont from the Middle Triassic of Yunnan Province, southwestern China. *Vertebrata PalAsiatica* 46:171-177.

SUPPLEMENTARY INFORMATION FOR:

The cranial anatomy of Chinese placodonts and the phylogeny of Placodontia

James M. Neenan, Chun Li, Da-Yong Jiang, Olivier Rieppel, Torsten M. Scheyer

CONTENTS:

1. Supplementary Figure

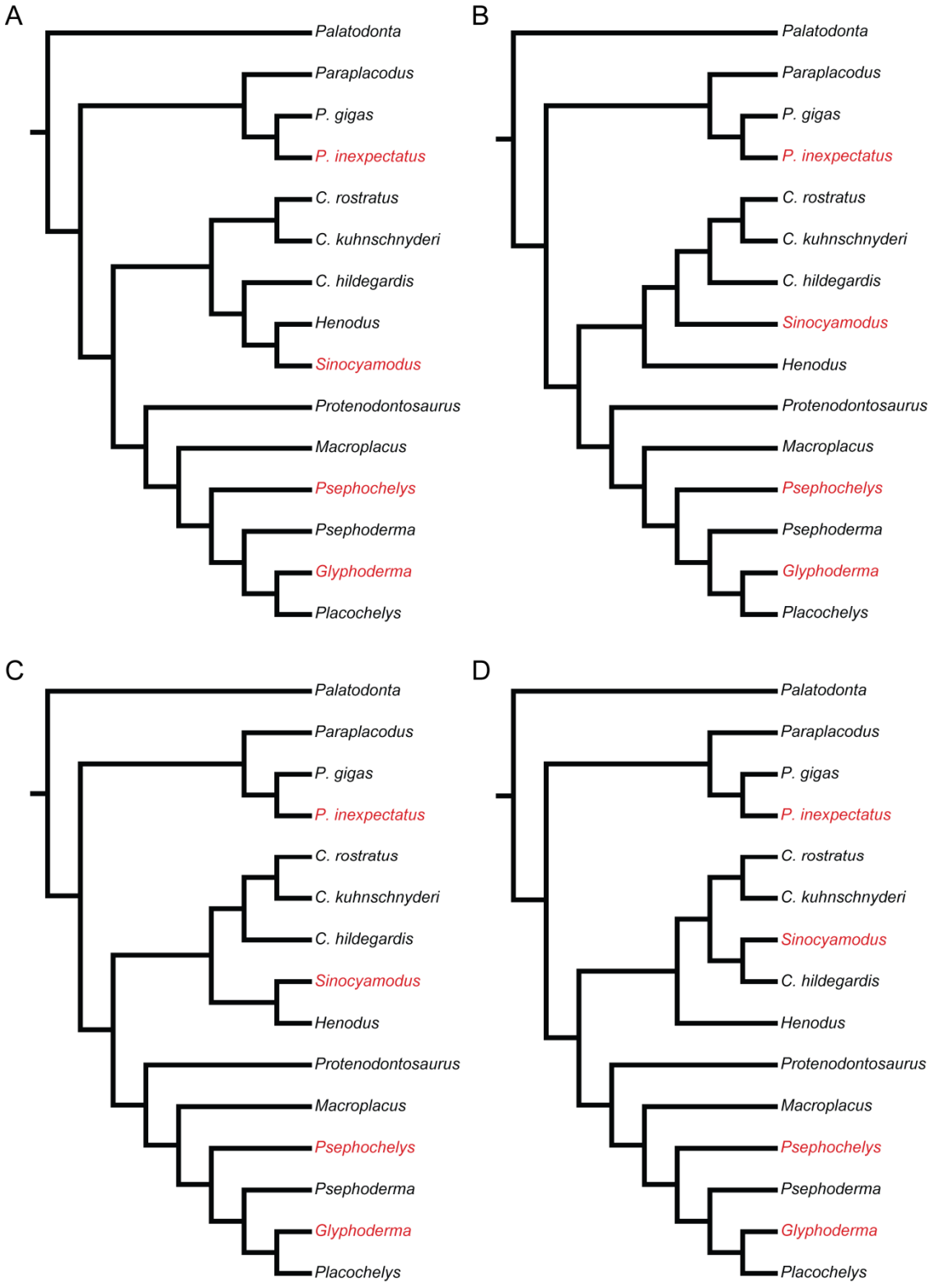

Supplementary Figure S6.1. The four most parsimonious trees from Analysis 2. **A**, tree 1. **B**, tree 2. **C**, tree 3. **D**, tree 4. Note that the topology is identical in every tree with the exception of the relationships between *C. hildegardis*, *Henodus* and *Sinocyamodus*. Chinese taxa shown in red.

2. Phylogenetic Character Descriptions

2.1 Analysis 1: Comprehensive diapsid analysis

Characters were taken directly from Neenan et al. (2013), which in turn were modified from Liu et al. (2011). The original matrix was constructed by Rieppel et al. (2002), and for reference, the original characters from this paper are given in parentheses (e.g. R1, R2, etc.). The scoring follows that of Neenan et al. (2013), apart from *Pararcus*, which was coded by Klein and Scheyer (in press), and the remaining new placodont taxa (i.e. *Placodus inexpectatus*, *Sinocyamodus*, *Glyphoderma*, *Henodus*, *Protenodontosaurus*, *Macroplacus* and *Psephochelys*).

(1) Bones in dermatocranium: distinctly sculptured (0); relatively smooth (1). (From Rieppel and Lin, 1995).

(2) Preorbital and postorbital region of skull: of subequal length (0); preorbital region distinctly longer (1); postorbital region distinctly longer (2). (R12)

(3) Snout: relatively short (0); elongated with broad anterior termination (1); elongated and tapering anteriorly (2). (R132)

(4) Distinct snout constriction in adult: absent (0); present (1). (R3)

(5) Premaxillae: small (0); large, forming most of snout in front of external nares (1). (R1)

(6) Postnarial process of premaxilla: absent (0); present, excluding maxilla from posterior margin of external naris (1). (R2)

(7) External nares: not retracted (0); retracted with a longitudinal diameter approaching or exceeding half the longitudinal diameter of orbit (1); retracted, narrow, and with a longitudinal diameter distinctly less than half the longitudinal diameter of orbit (2). (R133)

(8) Nasal(s): shorter than frontal(s) (0); longer than frontal(s) (1). (R5)

(9) Nasal(s): not reduced (0); reduced (1); absent (2). (R6)

(10) Nasal(s): meeting in dorsomedial suture (0); fused (1); seperated from one another by nasal processes of premaxillae extending back to frontal(s) and/or anterior processes of the frontals (2). (R8), this character has been changed to include the fact that the frontals may also extend anteriorly to separate the nasals.

(11) Lacrimal: present, entering external naris (0); present, excluded from external naris (1); (2) absent. (R9)

(12) Dorsal exposure of prefrontal: large (0); reduced (1). (R11)

(13) Prefrontal: without slender anteromedial process (0); with slender anteromedial process entering between maxilla and premaxilla (1). (R121)

(14) Frontal: participating in the formation of dorsal margin of orbit (0); excluded from dorsal margin of orbit by a contact of prefrontal and postfrontal (1). (R10)

(15) Frontal(s) in adult: paired (0); fused (1). (R14)

(16) Distinct posterolateral processes of frontal(s): (0) absent; (1) present. (R15)

(17) Frontal: widely separated from upper temporal fossa (0); narrowly approaching upper temporal fossa (1); entering the anteromedial margin of upper temporal fossa (2). (R16)

(18) Postfrontal: large and plate-like (0); with distinct lateral process overlapping the dorsal tip of postorbital (1); with reduced lateral process and hence more of an elongate shape (2). (R26)

(20) Jugal: extending backwards no farther than to the middle of cheek region (0); extending nearly to the posterior end of skull (1). (R24)

(21) Jugal: excluded from upper temporal arch (0); entering upper temporal arch (1). (R25)

(22) Parietal(s) in adult: paired (0); fused in their posterior part only (1); fully fused (2). (R17); *Wumengosaurus*: following Wu et al.[16], score changed from (2) to (0), as parietals are paired in adults and not fully fused.

(23) Parietal skull table: broad (0); weakly constricted (1); strongly constricted (at least posteriorly) (2); forming a sagittal crest (3). (R19)

(25) Postparietals: present (0); absent (1). (R20)

(26) Tabulars: present (0); absent (1). (R21)

(28) Temporal region of skull: relatively high (0); strongly depressed (1). (R4)

(29) Upper temporal fossa: absent (0); present and subequal in size or slightly larger than orbit (1); present and distinctly larger than orbit (2); present and distinctly smaller than orbit (3); secondarily closed (4). (R13)

(30) The anteromedial corner of upper temporal fossa: not (0); partially (1); (2) fully floored by a descensus from postorbital, which together with neighbouring elements (postfrontal, parietal) separates it from orbit. (R122)

(31) Lower temporal fossa: absent (0); present and closed ventrally (1); present but open ventrally (2). (R27)

(32) Squamosal: descending to ventral margin of skull (0); broadly separated from ventral margin of skull (1). (R28)

(33) A box-like suspensorium of squamosal: absent (0); present (1). (R123)

(34) Distinct notch of squamosal to receive distal tip of paroccipital process: absent (0); present (1). (R32)

(35) Quadratojugal: present (0); absent (1). (R29)

(36) Anterior process of quadratojugal: present (0); absent (1). (R30)

(37) Quadrate: covered by squamosal and quadratojugal in lateral view (0); exposed in lateral view (1). (R38)

(38) Posterior margin of quadrate: straight (0); concave (1). (R37)

(39) Lateral conch on quadrate: absent (0); present (1). (R40)

(40) Dorsal wing of epipterygoid: approximately as broad as its base (0); narrower than its base (1). (R39)

(41) Braincase: located at posterior end (0); deeply recessed below parietal skull roof (or parietal sagittal crest) (1). (R124)

(42) Occipital crest: absent (0); present but squamosals not meeting behind parietal (1); present and squamosals meeting behind parietal (2). (R36)

(43) Occiput: with paroccipital process forming the lower margin of posttemporal fossa and extending laterally (0); paroccipital processes trending posteriorly (1); plate-like with no distinct paroccipital process and with strongly reduced posttemporal fossae (2). (R31)

(44) Mandibular articulations: approximately at level with occipital condyle (0); displaced to a level distinctly behind occipital condyle (1); positioned anterior to occipital condyle (2). (R33)

(45) Supraoccipital: exposed more or less vertically on occiput (0); exposed more or less horizontally at posterior end of parietal skull table (1); U-shaped (2). (R35)

(46) Contact between exoccipitals and basioccipital condyle: present (0); absent (1). (R34)

(47) Basioccipital tubera: free (0); in complex relation to pterygoid, as they extend ventrally (1); in complex relation to pterygoid, as they extend laterally (2). (R42)

(48) Palate: kinetic (0); akinetic (1). (R41)

(49) Premaxillae: entering internal naris (0); excluded from internal naris (1). (R45)

(50) Posterior palatine vacuities: absent (0); present (1). (R125)

(51) Pterygoids: longer than palatines (0); shorter than palatines (1). (R130)

(52) Pterygoid flanges: well developed and transversely oriented (0); well developed and longitudinally oriented (1); strongly reduced (2). (R44)

(53) Ectopterygoid: present (0); absent (1). (R46)

(54) Suborbital fenestra: absent (0); present (1). (R43)

(55) Internal carotid passage: entering basicranium (0); entering quadrate ramus of pterygoid (1). (R47)

(56) Splenial bone: entering mandibular symphysis (0); excluded therefrom (1). (R52)

(57) Distinct coronoid process of lower jaw: absent (0); present (1). (R49)

(58) Strongly projecting lateral ridge of surangular defining the insertion area for superficial adductor muscle fibers on the lateral surface of lower jaw: absent (0); present (1). (R50)

(59) Mandibular symphysis: short (0); somewhat enforced (1); elongated and 'scoop-like' (2). (R51)

(60) Retroarticular process of lower jaw: absent (0); present (1). (R48)

(61) Trough on dorsal surface of retroarticular process: absent (0); present (1). (From Rieppel and Lin, 1995).

(62) Teeth: setting in shallow or deep sockets (0); superficially attached to bone (1). (R53)

(63) Durophagous dentition: absent (0); present (1). (R128)

(64) Number of premaxillary teeth: four or more (0); three or less (1); modified into a single row of denticles (2). (R129); character state (2) was added here to more accurately describe the condition in *Henodus*.

(65) Anterior (premaxillary and dentary) teeth: upright or only sightly procumbent (0); strongly procumbent (1); absent (2). (R54); character state (2) was added here to more accurately describe the anterior dentition of placochelyid placodonts.

(66) Premaxillary and anterior dentary fangs: absent (0); present (1). (R55)

(67) One or two enlarged teeth on maxilla: present (0); absent (1). (R56)

(68) Maxillary tooth row: restricted to a level in front of the posterior margin of orbit (0); extending backwards to a level below the posterior corner of orbit and/or the anterior corner of upper temporal fossa (1); extending backwards to a level below the anterior one third to one half of upper temporal fossa (2). (R57)

(69) Teeth on pterygoid flange: present (0); absent (1). (R58)

(70) Vertebrae: notochordal (0); non-notochordal (1). (R59)

(71) Vertebrae: amphicoelous (0); platycoelous (1); or other (2). (R60)

(72) Vertebral centrum: distinctly constricted in ventral view (0); with parallel lateral edges (1). (R67)

(73) Subcentral foramina: absent (0); present (1). (R127)

(74) Zygosphene-zygantrum articulation: absent (0); present (1). (R64)

(75) Zygapophyseal pachyostosis: absent (0); present (1). (R69)

(76) Number of cervical vertebrae: less than 30 (0); more than 30 (1). (R134)

(77) Cervical centra: rounded ventrally (0); keeled ventrally (1). (R63)

(78) Parapophysis: not shifting backwards on centrum along cervical vertebral column (0); shifting backwards on centrum along cervical vertebral column (1). (R135)

(79) Cervical intercentra: present (0); absent (1). (R62)

(80) Distal articular surface on transverse processes of dorsal vertebrae: oblong (0); evenly rounded (1). (R136)

(81) Transverse processes of neural arches in dorsal region: relatively short (0); distinctly elongated (1). (R66)

(82) Distal end of transverse processes of dorsal vertebrae: not increasing in diameter (0); distinctly thickened (1). (R68)

(83) Sutural facets receiving pedicels of neural arch on dorsal surface of centrum in dorsal region: narrow (0); expanded into a cruciform or ‘butterfly-shaped’ platform (1). (R65)

(84) Dorsal intercentra: present (0); absent (1). (R61)

(85) Anteroposterior trend of increasing inclination of pre- and postzygapophyses within dorsal and sacral region: absent (0); present (1). (R70)

(86) A distinct free anterior process of cervical ribs: absent (0); present (1). (R71)

(87) Pachyostosis of dorsal ribs: absent (0); present (1). (R72)

(88) Number of sacral ribs: two (0); three (1); four or more (2). (R73); *Sinocyamodus* and *Glyphoderma* are coded as (1), despite the original descriptions stating they each have 4 sacrals. They in fact have 3.

(89) Distinct expansion of distal head of sacral ribs: present (0); absent (1). (R74)

(90) Sacral (and caudal) ribs or transverse processes and their respective centrum: sutured (0); fused (1). (R75)

(91) Mineralized sternum: absent (0); present (1). (R118); *Cyamodus*: changed from (?) in Liu et al.[10] to (0).

(92) Median gastral element: angulated (0); straight (1). (R131)

(93) The medial gastral rib element: with a single lateral process (0); with two-pronged lateral process (1). (R119)

(94) Cleithrum: present (0); absent (1). (R76)

(95) Clavicles: broad medially (0); narrow medially (1). (R77)

(96) Clavicles: not meeting in front of interclavicle (0); meeting in an interdigitating anteromedial suture (1). (R79)

(97) Anterolaterally expanded corners of clavicles: absent (0); present (1). (R80)

(98) Clavicle: applied to anterior (lateral) surface of scapula (0); applied to medial surface of scapula (1). (R81)

(99) Relationship between clavicles and interclavicle: in simple overlapping contact (0); anteromedioventral end of clavicle embracing lateral tip of interclavicle in a complex contact (1). (R78)

(100) Interclavicle: rhomboidal (0); T-shaped (1). (R82)

(101) Posterior process on (T-shaped) interclavicle: elongate (0); short (1); rudimentary or absent (2). (R83)

(102) Scapula: represented by a broad blade of bone (0); with a constriction separating a ventral glenoidal portion from a posteriorly directed dorsal wing (1); rod-like (2). (R84)

(103) Dorsal wing or process of eosauropterygian scapula: tapers to a blunt tip (0); ventrally expanded at its posterior end (1). (R85)

(104) Supraglenoid buttress: present (0); absent (1). (R86)

(105) Number of coracoid ossifications: one (0); two (1). (R87)

(106) Coracoid: of rounded contours (0); slightly waisted (1); strongly waisted (2); with expanded medial symphysis and ridge-like thickening of the bone extending from glenoid facet posteriorly along lateral edge of the bone, coracoid foramen not enlarged (3); with expanded medial symphysis and ridge-like thickening of the bone extending from glenoid facet transversely through the bone, coracoid foramen much enlarged (4). (R88)

(107) Coracoid foramen: enclosed by coracoid ossification (0); between coracoid and scapula (1). (R89)

(108) Pectoral fenestration: absent (0); present (1). (R90)

(109) Limbs: short and stout (0); long and slender (1). (R91); *Psephochelys* coded from Wang et al. (2008).

(110) Foot: short and broad (0); long and slender (1). (R112); *Psephochelys* coded from Wang et al. (2008).

(111) Humerus: rather straight (0); ‘curved’ (1). (R92); *Psephochelys* coded from Wang et al. (2008).

(112) Deltopectoral crest: well developed (0); reduced (1); absent (2). (R93)

(113) Insertional crest for latissimus dorsi muscle: prominent (0); reduced (1). (R94)

(114) Epicondyles of humerus: prominent (0); reduced (1). (R95)

(115) Ectepicondylar groove: open and notched anteriorly (0); open without anterior notch (1); closed (2); absent (3). (R96)

(116) Entepicondylar foramen: present (0); absent (1). (R97)

(117) Radius: shorter than ulna (0); longer than ulna (1); approximately of same length (2). (R98); *Psephochelys* coded from Wang et al. (2008).

(118) Distal end of ulna: not expanded (0); distinctly expanded to at least the width of the proximal part (1). (R126)

(119) Total number of carpal ossifications: more than three (0); three (1); two (2). (R137)

(121) Pubis: with convex ventral (medial) margin (0); with concave ventral (medial) margin (1). (R100)

(122) Obturator foramen in adult: closed (0); open or absent (1). (R101)

(123) Thyroid fenestra: absent (0); present (1). (R102)

(124) Acetabulum: oval (0); circular (1). (R103)

(125) Femoral shaft: stout and straight (0); slender and sigmoidally curved (1). (R104); *Psephochelys* coded from Wang et al. (2008).

(128) Distal femoral condyles: prominent (0); not projecting markedly beyond shaft (1). (R107)

(130) Total number of tarsal ossifications: four or more (0); three (1); two or less (2). (R115)

(131) Perforating artery: passes between astragalus and calcaneum (0); between distal heads of tibia and fibula proximal to astragalus (1). (R109)

(132) Proximal concavity of astragalus: absent (0); present (1). (R110)

(133) Calcaneal tuber: absent (0); present (1). (R111)

(134) Distal tarsal 1: present (0); absent (1). (R113)

(135) Distal tarsal 5: present (0); absent (1). (R114)

(136) Metatarsal 5: long and slender (0); distinctly shorter than other metatarsals and with a broad base (1). (R116)

(137) Metatarsal 5: straight (0); ‘hooked’ (1). (R117)

(138) Dermal armour ("osteoderms"): absent (0); present (1); forming single carapace, excluding endoskeletal elements (2); same as (2) but forming distinctly separate dorsal and pelvic carapaces; forming carapace, including endoskeletal elements (4). Note: this character has been changed to include the fact that some placodont taxa have a separate pelvic carapace.

(139) Distinctly open L-shaped (boomerang-shaped) jugal: absent (0); present (1).

(140) Palatine dentition: multiple rows with small numerous teeth/denticles (0); single row with four or more teeth (1), single row with three to one teeth/tooth (2); absent (3).

2.2 Analysis 2: Placodont cranial analysis

The majority of characters for this analysis were taken directly from Rieppel (2001) (characters 1–54). Additional cranial characters (55–61) were taken from Rieppel (2000), however this was originally a genus-level phylogeny, so the three *Cyamodus* species are herein encoded. Characters 62 and 63 were taken from Jiang et al. (2008). *Palatodonta* was added to this matrix, as well as the Chinese placodont taxa. Note, while this is referred to as a cranial analysis, there are in fact two postcranial characters (1 and 63) that help to give additional resolution to the resulting trees.

(1) Osteoderms absent (0); osteoderms present (1); carapace present (2).

(2) Dividing the total length of the skull by the total height of the skull yields a ratio smaller (0) or larger (1) than 3.

(3) Rostrum relatively short and broad (0), narrow and distinctly elongated (1), or spatulate (2). Changed *Macroplacus* from 0 to ? as the shape of the rostrum is unknown.

(4) The ventral surface of the premaxilla is level with the ventral surface of the maxilla (0) or the rostrum is distinctly downturned (1). Changed *Henodus* from ? to 1 as the rostrum is distinctly downturned.

(5) The premaxilla extends backward for more (0) or less (1) than half of the length of the ventral margin of the external naris. Changed *Psephoderma* from ? to 1 due to observations from new specimen PIMUZ A/III 1491.

(6) Nasals in contact along midline of skull (0) or separated from one another by large posterior (nasal) processes of the premaxilla and/or anterior processes of the frontal. (1). This character has been changed from the original to include “and/or anterior processes of the frontal” to better describe the morphology of some placodonts.

(7) Anterior end of maxilla does not (0) or does (1) expand medially to form most of the dermal floor of the external naris. Changed *Psephoderma* from ? to 1 due to observations from new specimen PIMUZ A/III 1491.

(8) Anterior tip of the jugal does (0) or does not (1) extend anteriorly along the ventral margin of the orbit beyond the midpoint of the longitudinal diameter of the orbit. Changed *Psephoderma* from ? to 0 due to observations from new specimen PIMUZ A/III 1491.

(9) The jugal does not (0) or does (1) extend backward along the anteromedial margin of the subtemporal fossa.

(10) Pineal foramen placed in centre of parietal skull table (0), displaced anteriorly on parietal skull table (1) or is displaced anteriorly with frontal entering its anterior margin (2). Changed *Psephoderma* from 2 to 1&2 due to observations from new specimen PIMUZ A/III 1491.

(11) Anterolateral processes of frontals well developed (0) or reduced (1).

(12) Parietal without (0) or with (1) distinct an anterolateral processes embraced by postfrontal and frontal.

(13) Frontals do not (0) or do (1) reach posteriorly beyond the level of the anterior margin of the upper temporal fossa.

(14) Parietal skull table constricted in its posterior part (i.e., with concave lateral margins) (0) or square (i.e., with straight lateral margins in its posterior part) (1).

(15) Posterolateral margin of postfrontal weakly concave and evenly curved (0) or deeply concave and angulated (1). Changed *Macroplacus* from ? to 0.

(16) Postfrontal enters upper temporal fossa (0) is excluded from upper temporal fossa by a narrow (1), or broad (2) contact of the postorbital with the parietal. Changed *Macroplacus* from ? to 1.

(17) Postorbital extends along lateral margin of temporal fossa to a level in front of or at the midpoint of the longitudinal diameter of the upper temporal fossa (0) or further back (1).

(18) The vertical part of the suture separating the maxilla from the jugal is located behind the level of the posterior margin of the orbit (0), behind the level of the midpoint of the longitudinal diameter of the orbit but in front of the posterior margin of the latter (1), or at the level of the midpoint of the longitudinal diameter of the orbit (2).

(19) Dorsal process of the epipterygoid is narrow (0) or broad (1).

(20) Base of the epipterygoid is sutured predominantly to the pterygoid (0) or to the palatine (1).

(21) The postorbital does not (0) or does (1) form a medioventral process, which abuts against the lateral surface of the epipterygoid at the posterodorsal margin of the foramen interorbitale.

(22) Dividing the basicranial length (tip of snout to occipital condyle) by the transverse diameter of the upper temporal fossa yields a ratio which is larger (0) or smaller (1) than 3.

(23) Dividing the longitudinal diameter of the upper temporal fossa by the longitudinal diameter of the orbit yields a ratio that is smaller (0) or equal or larger (1) than 2 (in the adult). The subadult condition of *Sinocyamodus* is only speculative, so it was coded as (0).

(24) The epipterygoid does not (0) or does (1) form a posterior dorsal process that contacts the squamosal at the anterodorsal comer of posttemporal fossa.

(25) The epipterygoid is always fully ossified in the adult (0) or may be incompletely ossified in the adult (1).

(26) The (neomorph) otic process of the squamosal is absent (0), extends to the midpoint of the ventral margin of the posttemporal fossa (1), or extends beyond the level of the medial margin of the posttemporal fossa (2) (in lateral view of the skull). Changed *Psephoderma* from ? to 1 due to observations from new specimen PIMUZ A/III 1491.

(27) A palatoquadrate cartilage recess is absent (0) or present (1).

(28) A basiorbital furrow is absent (0) or present (1).

(29) The palatine does not (0) or does (1) contact the quadrate along the lateral margin of the palatoquadrate cartilage recess.

(30) The pteroccipital foramen is absent (0) or present (1).

(31) The prootic is not (0) or is (1) exposed in occipital view of the skull.

(32) Premaxillary teeth are present (0) or absent (1).

(33) Anterior premaxillary and dentary teeth pointed (0), chisel-shaped (I), or bulbous with anterior transverse ridge (2).

(34) A diastema separating premaxillary and maxillary teeth is absent (0) or present (I).

(35) Four or more (0), three (1), two (2), one (3), or no (4) maxillary teeth (tooth).

(36) More than three (0), three (1), two (2) or one (3) pair(s) of palatine teeth.

(37) Anterior palatal tooth plate(s) small and rounded (0), or transversely enlarged (1).

(38) The ratio of the longitudinal to the transverse diameter of the posterior palatine tooth plate less (0)- or equal or more (1) than 1.4 (in theadult). The subadult condition of *Sinocyamodus* is only speculative, so it was coded as (1).

(39) Maxilla without (0) or with (1) anterior process extending into rostrum in ventral view.

(40) Ventral surface of rostrum flat (0) or concave (1).

(41) Ventral surface of rostrum without (0) or with distinct grooves leading up to internal nares (1).

(42) Internal nares separated (0) or confluent (1).

(43) Ectopterygoid present (0) or absent; if absent, palatine extends laterally at the anterior margin of the subtemporal fossa to meet the jugal (1) or jugal extends medially to meet the palatine (2).

(44) The ratio of the length of palatal exposwe of pterygoid relative to length of palatine is less (0) or more (I) than 0.3.

(45) The ventral pterygoid flange has a single (0) or a double (1) ventral projection.

(46) The postemporal fossae are relatively large (0) or reduced (1) because of expansion of occipital exposure of parietal, squamosal, and opisthotic.

(47) The squamosal buttress against which abuts the distal tip of the paroccipital process is absent (0) or present (1).

(48) The posteroventral tubercle is absent (0) or present (1) at the distal tip of the patoccipital process.

(49) The exoccipitals do not (0) or do (1) meet above occipital condyle (above the basioccipital).

(50) The basioccipital tuber and the ventral opisthotic flange remain separate (0) or meet each other (1) ventral to passage of internal carotid.

(51) Anterior tip of dentary with teeth (0) or edentulous (1).

(52) The coronoid remains well separated from lower margin of the mandible (0) or closely approaches the lower margin of mandible (1).

(53) The retroarticular process is long and slender (0) or short with a sloping surface (1).

(54) Tubercular osteoderms, secondarily fused to the underlying bone, are absent (0), present along the posterior margin of the upper temporal fossa only (1), or present on lateral sur face of posterior part of temporal arch also (2).

(55) Quadratojugal present (0), or absent (1). (from Rieppel, 2000, character 52).

Note: this was coded the wrong way around in the original matrix of Rieppel (2000) but has now been corrected.

(56) Jugal–squamosal contact absent (0), or present (1). (from Rieppel, 2000, character 53)

(57) Coronoid process absent (0), distinct but low (1), or very high (2). (from Rieppel, 2000, character 54)

(58) Crushing tooth plates absent (0), or present (1). (from Rieppel, 2000, character 63)

(59) Diastema between symphyseal and posterior dentary teeth absent (0), or present (1). (from Rieppel, 2000, character 64)

(60) Palatines separated by pterygoids (0), or meeting in medial suture (1). (from Rieppel, 2000, character 65)

(61) Pterygoids longer (0), or shorter (1), than palatines. (from Rieppel, 2000, character 66)

(62) External naris not distinctly higher than long (0); distinctly higher than long (1). (from Jiang et al, 2008, character 68)

(63) Chevron morphology simple, y-shaped (0); complex as described by Rieppel (2000) for *Paraplacodus* (1). (from Jiang et al, 2008, character 69)

3. References

Jiang, D.-Y., R. Motani, W.-C. Hao, O. Rieppel, Y.-L. Sun, L. Schmitz, and Z.-Y. Sun. 2008. First record of Placodontoidea (Reptilia, Sauropterygia, Placodontia) from the Eastern Tethys. *Journal of Vertebrate Paleontology* 28:904-908.

Klein, N., and T. M. Scheyer. In press. A new placodont sauropterygian from the Middle Triassic of the Netherlands. *Acta Palaeontologica Polonica*. (doi:10.4202/app.2012.0147).

Liu, J., O. Rieppel, D.-Y. Jiang, J. C. Aitchison, R. Motani, Q.-Y. Zhang, C.-Y. Zhou, and Y.-Y. Sun. 2011. A new pachypleurosaur (Reptilia: Sauropterygia) from the Lower Middle Triassic of Southwestern China and the phylogenetic telationships of Chinese pachypleurosaurs. *Journal of Vertebrate Paleontology* 31:292-302.

Neenan, J. M., N. Klein, and T. M. Scheyer. 2013. European origin of placodont marine reptiles and the evolution of crushing dentition in Placodontia. *Nature Communications* 4:1621. (doi:10.1038/ncomms2633).

Rieppel, O. 2000. *Paraplacodus* and the phylogeny of the Placodontia (Reptilia: Sauropterygia). *Zoological Journal of the Linnean Society* 130:635-659.

Rieppel, O. 2001. The cranial anatomy of *Placochelys placodonta* Jaekel, 1902, and a review of the Cyamodontoidea (Reptilia, Placodonta*). Fieldiana: Geology, New Series* 45:1-104.

Rieppel, O., and K. Lin. 1995. Pachypleurosaurs (Reptilia: Sauropterygia) from the Lower Muschelkalk, and a review of the Pachypleurosauroidea. *Fieldiana (Geology), New Series* 32:1-44.

Rieppel, O., P. M. Sander, and G. W. Storrs. 2002. The skull of the pistosaur *Augustasaurus* from the Middle Triassic of northwestern Nevada. *Journal of Vertebrate Paleontology* 22:577-592.

Wang, X., G. H. Bachmann, H. Hagdorn, P. M. Sander, G. Cuny, X. Chen, C. Wang, L. Chen, L. Cheng, F. Meng, and G. Xu. 2008. The Late Triassic back shales of the

Guanling area, Guizhou Province, South-West China: a unique marine reptile and pelagic crinoid fossil lagerstätte. *Palaeontology* 51:27-61.

CHAPTER 7

CONCLUSIONS AND FUTURE PERSPECTIVES

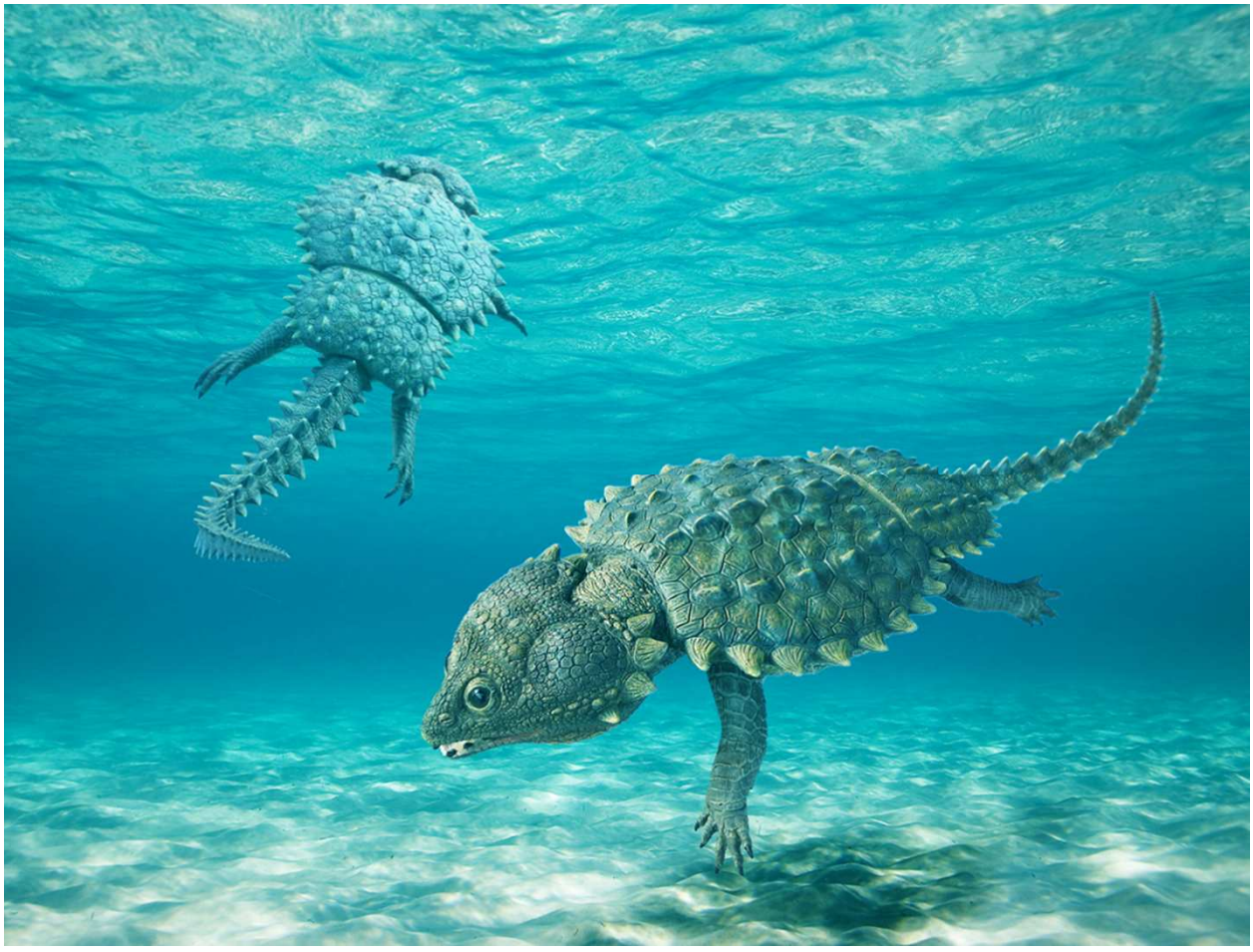

Cyamodus hildegardis by Beat Scheffold

The chapters of this thesis represent the first studies on placodonts using micro-computed tomographic (μCT) data. This has proven to be a very effective method, having provided insight into previously unknown cranial anatomy, and thus allowing the formation of conclusions regarding placodont palaeoecology, evolutionary origins and systematic relationships. Based on inner ear morphology, placodonts have been shown to have been extremely well adapted to life in an aquatic environment, despite their otherwise plesiomorphic postcranial anatomy. In addition, the highly specialised placodont crushing dentition has been shown to have evolved from much more gracile teeth, adapted for feeding on soft prey. μCT scanning was also used to reveal placodont replacement teeth in situ, allowing the first description of tooth replacement patterns, which resulting in the discovery that the group had a completely unique method of tooth replacement. Detailed cranial osteology was also revealed, with a revised description of the braincase of *Placodus gigas* being published, as well as the first detailed reconstructions of all Chinese holotype crania. These data were essential for the creation of the first comprehensive placodont phylogenies that incorporated all taxa from both the eastern and western Tethys. Placodonts appear to have first evolved in the west, with both unarmoured and armoured taxa first appearing here. However the highly-nested and specialised Placochelyidae evolved in the upper Middle Triassic of the eastern Tethys.

While we have learnt a great deal about placodonts using μCT data, there is still much that can be studied. In particular, poorly understood taxa such as *Paraplacodus broilii* and *Cyamodus hildegardis* are in special need of more analysis. The enigmatic *Henodus chelyops* also requires further attention, owing to its ‘wildcard’ occurrences at very different points in the phylogenies of Chapter 6. Indeed, our understanding of placodont evolution would be greatly improved with further study of Chinese (eastern Tethyan) taxa, of which many new specimens are

currently awaiting description and/or being prepared. It is safe to say that there is currently a bias in our understanding of Placodontia, as European taxa have been studied for far longer and in more detail than those from China. However, Chinese placodonts will, without a doubt, become increasingly important in our understanding of both placodont and sauropterygian evolution in the near future.

A future direction for the study of placodonts would be to examine the biomechanics of their feeding, using a modelling technique known as finite element analysis (FEA). This effective and increasingly inexpensive method is being used by vertebrate palaeontologists to study the effects of stress and strain on complex virtual structures (such as a skull), without damaging precious specimens. Indeed, this technique is a particularly viable option owing to the wealth of μCT data that have already been collected for this project.

NEENAN, JAMES MICHAEL

Paläontologisches Institut und Museum
Universität Zürich
Karl-Schmid-Strasse 4
8006 Zurich, Switzerland

Tel.: +41 44 634 21 47
Mob.: +41 78 648 63 32
Email: james.neenan@pim.uzh.ch

Date of birth: 3 January 1984
Marital status: Single
Nationality: British

EDUCATION

2010–2014: PhD (Natural Science)
University of Zurich, Palaeontological Institute and Museum, Switzerland
Supervisor: Dr. Torsten Scheyer
Title: Evolutionary origins, palaeoecology and systematics of placodont marine reptiles from the Triassic of Europe and China.

2008–2009: MSc Palaeobiology (with Merit)
University of Bristol, School of Earth Sciences, UK
Supervisors: Dr. Emily Rayfield and Prof. Jenny Clack
Thesis: Feeding in the early tetrapod *Acanthostega gunnari*: a combined finite element analysis and geometric morphometric approach

2002–2005: BSc Honours Palaeobiology
University College London, Department of Earth Sciences, UK.

1997–2002: A2-Levels in Biology, Chemistry and History, AS-Level in Physics
King's College, Taunton, UK.

GRANT APPLICATIONS AND AWARDS

Swiss National Science Foundation – **12 month PhD extension (No. 31003A 146440)**

Forschungskredit der Universität Zürich – **Withdrawn due to success of above application**

Winner of the 2013 Commission of the Swiss Palaeontological Memoirs Prize for Young Researchers

Gained a special commendation for my presentation at the 2013 PalAss Annual Meeting in Zurich

RESEARCH EXPERIENCE

RESEARCH INTERESTS

- Functional morphology of vertebrates
- Evolution and palaeobiology of Mesozoic reptiles
- Palaeoecology of terrestrial and marine vertebrates

TECHNICAL SKILLS

- Comparative vertebrate anatomy
- 3D data processing and manipulation (Avizo, some VGStudio MAX)
- 2D finite element modelling (Geostar) and geometric morphometrics (PAST)
- Theory and software for phylogenetic analysis of morphological data (PAUP, TNT)
- Microsoft Office and Adobe Creative Suite
- Excellent communication skills in English (native language), with conversational knowledge of German and French

GEOLOGICAL / PALEONTOLOGICAL FIELD EXPERIENCE

2002–2005: Undergraduate field courses:

- Isle of Wight
- Spanish Pyrenees
- Italian Apennines
- Southwest England
- Norfolk

2009: Master's field course:

- Avon Gorge

RELEVANT PROFESSIONAL DEVELOPMENT AND VOLUNTEER EXPERIENCE

TEACHING AND SUPERVISING

2010–Present: *Evolutionary Morphology of Vertebrates– Issues and Methods* (Biol 262), Palaeontological Institute and Museum, Univerity of Zurich

Role: Co-lecturer, student project supervisor

OTHER

Reviewer, Journal of Vertebrate Paleontology

Symposium organizer, 2011 Evolutionary Biology PhD student annual retreat (University of Zurich)

Lab meeting coordinator, I have helped to organise regular lab meetings in the Sánchez lab for the last two years

Volunteer, 'Lange Nacht der Museen' (annual public outreach) at the Palaeontological Museum, University of Zurich

OTHER QUALIFICATIONS AND PAST EMPLOYMENT

- Full UK driving license
- Canadian Ski Instructors' Alliance (2006): Level 2 Ski Instructor
- Canadian Association for Disabled Skiers (2006): Level 1 Disabled Ski Instructor
- Wine and Spirits Education Trust (2006): Level 2 Certificate with Merit

2006: Wine Advisor, Laithwaite's Wine Club

2007–2008: Production Runner, British Broadcasting Corporation (BBC)

2008: Bar Manager, Royal Standard Pub, Mary Tavy, Devon

PUBLICATIONS AND PRESENTATIONS

PEER-REVIEWED PUBLICATIONS

In Press

Neenan, J. M., M. Ruta, J. A. Clack and E. J. Rayfield. Feeding biomechanics in *Acanthostega* and across the fish-tetrapod transition. *Proceedings of the Royal Society B, Biological Sciences* 281:1781. doi: 10.1098/rspb.2013.2689.

2014

Neenan, J. M., C. Li, O. Rieppel, F. Bernardini, C. Tuniz, G. Muscio and T. M. Scheyer. Unique method of tooth replacement in durophagous placodont marine reptiles, with new data on the dentition of Chinese taxa. *Journal of Anatomy* 224(5):603-613. doi: 10.1111/joa.12162.

2013

Neenan, J. M., N. Klein and T. M. Scheyer. 2013. European origin of placodont marine reptiles and the evolution of crushing dentition in Placodontia. *Nature Communications* 4:1621, doi:10.1038/ncomms2633.

2012

Neenan, J. M. and T. M. Scheyer. 2012. The braincase and inner ear of *Placodus gigas* (Sauropterygia, Placodontia) - a new reconstruction based on micro-computed tomographic data. *Journal of Vertebrate Paleontology* 32(6):1350-1357, doi:10.1080/02724634.2012.695241.

Scheyer, T. M., J. M. Neenan, S. Renesto, F. Saller, H. Hagdorn, H. Furrer, O. Rieppel and A. Tintori. 2012. Revised paleoecology of placodonts – with a comment on 'The shallow marine placodont *Cyamodus* of the central European Germanic Basin: its evolution, paleobiogeography and paleoecology' by C.G. Diedrich (Historical Biology, iFirst article, 2011, 1–19, doi: 10.1080/08912963.2011.575938). *Historical Biology* 24:257-267, doi:10.1080/08912963.2011.621083.

CONFERENCE ABSTRACTS

2013

Neenan, J. M. and T. M. Scheyer. 2013. Systematics, origins and palaeoecology of placodont marine reptiles (Sauropterygia, Placodontiformes). *57th Annual Meeting of the Palaeontological Association*, Zurich, CH. **Winner: Special Commendation.**

Neenan, J. M., C. Li, O. Rieppel, F. Bernardini, C. Tuniz, G. Muscio & T. M. Scheyer 2013. Unique method of tooth replacement in Placodontia (Diapsida, Sauropterygia), with new data on the dentition of Chinese taxa. *11th Swiss Geoscience Meeting*, Lausanne, Switzerland. **Winner: Commission of the Swiss Palaeontological Memoirs Prize for Young Researchers.**

Neenan, J. M. 2013. Origins, systematics and paleoecology of placodont marine reptiles (Sauropterygia, Placodontia). *73rd Society of Vertebrate Paleontology Annual Meeting*, Los Angeles, USA, p. 184. **Romer Prize Session Participant**.

Neenan, J. M. 2013. Tooth replacement in durophagous placodont marine reptiles (Sauropterygia, Placodontia), with new data on the dentition of Chinese taxa. *61st Symposium on Vertebrate Palaeontology and Comparative Anatomy*, Edinburgh, UK, p. 32.

2012

Neenan, J. M. and T. M. Scheyer. 2012. Comparative skull anatomy of placodonts (Diapsida: Sauropterygia) using µCT scanning - implications for palaeobiogeography and palaeoecology. *10th Swiss Geoscience Meeting*, Bern, Switzerland, p. 203.

Neenan, J. M., C. Li and T. M. Scheyer. 2012. The cranial morphology of the Chinese placodont *Psephochelys polyosteoderma* (Sauropterygia, Placodontia), a reconstruction based on µCT data. *60th Symposium on Vertebrate Palaeontology and Comparative Anatomy*, Oxford, UK, p. 18–19.

2011

Neenan, J. M. and T. M. Scheyer. 2011. The braincase of *Placodus gigas* - a new reconstruction based on µCT scanning. *71st Society of Vertebrate Paleontology Annual Meeting*, Las Vegas, USA, p. 165–166.

Neenan, J. M. 2011. The skulls of placodont reptiles (Sauropterygia) - a study using microCT-imaging. *Symposium on the fossils from the Lower Muschelkalk of Winterswijk and stratigraphic equivalents*, Bonn, Germany.

Neenan, J. M. and T. M. Scheyer. 2011. The braincase and inner ear region of *Placodus* (Sauropterygia: Placodontia). *55th Annual Meeting of the Palaeontological Association*, Plymouth, UK, p. 69.

2010

Scheyer, T. M. and J. M. Neenan. 2010. Evolution and paleobiology of marine reptiles: using Placodontia as a case study for integrating osteological and 3D imaging, developmental, and paleohistological data. *International Symposium on Triassic and later Marine Vertebrate Faunas*, Beijing, China, p. 78–81.

2009

Neenan, J. M., J. A. Clack and E. J. Rayfield. 2009. Jaw mechanics and feeding in the early tetrapod *Acanthostega gunnari*. *Progressive Palaeontology*, Birmingham, UK.

THESES

2009

Neenan, J. M. 2009. Feeding in the early tetrapod *Acanthostega gunnari*: a combined finite element analysis and geometric morphometric approach. Master's Thesis, University of Bristol, UK, 60 pp.